Synthesis of Batch Processes with Integrated Solvent Recovery

by

Berit Sagli Ahmad

Submitted to the Department of Chemical Engineering
in partial fulfillment of the requirements for the degree of

Doctor of Philosophy in Chemical Engineering

at the

MASSACHUSETTS INSTITUTE OF TECHNOLOGY

June 1997

Author .....
Department of Chemical Engineering
March 3, 1997

Certified by .....
Paul I. Barton
Assistant Professor
Thesis Supervisor

Accepted by .....
Robert Cohen
St. Laurent Professor of Chemical Engineering
Chairman, Committee on Graduate Students

Synthesis of Batch Processes with Integrated Solvent Recovery

by

Berit Sagli Ahmad

Submitted to the Department of Chemical Engineering
on March 3, 1997, in partial fulfillment of the
requirements for the degree of
Doctor of Philosophy in Chemical Engineering

Abstract

One of the many environmental challenges faced by the chemical industries is the widespread use of organic solvents. With a solvent-based chemistry, the solvent necessarily has to be separated from the product. Although intermediate storage may be required before the solvent can be recycled, this should be preferred to disposal of the solvent as waste. This issue provides the motivation for this research, which focuses on development of synthesis tools to address the pollution prevention challenges posed by the use of solvents in the pharmaceutical and specialty chemical industries. In particular, the effective recovery and recycling of solvents is a primary concern.

Chemical species in waste-solvent streams typically form multicomponent azeotropic mixtures. This highly nonideal behavior often complicates separation and hence recovery of solvents. Our approach is based on understanding and mitigating such obstacles. A prototype technology is proposed which combines rigorous dynamic simulation models and/or plant data to quantify waste-solvent streams with residue curve maps to target for maximum feasible recovery when using batch distillation. The theory for ternary residue curve maps applied to batch distillation is extended and generalized to homogeneous systems with an arbitrary number of components. The body of theory is derived from the fields of nonlinear dynamics and topology. Based on these results an algorithm for characterizing the batch distillation composition simplex for a multicomponent system is developed. This algorithm is exploited in a sequential design approach where process modifications proposed by the engineer are evaluated using a targeting procedure. Furthermore, a framework that allows simultaneous evaluation of all feasible distillation sequences from both thermodynamic and environmental or economic perspectives is developed. The framework is realized as a mathematical program and can be applied to a single batch process, or to multi-product facilities in which solvent use is integrated across parallel processes.

Thesis Supervisor: Paul I. Barton
Title: Assistant Professor

To my two lovely daughters,
Ida Rebecca and Jasmine Helena

Acknowledgments

My sincere thanks are due to Professor Paul I. Barton for experienced and extremely fruitful guidance in this research project. Many discussions over the past years have provided a carefully balanced mixture of criticism, encouragement, and advice. He has been a great source of inspiration.

Prof. Larry Evans was my original research supervisor when I started at MIT. I would like to thank him for introducing me into the graduate research program, and I wish him all the best now that he is engaged full time at Aspen Technology, Inc.

Dr. John Ehrenfeld was a source and inspiration to my interest in environmental issues in the early stages of my graduate studies.

Thanks go to Truls Gundersen at the Norwegian University of Science and Technology who encouraged me to pursue graduate work.

I would like to express gratitude to the Norwegian Research Council, the Emission Reduction Research Center, the Chlorine Project of the MIT Initiative in Environmental Leadership, the Fulbright Foundation, and Norsk Hydro as. for providing financial resources.

Within the research group I have enjoyed many hours of discussion with my friends and colleagues. In particular, my thanks go to Russell Allgor, William Feehery, Wade Martinson, Taeshin Park, and John Tolsma. I would also like to thank my UROP students Sarwat Khattak and Mingjuan Zhu for helping out with some of case studies, and Yong Zhang for coding up parts of the solvent recovery targeting algorithm.

Outside the research group I would like to thank Susan Allgor, Aurelie Edwards, Karen Fu, Susan Hobbs, Rahda Nayak, Margaret Speed, Colleen Vandervoorde, and Diane Yen who made these last five or so years at MIT a unique experience. Sue and Diane, I will miss our jogs around Charles River. I am very grateful to Elaine E. Aufiero and Janet Fischer in the graduate student headquarters for being so helpful.

Finally, my warmest thanks go to all those friends and relatives in private life who have supported me through all my efforts. In particular, I would like to express tremendous gratitude as well as amazement to my husband Su Ahmad for putting up with me during what must have been demanding times. Without his immense support and encouragement this work would not have resulted. I would also like to thank my parents for always being there when I have needed some extra encouragement. Throughout my upbringing they always emphasized the importance of a good education, although I do not think they expected me to go this far.

Contents

List of Figures

List of Tables

Chapter 1

Introduction

Together the pharmaceutical and specialty chemical industries made up $380 billion of a total $1 trillion world chemical market in 1988 (Shell, 1990). In comparison to bulk chemical manufacturing or oil refining, the ratio of waste generated to mass of final product is extremely high (5-100+) (Sheldon, 1994). One of the many environmental challenges faced by the synthetic pharmaceutical and specialty chemical industries is the widespread use of organic solvents. The U.S. Environmental Protection Agency (1976) reports that the pharmaceutical industry in 1973 produced about 244,000 metric tons of land-destined process waste. The amount of hazardous waste was approximately 61,000 metric tons, out of which waste solvents amounted to 40,100 metric tons. With an estimated 5% compounded annual increase in production, projections for 1983 for total waste amounted to nearly 400,000 metric tons. The expected generation of hazardous waste was 100,000 metric tons, out of which waste solvents amounted to almost 67,200 metric tons.

Solvents are used in a broad spectrum of unit operations ranging from reaction and separation to product washing and equipment cleaning. A large number of these solvents have traditionally been chlorinated hydrocarbons. Many of the solvents are being phased out of products and processes for environmental and health reasons (Kirschner, 1994). For example, cleaning solvents are relatively easy to change or eliminate (Heckman, 1991) . On the other hand, solvents in process reactions are much more difficult to substitute, because most process solvents influence the character of

the reaction product (Kirschner, 1994).

With a solvent-based chemistry, the solvent necessarily has to be separated from the product stream. Although intermediate storage may be required before the solvent can be recycled to subsequent batches, this should be preferred to disposal of the solvent as toxic waste. This issue provides the motivation for this work, which focuses on the development of analysis and design tools that can facilitate assessment and reduction of the environmental impact of entire chemical manufacturing systems. Attention is devoted to the pollution prevention challenges posed by the use of organic solvents in the bulk synthesis and separation operations employed for the manufacture of active ingredients in the pharmaceutical and specialty chemical industries. This chapter discusses the role of pollution prevention in batch process design, followed by a review of batch process design, and concludes with an overview of the problems that are addressed in this research and a presentation of the approach to deal with these problems.

1.1 Pollution Prevention

Increasingly aggressive legislation and growing concern over environmental impacts are motivating the chemical manufacturing industry to reassess their current operations. The traditional approach has been to employ ever more sophisticated end-of-pipe treatment technologies. These devices are typically designed to meet government emission standards for targeted chemical compounds. The accompanying non-regulated substances, however, almost always remain untouched (Friedlander, 1989). More recently, the more forward looking policy of *pollution prevention* has been adopted; defined by the U.S. Environmental Protection Agency as "the use of materials, processes, or practices that reduce or eliminate the creation of pollutants or waste at the source" (Freeman *et al.*, 1992). For example, in the Resource Conservation and Recovery Act (U.S. Congress, 1984), which regulates the management and disposal of solid and hazardous wastes, the Congress declares that wherever possible the generation of hazardous waste is to be reduced or eliminated. The federal Clean

Air Act Amendments of 1990 (U.S. Congress, 1990a) incorporate innovative strategies and a preventive approach to tackle some of the most serious air pollution problems. In the Pollution Prevention Act (U.S. Congress, 1990b) the U.S. Congress declares it to be the national policy of the United States that pollution should be prevented or reduced at the source whenever feasible. The 33/50 Program, administered by the Office of Toxic Substances, is a voluntary pollution prevention initiative that builds on the U.S. Environmental Protection Agency's pollution prevention policies and programs. The program aims to reduce the release and off-site transfer of 17 chemicals and chemical compounds used in manufacturing. Freeman *et al.* (1992) provide an excellent overview of the current state of activities related to pollution prevention in both public and private institutions

Pollution prevention ranks at the top of the national waste management hierarchy. Source reduction and on-site, closed loop recycling are the recommended methods, with less desirable strategies ranked in order of decreasing preference (see Figure 1-1) (The Pollution Prevention Act (U.S. Congress, 1990b)). As increased attention is devoted to waste management, we should observe a load shift from the alternatives in the lower part of the hierarchy to the alternatives in the upper part. Experience indicates that on average about 80% of emissions from chemical facilities are generated by 20% of the sources (Chadha and Parmele, 1993). It is therefore important to identify and focus on the major contributors. As stated by Friedlander (1989): "Although waste reduction is an attractive concept, the total elimination of manufacturing waste is beyond the capability of modern technology. The issue is really how to approach the limiting goal in an expeditious and cost-effective manner."

Opportunities for waste elimination are present during the design and construction of a new process, and when the process is in normal operation (Jacobs, 1991). Pollution prevention aims to fundamentally redesign chemical manufacturing systems in order to achieve or approach zero environmental impact. This philosophy should be applied both to the design of new processes and to the modification of existing ones. In both cases this requires an approach that considers the overall impact of any modification on the entire processing system, and must encompass all aspects

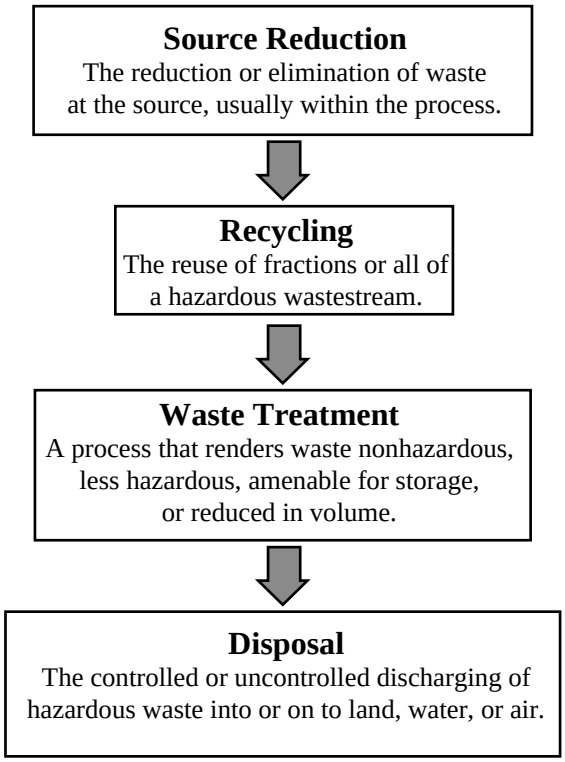

Figure 1-1: The national waste management hierarchy.

of process operation. The design phase involves the selection of chemical pathways, unit operations, the overall flowsheet, operating procedures, etc., and provides the greatest potential for waste reduction. Currently, much attention is devoted to the development of new chemical pathways and novel unit operations that reduce or eliminate materials that are harmful to the environment (e.g., Knight and McRae (1993), Crabtree and El-Halwagi (1994), and Baker *et al.* (1990)). A necessary complement to these efforts is the ability to predict and analyze process behavior at a plant wide level. For example, Grossman *et al.* (1982) present a solution procedure for maximizing net present value while minimizing overall toxicity during the synthesis of chemical complexes. The problem is posed as a bicriteria mixed-integer programming problem. Douglas (1992) demonstrates how his hierarchical design procedure for continuous processes (Douglas, 1988) can be extended to identify waste minimization problems as a design is evolving, and to identify process alternatives that can be used to avoid or reduce these problems. The systematic approach proceeds

through a series of hierarchical levels, where additional process details are added at each level. Some of the decisions that are made result in emission problems, which, if identified early in the design phase, can be eliminated. Rossiter (1994) discusses how process integration techniques are being applied to pollution prevention problems. Illustrations are drawn from the three main areas of process integration: pinch analysis, knowledge-based approaches, and numerical/graphical optimization approaches. Linninger *et al.* (1994) presents a hierarchical approach leading to the synthesis of batch processes with zero avoidable pollution, followed by a guided evolution to processes with minimum avoidable pollution. Lakshmanan and Biegler (1994) apply the concepts of reactor network targeting to the synthesis of process flowsheets with minimum waste. Pistikopoulos *et al.* (1994) introduce a systematic methodology for obtaining process designs with minimum environmental impact. The methodology embeds principles from life cycle analysis within a process optimization framework. Diwekar (Summer 1993; 1994) discusses how existing process simulation technologies and mathematical methods can be applied to addressing environmental concerns in chemical process engineering. In particular, the incorporation of uncertainties into the synthesis of advanced environmental control systems is emphasized.

So far, research activities have been successful only to a limited extent in addressing the problems of waste generation in chemical processes. It is our opinion that much of this deficiency has arisen from a failure to recognize that the environmental problems faced by the chemical industries require new approaches, as opposed to adapting current design technologies. Systematic methods developed specifically to address the needs of the industry and the legislators are essential to successfully resolve the problems at hand. The recognition that the real opportunities lie in how the environmental debate should change the way design is performed, rather than *vice versa*, inspired formulation of the following procedure:

- study particular industries and specific environmental problems
- employ the insight and understanding gained to conceive one or more concrete innovative approaches to address these problems

- define a series of genuine technical problems that need to be resolved

This thesis serves as a modest example of how this approach can yield concrete technical solutions leading to significant environmental benefits.

1.2 Batch Process Design

Smaller companies especially find it hard to devote the effort needed for effective process development (Stinson, 1993). This is partly due to pressure from the market, and partly due to the fact that the cost of manufacturing pharmaceutical intermediates and specialty chemicals is often marginal compared to the cost of the development work up to the stage when the product is ready for large-scale production. Hence, there are often small economic incentives to improve manufacturing efficiency. With increased environmental pressure from regulatory agencies and government this is likely to change.

Pharmaceutical products are typically required in small volumes, and are subject to short product life cycles as well as fluctuating demand. Hence these industries are dominated by the use of multipurpose equipment in batch processes, and waste is generated in relatively small volumes with large variability and high concentration of toxic species. These factors coupled with the inherently time dependent behavior of the unit operations will strongly influence the manner in which pollution prevention is pursued in batch process design.

In batch processing facilities a strong distinction exists between the batch process and the batch plant. The plant refers to the multi-purpose facility in which a variety of products can be produced, while the process refers to the operating procedures and production plans to manufacture an individual product within the facility. Allgor *et al.* (1996) observe that far more frequently the goal of batch mode engineering activities is the design of an efficient process for a new or existing product rather than the design of a flexible manufacturing facility. In fact, the new process is usually incorporated into an existing facility. Extensive reviews of academic progress in this field have been published (Rippin, 1983a; Rippin, 1983b; Reklaitis, 1989; Rippin,

1993) and show that typical engineering tasks addressed by academic research include equipment selection and sizing for plant construction, production planning and scheduling, the treatment of uncertainty in these tasks, and batch process simulation. However, the rapid design of efficient batch processes has received little academic attention (Allgor *et al.*, 1996).

Some of the problems arising in the design of batch processes can be identified (Rippin, 1983b):

- Understand and optimize the performance of tasks carried out in individual items of equipment.
- Optimize the performance of a sequence of tasks in several equipment items to produce a single product.

A task carried out in a particular item can be characterized by the extent to which the task is performed, the time required, and the capacity requirement (Rippin, 1983a). Rippin (1983b) observed that although optimal operation of individual equipment items is important, coordination of tasks is necessary to give optimal operation at a system level, as the performance of an upstream unit determines the input to a downstream unit (and *vice versa* if material is recycled). This issue has been addressed by several workers in the field, e.g., Hatipoglu and Rippin (1984), Wilson (1987), Barrera and Evans (1989), Salomone and Iribarren (1992), and Allgor *et al* (1996). An important observation made by Barrera and Evans (1989) is that in previous research the objective had been to minimize capital cost, although a more appropriate objective function would be the minimization of total manufacturing cost, including rental cost of the capital equipment, raw materials, energy, and labor. Three generic trade-offs in the optimal design problem are also formally introduced. The first type occurs within an individual unit, where there is a trade-off between the cycle time of the unit and the intensity of processing. The second type of trade-off occurs amongst units, as the performance of an upstream unit determines the input to a downstream unit. The third trade-off is a combination of the two other types, and trades off the total rental costs for all the units against the cost factors

determined by the total processing rate for the entire system. Optimal batch process design requires that all these trade-offs are considered simultaneously. Increasing environmental concerns introduces an additional design objective: the environmental impact of the process. Today, the ability to take into account these issues at the development stage is vital to generating an attractive and acceptable process.

Unfortunately, today's environmental legislation appears to be solely focused on continuous processing and dedicated batch manufacturing. For example, recovery of toxic materials through recycling is only credited if it is an on-site closed loop process with no intermediate storage. This is typically very difficult to satisfy in a batch process, as the intermittent nature of the process almost always requires some temporary intermediate storage to make recycling feasible. A more appropriate definition for pollution prevention in multi-product batch facilities is therefore the task of *integrating source reduction and recovery of materials in such a way that any waste treatment or disposal is made redundant.* In this context, the effective recovery and recycling of solvents is a primary concern. As De Wahl and Peterson (1991) note: "though changing an industrial process is frequently cited as the most desirable way to reduce waste for true pollution prevention, the benefits of recycling, however, tend to be more obvious and often affect waste volumes dramatically." Berglund and Lawson (1991) suggest that the permitting process for environmentally sound recycling of waste streams should be streamlined to enhance the attractiveness of such pollution prevention options.

1.3 Approach

Several technologies are available to analyze different aspects of a process design. For example, batch process development is typically conducted by the use of laboratory scale experiments and test runs in pilot plants. In addition, steady-state simulators for extraction of physical properties, and dynamic simulation models customized for selected unit operations (e.g., BATCHFRAC (Aspen Technology, 1991)) are sometimes employed. However, no single tool or approach can appropriately capture all

the issues. In this research we propose a prototype technology which utilizes a combination of tools:

1. Rigorous dynamic simulation models and/or plant data are used to predict the compositions and magnitude of waste-solvent streams.
2. Recent research results from the analysis of residue curve maps are exploited and extended to target for the maximum feasible recovery when using batch distillation.
3. This information is used to suggest design modifications. The new design is then analyzed for further improvements, returning to step (2) if necessary.
4. Dynamic simulation models are employed to analyze the dynamic behavior of the generated process alternatives.

Chemical species in waste-solvent streams typically form multicomponent azeotropic mixtures. This highly nonideal behavior often complicates separation and hence recovery of the solvents. Our approach is based on understanding and mitigating such obstacles. A simple batch process consisting of a reactor and a rectifier is presented in Figure 1-2 to illustrate the procedure. Although simple, the problems encountered in this flowsheet are representative of the class of processes studied in this work. Component R reacts to form product P and byproduct BP. R is exhausted by the reaction, BP is undesired and is treated as organic waste, while it is desirable to recover and recycle the solvent S. The feasibility of distilling the ternary mixture P, BP, and S can be determined from a study of the relevant ternary *residue curve map* (see Figure 1-2b). S and BP form a maximum boiling binary azeotrope S-BP. As a consequence, only one of the species S and BP can be recovered in pure form. The two possible distillation sequences are 1) S $\rightarrow$ S-BP $\rightarrow$ P and 2) BP $\rightarrow$ S-BP $\rightarrow$ P, depending on the initial composition in the reboiler. If alternative 1 is chosen, pure S is recovered and can be recycled to the subsequent batch. However, the binary azeotrope S-BP will have to be disposed of, as it is the only means by which BP can be removed from the system. Hence, extra solvent has to be added to the process with every batch,

and subsequently disposed. On the other hand, alternative 2 will result in recovery of nearly pure BP, which is also subject to disposal, while the binary azeotrope can be recycled to the subsequent batch. Alternative 2 obviously provides environmental benefits over alternative 1 because nearly all of the solvent is recovered and recycled. Some organic waste (BP) is generated, but this is a result of the stoichiometry and is unavoidable without altering the chemistry. In conclusion, this analysis has revealed that the final reaction mixture should ideally have a composition that is located in the region bounded by BP, S-BP, and P. This can be achieved in principle by adjusting the amount of solvent added to the reactor during start-up before cyclic steady-state is reached. Before implementation in plant the impact of recycling BP through the S-BP azeotrope on the reaction kinetics must be analyzed.

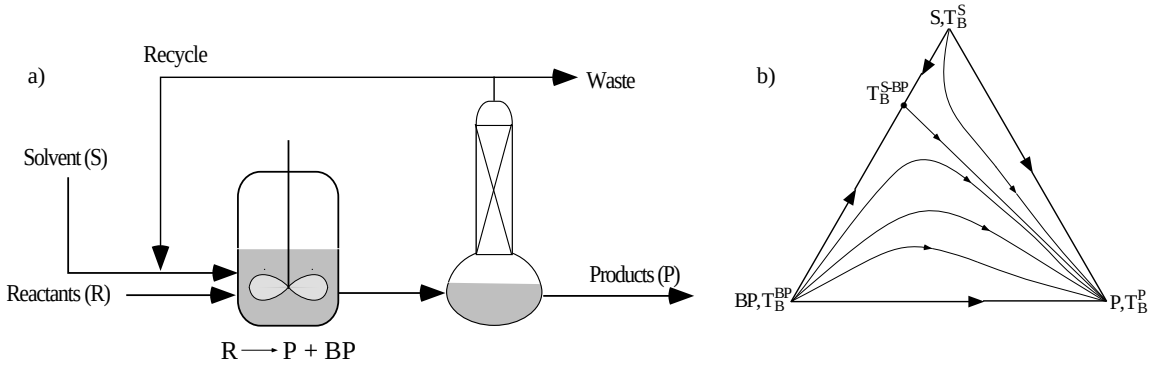

Figure 1-2: a) A simple process consisting of a reaction task and a separation task. b) The residue curve map for the mixture leaving the reactor.

As demonstrated in the example, the sequence of pure component and azeotropic cuts generated by batch distillation of a multicomponent azeotropic mixture, and the maximum feasible recovery in each cut, is highly dependent on the initial composition of the mixture. Any species that is recovered in azeotropic cuts that cannot be recycled is likely to leave the process and be treated as toxic waste. The ability to predict the feasibility of recovering components in pure form from a process stream is therefore essential to pollution prevention in these manufacturing systems. The use of batch distillation as a multipurpose separation operation is typical in the industries concerned. Economics and simplicity of control make batch distillation one of the

most attractive methods for solvent recovery (Hassan and Timberlake, 1992). This work presents a rapid and automated approach to generating this prediction, assuming that batch distillation is the separation technique employed.

The approaches currently available to obtain such predictions, e.g., test runs in pilot plants or detailed dynamic simulation models are typically very elaborate and time consuming. On the other hand, Van Dongen and Doherty (1985a) show that the desired information can be readily extracted from the residue curve map that is characteristic of *simple distillation*. In this research the theory for ternary and quaternary residue curve maps is extended and generalized to *systems with an arbitrary number of components*. The body of theory is derived from the fields of nonlinear dynamics and topology (see, for example, Guckenheimer and Holmes (1983) or Hale and Koçak (1991)).

These theoretical results lead to the development of systematic and general tools for the design of batch processes with minimum waste. An algorithm for elucidating the structure of the batch distillation composition simplex for a system with an arbitrary number of components is developed. Identification of the batch distillation regions is accomplished through completion of the unstable boundary limit sets. The completed boundary limit sets accurately represent the topological structure of the composition simplex, and also makes it possible to extract all product sequences achievable when applying batch distillation.

The algorithm for characterizing the batch distillation composition simplex for a system with an arbitrary number of components is then exploited in a sequential approach where the process modifications proposed by the engineer are evaluated. This approach places the composition of the mixture correctly in the map, and computes the maximum feasible amounts that can be recovered when employing batch distillation. This procedure will be termed *solvent recovery targeting*.

Furthermore, a framework that allows automatic and simultaneous evaluation of all feasible distillation sequences from both thermodynamic and environmental or economic perspectives is developed. The framework is realized as a *mathematical program*. This methodology can be employed to generate various designs alternatives

by adding or removing design constraints, thereby furnishing the engineer with a set of different process designs that can be evaluated based on other criteria not embedded in the program, such as reaction rates (which is a function of selected solvent), production times, safety, etc.

Chapter 2 demonstrates and addresses the deficiencies in earlier work on ternary residue curve maps. In Chapter 3 these results are used to guide the development of a complete set of concepts to describe batch distillation of an azeotropic mixture with an arbitrary number of components. The material in Chapters 2 and 3 is an extended version of the material in Ahmad and Barton (1996b). Chapter 4 presents the algorithm for characterizing the batch distillation composition space. Chapter 5 introduces solvent recovery targeting, and presents results from two case studies where solvent recovery targeting is applied. Chapter 6 presents a systematic approach to the generation of batch process designs that have solvent recovery and recycling integrated into the flowsheet. The approach is realized as a mathematical program. In Chapter 7 the results from two case studies where the mathematical programming approach is used are discussed. The material in Chapters 6 and 7 is an extended version of the material in Ahmad and Barton (1995). Chapter 8 extends the mathematical programming approach to provide a general framework for the design of multi-product batch manufacturing facilities in which solvent use is integrated across parallel processes. Chapter 9 discusses the results from two case studies where the extended mathematical programming approach is utilized. The material in Chapters 8 and 9 is an extended version of the material in Ahmad and Barton (1996a). Finally, Chapter 10 presents conclusions and recommendations for future work.

Chapter 2

Analysis of Batch Distillation Systems

Separation of multicomponent azeotropic mixtures into pure products is a common problem in most sectors of the chemical industry, whether it be through the use of continuous distillation or batch distillation. It is now generally recognized that dynamic investigations of processes and equipment are essential to understand adequately the behavior and performance of these operations. A good deal of effort has been spent on exploring the dynamic behavior of *simple distillation* of multicomponent mixtures. The concept of *residue curve maps* has been introduced to facilitate graphical analysis of such systems. This has led to a number of results that can be used in the synthesis and design of complex distillation systems. A number of articles have addressed continuous systems (Doherty and Caldarola, 1985; Levy *et al.*, 1985; Stichlmair and Herguijuela, 1992; Stichlmair *et al.*, 1993; Van Dongen and Doherty, 1985a; Wahnschafft *et al.*, 1992; Wahnschafft *et al.*, 1993). To a lesser extend the synthesis of batch distillation systems has been addressed. The bulk of this research has focused on low dimension systems (binary, ternary and quaternary systems) and the generation of ternary residue curve maps. The work on simple distillation and ternary batch distillation is reviewed, and the deficiencies are identified and addressed. In subsequent chapters these results are used to guide the development of a complete set of concepts to describe batch distillation of an azeotropic mixture with an arbitrary

number of components.

2.1 Characterizing Distillation Systems

Binary distillation, where one component is separated from another, is the simplest form of distillation. The homogeneous phase equilibrium between two components can be represented by a *vapor-liquid equilibrium curve* at constant pressure. This curve contains all possible pairs of liquid and vapor compositions in equilibrium with each other and is completely independent of any consideration concerning the distillation setup except the total pressure. Corresponding plots also showing the equilibrium temperature are termed *Txy-diagrams* and include both bubble- and dew-point curves. Given a boiling temperature the corresponding vapor and liquid compositions can be read directly off the diagram. Alternatively, for a given liquid (or vapor) composition the composition of the vapor (or liquid) at equilibrium can be found, as well as the boiling- or dew-temperature. Depending on the system, the diagram takes on qualitatively different forms as shown in Figure 2-1: a) the system forms no azeotropes, b) the two components form a minimum boiling binary azeotrope, and c) the two components form a maximum boiling binary azeotrope. Although extremely rare, multiple azeotropy may be observed, where the same components form azeotropes with different compositions and boiling temperatures. This occurs when the system exhibits very strong positive and negative deviations from Raoult's law in different areas of the composition space. The only known example of a double azeotropic mixture is the system C_6H_6-C_6F_6 (see, for example, Dechema's Vapor-Liquid Equilibrium Data Collection Vol.1, Part 7 (1980) or Doherty and Perkins (1978a)). In this work multiple azeotropy is not discussed. However, the theory derived in Chapters 2 and 3 is also applicable to such phenomena.

Vapor-liquid equilibrium data can be generated using the least complicated of all distillation processes, the simple distillation (or open evaporation) process. Here a multicomponent mixture is boiled in an open vessel at constant pressure such that the vapor is removed as soon as it is formed (see Figure 2-2 where x_i and y_i are the

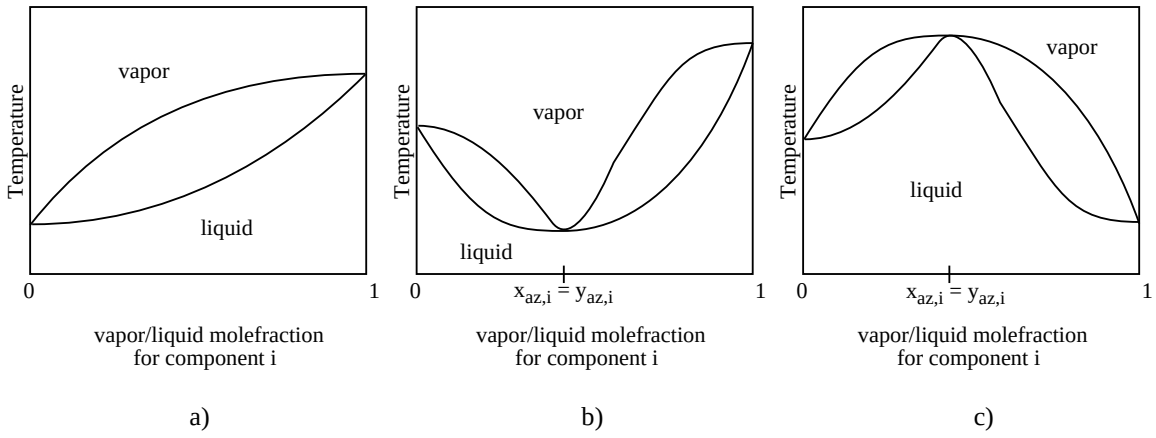

Figure 2-1: Binary vapor-liquid equilibrium diagrams exhibiting a) no azeotrope, b) a minimum boiling binary azeotrope, and c) a maximum boiling binary azeotrope.

mole fractions of component i in the liquid and the vapor phase, respectively). The liquid (or *residue*) will become increasingly depleted in the more volatile component as the distillation progresses. The change in the composition of the residue during simple distillation of an nc component mixture can be represented as curves that lie in an $nc-1$ dimensional composition hyperplane called a residue curve map. The residue curve maps for the binary systems in Figure 2-1 are shown in Figure 2-3.

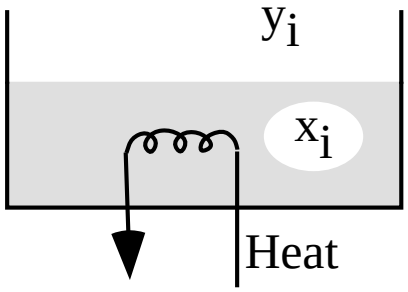

Figure 2-2: Setup for simple distillation.

A study of the residue curve maps in Figure 2-3 yields the important information that an azeotrope acts as some kind of barrier to separation. For example, if the liquid feed composition is located to the right of the azeotrope in Figure 2-3c, the vapor will initially be rich in component i. As the liquid composition approaches $\mathbf{x}_{az,i}$, the vapor composition will do the same. However, when the liquid reaches the azeotropic composition it will not change, no matter how much heat is applied. On

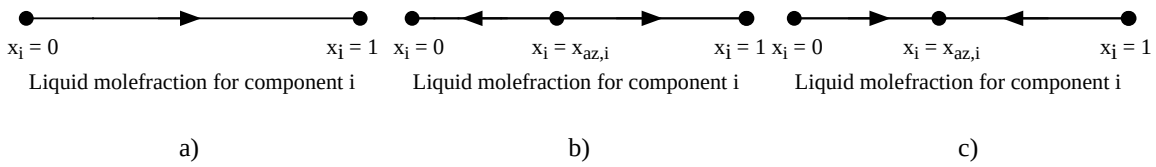

Figure 2-3: Binary residue curve maps for systems exhibiting a) no azeotrope, b) a minimum boiling binary azeotrope, and c) a maximum boiling binary azeotrope. Direction of arrow indicates increasing boiling temperature.

the other hand, with the liquid feed composition located to the left of the azeotrope, we will observe vapor compositions in the range from very little i to the azeotropic composition. Hence, we also observe that depending on which side of the azeotrope we are operating different separation alternatives will result. Residue curve maps can provide the means to enumerate the number of possible separation alternatives. Obviously, Txy-diagrams yield more information than residue curve maps and would be preferred. However, as the number of components increases graphical representation becomes increasingly difficult. Vapor-liquid equilibrium of ternary systems is most easily studied in residue curve maps, and for systems with more than four components there is no straightforward way of studying the separation behavior of a mixture graphically. Now, going from binary to ternary to multicomponent systems, there is literally an explosion in the number of separation alternatives. The main focus of this work is to try to understand this vast number of alternatives, and if possible provide an automatic means to enumerate them for a given system.

2.2 Simple Distillation Residue Curve Maps

For ternary systems the residue curves may be represented either in a regular simplex or in a right simplex. The regular simplex is the well known Gibb's composition triangle, and the right simplex is generated by projecting the composition plane onto a plane defined by $x_i = 0, i \in \{1, 2, 3\}$. The relationship between the two representations is shown in Figure 2-4, where the vertices represent pure components, binary azeotropes are located on the edges, and any ternary azeotrope is found inside the simplex. For the purposes of this work, it is most valuable to imagine the Gibb's

composition simplex suspended in the host nc space.

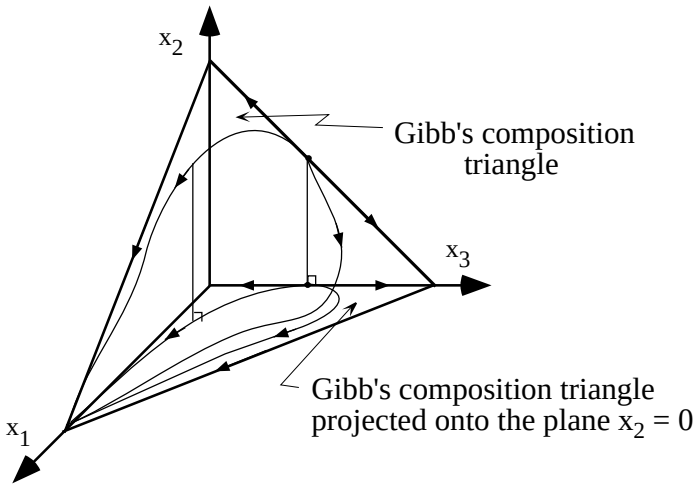

Figure 2-4: The relationship between the regular and the right simplex representations of ternary residue curve maps.

The vectors through the three pure component vertices form a basis for the three dimensional vector space $\mathbf{R}^3$, but because the mole fractions must sum to unity, the actual feasible composition space is a regular simplex that lies on the plane $x_1 + x_2 + x_3 = 1$ and is constrained by $x_i \geq 0 \ \forall i = 1, 2, 3$. Hence, in an nc component system the vectors through the nc pure component vertices form the basis for the nc dimensional vector space $\mathbf{R}^{nc}$, and the composition space is a closed $nc - 1$ dimensional regular simplex on the hyperplane $\sum_{i=1}^{nc} x_i = 1$ constrained by the closed half planes $x_i \geq 0 \ \forall i = 1, 2, \ldots, nc$. The simple distillation residue curves can be constructed experimentally using the distillation setup described above, or can be found numerically by solving a set of equations describing the composition path of the residue. The derivation of these equations can be found in Doherty and Perkins (1977):

$$\frac{dx_i}{d\xi} = x_i - y_i(\mathbf{x}) \ \ \forall i = 1, \ldots, nc - 1 \tag{2.1}$$

The relationship between x_i and y_i can, for example, be described by a suitable vapor-liquid equilibrium model (see, for example, Prautsnitz *et al.* (1986)). The independent variable ξ is a dimensionless measure of time. Residue curves $(orbits)^{\ddagger}$ are projections of the trajectories defined by Equations (2.1) onto the plane $\xi = 0$ (i.e., the *phase*

portrait of the dynamic system). Equations (2.1) can be analyzed, and a number of properties regarding the structure of the residue curve map for the system of interest can be extracted. The mathematical basis for multicomponent simple distillation theory can be found in a series of papers by Doherty and Perkins (1978a; 1978b; 1979). The residue curves also represent the column profile in a column that is operated at total reflux, indicating that the top and the bottom product compositions in that case have to be located on the same residue curve. The residue curves can be grouped into families of curves that have qualitatively similar trajectories. Most of the residue curve maps presented here are for simplicity shown with only one or two residue curve representing a certain family of curves, but, of course, an infinite number of curves may be drawn. An example of the residue curve map (regular simplex) for a ternary system with components L, I, and H is shown in Figure 2-5. Components L and I form a maximum boiling azeotrope. The arrows point in the direction of increasing temperature and time.

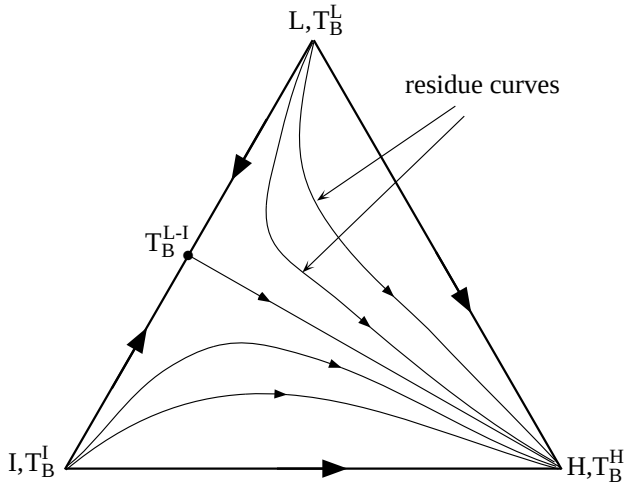

Figure 2-5: Simple distillation residue curve map for ternary system with a binary maximum boiling azeotrope. L, I, and H are the low, intermediate, and high boiling pure components in the system, respectively. The order of boiling temperatures is $T_B^L < T_B^I < T_B^{L-I} < T_B^H$. • indicates azeotrope.

The problem of computing the temperatures and compositions of all the azeotropes in a multicomponent system can be formulated as a multi-dimensional root-finding

[‡]The terminology describing the dynamic system $\mathbf{x}(\xi)$ is adopted from Hale and Koçak (1991).

problem, where the pure components and azeotropes are the fixed points (critical points, equilibrium points, steady-state solutions) of the dynamic system. The fixed points can be shown to have the properties of nodes or saddles (Doherty and Perkins, 1977; Doherty and Perkins, 1978a). The nodes represent either low-boiling or high-boiling compositions, while the saddles represent intermediate-boiling compositions, here referred to as $\mathbf{x}_m^*$, $\mathbf{x}_q^*$, and $\mathbf{x}_n^*$, respectively. $\mathbf{x}_m^*$ is an unstable node which all residue curves in the same family will enter as $\xi \to -\infty$, $\mathbf{x}_q^*$ is a stable node which all residue curves in the same family will enter as $\xi \to +\infty$, and $\mathbf{x}_n^*$ has no residue curves entering except for the residue curves that are also *separatrices* (see Section 2.4). In Figure 2-5 the pure components L and I are unstable nodes, component H is a stable node, and the binary azeotrope L-I has the properties of a saddle point. The nature of the fixed points can be classified using topology theory (Doherty and Perkins, 1979; Fidkowski *et al.*, 1993). The set $\alpha(\hat{\mathbf{x}}) = \lim_{\xi \to -\infty} \varphi(\xi, \hat{\mathbf{x}})$ is called the α-limit set of composition point $\hat{\mathbf{x}}$. Similarly, the set $\omega(\hat{\mathbf{x}}) = \lim_{\xi \to +\infty} \varphi(\xi, \hat{\mathbf{x}})$ is called the ω-limit set of $\hat{\mathbf{x}}$ (Hale and Koçak, 1991). $\varphi(\xi, \hat{\mathbf{x}})$ refers to the trajectory through $\hat{\mathbf{x}}$. Clearly, following from the properties above $\alpha(\hat{\mathbf{x}})$ and $\omega(\hat{\mathbf{x}})$ only contain fixed points, as all trajectories approach fixed points as $\xi \to -\infty$ and $\xi \to +\infty$, and the trajectories fill the entire composition simplex. Therefore, each composition point in the composition simplex may be characterized by a fixed point as its α-limit set and another fixed point as its ω-limit set.

2.3 The Use of Residue Curve Maps in Batch Distillation

Reinders and De Minjer (1940) study the differences between residue curves (simple distillation lines) and *distillation lines* that describe *rectification*, or traditional batch distillation. In rectification the feed is heated in a reboiler and product is condensed and drawn overhead (see Figure 2-6). They present several examples of ternary residue curve maps, and indicated that under certain conditions the lines of rectifying

distillation will be almost straight. Figure 2-7 illustrates this behavior for a system with no azeotropes. The conditions under which this behavior may be observed, however, are less clear. The authors argue that the distillation lines may deviate from this behavior if the hold-up in the tray section is large compared to the reboiler volume, and the less ideally the column works.

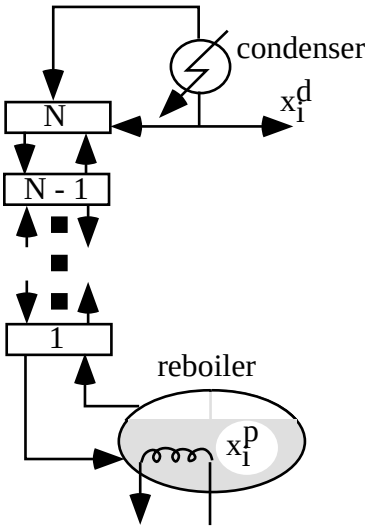

Figure 2-6: Setup for rectification or traditional batch distillation.

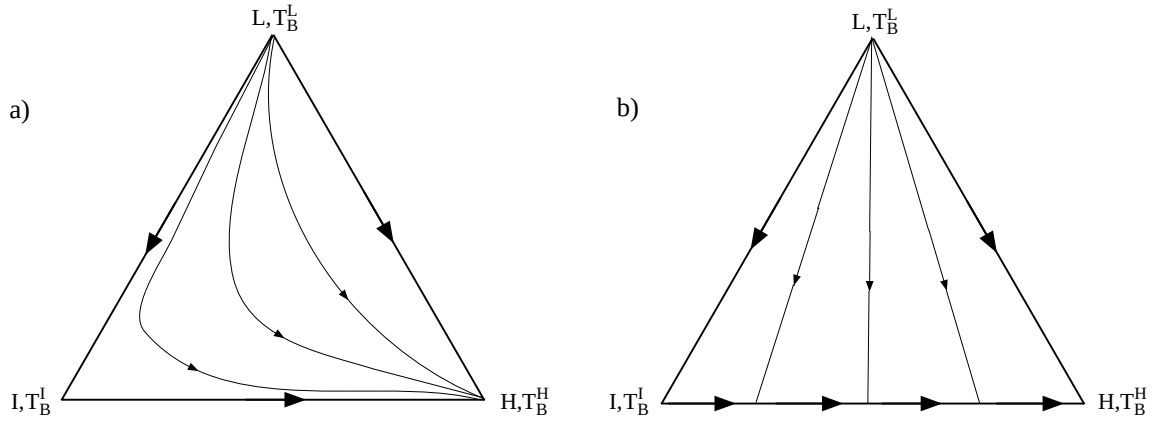

Figure 2-7: Residue curve map for a ternary system with no azeotropes: a) simple residue curve map, b) residue curve map with distillation lines that describe rectification.

Van Dongen and Doherty (1985b) prove that for ternary batch distillation with high reflux and a large number of equilibrium stages the rectifying distillation lines

do indeed move in such a manner. They demonstrate that when distilling a ternary mixture under these limiting conditions it is possible to draw the exact orbits following the composition of the liquid in the still, and to predict the sequence of constant-boiling vapor distillates overhead; provided only that the structure of the residue curve map for the system of interest is known. This is particularly important for azeotropic mixtures, as the sequence of products will typically change with feed composition. A simple batch distillation model was developed describing the time evolution of the composition in the still pot:

$$\frac{dx_i^p}{d\xi} = x_i^p - x_i^d(\mathbf{x}^p) \; \forall i = 1, \ldots, nc-1 \tag{2.2}$$

where x_i^p is the mole fraction of component i in the still pot and x_i^d is the fraction in the distillate as illustrated in Figure 2-6. It is important to note that this equation is different to the simple distillation Equations (2.1) as x_i^d is not in equilibrium with x_i^p. Rather, x_i^d is calculated (given x_i^p) using the design equations for the column. The set of equations used was based on the assumption of high reflux ratio ($rr \geq 7$). With few theoretical stages (small N), the batch distillation residue curves calculated look similar to the residue curves from simple distillation, as expected. When N is increased to a high value (i.e., N $\geq$ 10-20), the batch distillation residue curves ($\mathbf{x}^p(\xi)$) appear to move directly away from the initial composition point $\mathbf{x}^{p,0}$ in a direction opposite from the position of the low-boiling fixed point (pure component or azeotrope) in the region where $\mathbf{x}^{p,0}$ was located. $\mathbf{x}^p(\xi)$ denotes the pot composition trajectory ($\varphi^p(\xi)$) projected onto the plane $\xi = 0$. The change in the pot composition $\mathbf{x}^p(\xi)$ is almost linear because a large number of trays and high reflux ratio cause the composition of the distillate $\mathbf{x}^d(\xi)$ to be approximately constant at a value near the low-boiling fixed point. The composition of the pot will move along this straight line until it hits a *pot composition barrier* (see Section 2.6), then it will turn and follow the limiting boundary towards the higher boiling fixed point. For each batch distillation residue curve there will be a corresponding *distillate curve* that denotes the locus of distillate compositions $\mathbf{x}^d(\xi)$ as they change with time during the course of distillation.

The relationship between these two curves is precisely the same as the relationship between a simple distillation residue curve and its vapor boil-off curve. Hence, the distillate composition $\mathbf{x}^d(\xi^{'})$ corresponding to any particular instantaneous still pot liquid composition $\mathbf{x}^p(\xi^{'})$ will lie on the tangent line to the batch distillation residue curve through $\mathbf{x}^p(\xi^{'})$ (see Equations (2.2)). The two instantaneous compositions also have to lie on the same simple distillation residue curve due to the assumption of close to total reflux in the column. In Figure 2-8 the relationship between the pot liquid composition $\mathbf{x}^p(\xi)$ and the distillate composition $\mathbf{x}^d(\xi)$ during the course of distillation is shown for a ternary mixture. $\mathbf{x}^{p,0}$ is the initial composition in the reboiler. The white arrow indicates the orbit $\mathbf{x}^p(\xi)$. The set of points $\mathbf{x}^{d,1}$, $\mathbf{x}^{d,2}$, and $\mathbf{x}^{d,3}$ represents the distillate curve, i.e., the sequence of distillate compositions that will appear overhead if the column is run until the reboiler is dry.

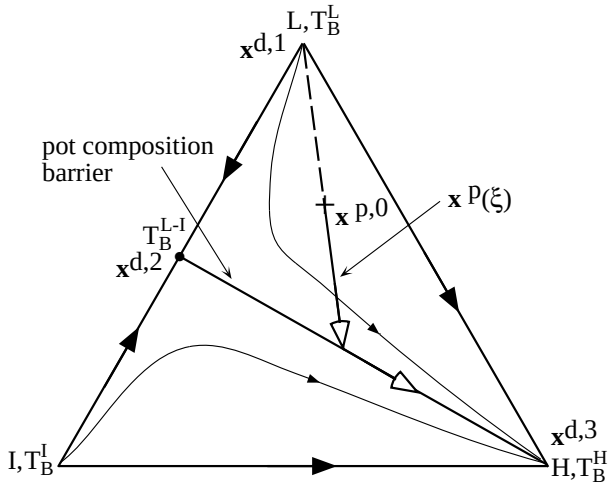

Figure 2-8: Relationship between pot composition $\mathbf{x}^p(\xi)$ and the distillate composition $\mathbf{x}^d(\xi)$ during the course of distillation of a ternary mixture.

It has been demonstrated that this behavior also applies to mixtures with more than three components. For example, Bernot *et al.* (1991) present an example with four components. However, no attempt has been reported at extending and generalizing the theory to mixtures with an arbitrary number of components. In this work the theory governing the behavior of such a mixture is introduced. A rectifier configuration is assumed, but the same arguments will apply for a stripper configuration

(see Appendix A).

2.4 Distillation Boundaries

The presence of *distillation boundaries* in the composition space, and whether these boundaries can be crossed or not using continuous or batch distillation, have been the topic of considerable debate in the literature over the years. The separatrices play a central role, where a separatrix is defined in the following manner: if in each neighborhood[§] $N_r(\mathbf{p})$ of a point $\mathbf{p}$ there is a point $\mathbf{q}$ such that $\omega(\mathbf{q}) \neq \omega(\mathbf{p})$, or $\alpha(\mathbf{q}) \neq \alpha(\mathbf{p})$, then the orbit through $\mathbf{p}$ is called a separatrix (Hale and Koçak, 1991). It is important to understand the difference between stable and unstable separatrices. A stable separatrix is defined as a residue curve where the residue curves on each side are moving towards the same fixed point, and which are moving towards this same fixed point even at long time. Otherwise the separatrix is an unstable separatrix. Doherty and Perkins (1978a) conclude that unstable separatrices correspond to simple distillation boundaries.

Much discussion has evolved around the difference between simple distillation boundaries and the distillation boundaries related to a specific distillation configuration (e.g., continuous, batch rectifier, batch stripper, etc.). Reinders and De Minjer (1940) analyze the general structure of simple distillation curves and distillation curves of rectifying distillation for systems with no azeotropes, one minimum boiling binary azeotrope, one maximum boiling binary azeotrope, and combinations of binary and ternary azeotropes, and conclude that for some systems a boundary line for simple distillation may induce a similar boundary line for rectification. However, for other systems this correlation may be lacking. Ewell and Welch (1945), after studying five ternary systems using a rectifier, summarize that three types of boundaries are observed: 1) straight boundaries associated with valleys in the boiling temperature surface, 2) curved boundaries associated with ridges in the boiling temperature

[§]A *neighborhood* of a point p is a set $N_r(p)$ consisting of all points q such that the distance $d(p,q) < r$. The number r is called the radius of $N_r(p)$ (Rudin, 1976).

surface, and 3) straight boundaries that are not associated with any feature in the boiling temperature surface. Although it appeared to Ewell and Welch that some of the boundaries they observed were associated with valleys and ridges in the boiling temperature surface, we know now that this correlation with features on the boiling temperature surface was only an artifact of the particular systems they were studying.

It has been widely believed that separatrices in a simple distillation residue curve map coincide with the projection of ridges and valleys in the boiling temperature surface onto the composition simplex. Hence, the separatrices can be located by studying the structure of the boiling temperature surface. For example, Doherty and Perkins (1978a) describe a simple algorithm to locate the boundary structure for an nc component system by detecting the valleys and ridges based on stability criteria for the boiling temperature surface. However, over the years there have been indications that this prevailing opinion is false. Swietoslawski (1963) compares experimental data for valleys and ridges with the corresponding simple distillation residue curve maps, and demonstrates that there are deviations. Naka *et al.* (1976) without rigorous proofs also come to the same conclusion. The last words on the subject may have been said when Van Dongen and Doherty (1984) demonstrate that valleys and ridges do not necessarily coincide with separatrices by analyzing the equations governing the boiling temperature surface and the simple distillation process. They show through several examples that there is no correlation between the separatrices and the valleys and ridges in the boiling temperature surface. The curved boundaries actually correspond to separatrices. In simple distillation unstable separatrices, by definition, cannot be crossed by the orbit of the liquid composition (a separatrix is just another residue curve, and residue curves cannot cross). On the other hand, it may be feasible to achieve distillate compositions on the other side of the boundary. In continuous distillation, unstable separatrices can be crossed under certain conditions: if the boundary is highly curved and the feed composition is in the concave region of the boundary line, it may be possible to achieve product compositions on the other side of the boundary (Stichlmair and Herguijuela, 1992; Wahnschafft *et al.*, 1992). Ewell and Welch (1945) speculate concerning the crossing of curved boundary lines using a

traditional batch column. They conclude that both residue and distillate composition orbits can cross the boundary when approaching from the concave side, but not from the convex side. As Doherty and Perkins (1978a) later point out, the residue composition orbit cannot cross the boundary (as this would give rise to intersecting residue curves). However, as the distillate is not in equilibrium with the residue in a batch column, it is feasible for the distillate composition orbit to cross the boundary. This issue is elaborated further in the next section.

2.5 Distillation Regions

The definition of distillation regions and boundaries are closely related. Doherty and Perkins (1978a) state that two simple distillation residue curves that are initially close together and are still close at long time belong to the same simple distillation region. Clearly, the residue curves in Figure 2-5 can be divided into two families, those that enter L as $\xi \to -\infty$ and H as $\xi \to +\infty$, and those that enter I as $\xi \to -\infty$ and H as $\xi \to +\infty$. However, according to the definition by Doherty and Perkins (1978a), all the residue curves belong to the same region, and hence there is only one simple distillation region in the map. In batch distillation the situation is different. At this point it is necessary to define a *batch distillation region*, and we adopt a modification of the definition due to Ewell and Welch (1945):

Definition 2-1 *A batch distillation (rectification or stripping)*[¶] *region* $B(\mathbf{P})$ *is the set of compositions that lead to the same sequence of product cuts* $\mathbf{P} = \{\mathbf{p}_0, \mathbf{p}_1, \ldots\}$ *upon distillation (rectification or stripping) under the limiting conditions of high reflux ratio and large number of equilibrium stages.*

Under the limiting conditions, a product cut sequence is defined as the sequence of pure component and azeotropic compositions ($\mathbf{p}_k \ \forall k = 0, 1, \ldots$) drawn overhead when distilling a multicomponent mixture using batch distillation. The element p_{ki} in the nc vector $\mathbf{p}_k$ is the mole fraction of pure component i in product cut k. For an azeotropic

[¶]The theory is derived for the more common rectifier configuration.

mixture this product cut sequence depends on the location of the composition of the feed, and by definition any initial composition that is taken interior to a given batch distillation region will always result in the *same* sequence of cuts. Hence, once the batch distillation regions are defined, the set of products can be predicted from the distillate path thus defined. As Figure 2-8 shows, the residue curve map for the components L, I, and H presented in Figure 2-5 can actually be divided into two batch distillation regions: one defined by the straight lines connecting L,L-I, and H giving rise to $\mathbf{P}_1 = \{\text{L,L-I,H}\}$, and one defined by the straight lines connecting I,L-I, and H resulting in $\mathbf{P}_2 = \{\text{I,L-I,H}\}$. Figure 2-9 presents another example. Components L and I form a minimum boiling binary azeotrope, and so do components I and H. The composition space is divided into three batch distillation regions, B_1, B_2, and B_3. The feed composition $\mathbf{x}^{p,0}$ is located in batch distillation region B_3. The resulting product cuts therefore are: 1) the binary azeotrope L-I with composition $\mathbf{x}^{d,1}$, 2) the pure component L with composition $\mathbf{x}^{d,2}$, and 3) the pure component H with composition $\mathbf{x}^{d,3}$.

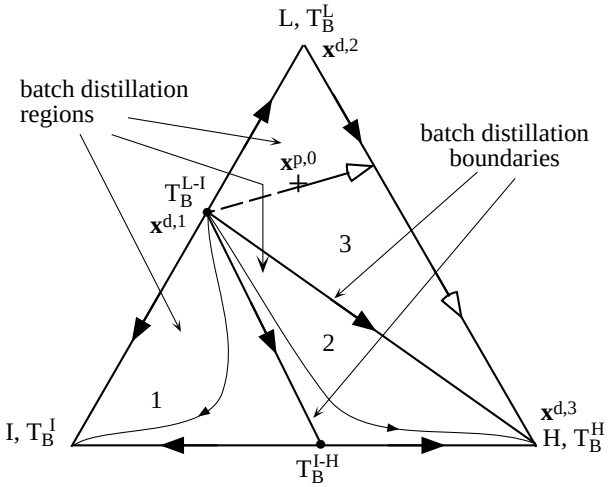

Figure 2-9: Ternary residue curve map with batch distillation boundaries and regions. The order of the boiling temperatures is $T_B^{L-I} < T_B^L < T_B^{I-H} < T_B^I < T_B^H$.

The boundaries that Ewell and Welch (1945) observed have later been termed *batch distillation boundaries* (see Figure 2-9). Bernot *et al.* (1990; 1991) propose how the batch distillation boundaries can be found for a ternary system:

1. The stable separatrices dividing the simplex into subdomains each containing an unstable node constitute batch distillation boundaries.

2. Within each of these subdomains (or the entire simplex in the case of only one domain), connections between the unstable node and all the other species in the domain may be introduced as straight line batch distillation boundaries.

A straight line boundary should not intersect a stable separatrix, and if a stable separatrix is highly curved, the straight line boundary is tangent to the separatrix. For example, in the ternary residue curve map in Figure 2-10a the boundary connecting component I and the binary azeotrope L-H will intersect the stable separatrix between L-I-H and L-I and should therefore be discarded. Figure 2-10b illustrates another example. When placing batch distillation boundaries according to the above rules a boundary connecting L and H will be introduced. However, as this boundary will intersect the binary edge L-H, it should be discarded. Another interesting feature of the latter system is that any initial pot composition $\mathbf{x}^{p,0}, x_i > 0$ will yield the product sequence $\mathbf{P}$ = {L,I,H}. Compositions on the (L,I) edge, or the (I,H) edge will yield a subset of $\mathbf{P}$, {L,H}, or {I,H}, respectively. In contrast, compositions on the binary edge (L,H) will yield {L,L-H}, or {H,L-H}, depending on which side of the L-H azeotrope the initial composition is located. This irregular behavior will only be apparent if the initial composition is located on the edge. In Section 3.3 a clear distinction will be made between the case when the initial composition is located internal to a batch distillation region, and when it is located on the boundary of a batch distillation region.

As demonstrated by Ewell and Welch (1945) it is possible to obtain distillate compositions on the other side of a stable separatrix when running a rectifier under the limiting conditions of high reflux ratio and large number of trays. When distilling mixtures of acetone, chloroform, and methanol, the researchers observed a nonmonotonic variation in the distillate temperature for certain initial reboiler compositions. Ewell and Welch could not explain their findings, and concluded that the temperature drop was an anomaly. Van Dongen and Doherty (1985b) showed that this "anomaly"

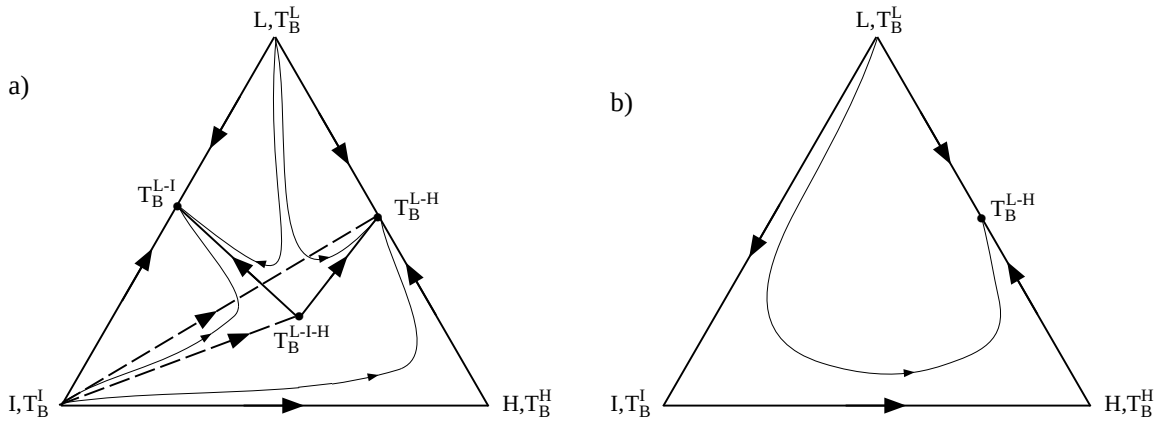

Figure 2-10: Residue curve maps where some batch distillation boundaries are discarded. The order of boiling temperatures: a) $T_B^{L,m} < T_B^{I,m} < T_B^{H,m} < T_B^{L-I-H,n} < T_B^{L-I,q} < T_B^{L-H,q}$ and b) $T_B^{L,m} < T_B^{I,n} < T_B^{H,n} < T_B^{L-I,q}$.

has a logical explanation related to the curvature of stable separatrices. Figure 2-11 shows the residue curve map for the system acetone, methanol, and chloroform with batch distillation boundaries placed according to the above rules. Stable separatrices are indicated with solid lines, while the other boundaries are dashed (long dash segments). Unstable separatrices are shown for clarity (short dash segments). When the pot orbit starting in $\mathbf{x}_1^{p,0}$ hits the stable separatrix connecting the binary acetone-chloroform azeotrope and the ternary azeotrope it is forced to stay on this boundary, and the pot composition $\mathbf{x}^p(\xi)$ will therefore follow the curvature of the separatrix. The instantaneous distillate composition $\mathbf{x}^d(\xi^{'})$ will lie on the tangent line to the pot orbit through the instantaneous pot composition $\mathbf{x}^p(\xi^{'})$ (see Equations (2.2)). Hence, the distillate composition will not be equal to the ternary saddle azeotrope, but will have a composition which will vary along the unstable separatrix connecting the binary azeotrope acetone-methanol and the ternary azeotrope. A decrease in the distillate temperature may therefore be detected, before the temperature eventually increases again as the distillate composition path reaches the binary acetone-methanol azeotrope. The deviation from the ternary saddle azeotropic composition will depend on the curvature of the stable separatrix. Distillation of an initial reboiler composition located in batch distillation region B^2 will result in a similar outcome with some distillate compositions located on the other side of the stable separatrix. On the other

hand, initial compositions taken within regions B^3 and B^4 will not result in distillate compositions located on the other side of the stable separatrices. For example, when the pot orbit starting with $\mathbf{x}_3^{p,0}$ hits the stable separatrix connecting the ternary azeotrope and the binary acetone-chloroform azeotrope the corresponding distillate orbit will follow the same path as the distillate orbit resulting from $\mathbf{x}_1^{p,0}$ (i.e., at that point the distillate composition will vary along the unstable separatrix connecting the binary azeotrope acetone-methanol and the ternary azeotrope). Hence, the distillate orbit will not cross the stable separatrix. A detailed discussion of the other possible product sequences can be found in Bernot *et al.* (1990).

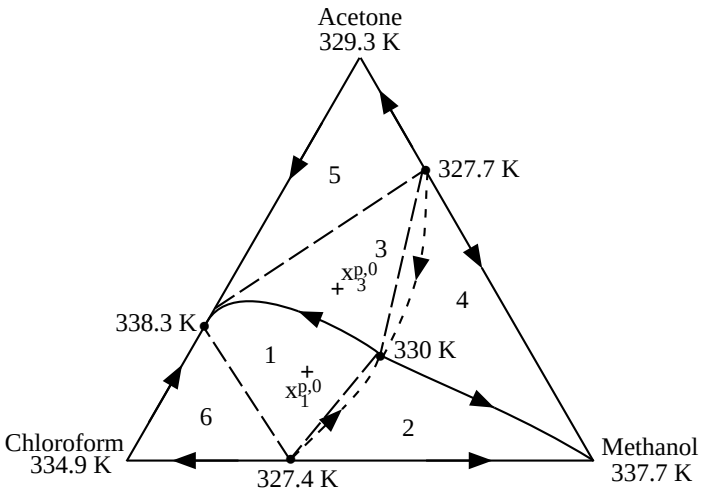

Figure 2-11: Residue curve map (qualitative) for the system acetone, chloroform, and methanol.

The significance of these results is that highly curved stable separatrices may lead to distillate orbits where the temperature is not monotonically increasing. If the pot orbit hits the stable separatrix from the concave side, distillate compositions on the other side of the separatrix may be achieved. Conversely, when the pot orbit hits the stable separatrix from the convex side, the distillate orbit will not cross the separatrix, but will move back into the original batch distillation region.

2.6 Pot Composition Boundaries in Ternary Mixtures

A stable separatrix does not necessarily divide the composition space. Figure 2-12a shows a topologically consistent residue curve map with a single simple distillation region where a stable ternary node is connected to a binary saddle azeotrope with a stable separatrix. There is only one unstable node (L) in the composition space. However, when the pot orbit hits the stable separatrix, it will be constrained to stay on this boundary. Three batch distillation regions can therefore be constructed, as indicated in Figure 2-12b. Feed compositions in region B_1 will give rise to $\mathbf{P}_1 = \{$L,I,I-H$\}$, B_2 will give rise to $\mathbf{P}_2 = \{$L,I-H,L-I-H$\}$, and B_3 will give rise to $\mathbf{P}_3 = \{$L,H,I-H$\}$. This behavior is, in fact, completely ignored by other workers, for example Bernot *et al.* (1991) and Safrit and Westerberg (1996).

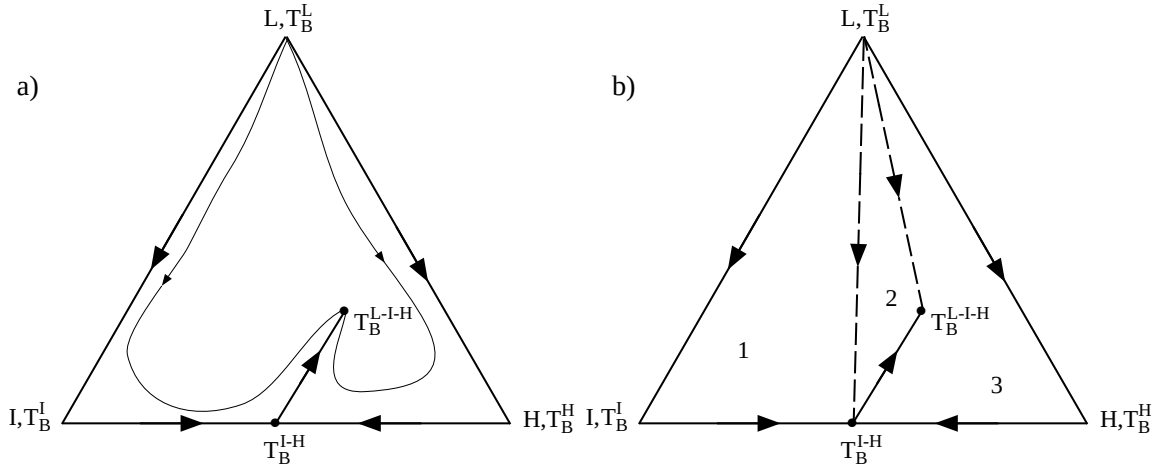

Figure 2-12: Ternary residue curve map where stable separatrix does not divide the composition space. The order of boiling temperatures: $T_B^{L,m} < T_B^{I,n} < T_B^{H,n} < T_B^{L-I,n} < T_B^{L-I-H,q}$.

It is now evident that all stable separatrices will constrain the movement of the pot orbit. Residue curves are approaching from either side. Hence, the pot orbit is restricted to move ever closer to the stable separatrix, and finally, to follow the same path as the separatrix. Here, we present the less obvious result that certain unstable separatrices also play the role of impassable boundaries. Figure 2-13a shows a topo-

logically consistent residue curve map containing a saddle ternary connected to three binary azeotropes and pure component H by separatrices. Only stable separatrices are shown. Two of the binaries are unstable nodes (L-I and I-H), while the third binary is a saddle point (L-I). The stable separatrix connecting L-I-H and H does not divide the composition space, but there are two unstable nodes (I-H and L-H) present indicating that two subdomains exist. In this case the previous rules will lead to intersecting batch distillation boundaries (see Figure 2-13b), and no guidelines are provided by previous work to deal with this situation. There is actually a boundary constraining the movement of the pot composition path between the ternary azeotrope and the binary azeotrope L-I, as illustrated in Figure 2-14. Initial composition $\mathbf{x}^{p,0}$ will produce the binary azeotrope L-H as the first product cut, while the pot composition is moving towards the unstable separatrix connecting the ternary azeotrope L-I-H and the binary azeotrope L-I. When $\mathbf{x}^p(\xi)$ hits the unstable separatrix, there is apparently nothing preventing it from crossing the separatrix. However, at that point it will switch to a different family of residue curves where the corresponding unstable node is the binary azeotrope I-H. Hence, the composition path will turn and move in a straight line away from I-H, and as $\mathbf{x}^p(\xi)$ tries to cross the unstable separatrix in the opposite direction it will again be forced back to the separatrix, this time by L-H. The two opposing unstable nodes L-H and I-H will in fact constrain the pot composition to stay on the unstable separatrix. If the unstable separatrix is highly curved, a similar behavior to the one encountered for stable separatrices in the acetone, chloroform, and methanol system will be observed. Following the analogy with stable separatrices this type of unstable separatrix can be defined as a residue curve where the residue curves on each side *at least locally* are moving towards the same fixed point.

Note that most unstable separatrices will not behave in this manner. The type of unstable separatrix shown in Figure 2-14 is a consequence of the presence of three stable nodes, and was only found in 6 of the 113 possible ternary residue maps presented by Matsuyama and Nishimura (1977). For example, an unstable separatrix that is connected to an unstable node (e.g. the unstable separatrix between L-H and

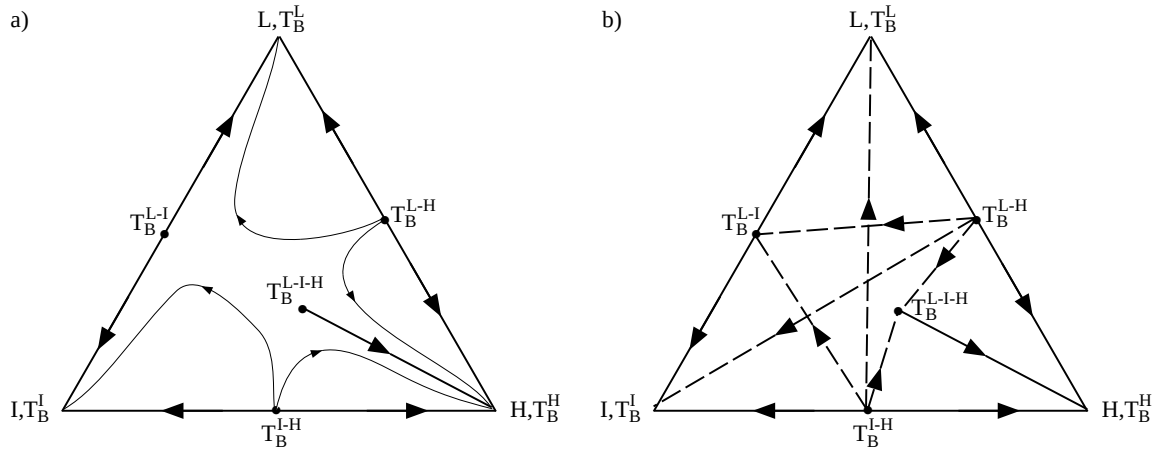

Figure 2-13: Ternary residue curve map where stable separatrix does not divide the composition space, but which has two unstable nodes. The order of boiling temperatures: $T_B^{L-H,m} < T_B^{I-H,m} < T_B^{L-I-H,n} < T_B^{L-I,n} < T_B^{L,q} < T_B^{I,q} < T_B^{H,q}$.

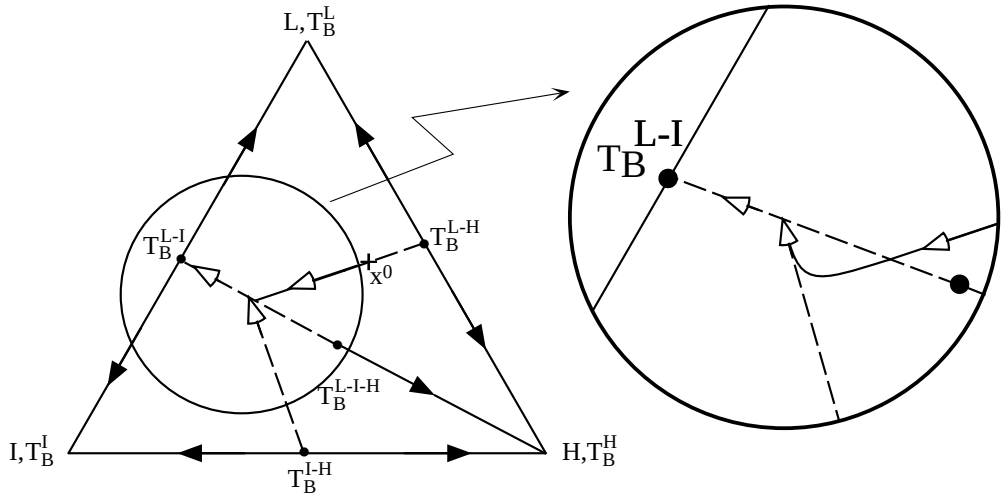

Figure 2-14: Ternary residue curve map with unstable separatrix constraining the movement of the pot composition.

L-I-H in Figure 2-14) will not constrain the movement of the residue path. On the other hand, the path will not cross it either, but that is due to the fact that the path under the limiting assumptions above is composed of segments of straight lines. Therefore, we cannot achieve distillate compositions on the other side. Consequently, a new term may be introduced:

Definition 2-2 *A pot composition barrier is a barrier that will constrain the movement of the pot composition during the course of batch distillation. When the pot*

composition orbit intersects a pot composition barrier, it is restricted to stay relatively close to that barrier.

The geometric and algebraic definitions will be introduced later. At the moment we are only interested in knowing that such a barrier might be present.

Obviously, if the pot orbit hits one of the edges or vertices of the ternary composition simplex, it will be constrained to stay on this edge or vertex, as one or more of the species are exhausted, and, following the definition of a separatrix, any segment of an edge connecting two fixed points is also a separatrix. However, as with separatrices internal to the composition space, not all the edges may be pot composition barriers. For example, in the ideal system shown in Figure 2-7 the binary edge between the pure components I and H will constrain the pot orbit during the first product cut (when L is boiled off). During the second product cut (when I is boiled off) the pot orbit is constrained by the vertex H. But, the edge [L,I] is not a pot composition barrier.

To summarize, we argue that the following types of pot composition barriers of dimension 1 are observed in ternary systems:

- Stable separatrices
- Certain unstable separatrices
- Some of the edges

In ternary residue curve maps all pot composition barriers will be composed of straight lines except the ones resulting from curved separatrices. Accounting for the curvature of the separatrices will require integration of Equations (2.1). Although a separatrix will almost always have some curvature (Reinders and Minjer, 1940), for many systems assuming that the separatrices are straight will suffice. The consequence and desired outcome of this assumption is that the composition path $\mathbf{x}^p(\xi)$ will be composed of segments of straight lines. Therefore, all distillation cuts will have compositions equal to fixed points, and no other distillation cuts may be achieved.

In Chapter 3 we will develop the extension of this assumption to multicomponent systems.

2.7 Summary

In this chapter it has been demonstrated that earlier work on ternary residue curve maps for batch distillation is not complete. For example, several topologically consistent residue curve maps exist that cannot be dealt with using previous work. In order to explain and address these shortcomings the concept of *pot composition barriers* in the composition space is introduced and defined. The following types of pot composition barriers of dimension 1 are observed in ternary systems: stable separatrices, certain unstable separatrices, and some of the edges.

It should be noted that many of the exceptions or special cases described throughout this chapter, and in Chapters 3, 4, and 5 involve multiple high boiling azeotropes, which physically is unlikely. However, if we are to analyze other column configurations than a rectifier, e.g., a stripper, these topologies are more likely to occur (see, for example, Appendix A).

Chapter 3

Multicomponent Batch Distillation

The theory for multicomponent batch distillation is derived for a homogeneous system based on the limiting assumptions of very high reflux ratio and large number of trays. First pot composition barriers and batch distillation regions in multicomponent systems will be discussed, and then the theory governing prediction of the number of product cuts and their sequence will be introduced. The exceptions for ternary systems discussed in Chapter 2 are used throughout to motivate derivation of the theory. The results will allow complete characterization of the structure of the composition space for a multicomponent system when using batch distillation based only on the information of the compositions, boiling temperatures, and stability of the fixed points. A rectifier configuration is assumed, but it should be noted that the same arguments will apply to a stripper configuration. Appendix A demonstrates how the approach can be extended to such a column configuration. The derived properties are demonstrated in a four-component example.

3.1 Simple Distillation

First, we examine multicomponent simple distillation described by Equations (2.1). The concept of separatrices as distillation boundaries is only useful in ternary systems. A separatrix is an orbit and will form an infinitely thin barrier in higher dimensions. In order to extend the notion of distillation boundaries for ternary systems to systems

with an arbitrary number of components it is advantageous to introduce the concept of *global unstable and stable manifolds* of a fixed point $\mathbf{x}^*$, $W^u(\mathbf{x}^*)$ and $W^s(\mathbf{x}^*)$, respectively (Hale and Koçak, 1991):

$$W^u(\mathbf{x}^*) \equiv \{\hat{\mathbf{x}} \in \mathbf{R}^{nc} : \varphi(\xi, \hat{\mathbf{x}}) \to \mathbf{x}^* \text{ as } \xi \to -\infty\} \tag{3.1}$$

$$W^s(\mathbf{x}^*) \equiv \{\hat{\mathbf{x}} \in \mathbf{R}^{nc} : \varphi(\xi, \hat{\mathbf{x}}) \to \mathbf{x}^* \text{ as } \xi \to +\infty\} \tag{3.2}$$

where $\varphi(\xi, \hat{\mathbf{x}})$, defined by Equations (2.1), refers to the simple distillation trajectory through the composition point $\hat{\mathbf{x}}$. $W^u(\mathbf{x}^*)$ can also be defined as all compositions that have $\mathbf{x}^*$ as their α-limit set, and similarly, $W^s(\mathbf{x}^*)$ as all compositions that have $\mathbf{x}^*$ as their ω-limit set. The trajectory $\varphi(\xi, \mathbf{x}^*)$ is $\mathbf{x}^*$ itself, and $\mathbf{x}^*$ therefore belongs to both $W^u(\mathbf{x}^*)$ and $W^s(\mathbf{x}^*)$. For convenience a fixed point is allocated to its unstable manifold, and the notation $\overline{W}^w(\mathbf{x}^*)\ \forall w \in \{u, s\}$ will in the following refer to $W^u(\mathbf{x}^*)$ and $W^s(\mathbf{x}^*) \setminus \{\mathbf{x}^*\}$ projected onto the plane $\xi = 0$. For consistency, $\alpha(\mathbf{x}^*) \equiv \{\mathbf{x}^*\}$, and $\omega(\mathbf{x}^*) \equiv \emptyset$.

If $\mathbf{x}^*$ is an unstable node[‖] $\{\mathbf{x}^*\} \subset \overline{W}^u(\mathbf{x}^*) \subset Q$, while $\overline{W}^s(\mathbf{x}^*) = \emptyset$, where Q defines the whole composition simplex. If $\mathbf{x}^*$ is a stable node $\overline{W}^u(\mathbf{x}^*) = \{\mathbf{x}^*\}$, and $\emptyset \subset \overline{W}^s(\mathbf{x}^*) \subset Q$. If $\mathbf{x}^*$ is a saddle point $\{\mathbf{x}^*\} \subset \overline{W}^u(\mathbf{x}^*) \subset Q$ and $\emptyset \subset \overline{W}^s(\mathbf{x}^*) \subset Q$. From the definition above it follows that $\overline{W}^u(\mathbf{x}^*) \cap \overline{W}^s(\mathbf{x}^*)$ does not contain the fixed point itself. Furthermore, the absence of homoclinic orbits[**] (Doherty and Perkins, 1978a) (except the fixed points themselves) indicates that $\overline{W}^u(\mathbf{x}^*) \cap \overline{W}^s(\mathbf{x}^*) = \emptyset$. In addition, because orbits do not intersect $\overline{W}^w(\mathbf{x}_a^*) \cap \overline{W}^w(\mathbf{x}_b^*) = \emptyset\ \forall w \in \{u, s\}$ unless $\mathbf{x}_a^*$ and $\mathbf{x}_b^*$ are the same fixed point. The composition space Q can therefore be expressed as the following union of disjoint sets:

$$Q = \bigcup_{e=1}^{ep} \overline{W}^u(\mathbf{x}_e^*) = \bigcup_{m=1}^{un} \overline{W}^u(\mathbf{x}_m^*) \cup \bigcup_{n=1}^{s} \overline{W}^u(\mathbf{x}_n^*) \cup \bigcup_{q=1}^{sn} \overline{W}^u(\mathbf{x}_q^*) \tag{3.3}$$

where $\mathbf{x}_m^*$, $\mathbf{x}_q^*$, and $\mathbf{x}_n^*$ refer to unstable, and stable nodes, and saddle points, respectively, ep is the number of fixed points in the system, and un, s, and sn are the

number of unstable nodes, saddle points, and stable nodes in the system.

Definition 3-3 *$\overline{\omega}^u(\mathbf{x}^*)$ is the set of fixed points that are also limit points[††] of $\overline{W}^u(\mathbf{x}^*)$ excluding $\mathbf{x}^*$. Likewise, $\overline{\omega}^s(\mathbf{x}^*)$ is the set of fixed points that are also limit points of $\overline{W}^s(\mathbf{x}^*)$ excluding $\mathbf{x}^*$. $\overline{\omega}^u(\mathbf{x}^*)$ and $\overline{\omega}^s(\mathbf{x}^*)$ are termed the unstable and stable boundary limit sets of $\mathbf{x}^*$, respectively.*

Alternatively, the boundary limit sets can be defined as:

$$\overline{\omega}^u(\mathbf{x}^*) \equiv \bigcup_{\hat{\mathbf{x}} \in \overline{W}^u(\mathbf{x}^*)} \omega(\hat{\mathbf{x}}) \cup \{\mathbf{x}^*_{n'}\} \tag{3.4}$$

$$\overline{\omega}^s(\mathbf{x}^*) \equiv \bigcup_{\hat{\mathbf{x}} \in \overline{W}^s(\mathbf{x}^*)} \alpha(\hat{\mathbf{x}}) \cup \{\mathbf{x}^*_{n''}\} \tag{3.5}$$

where $\{\mathbf{x}^*_{n'}\}$ represents the set of saddle points that are passed infinitesimally close but not entered by any of the orbits in $\overline{W}^u(\mathbf{x}^*)$, and $\{\mathbf{x}^*_{n''}\}$ represents the set of saddle points that are passed infinitesimally close but not entered by any of the orbits in $\overline{W}^s(\mathbf{x}^*)$. As defined, $\overline{\omega}^w(\mathbf{x}^*) \not\subset \overline{W}^w(\mathbf{x}^*)\ \forall w \in \{u, s\}$. It is evident that $\overline{\omega}^u(\mathbf{x}^*)$ does not contain unstable nodes. Similarly, $\overline{\omega}^s(\mathbf{x}^*)$ does not contain stable nodes. The term *boundary limit set* of $\mathbf{x}^*$ refers to $\overline{\omega}(\mathbf{x}^*) = \overline{\omega}^u(\mathbf{x}^*) \cup \overline{\omega}^s(\mathbf{x}^*) \cup \{\mathbf{x}^*\}$.

The closure of $\overline{W}^u(\mathbf{x}^*)$, denoted by $\overline{\overline{W}^u}(\mathbf{x}^*)$, can be expressed as:

$$\overline{\overline{W}^u}(\mathbf{x}^*) = \overline{W}^u(\mathbf{x}^*) \cup \{\hat{\mathbf{x}} \in \mathbf{R}^{nc} : \gamma(\xi, \hat{\mathbf{x}}) \to \mathbf{x}^*_j \in \overline{\omega}^u(\mathbf{x}^*) \text{ as } \xi \to \pm\infty\} \tag{3.6}$$

where $\gamma(\xi, \hat{\mathbf{x}})$ represents the residue curve through $\hat{\mathbf{x}}$. For example, this can be illustrated by Figure 2-10b. There $\overline{W}^u(L)$ includes the whole composition simplex except the binary compositions between I and H and between H and L-H, and $\overline{\omega}^u(\text{L}) = \{\text{I,H,L-H}\}$. Therefore, $\overline{\overline{W}^u}(\text{L}) = \overline{W}^u(\text{L}) \cup \{\hat{\mathbf{x}} \in \mathbf{R}^3 : \gamma(\xi, \hat{\mathbf{x}}) \to \mathbf{x}^*_j \in \{\text{I,H,L-H}\} \text{ as } \xi \to \pm\infty\} = Q$, the whole composition simplex.

[‖]The definitions are based on systems with at least two components, as there makes little sense to define the nature of the fixed point of a pure component system. $\subset$ denotes a proper subset.

[**]A homoclinic orbit is an orbit which will approach the same fixed point for $\xi \to -\infty$ and $\xi \to +\infty$ (Hale and Koçak, 1991).

[††]A point p is a limit point of the set E if every neighborhood of p contains a point $q \neq p$ such that $q \in E$.

The closure of $\overline{W}^s(\mathbf{x}^*)$, $\overline{\overline{W}^s}(\mathbf{x}^*)$, can be expressed in a similar manner.

3.2 Pot Composition Barriers and Batch Distillation Regions

We now consider multicomponent batch rectification described by Equations (2.2).

Theorem 3-1 *Distillation cut 1 starting with pot composition* $\mathbf{x}^{p,0} \in \overline{W}^u(\mathbf{x}_m^*)$, *where* $\mathbf{x}_m^*$ *is an unstable node, will at limiting conditions of very high reflux ratio and large number of trays have a distillate composition* $\mathbf{x}^{d,1}$ *close to* $\mathbf{x}_m^*$ *as long as pot composition* $\mathbf{x}^p(\xi) \in \overline{W}^u(\mathbf{x}_m^*)$.

Proof. At very high reflux $\mathbf{x}^p(\xi^{'})$ and $\mathbf{x}^d(\xi^{'})$ are located on the same simple residue curve, where $\mathbf{x}^p(\xi^{'})$ and $\mathbf{x}^d(\xi^{'})$ refers to the instantaneous reboiler composition and distillate composition, respectively. Thus, $\mathbf{x}^d(\xi^{'}) \in \overline{W}^u(\mathbf{x}_m^*)$. The assumption of large number of trays ensures that $\mathbf{x}^d(\xi^{'})$ stays constant at the α-limit set of $\mathbf{x}^p(\xi^{'})$, i.e., $\mathbf{x}_m^*$. □

Corollary 3-1 *Equations (2.2) state that* $\mathbf{x}^d(\xi^{'})$ *lies on the tangent to the pot composition path* $\mathbf{x}^p(\xi)$ *through* $\mathbf{x}^p(\xi^{'})$. *Hence, since* $\mathbf{x}^d(\xi^{'}) = \mathbf{x}_m^*$, $\mathbf{x}^p(\xi)$ *will move in a straight line away from* $\mathbf{x}_m^*$. *This can also be confirmed by an overall material balance.*

Theorem 3-1 is a more formal statement of the results discussed in Van Dongen and Doherty (1985b).

At the limit, $\mathbf{x}^p(\xi)$ will intersect PCB($\mathbf{x}_m^*$), the pot composition barrier for any pot composition orbit with initial condition $\mathbf{x}^{p,0} \in \overline{W}^u(\mathbf{x}_m^*)$. The intersection, $\mathbf{x}^{p,1}$, has to be a limit point of $\overline{W}^u(\mathbf{x}_m^*)$. However, $\mathbf{x}^{p,1} \notin \overline{W}^u(\mathbf{x}_m^*)$. It therefore follows from Equation (3.6) that the pot composition barrier can be defined as:

$$\begin{aligned} \mathrm{PCB}(\mathbf{x}_m^*) &= \overline{\overline{W}^u}(\mathbf{x}_m^*) \setminus \overline{W}^u(\mathbf{x}_m^*) \\ &= \{\hat{\mathbf{x}} \in \mathbf{R}^{nc} : \gamma(\xi, \hat{\mathbf{x}}) \to \mathbf{x}_j^* \in \overline{\omega}^u(\mathbf{x}_m^*) \text{ as } \xi \to \pm\infty\} \end{aligned} \tag{3.7}$$

$\mathbf{x}^{p,1} \in \overline{W}^u(\mathbf{x}_j^*)$ for some $\mathbf{x}_j^* \in \overline{\omega}^u(\mathbf{x}_m^*)$, will be the starting point of distillation cut 2. The relationship between the instantaneous distillate composition $\mathbf{x}^d(\xi^{'})$ and the instantaneous pot composition $\mathbf{x}^p(\xi^{'})$ is still governed by Equations (2.2). However, if $\overline{W}^u(\mathbf{x}_j^*)$ is curved, the tangent to $\mathbf{x}^p(\xi)$ at $\mathbf{x}^p(\xi^{'})$ may not lie within $\overline{W}^u(\mathbf{x}_j^*)$, and hence $\mathbf{x}^d(\xi^{'})$ may not equal $\mathbf{x}_j^*$. Moreover, as $\mathbf{x}^p(\xi)$ is forced to move relatively close to this curved surface (see Definition 2-2), the slope of the tangent will vary, and hence the distillate composition $\mathbf{x}^d(\xi^{'})$ will not stay constant. However, if we could ensure that $\mathbf{x}^p(\xi)$ will always move in a straight line during a certain distillation cut, Theorem 3-1 could be generalized to apply for all subsequent distillation cuts. Assuming that $\overline{W}^u(\mathbf{x}_e^*)\ \ \forall e = 1, \ldots, ep$ are linear would lead to the desired outcome. As will be demonstrated, this is too restrictive, and may introduce large inaccuracy in the analysis. For example, consider the ternary system in Figure 3-1a. The unstable manifolds of L and I-H are inherently linear as they have dimension $nc - 1 = 2$. Likewise, $\overline{W}^u$(I), $\overline{W}^u$(L-I), and $\overline{W}^u$(H) are linear because they are located on the binary edges. However, $\overline{W}^u$(L-I-H) is not linear as it is composed of the two line segments connecting the ternary saddle point L-I-H to L-I and H including L-I-H, but excluding L-I and H. The dashed lines in Figure 3-1b labeled a and b show two possible linearizations of $\overline{W}^u$(L-I-H). Both of them will require a shift in the position of a fixed point (either L-I (a) or L-I-H (b)). A closer look at Figure 3-1a reveals that the composition space can be divided into five batch distillation regions, as indicated by the dashed lines. The composition paths in regions 2, 3, 4, and 5 will all approach and intersect $\overline{W}^u$(L-I-H). The composition paths starting in regions 2 and 4 will intersect to the left of L-I-H and then turn and move towards L-I, and the composition paths starting in regions 3 and 5 will intersect to the right of L-I-H and then turn and move towards H. Hence, both linearizations a and b will serve to satisfy the requirement that $\mathbf{x}^p(\xi)$ should move in a straight line during a certain distillation cut. In this case, while L-I-H is boiling off. However, non-linearity in the line segment between L-I-H and L-I will not effect the path of the orbit with initial composition in regions 3 and 5, in the same way as non-linearity in the line segment between L-I-H and H will not effect the orbit with initial composition in regions 2 and

4. A third linearization of $\overline{W}^u$(L-I-H) may therefore be considered where the two line segments between L-I-H and L-I, and L-I-H and H are linearized separately (labeled c in Figure 3-1b).

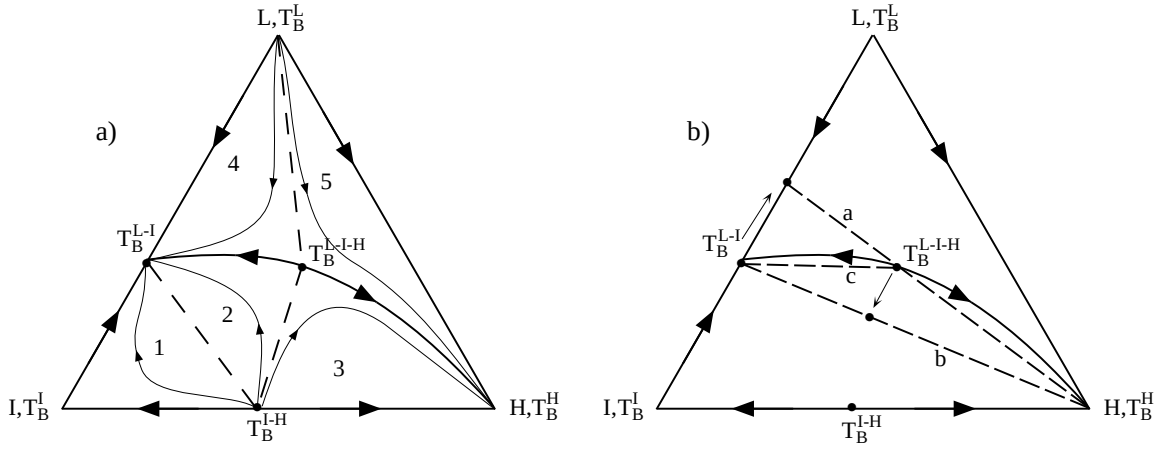

Figure 3-1: Linearization of $\overline{W}^u(\mathbf{x}^*)$ to ensure that the pot composition will move in a straight line during a certain distillation cut.

In conclusion, it has been found that PCB($\mathbf{x}_j^*$) can be divided into one or more domains, termed *pot composition boundaries*:

Definition 3-4 *A pot composition boundary is the set of compositions that lead to the same sequence of product cuts* $\hat{\mathbf{P}} = \{\mathbf{p}_{k+1}, \mathbf{p}_{k+2}, \ldots\}$ *upon distillation under the limiting conditions of very high reflux ratio and large number of trays. The pot composition boundaries are subsets of the respective unstable manifolds of PCB*($\mathbf{p}_k$) *where* $\mathbf{p}_k$ *represents the composition of cut* k.

We can now proceed to generalize Theorem 3-1:

Theorem 3-2 *Distillation cut* k *starting with pot composition* $\mathbf{x}^{p,k-1} \in \overline{W}^u(\mathbf{x}_j^*)$ *will at limiting conditions of very high reflux and large number of trays, and with linear pot composition boundaries have a distillate composition* $\mathbf{x}^{d,k}$ *close to* $\mathbf{x}_j^*$ *as long as pot composition* $\mathbf{x}^p(\xi) \in \overline{W}^u(\mathbf{x}_j^*)$.

Proof. At very high reflux $\mathbf{x}^p(\xi')$ and $\mathbf{x}^d(\xi')$ are located on the same residue curve. Thus, $\mathbf{x}^d(\xi') \in \overline{W}^u(\mathbf{x}_j^*)$. Furthermore, $\mathbf{x}^d(\xi')$ lies on the tangent to $\mathbf{x}^p(\xi)$ through

$\mathbf{x}^p(\xi^{'})$. The assumption of linear pot composition boundaries ensures that the tangent lies within $\overline{W}^u(\mathbf{x}_j^*)$. Combined with the assumption of large number of trays this ensures that $\mathbf{x}^d(\xi^{'})$ stays constant at the α-limit set of $\mathbf{x}^p(\xi^{'})$, i.e., $\mathbf{x}_j^*$. $\square$

Of course, if $\mathbf{x}^{p,k-1} = \mathbf{x}_j^*$ then $\mathbf{x}^p(\xi) = \mathbf{x}^{d,k} = \mathbf{x}_j^*$ as $\xi \to +\infty$.

Corollary 3-2 *If batch distillation region $B(\mathbf{P})$ gives rise to the product sequence $\mathbf{P} = \{\mathbf{p}_0, \mathbf{p}_1, \ldots\}$, then at limiting conditions $B(\mathbf{P})$ is the set of composition points $\hat{\mathbf{x}} \in \overline{W}^u(\mathbf{p}_0)$ such that the resulting pot composition path $\mathbf{x}^p(\xi)$ will intersect $\overline{W}^u(\mathbf{p}_k)$ $\forall \mathbf{p}_k \in \mathbf{P}$ as $\xi \to +\infty$. Composition points that give rise to a subset of $\mathbf{P}$ form the batch distillation boundaries of $B(\mathbf{P})$.*

Corollary 3-3 *The pot composition boundary for product cut k is at limiting conditions the set of composition points $\hat{\mathbf{x}} \in PCB(\mathbf{p}_k)$ such that the subsequent pot composition path will intersect $\overline{W}^u(\mathbf{p}_l)$ $\forall \mathbf{p}_l \in \hat{\mathbf{P}} = \{\mathbf{p}_{k+1}, \mathbf{p}_{k+2}, \ldots, \} \subset P$ as $\xi \to +\infty$, where $\mathbf{P}$ is the product sequence for a particular batch distillation region. Thus, assuming linear pot composition boundaries is equivalent to assuming that the boundaries of a batch distillation region are linear.*

Figure 3-2 illustrates what would happen if the pot composition boundary was curved. The initial reboiler composition $\mathbf{x}^{p,0} \in \overline{W}^u(\mathrm{L})$, and the first distillate composition therefore will be equal to L according to Theorem 3-1. The pot composition barrier for $\mathbf{x}^{p,0}$ while in $\overline{W}^u(\mathrm{L})$, PCB(L), is equal to the separatrix connecting L-I and H including the endpoints, and in this case the pot composition boundary coincides with PCB(L). At the end of the first cut $\mathbf{x}^p(\xi)$ will intersect $\overline{W}^u$(L-I), or so it appears. However, the conditions that $\mathbf{x}^p(\xi^{'})$ and $\mathbf{x}^d(\xi^{'})$ lie on the same residue curve, and $\mathbf{x}^d(\xi^{'})$ lies on the tangent to $\mathbf{x}^p(\xi)$ through $\mathbf{x}^p(\xi^{'})$ can only be satisfied if $\mathbf{x}^p(\xi)$ remains in $\overline{W}^u(\mathrm{L})$. The distillate will therefore take on compositions as indicated in Figure 3-2. $\mathbf{x}^p(\xi)$ may move ever closer to $\overline{W}^u$(L-I), but it will not intersect it. On the other hand, if $\mathbf{x}^{p,0} \in \overline{W}^u(\mathrm{I})$, $\mathbf{x}^p(\xi)$ will necessarily have to intersect and cross $\overline{W}^u$(L-I) in order to satisfy the same conditions. Note that this does not result in crossing trajectories because $\mathbf{x}^p(\xi)$ is governed by Equations (2.2), while $\overline{W}^u$(L-I) is governed by Equations (2.1). At that point $\mathbf{x}^p(\xi)$ will follow the same path as the

orbits starting on the convex side. As the temperature in the reboiler must increase monotonically, $\mathbf{x}^p(\xi)$ must remain relatively close to $\overline{W}^u$(L-I) in both cases. This behavior has been observed and discussed by several other authors (Ewell and Welch, 1945; Van Dongen and Doherty, 1985b; Bernot *et al.*, 1990).

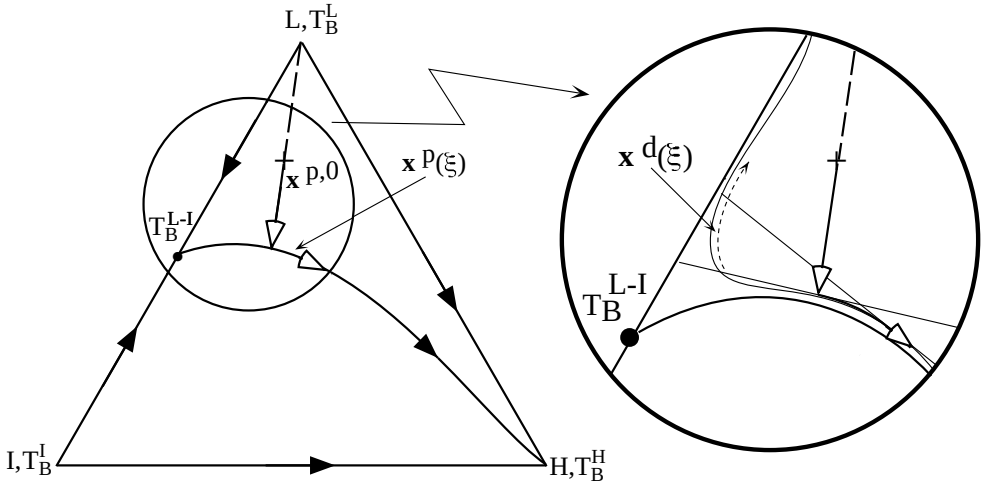

Figure 3-2: Ternary system with curved pot composition boundary.

3.3 The Product Sequence

As stated in Definition 2-1, any composition taken interior to a specific batch distillation region will always result in the same sequence of product cuts. It is demonstrated here that, subject to the assumptions at the beginning of this chapter, the number of cuts can be predicted *a priori*.

Theorem 3-3 *At very high reflux, large number of trays, and with linear pot composition boundaries, an nc component mixture located interior to a batch distillation region will produce exactly nc product cuts.*

Proof. By definition, initial composition $\mathbf{x}^{p,0}$ interior to B($\mathbf{P}$) will always result in the same sequence of cuts $\mathbf{P} = \{\mathbf{p}_0, \mathbf{p}_1, \mathbf{p}_2, \ldots\}$. Following Theorem 3-1 the pot composition path $\mathbf{x}^p(\xi)$ will move in $\overline{W}^u(\mathbf{p}_0)$ until it intersects $\overline{W}^u(\mathbf{p}_1) \subseteq \mathrm{PCB}(\mathbf{p}_0)$, then it will continue in $\overline{W}^u(\mathbf{p}_1)$ until it intersects $\overline{W}^u(\mathbf{p}_2) \subseteq \mathrm{PCB}(\mathbf{p}_1) \subseteq \mathrm{PCB}(\mathbf{p}_0)$, etc.

Initially, $\mathbf{x}^p(\xi)$ is free to move in the hyperplane defined by $\sum_{i=1}^{nc} x_i = 1$. However, the number of degrees of freedom is reduced by one each time a pot composition barrier is encountered, until $\mathbf{x}^p(\xi)$ moves in a fixed point in the composition space. Thus, this point (azeotrope or pure component) is the final value of the pot composition. Hence, the number of product cuts including the final composition left in the pot is equal to the number of pure components in the initial mixture. We can conclude from this exercise that the distillate path consists of exactly nc vertices. □

Corollary 3-4 *Following Corollary 3-2, an nc component mixture located on the boundary of a batch distillation region will at very high reflux, large number of trays, and with linear pot composition boundaries produce at most* $nc - 1$ *product cuts.*

The nc product cuts form a string of nc fixed points where each consecutive fixed point has a higher boiling temperature then the previous fixed point. The first fixed point is always an unstable node ($\mathbf{p}_0$), the intermediate fixed points are saddle points, and the last fixed point will be either a saddle point or a stable node. The distillate curve for the separation is the set of these points.

Definition 3-5 *(Hocking and Young, 1961) Let* $A = \{a_0, a_1, \ldots, a_k\}$ *be a set of* $k+1$ *pointwise independent points in* $\mathbf{R}^{nc}$*. The geometric k-simplex in* $\mathbf{R}^{nc}$ *determined by A is the set of all points of the hyperplane* H^k *containing A for which the barycentric coordinates with respect to A are all nonnegative. The barycentric coordinates of a vector* $\mathbf{h}$ *with respect to A are the real numbers* $f_0, f_1, \ldots, f_k$ *if and only if (i)* $\mathbf{h} = \sum_{i=0}^{k} f_i \mathbf{a}_i$ *and (ii)* $\sum_{i=0}^{k} f_i = 1$*.* $\mathbf{a}_i$ *is the vector from the origin to the point* a_i*.*

Theorem 3-4 *The nc vertices representing product cuts bound an* $(nc-1)$*-simplex.*

Proof. The composition simplex for an nc component system is an $(nc-1)$-simplex defined by the nc pure component fixed points on the hyperplane H^{nc-1} described by $\sum_{i=1}^{nc} x_i = 1$. Any composition $\mathbf{x}^{p,0}$ located in batch distillation region B($\mathbf{P}$) will produce the set of product cuts $\mathbf{P}$= $\{\mathbf{p}_0, \ldots, \mathbf{p}_{nc-1}\}$. The vertices are necessarily pointwise independent, as the dimensionality is reduced by one every time a new pot

composition boundary is encountered and a new product cut is produced (a set of vertices would be pointwise dependent if and only if the dimensionality remained the same even after a vertex has been exhausted.) A vector $\mathbf{h}$ through any composition $\hat{\mathbf{x}}$ lying in the interior of $\mathbf{P}$ will have positive barycentric coordinates that sum to unity as they would represent the fractions of a mixture with composition $\hat{\mathbf{x}}$ that would be recovered in each product cut. Hence, $\mathbf{P}$ bounds an $(nc-1)$-simplex, which we will term the *product simplex* $\mathbf{\Pi}^{nc}$. $\square$

It is evident that any point in B($\mathbf{P}$) must be a point in $\mathbf{\Pi}^{nc}$. However, the converse is not necessarily true. The residue curve map in Figure 3-3 has three batch distillation regions, and hence three product simplices. Product simplex $\mathbf{\Pi}_1^3$ is bounded by the pure components L, I, and maximum boiling binary azeotrope I-H, product simplex $\mathbf{\Pi}_2^3$ is bounded by L, I-H, and ternary azeotrope L-I-H, and product simplex $\mathbf{\Pi}_3^3$ is bounded by L, H, and I-H. $\mathbf{\Pi}_2^3$ and $\mathbf{\Pi}_3^3$ intersect, and hence a reboiler composition $\mathbf{x}^{p,0}$ interior to $\mathbf{\Pi}_2^3$ will in fact produce positive barycentric coordinates for both product sets. However, the correct product sequence is {L,I-H,L-I-H}. Therefore, $\mathbf{x}^{p,0}$ is truly located in batch distillation region B_2. On the other hand, a composition located in batch distillation region B_3 (bounded by the straight lines connecting L, I, I-H, and L-I-H) will only produce positive barycentric coordinates for this region. The product sequence will be {L,I,I-H}. Hence, region B_3 is an exception where the simplex bounded by the product compositions does not coincide with the batch distillation region itself. Therefore, a batch distillation region may not be a simplex. However, from the above properties, each batch distillation region can be characterized by a product simplex.

From the properties of simplices the result implies that any subset of the vertices of $\mathbf{P}$ is itself the set of vertices for a geometric simplex (Hocking and Young, 1961). Each such subsimplex is called a *face* of the product simplex. In particular, the subsets of $nc-1$ vertices are the highest order faces (facets). There exist $nc-1$ such facets. These will be termed *product simplex facets* and are $(nc-2)$-simplices. The product simplex facet defined by the points $\mathbf{p}_1, \mathbf{p}_2 \ldots, \mathbf{p}_{nc-1}$ will be termed *a product simplex boundary*. A product simplex boundary does not necessarily coincide with a

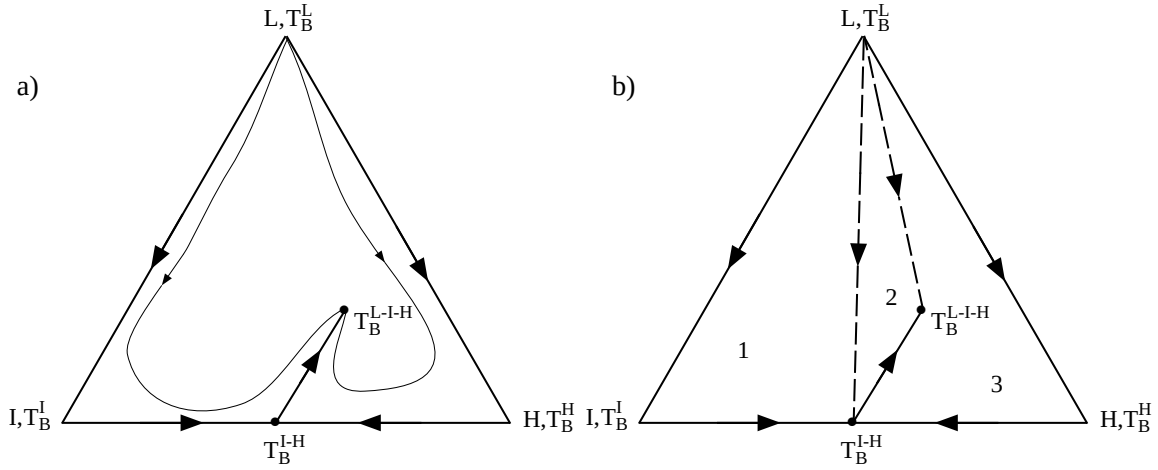

Figure 3-3: Intersecting product simplices. The order of boiling temperatures: $T_B^{L,m} < T_B^{I,n} < T_B^{H,n} < T_B^{L-I,n} < T_B^{L-I-H,q}$.

pot composition boundary, in the same way product simplices and batch distillation regions do not necessarily coincide. A product simplex boundary can be found by removing the unstable node from the set describing the product simplex. Conversely, a product simplex is an $(nc-1)$-simplex defined by a set of nc fixed points, where $nc-1$ points form a product simplex boundary and the remaining point is the unstable node in the set.

Theorem 3-5 *Let* $\mathbf{P}$ *represent the set of product cuts achievable, and* $\mathbf{p}_k$ *a product cut in* $\mathbf{P}$. *Then* $PCB(\mathbf{p}_k) \subset PCB(\mathbf{p}_l)\ \forall l = 0, \ldots, k-1$ *and* $\forall k = 1, \ldots, nc-2$.

Proof. Let $\mathbf{x}^p(\xi)$ represent the pot composition orbit and $\mathbf{x}^d(\xi)$ the corresponding distillate composition orbit related through the set of differential equations (2.2). Furthermore, let $\mathbf{x}^{p,k}$ be the pot composition at the beginning of product cut $\mathbf{p}_k$. $\mathbf{x}^{p,k}$, $\mathbf{x}^{p,k+1}$, etc., are points on $\mathbf{x}^p(\xi)$, while $\mathbf{p}_k$, $\mathbf{p}_{k+1}$, etc., are points on $\mathbf{x}^d(\xi)$. $\mathbf{x}^{p,k} \in \mathrm{PCB}(\mathbf{p}_{k-1})$, $\mathbf{x}^{p,k+1} \in \mathrm{PCB}(\mathbf{p}_k)$, etc. If the theorem is not true, this implies that initial condition $\mathbf{x}^{p,k+1}$ would result in a different distillate orbit than initial condition $\mathbf{x}^{p,k}$. However, since $\mathbf{x}^{p,k}$ and $\mathbf{x}^{p,k+1}$ lie on the same orbit, this is infeasible. Therefore $\mathbf{x}^{p,k+1}$ must also be in $\mathrm{PCB}(\mathbf{p}_{k-1})$. □

Corollary 3-5 *It follows from Theorem 3-5 that* $\mathbf{p}_k \in \overline{\omega}^u(\mathbf{p}_l)\ \forall l = 1, \ldots, k-1$.

3.4 Relaxing Limiting Assumptions

The theory for multicomponent homogeneous batch distillation is derived based on the assumptions of very high reflux ratio, large number of theoretical stages, and linear pot composition boundaries. If any of these limiting conditions are relaxed, a slight deviation from the predicted behavior may be observed:

Finite number of stages and reflux ratio: if the assumptions of large number of theoretical stages and very high reflux ratio are relaxed, the column profile will no longer follow a simple residue curve and the pot composition path will not move in a straight line, but take on some curvature. Bernot *et al.* (1991) demonstrate that the pot and distillate paths can move slightly into another batch distillation region, and one may get a small fraction of an additional product cut ($nc + 1$ cuts). Nevertheless, the pot and distillate paths will have the same basic shape as before. We have observed that the theory is still valid for columns with as little as 6-8 trays.

Curved pot composition boundaries: in the case of a highly curved pot composition boundary the pot composition path will move along the boundary, while the distillate path may move into another batch distillation region resulting in additional product cuts (Van Dongen and Doherty, 1985b; Bernot *et al.*, 1990).

Holdup on trays: Watson *et al.* (1995) study the distillation of quaternary component mixtures and claim that large holdup in the traysection and the condenser may result in separation sequences other than the ones predicted by the theory. However, large holdup in the column will only decrease the sharpness of splits. On the other hand, the theory only applies to homogeneous systems. Watson and his coworkers apply the theory to a heterogeneous mixture, which residue curve map is derived using a vapor-liquid-liquid equilibrium model. In their simulations, performed to confirm their predictions, however, they used a vapor-liquid equilibrium model. The results therefore, not so surprisingly, were not consistent with the predictions.

3.5 Example: Quaternary System

To demonstrate the applications of the results derived in this chapter, the quaternary system acetone (A), chloroform (C), ethanol (E), and benzene (B) has been characterized using the new concepts. The fixed points of this system at 1 atm. were found by Fidkowski *et al.* (1993) and are shown in Table 3.1. The system features four azeotropes, and its composition simplex is shown in Figure 3-4.

Table 3.1: Compositions, boiling temperatures, and stability of fixed points for the system acetone (A), chloroform (C), ethanol (E), and benzene (B) at 1 atm.

e	A	C	E	B	T_B[K]	Type
A	1	0	0	0	329.22	un
CE	0	0.8536	0.1464	0	333.08	un
C	0	1	0	0	334.94	s
ACE	0.3383	0.4642	0.1967	0	337.04	s
AC	0.3437	0.6563	0	0	338.62	s
EB	0	0	0.4514	0.5486	340.98	s
E	0	0	1	0	351.44	sn
B	0	0	0	1	353.25	sn

A and the binary azeotrope CE are both unstable nodes, and their unstable manifolds fill most of the composition space. $\overline{W}^u$(A) includes all the compositions above the shaded area in Figure 3-4a including the point A itself but excluding the shaded area and the fixed points located on it. Similarly, $\overline{W}^u$(CE) includes the compositions below the shaded area including CE, but excluding the shaded area and all the compositions not involving E, while $\overline{W}^s$(A) = $\overline{W}^s$(CE)= $\emptyset$. $\overline{W}^u$(C) includes all the compositions not involving E below the unstable separatrix connecting AC and B, while $\overline{W}^s$(C) includes the binary compositions between CE and C excluding CE and C. $\overline{W}^u$(AC) includes the compositions along the stable separatrix connecting AC and B excluding B, while $\overline{W}^s$(AC) includes all the compositions not involving B to the left of the unstable separatrices between A and ACE, and CE and ACE excluding the fixed points and the binary edge between CE and C. $\overline{W}^u$(ACE) includes all the compositions on the shaded area in Figure 3-4a excluding the edges between AC and

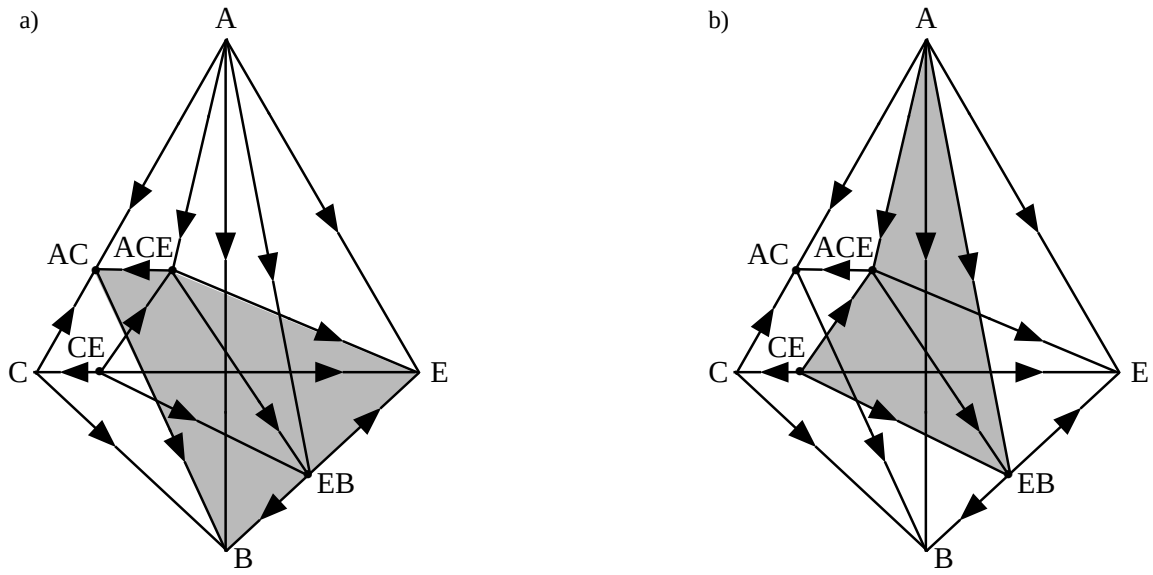

Figure 3-4: The composition simplex for acetone, chloroform, ethanol, and benzene. a) Shaded area separates $\overline{W}^u$(A) and $\overline{W}^u$(CE). b) Shaded area separates $\overline{W}^s$(E) and $\overline{W}^s$(B).

B, and E and B. $\overline{W}^s$(ACE) includes the compositions along the two unstable separatrices connecting the ternary azeotrope to A and CE excluding the fixed points. $\overline{W}^u$(EB) includes the entire binary edge between E and B excluding the pure components, while $\overline{W}^s$(EB) includes the entire shaded area in Figure 3-4b excluding the fixed points and the unstable separatrices between A and ACE, and CE and ACE. Finally, $\overline{W}^u$(E) = $\{E\}$, and $\overline{W}^u$(B) = $\{B\}$. $\overline{W}^s$(E) includes all the compositions to the right of the shaded area in Figure 3-4b excluding the fixed points, while $\overline{W}^s$(B) includes all the compositions to the left of the shaded area in Figure 3-4b excluding all compositions not involving B and the fixed points.

When the unstable and stable manifolds are established, we can determine the boundary limit sets from Definition 3-3. $\overline{\omega}^u$ and $\overline{\omega}^s$ are presented in Table 3.2.

We now proceed to determine the pot composition boundaries for the two unstable nodes. Application of Equation (3.7) leads to Equations (3.8) and (3.9). Hence PCB(A) is equal to the shaded area in Figure 3-4a including the fixed points, while PCB(CE) is equal to PCB(A) plus the compositions below the stable separatrix

Table 3.2: Unstable and stable boundary limit sets for the system acetone, chloroform, ethanol, and benzene.

e	$\overline{\omega}^u$	$\overline{\omega}^s$
A	ACE, AC, EB, E, B	$\emptyset$
CE	C, ACE, AC, EB, E, B	$\emptyset$
C	AC, B	CE
ACE	AC, EB, E, B	A, CE
AC	B	A, CE, C, ACE
EB	E, B	A, CE, ACE
E	E	A, CE, ACE, EB
B	B	A, CE, C, ACE, AC, EB

between AC and B in the ternary subsystem A, C, and B:

$$\text{PCB(A)} = Q \cap \bigcup_{\mathbf{x}_j^* \in \{ACE, AC, EB, E, B\}} \overline{W}^u(\mathbf{x}_j^*) \tag{3.8}$$

$$\text{PCB(CE)} = Q \cap \bigcup_{\mathbf{x}_j^* \in \{C, ACE, AC, EB, E, B\}} \overline{W}^u(\mathbf{x}_j^*) \tag{3.9}$$

PCB(A) can be divided into three pot composition boundaries, the 3-simplices described by the set of vertices {ACE,EB,E}, {ACE,EB,B}, and {ACE,AC,B}, as illustrated in Figure 3-5. Hence, an initial composition $\mathbf{x}^{p,0} \in \overline{W}^u$(A) may give rise to three different product sequences starting with A: $\mathbf{P}_1$ = {A,ACE,EB,E}, $\mathbf{P}_2$ = {A,ACE,EB,B}, and $\mathbf{P}_3$ = {A,ACE,AC,B} (see Figure 3-6). PCB(CE) can be divided into four pot composition boundaries, the same three 3-simplices as above plus the 3-simplex described by {C,AC,B}. Therefore, $\mathbf{x}^{p,0} \in \overline{W}^u$(CE) may give rise to four different product sequences starting with CE: $\mathbf{P}_4$ = {CE,ACE,EB,E}, $\mathbf{P}_5$ = {CE,ACE,EB,B}, $\mathbf{P}_6$ = {CE,ACE,AC,B}, and $\mathbf{P}_7$ = {CE,C,AC,B} (see Figures 3-7 and 3-8). Note that in this system the batch distillation regions coincide with their corresponding product simplices.

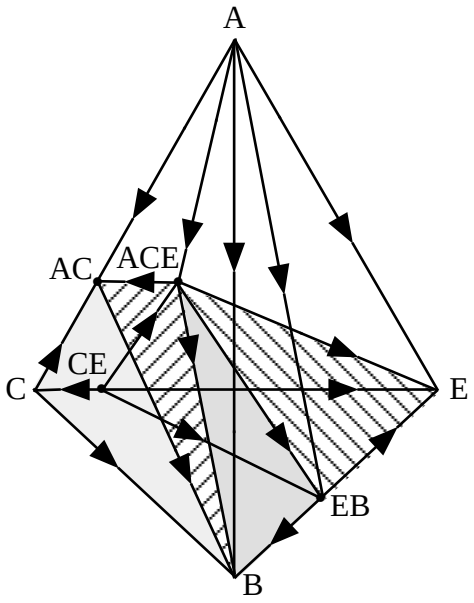

Figure 3-5: Pot composition boundaries.

3.6 Summary

In this chapter the theory of residue curves maps for analysis of batch distillation of homogeneous mixtures has been generalized to homogeneous systems with an arbitrary number of components. The following properties for simple distillation have been demonstrated:

- The whole composition simplex can be defined in terms of the respective disjoint unstable manifolds of the fixed points: $Q = \bigcup_{e=1}^{ep} \overline{W}^u(\mathbf{x}_e^*) = \bigcup_{m=1}^{un} \overline{W}^u(\mathbf{x}_m^*) \cup \bigcup_{n=1}^{s} \overline{W}^u(\mathbf{x}_n^*) \cup \bigcup_{q=1}^{sn} \overline{W}^u(\mathbf{x}_q^*)$.
- Each fixed point can be characterized by its *unstable* and *stable boundary limit sets*, $\overline{\omega}^u(\mathbf{x}^*)$ and $\overline{\omega}^s(\mathbf{x}^*)$, respectively.

Moreover, based on the limiting assumptions of very high reflux ratio, large number of trays, linear pot composition boundaries, and a rectifier configuration, properties of the batch distillation composition simplex have been introduced:

- The movement of the pot composition orbit will be constrained by *pot composition barriers* present in the composition simplex. If $\mathbf{x}^p(\xi) \in \overline{W}^u(\mathbf{x}^*)$, the unsta-

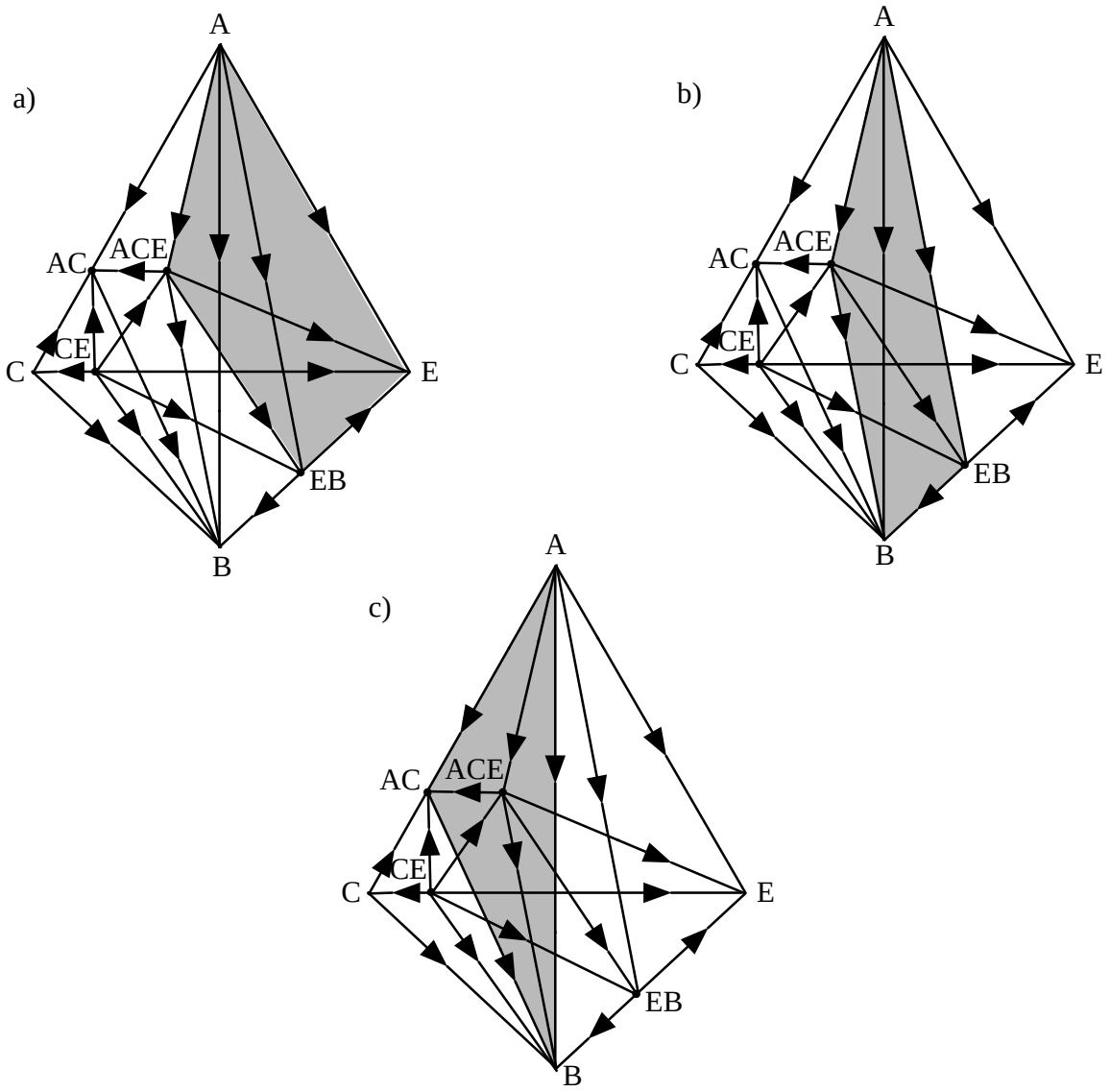

Figure 3-6: The composition simplex divided into batch distillation regions: a) $\mathrm{B}(\mathbf{P}_1) \rightarrow \mathbf{P}_1 = \{\mathrm{A,ACE,EB,E}\}$, b) $\mathrm{B}(\mathbf{P}_2) \rightarrow \mathbf{P}_2 = \{\mathrm{A,ACE,EB,B}\}$, and c) $\mathrm{B}(\mathbf{P}_3) \rightarrow \mathbf{P}_3 = \{\mathrm{A,ACE,AC,B}\}$.

ble manifold of fixed point $\mathbf{x}^*$, the constraining barrier is defined as $\mathrm{PCB}(\mathbf{x}^*) = \{\hat{\mathbf{x}} \in \mathbf{R}^{nc} : \gamma(\xi, \hat{\mathbf{x}}) \rightarrow \mathbf{x}_j^* \in \overline{\omega}(\mathbf{x}^*) \text{ as } \xi \rightarrow \pm\infty\}$. *Pot composition boundaries* are subsets of the pot composition barriers.

- If batch distillation region $\mathrm{B}(\mathbf{P})$ gives rise to the product sequence $\mathbf{P} = \{\mathbf{p}_0, \mathbf{p}_1, \mathbf{p}_2, \ldots\}$, than at limiting conditions $\mathrm{B}(\mathbf{P})$ is the set of composition points $\hat{\mathbf{x}} \in \overline{W}^u(\mathbf{p}_0)$ such that the resulting pot composition path $\mathbf{x}^p(\xi)$ will intersect the

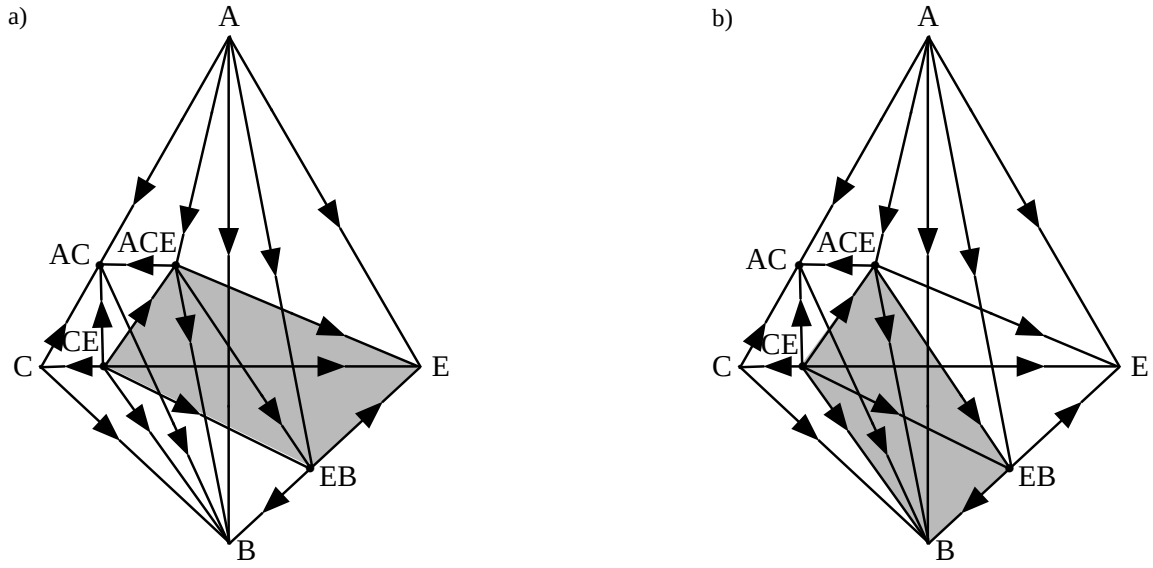

Figure 3-7: The composition simplex divided into batch distillation regions: a) $B(\mathbf{P}_4) \rightarrow \mathbf{P}_4 = \{CE,ACE,EB,E\}$, and b) $B(\mathbf{P}_5) \rightarrow \mathbf{P}_5 = \{CE,ACE,EB,B\}$.

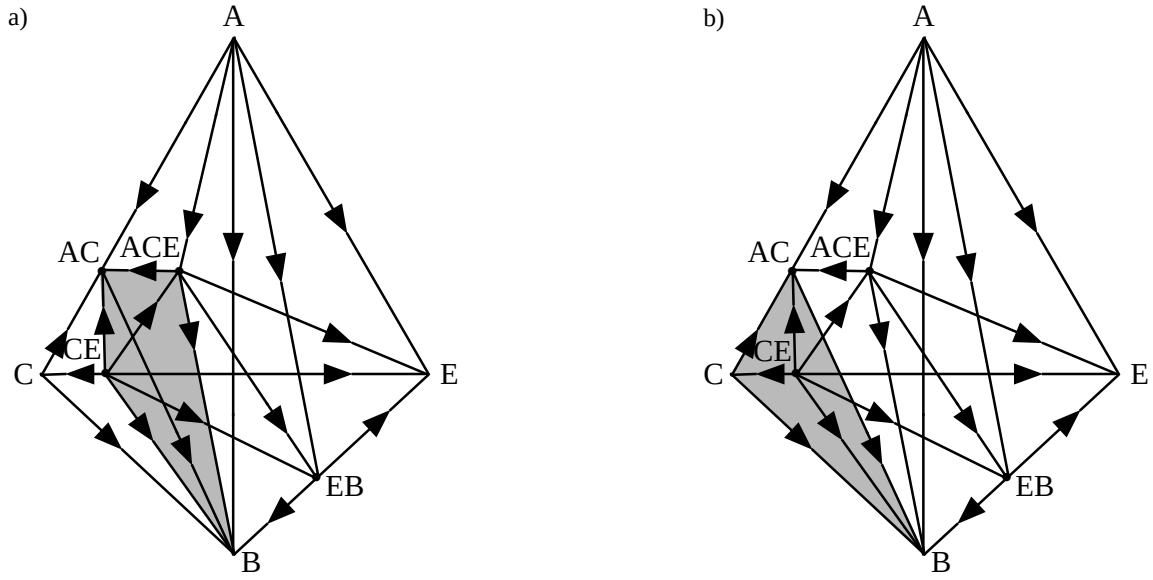

Figure 3-8: The composition simplex divided into batch distillation regions: a) $B(\mathbf{P}_6) \rightarrow \mathbf{P}_6 = \{CE,ACE,AC,B\}$, and b) $B(\mathbf{P}_7) \rightarrow \mathbf{P}_7 = \{CE,C,AC,B\}$.

unstable manifolds of $\mathbf{p}_k$, $\overline{W}^u(\mathbf{p}_k)$ $\forall \mathbf{p}_k \in \mathbf{P}$ as $\xi \rightarrow +\infty$. Composition points that give rise to a subset of $\mathbf{P}$ form the batch distillation boundaries of $B(\mathbf{P})$.

- An initial composition $\mathbf{x}^{p,0}$ located interior to batch distillation region B at limiting conditions will give rise to exactly nc product cuts, and these nc cuts

form an *nc product simplex*.

- A batch distillation region and its corresponding product simplex defined by the the *nc* fixed points in $\mathbf{P} = \{\mathbf{p}_0, \ldots, \mathbf{p}_{nc-1}\}$ do not necessarily coincide.

The derived properties will allow complete characterization of the structure of the composition space for a multicomponent system when using batch distillation based only on the information of the compositions, boiling temperatures, and the stability of the fixed points. The composition space of the quaternary system acetone, chloroform, ethanol, and benzene has been characterized using the derived properties.

Chapter 4

Characterization of the Batch Distillation Composition Simplex

Chapters 2 and 3 explore the structure imposed on the composition simplex (residue curve map) of a multicomponent system describing batch distillation by the presence of azeotropes. This structure can be visualized by dividing the composition simplex (regular simplex) into a series of distinct batch distillation regions. All initial compositions within a particular batch distillation region will result in the same sequence of product cuts, and these cuts will have compositions close to pure components or azeotropes. Each batch distillation region can therefore be characterized by a product simplex. In this chapter an algorithm for constructing the *batch distillation composition simplex* is described based on the theoretical results developed in Chapter 3. The algorithm is based solely on information about the individual fixed points (pure components and azeotropes), i.e., composition, boiling temperature, and nature of point (unstable or stable node, or saddle point). In particular, no numerical integration is required. The algorithm assumes high reflux ratio, large number of trays, and linear pot composition boundaries. Furthermore, it is assumed that a single batch distillation column with a rectifier configuration is employed. Other studies on batch distillation have proposed more sophisticated column configurations. Bernot *et al.* (1991) demonstrate that a stripper configuration may reduce the number of cuts if the stable separatrix is highly curved. Davidyan *et al.* (1994) and Safrit *et al.* (1995)

propose a batch distillation column consisting of a stripper section, a rectifier section, and a vessel in between. With the latter configuration material is taken off both as top and bottom products. Skogestad *et al.* (1995) discuss the benefits of a multi-vessel configuration. Ultimately, the presented methodology can be extended to include a set of specific rules associated with each alternative technology. These rules can then be applied automatically for each relevant technology to generate more separation alternatives for the engineer. For example, the algorithm presented here can be applied directly to a stripper configuration under the same limiting conditions simply by reversing time in the governing differential equations as demonstrated in Appendix A.

4.1 Constructing the Composition Simplex

For binary, ternary, and even quaternary systems the structure of the composition simplex (residue curve map) can be extracted through relatively straightforward experiments, or through integration of the system of differential equations describing simple distillation and sampling a representative number of trajectories. However, for systems with more than four components this approach is neither feasible nor practical. Therefore, a general, less elaborate procedure for describing the composition simplex for a multicomponent system is desired. For instance, exhaustive search algorithms have been developed for continuous distillation of systems exhibiting only binary azeotropes (Serafimov *et al.*, 1974; Petlyuk *et al.*, 1975a; Petlyuk *et al.*, 1975b; Petlyuk *et al.*, 1977). Matsuyama and Nishimura (1977) and Doherty and Calderola (1985) classify all possible ternary residue curve maps. Knight and Doherty (1989) present a graph-theoretic representation of the boundary structure for general ternary systems. An improved algorithm for ternary systems is described by Foucher *et al.* (1991). Malenko (1970a; 1970b; 1970c) proposes a graphical approach for isolating regions of ideal fractionation for multicomponent systems based on the search for maximum-temperature hypersurfaces representing divisions in the composition simplex. Bernot *et al.* (1990) introduce a set of rules for placing batch distillation

boundaries in a ternary system provided that the simple residue curve map is known beforehand. Ahmad and Barton (1994) propose an algorithm for finding the batch distillation regions for multicomponent systems by systematically generating all subsystems starting with ternary systems. Safrit and Westerberg (1996) present an expanded algorithm based on the same evolutionary approach.

There are a number of deficiencies in the approaches described in the existing literature. In particular, 1) it is not possible to characterize the composition simplex for all possible configurations only from information about each fixed point, as pointed out by Foucher *et al.* (1991), even for ternary systems, 2) not all possible topological configurations are taken into account (some of the exceptions are pointed out in Chapter 2), and 3) a batch distillation region may not necessarily coincide with its characteristic product simplex as discussed in Chapter 3. Our algorithm accounts for all possible configurations subject to some relatively mild assumptions.

Chapter 3 demonstrates that the composition simplex of a system can be completely characterized by knowing the *boundary limit sets* of each fixed point in the system. The completed boundary limit sets will accurately represent the topological structure of the composition simplex, and also make it possible to extract all product sequences achievable when applying batch distillation. In this work characterizing of the composition simplex is accomplished through completion of the boundary limit sets. The methodology for generating the unstable boundary limit sets is presented, but by reversing time the exact same methodology can be applied to generating the stable boundary limit sets. The methodology is guaranteed to find the correct boundary limit sets for all fixed points in the system provided that the system is *globally determined*. A system is *globally undetermined* if topological requirements for the composition simplex given by the compositions, boiling temperatures, and stability of each fixed point can be met by more than one combination of boundary limit sets. In Section 4.1.3 it is demonstrated that this may occur if the number of unstable nodes is two and the number of stable nodes is greater than two, and *vice versa*. In such cases integration of the equations governing simple distillation is necessary to determine the correct boundary limit sets. The different steps of the algorithm for

constructing the composition simplex are shown in Figure 4-1.

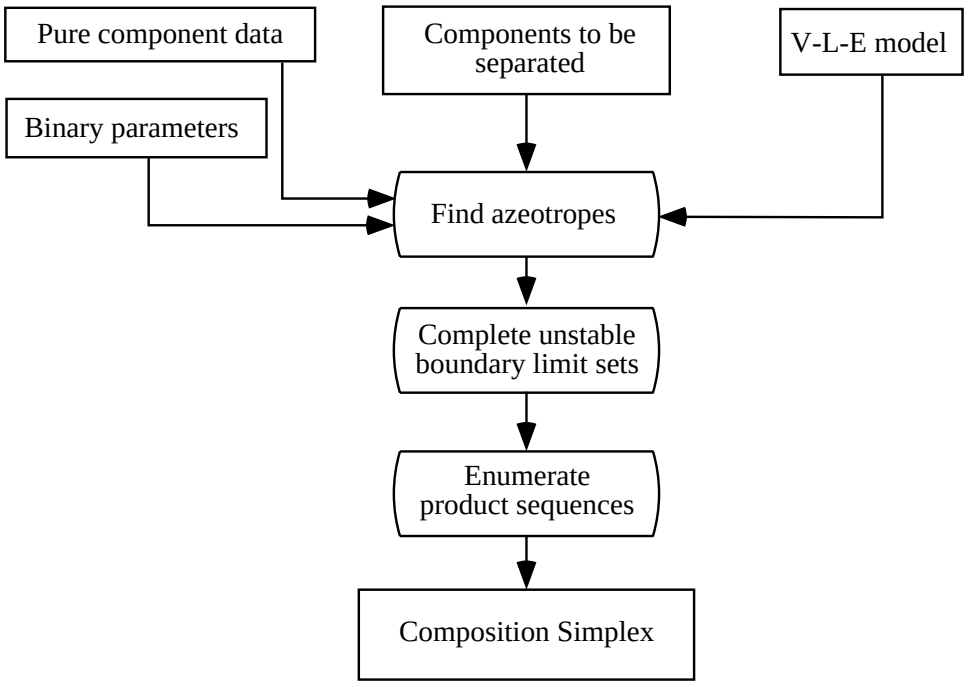

Figure 4-1: Algorithm for constructing the composition simplex.

4.1.1 Predicting the Azeotropes

First the azeotropes of the system of interest are predicted. A suitable vapor-liquid equilibrium model is chosen and the necessary data is gathered to compute the temperatures and compositions of all the azeotropes. The pure components and azeotropes are exactly the fixed points of the differential equations describing simple distillation (Equations (2.1)). The azeotropes can therefore be found by formulating a multi-dimensional root-finding problem, and solving for all physically valid roots. For example, a homotopy method combined with arc length continuation, restricted to those systems not exhibiting multiple azeotropy, is proposed by Fidkowski *et al.* (1993). Similarly, the global optimization based approach by Maranas *et al.* (1996) is applicable to a limited class of vapor-liquid equilibrium models. Vapor-liquid equilibrium calculations rely on accurate binary interaction parameters, and missing or inadequate data (as well as limitations of the vapor-liquid equilibrium model of choice)

can undermine the accuracy of these predictions. Unfortunately, complete equilibrium data for the system of interest are often not available. Usually, however, some other type of data can be located readily. Twu and Coon (1995) and Carlson (1996) provide techniques and guidelines on how to accurately perform vapor-liquid equilibrium calculations in such cases.

Doherty and Perkins (1979) conclude that the only type of fixed points which can occur are: unstable and stable nodes, saddle points, and armchair-like points. The three first types are elementary fixed points, while the latter type is a non-elementary fixed point. The stability of the fixed points can be found by performing a linear stability analysis around each fixed point (Fidkowski *et al.*, 1993). Non-elementary fixed points will have one or more eigenvalues equal to zero, and may correspond to bifurcation points with respect to a parameter, i.e., the global structure changes from one type to another (see, for example, Knapp (1991)). The bifurcation parameter is usually pressure, but it could also be a model parameter, etc. Although it is possible that a column is operating at the bifurcation pressure, and hence that the calculations will predict one or more non-elementary fixed point, it is not very likely. The algorithm therefore assumes elementary fixed points. In that case the eigenvalues of the linearized system in the neighborhood of a fixed point must be real and nonzero, and the fixed points have the properties of nodes or saddles. A system of nc components will exhibit $nc-1$ real valued eigenvalues for each fixed point. A stable (unstable) node has only negative (positive) eigenvalues, while a saddle point has some negative and some positive eigenvalues. A test must be applied to the fixed points predicted to establish that the data is topologically consistent (Fidkowski *et al.*, 1993).

4.1.2 Dividing Boundaries

The eigenvectors defined by the positive eigenvalues and the eigenvectors defined by the negative eigenvalues span the unstable eigenspace and the stable eigenspace, respectively, of the linearized system in the neighborhood of a particular fixed point. The *unstable and stable manifolds* of the nonlinear system will have the same dimen-

sions as those of the eigenspaces of the linearized system, and the eigenvectors will be tangent to the manifolds through the fixed point (Guckenheimer and Holmes, 1983). The unstable (stable) manifold of an unstable (stable) node therefore has dimension $nc-1$, while the stable (unstable) manifold has zero dimension. The unstable and stable manifolds of a fixed point are defined in Chapter 3.

In a system containing two unstable nodes an $nc-2$ dimensional hypersurface must separate their unstable manifolds. Likewise, if there are two stable nodes present an $nc-2$ dimensional hypersurface must separate their stable manifolds. Such a surface separating the unstable manifolds of two unstable nodes is termed a *stable dividing boundary* and is denoted by $\mathrm{SDB}(\mathbf{x}^*_{m_a}, \mathbf{x}^*_{m_b})$, where $\mathbf{x}^*_{m_a}$ and $\mathbf{x}^*_{m_b}$ are unstable nodes. A surface separating the stable manifolds of two stable nodes is termed an *unstable dividing boundary* and is denoted by $\mathrm{UDB}(\mathbf{x}^*_{q_a}, \mathbf{x}^*_{q_b})$, where $\mathbf{x}^*_{q_a}$ and $\mathbf{x}^*_{q_b}$ are stable nodes. For example, in a binary system a dividing boundary is just a point and has dimension zero, in a ternary system a dividing boundary consists of one or more connected line segments and has dimension 1, etc. A simple distillation trajectory through a composition point on the boundary will remain on the boundary both as $\xi \to -\infty$ and $\xi \to +\infty$. ξ denotes a dimensionless measure of time. $\mathrm{SDB}(\mathbf{x}^*_{m_a}, \mathbf{x}^*_{m_b})$ and $\mathrm{UDB}(\mathbf{x}^*_{q_a}, \mathbf{x}^*_{q_b})$ are defined formally by Equations (4.1) and (4.2), where $\gamma(\xi, \hat{\mathbf{x}})$ is the simple distillation orbit through $\hat{\mathbf{x}}$.

$$\mathrm{SDB}(\mathbf{x}^*_{m_a}, \mathbf{x}^*_{m_b}) \equiv \{\hat{\mathbf{x}} \in \mathbf{R}^{nc} : \gamma(\xi, \hat{\mathbf{x}}) \to \mathbf{x}^* \in \overline{\omega}^{uc}(\mathbf{x}^*_{m_a}, \mathbf{x}^*_{m_b}) \text{ as } \xi \to \pm\infty\} \quad (4.1)$$

$$\mathrm{UDB}(\mathbf{x}^*_{q_a}, \mathbf{x}^*_{q_b}) \equiv \{\hat{\mathbf{x}} \in \mathbf{R}^{nc} : \gamma(\xi, \hat{\mathbf{x}}) \to \mathbf{x}^* \in \overline{\omega}^{sc}(\mathbf{x}^*_{q_a}, \mathbf{x}^*_{q_b}) \text{ as } \xi \to \pm\infty\} \quad (4.2)$$

The *common unstable boundary limit set* of $\mathbf{x}^*_{m_a}$ and $\mathbf{x}^*_{m_b}$, $\overline{\omega}^{uc}(\mathbf{x}^*_{m_a}, \mathbf{x}^*_{m_b})$, and the *common stable boundary limit set* of $\mathbf{x}^*_{q_a}$ and $\mathbf{x}^*_{q_b}$, $\overline{\omega}^{sc}(\mathbf{x}^*_{q_a}, \mathbf{x}^*_{q_b})$, are defined by Equations (4.3) and (4.4):

$$\overline{\omega}^{uc}(\mathbf{x}^*_{m_a}, \mathbf{x}^*_{m_b}) \equiv \overline{\omega}^{u}(\mathbf{x}^*_{m_a}) \cap \overline{\omega}^{u}(\mathbf{x}^*_{m_b}) \quad (4.3)$$

$$\overline{\omega}^{sc}(\mathbf{x}^*_{q_a}, \mathbf{x}^*_{q_b}) \equiv \overline{\omega}^{s}(\mathbf{x}^*_{q_a}) \cap \overline{\omega}^{s}(\mathbf{x}^*_{q_b}) \quad (4.4)$$

As defined, $\mathrm{SDB}(\mathbf{x}^*_{m_a}, \mathbf{x}^*_{m_b})$ must be a subset of the pot composition barrier $\mathrm{PCB}(\mathbf{x}^*_{m_a})$. This is because $\mathrm{PCB}(\mathbf{x}^*_{m_a})$ contains all orbits that approach a fixed point in $\overline{\omega}^u(\mathbf{x}^*_{m_a})$ as $\xi \to \pm\infty$, and $\overline{\omega}^{uc}(\mathbf{x}^*_{m_a}, \mathbf{x}^*_{m_b})$ is a subset of $\overline{\omega}^u(\mathbf{x}^*_{m_a})$. Likewise, $\mathrm{SDB}(\mathbf{x}^*_{m_a}, \mathbf{x}^*_{m_b})$ is also a subset of $\mathrm{PCB}(\mathbf{x}^*_{m_b})$.

To illustrate these new concepts consider the quaternary system A, B, C, and D in Figure 4-2. It contains two unstable nodes AC and B. The unstable boundary limit set of AC consists of A, AB, CD, C, and D, and the unstable boundary limit set of B consists of AB, CD, C, and D. Hence, $\overline{\omega}^{uc}(\mathbf{x}^*_{AC}, \mathbf{x}^*_B) = \{\mathrm{AB,CD,C,D}\}$, and $\mathrm{SDB}(\mathbf{x}^*_{AC}, \mathbf{x}^*_B)$ is equal to the shaded area.

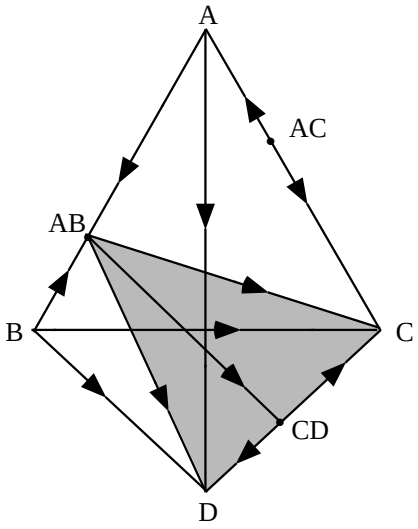

Figure 4-2: Quaternary system with stable dividing boundary. The fixed points are listed in order of increasing boiling temperature: AC (un), B (un), A (s), AB (s), CD (s), C (sn), D (sn). un, s, and sn denote unstable node, saddle point, and stable node, respectively.

4.1.3 Feasible Topological Configurations

The structures that can arise in a system are analyzed in a systematic fashion. This set of topological structures will form the basis for the algorithm for finding the unstable boundary limit sets. To avoid the need to consider multiple azeotropy it is assumed that there is only one fixed point involving a particular set of components, i.e., at most one binary azeotrope in a binary subset of components, at most one ternary

azeotrope in a ternary subset of components, etc. It is also assumed that a system involves at least two components. The latter assumption is included because it makes little sense to analyze a system of one component. The systems are characterized by the number of unstable and stable nodes, whether there is an azeotrope involving all components, and the stability of this azeotrope.

Theorem 4-6 *If a system has only one unstable node, the unstable node's unstable boundary limit set will contain all the other fixed points in the system.*

Proof. Let $\overline{W}^u(\mathbf{x}_m^*)$ be the unstable manifold of the unstable node $\mathbf{x}_m^*$. $\overline{W}^u(\mathbf{x}_m^*)$ has dimension $nc-1$, while any other unstable manifold in the composition simplex has at most dimension $nc-2$. Any neighborhood of a fixed point $\mathbf{x}^*$ must therefore intersect at least one orbit that approaches the unstable node as $\xi \to -\infty$. Hence, $\mathbf{x}^*$ is a limit point of $\overline{W}^u(\mathbf{x}_m^*)$. If $\mathbf{x}^*$ is not the unstable node itself it follows from Definition 3-3 that $\mathbf{x}^*$ must be in the unstable boundary limit set of $\mathbf{x}_m^*$. □

Theorem 4-7 *A saddle point involving all components cannot exist in an nc component system with only one unstable node.*

Proof. Assume that such a fixed point $\mathbf{x}^*$ exists, and that the unstable node is located on one of the facets. $\mathbf{x}^*$ is then located internal to the unstable node's unstable manifold. Only isolated fixed points may exist in the composition space (Doherty and Perkins, 1979). Let R be a neighborhood of $\mathbf{x}^*$. By Theorem 4-6 $\mathbf{x}^*$ is a limit point of the unstable node's unstable manifold. Orbits intersecting the boundary of R will therefore all point inwards. Since all orbits approach a fixed point as $\xi \to \pm\infty$ R must contain a stable node, but this contradicts the assumption that R contains a saddle point. □

Corollary 4-6 *It follows from Theorem 4-7 that an azeotrope involving all components in an nc component system with only one unstable node located on one of the facets must be a stable node.*

By similar reasoning, it is evident that if a system has only one stable node, and the stable node is located on one of the facets, a fixed point involving all components must be an unstable node. We can also conclude that for a system to contain a saddle point involving all components the system must feature at least two unstable and two stable nodes. The ternary system acetone, chloroform, and methanol shown in Figure 2-11 is an example of such a system. In fact, a ternary system with two unstable and two stable nodes will always feature a ternary saddle point.

Theorem 4-8 *Assume that an nc component system features two unstable nodes, two stable nodes, and a saddle point involving all the components. Then the saddle point must be in the unstable boundary limit sets of both unstable nodes, and in the stable boundary limit sets of both stable nodes.*

Proof. Assume that a fixed point $\mathbf{x}^*$ involving all components exists and that the point is an element of the unstable boundary limit set of only one of the unstable nodes. $\mathbf{x}^*$ must therefore be located internal to this unstable node's unstable manifold. By Theorem 4-7 and Corollary 4-6 this makes $\mathbf{x}^*$ a stable node. Similarly, if the point is an element of the stable boundary limit set of only one stable node $\mathbf{x}^*$ must be unstable. The only possible explanation is that $\mathbf{x}^*$ is a limit point of both unstable nodes' unstable manifolds and both stable nodes' stable manifolds. □

Corollary 4-7 *It follows from Theorem 4-8 that an nc saddle point must lie in the intersection between the stable and the unstable dividing boundary.*

Theorem 4-9 *If a system contains three or more unstable nodes, two stable nodes, and a saddle point involving all components the system is globally undetermined.*

Proof. From Theorem 4-8 it follows that the saddle point must be an element of the unstable boundary limit sets of at least two unstable nodes and an element of the stable boundary limit sets of at least two stable nodes. With three unstable nodes several possible combinations exist. Hence, there is insufficient information available to determine the unstable boundary limit sets of the system uniquely. □

Similarly, it is evident that a system which exhibits two unstable nodes, three or more stable nodes, and a saddle point involving all components is globally undetermined.

The results derived in Theorems 4-6 to 4-9 are consistent with earlier work on ternary systems: Foucher *et al.* (1991) demonstrate by using a consistent topology test that if the sum of binary azeotropes (saddles and nodes) and pure component nodes is equal to six for a ternary system containing a ternary saddle point the system is globally undetermined. A ternary saddle point in a ternary system has exactly two orbits approaching as $\xi \to -\infty$ and exactly two orbits approaching as $\xi \to +\infty$. Foucher *et al.* (1991) demonstrate that these special orbits may either approach pure component nodes or binary azeotropes (saddles and nodes) as $\xi \to +\infty$ and $-\infty$. In other words, there exists exactly four orbits connecting the ternary saddle point to either pure component nodes or binary azeotropes. A necessary condition for the existence of a ternary saddle point in a ternary system is therefore that the sum of pure component nodes and binary azeotropes (saddles and nodes) must be greater or equal to four. Only if the sum of binary azeotropes (saddles and nodes) and pure component nodes is equal to four a unique solution exists.

The consistent topology test for ternary systems used by Foucher *et al.* (1991) is derived by Doherty and Perkins (1979). The set of restrictions imposed on the complexity of the ternary system can be written as:

$$2N_3 - 2S_3 + N_2 - S_2 + N_1 = 2 \tag{4.5}$$

$$N_1 + S_1 = 3 \tag{4.6}$$

$$N_2 + S_2 \leq 3 \tag{4.7}$$

$$N_3 + S_3 \leq 1 \tag{4.8}$$

where N_i refers to the number or nodes (unstable and stable) involving i components, and S_i refers to the number of saddle points involving i components. In a ternary system with two unstable and two stable nodes, and a ternary saddle point, $S_3 = 1$, $N_3 = 0$, and $N_1 + N_2 = 4$. When inserting these values into Equation (4.5) we get

$S_2 = 0$, i.e., there may be no binary saddle points in the system. The ternary saddle point must therefore be connected to nodes only. These nodes are exactly the two unstable and two stable nodes. In conclusion, the criterion derived by Foucher *et al.* (1991) is equivalent to requiring that for a ternary system containing a ternary saddle point to be globally determined, it must contain exactly two unstable and two stable nodes.

An example of a ternary system that is globally undetermined is shown in Figure 4-3. The system exhibits two unstable nodes (AB and AC), three stable nodes (A, B, and C), and a ternary saddle point (ABC). Also, the ternary system exhibits a binary saddle point (BC). Figure 4-3a shows one feasible topological structure that satisfies the stability requirements of each fixed point, and Figure 4-3b shows another feasible topological structure. As indicated, the unstable boundary limit sets for the two configurations are different. A third topology is feasible where the binary saddle point BC is connected to unstable node AC rather than AB, and ternary saddle point ABC is connected to stable node B rather than C.

Although Theorem 4-9 does not exclude the possibility of having a system with three or more unstable nodes, two stable nodes (or *vice versa*), and no *nc* component saddle point, such characteristics can only be observed in systems with four or more components. The *nc* component saddle point lies in the intersection between the stable and the unstable dividing boundaries (Theorem 4-7). In a ternary system the intersection is a point, and hence must be equal to a fixed point. In systems with more than three components the intersection will have dimension greater or equal to one. The existence of a saddle point in the intersection therefore depend on the topological structure locally on the dividing boundaries. Experience shows that the number of nodes in a system typically goes down rather than up as the number of components increases. The algorithm will therefore be restricted to systems where the system itself and all its subsystems exhibit at most two unstable and at most two stable nodes. A fixed point that is a saddle point in the system itself may remain a saddle point locally on a stable dividing boundary, or it may have the properties of an unstable or stable node. Similarly, we must therefore require that a stable dividing

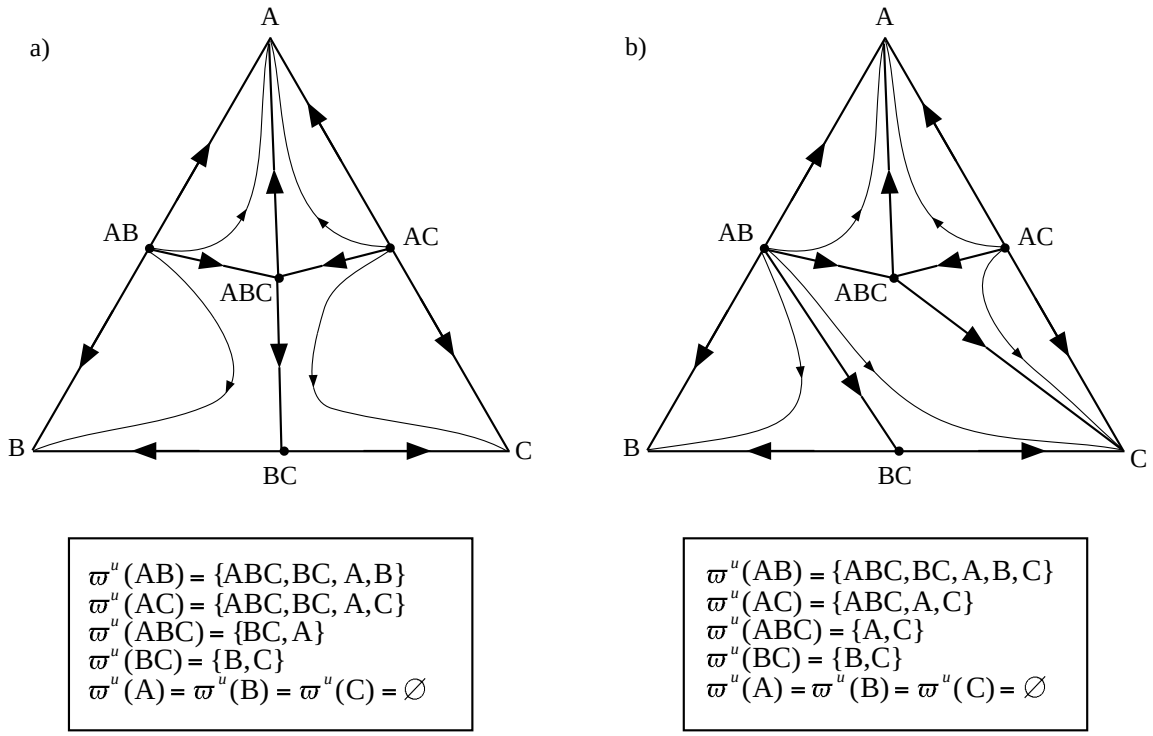

Figure 4-3: Globally undetermined ternary system. The fixed points are listed in order of increasing boiling temperature: AB (un), AC (un), ABC (s), BC (s), A (sn), B (sn), C (sn). un, s, and sn denote unstable node, saddle point, and stable node, respectively.

boundary locally exhibits at most two unstable and at most two stable nodes.

Theorem 4-10 *In a system with two unstable nodes and two stable nodes the stable nodes will be elements of the unstable boundary limit set of both unstable nodes, and the unstable nodes will be elements of the stable boundary limit sets of both stable nodes.*

Proof. Two unstable nodes introduce a stable dividing boundary and two stable nodes introduce an unstable dividing boundary. The two boundaries will intersect and hence divide the composition simplex into four sectors. The orbits through composition points internal to each sector must approach an unstable node as $\xi \to -\infty$ and a stable node as $\xi \to +\infty$. Since an orbit through a composition point internal to a sector may not cross any of the boundaries, this is possible only if the stable nodes are located on the stable dividing boundary, and the unstable nodes are located on the

unstable dividing boundary. The stable nodes are therefore in the common unstable dividing boundary limit set, and hence elements of the unstable boundary limit sets of both unstable nodes. Likewise, the unstable nodes must be in the common stable boundary limit set, and hence the unstable nodes will be elements of the stable boundary limit sets of both stable nodes. □

Theorem 4-11 *Let* $\mathbf{x}^*_{m_a}$ *be an unstable node and* $\mathbf{x}^*_j$ *an element in the unstable boundary limit set of* $\mathbf{x}^*_{m_a}$*. Then if a system and all its subsystems can be characterized as having at most two unstable nodes and at most two stable nodes the unstable boundary limit set of* $\mathbf{x}^*_j$ *is a subset of the unstable boundary limit set of* $\mathbf{x}^*_{m_a}$*.*

Proof. It follows from Theorem 4-6 that if $\mathbf{x}^*_{m_a}$ is the only unstable node the theorem is always true. Also note that the theorem is true if $\mathbf{x}^*_j$ is a stable node since the boundary limit set of a stable node is the empty set. Therefore it only remains to prove that the theorem is true for the system and all its subsystems having two unstable nodes, e.g., $\mathbf{x}^*_{m_a}$ and $\mathbf{x}^*_{m_b}$, and $\mathbf{x}^*_j$ being a saddle point.

The fixed points in the unstable boundary limit set of $\mathbf{x}^*_j$, $\overline{\omega}^u(\mathbf{x}^*_j)$, are limit points of the unstable manifold to $\mathbf{x}^*_j$. For the theorem to be true the fixed points in $\overline{\omega}^u(\mathbf{x}^*_j)$ must also be limit points to the unstable manifold of $\mathbf{x}^*_{m_a}$ (see Definition 3-3). $\overline{\omega}^u(\mathbf{x}^*_{m_a}) \cup \overline{\omega}^u(\mathbf{x}^*_{m_b})$ contains all the fixed points in the system except the unstable nodes themselves. Hence, if a fixed point in $\overline{\omega}(\mathbf{x}^*_j)$ is not an element of $\overline{\omega}^u(\mathbf{x}^*_{m_a})$, it must be an element of $\overline{\omega}^u(\mathbf{x}^*_{m_b})$. Let $\mathbf{x}^*_j \notin \overline{\omega}^{uc}(\mathbf{x}^*_{m_a}, \mathbf{x}^*_{m_a})$, i.e., $\mathbf{x}^*_j$ is not an element of the common unstable boundary limit set. Then the limit points of the unstable manifold of $\mathbf{x}^*_j$ will necessarily be a subset of the unstable boundary limit set of $\mathbf{x}^*_{m_a}$. Otherwise at least one orbit in the unstable manifold of $\mathbf{x}^*_j$ would intersect the stable dividing boundary and approach a fixed point on the other side of the boundary as $\xi \to +\infty$. Since orbits can only intersect the stable dividing boundary at fixed points, this is infeasible. On the other hand, if the orbit approaches a fixed point on the stable dividing boundary as $\xi \to +\infty$, the theorem is true since the fixed points on the stable dividing boundary are elements of the unstable boundary limit set of $\mathbf{x}^*_{m_a}$.

The last part of the proof involves demonstrating that the theorem is true when $\mathbf{x}_j^*$ is an element of the common unstable boundary limit set and hence located on the stable dividing boundary. With at most two unstable nodes and at most two stable nodes in the system itself and all its subsystems, it is guaranteed that stable nodes in the system itself and all its subsystems will lie on the stable dividing boundary (Theorem 4-10). Orbits through composition points internal to the composition simplex approaching an unstable node as $\xi \to -\infty$ will therefore monotonically approach the stable dividing boundary as $\xi \to +\infty$ (i.e., monotonicity is guaranteed by the location of the stable nodes on the stable dividing boundary). Hence, orbits that approach a fixed point located on the stable dividing boundary as $\xi \to -\infty$ will also approach a fixed point on the stable dividing boundary as $\xi \to +\infty$. Consequently, if $\mathbf{x}_j^*$ is located on the stable dividing boundary, the unstable manifold of $\mathbf{x}_j^*$ will be a subset of the composition points on the stable dividing boundary. Its limit points will therefore also be a subset of the stable dividing boundary, and hence limit points of the unstable manifold of $\mathbf{x}_{m_a}^*$. $\square$

We return to the ternary system in Figure 4-3 to demonstrate how this property may break down for an undetermined system. Consider the topological structure in Figure 4-3a. The binary azeotrope BC is an element of $\overline{\omega}^u$(AB). Both stable nodes B and C are elements of $\overline{\omega}^u$(BC). However, C is not an element of $\overline{\omega}^u$(AB). On the other hand, note that the alternative topological structure in Figure 4-3b satisfies the property.

Hence, by the reasoning above, only systems listed in Table 4.1 are included in the algorithm. Note that this set of structures is a complete description of all systems with less that three unstable nodes and less than three stable nodes assuming that there is only one fixed point involving a particular set of components.

4.1.4 The Algorithm

The algorithm completes the boundary limit sets of all the fixed points in a system by systematically generating all subsystems starting with the binary edges, and combining the data to complete the unstable boundary limit sets for the overall system.

Table 4.1: Topological structures included in the algorithm.

System	Unstable nodes	Stable nodes	nc-azeotrope
1	1	1	none
2	1	1	unstable node
3	1	1	stable node
4	1	2	none
5	1	2	unstable node
6	1	2	stable node
7	2	1	none
8	2	1	unstable node
9	2	1	stable node
10	2	2	none
11	2	2	saddle

The number of subsystems involving i components in a system with nc components is given by $\binom{nc}{i} = \frac{nc!}{i!(nc-i)!}$. Hence, the number of subsystems necessary to analyze is therefore $\mathrm{N}_{nc} = \sum_{i=2}^{nc} \frac{nc!}{i!(nc-i)!}$. For $i = 0$, we get $\sum_{i=0}^{nc} \frac{nc!}{i!(nc-i)!} = 2^{nc}$ (Cormen *et al.*, 1993). Therefore, $\mathrm{N}_{nc} = 2^{nc} - 1 - nc$. Assuming that analyzing a particular subsystem requires a fixed amount of time, the worst-case running time when analyzing a system of nc components is therefore of $\mathrm{O}(2^{nc})$, i.e., exponential. However, as it is expected that nc typically will be in the order of 5-10, the running time should not impose a great limitation on the applicability of the algorithm.

By Definition 3-3, the elements in the unstable boundary limit set of a fixed point are limit points to the fixed point's unstable manifold. If the fixed point itself and the other composition points in its unstable manifold are located on one of the faces of the overall composition simplex, i.e., only involve a subset of the components in the overall system, the elements in the unstable boundary limit set will also be located in the same subsystem. This implies that when the unstable boundary limit sets for this particular subsystem are complete, the unstable boundary limit set for the fixed point with respect to the overall system is complete. When completing the unstable boundary limit set of a system involving k components we therefore only need to focus on the fixed points that have composition points involving all k components in their unstable manifolds. These are:

1. Unstable nodes

2. Fixed points on a stable dividing boundary

3. Saddle points involving $k-1$ components in a system with a stable node involving all k components

The unstable manifold of an unstable node has dimension $k-1$ and must therefore contain composition points involving all k components. The unstable manifolds of the fixed points in the common unstable boundary limit set are subsets of the stable dividing boundary. The boundary divides the composition space and must therefore contain composition points involving all k components. Appendix B demonstrates that a stable node involving all k components must be connected to saddle points involving $k-1$ components through stable separatrices. Such a stable separatrix will be a subset of the unstable manifold of the saddle point and is composed of composition points involving all k components. Appendix B also shows that if the unstable manifold of a saddle point involving less than $k-1$ components contains k-component composition points, it is because the saddle point is located on the stable dividing boundary. In that case, the saddle point belongs to category 2 above. No other fixed points have composition points involving all k components in their unstable manifolds.

The data for the unstable boundary limit sets can be arranged in an adjacency matrix $\mathbf{A}_{nc}$ where the rows and the columns represent the fixed points in order of increasing boiling temperature. For each pair of fixed points ij, it is determined whether fixed point j is in the boundary limit set of i, where i is a fixed point from one of the categories in the list above. Each element a_{ij} in $\mathbf{A}_{nc}$ is visited only once. If element $a_{ij}=0$ fixed point j is not in the unstable boundary limit set of fixed point i, if $a_{ij}=1$ j is in the unstable boundary limit set of i, and if $a_{ij}=-1$ the relationship between i and j remains to be determined. Hence, the unstable boundary limit sets are completed if all elements in $\mathbf{A}_{nc}$ have a value of either 0 or 1.

The main steps of the algorithm (**OmegaAll**(overall_system)) are shown in Figure 4-4 as pseudo-code. The subroutine **Omega**(current_system,host_system) (see Figure

4-5) is called recursively until the unstable boundary limit sets for *current_system* is complete. The input to **OmegaAll**(overall_system) consists of the set of pure components, and the set of fixed points in *overall_system* with compositions, temperatures, and their stability. The input to **Omega**(current_system,host_system) consists of the set of pure components, and the set of fixed points in *current_system* with compositions, temperatures, and their stability, and the same for *host_system*. The individual steps are described in detail below. Note that the procedures for systems 7-11 only differ in the first step.

OmegaAll(overall_system)
  Initialize $\mathbf{A}_{nc}$ (step 1)
  Complete binary edges (step 2)
  If (number of components in overall_system) ≥ 3
    Set current_system = overall_system
    Omega(current_system,overall_system)
  EndIf
  Complete $\mathbf{A}_{nc}$ (step 14)

Figure 4-4: The overall algorithm for completing the unstable boundary limit sets.

Step 1: initialize $\mathbf{A}_{nc}$: set $a_{ij} = 0$ if j is an unstable node, i is a stable node, or if $\mathrm{T}_B^i \geq \mathrm{T}_B^j$. Set all other elements equal to -1.

Step 2: complete binary edges: if two pure components i and j form a minimum boiling binary azeotrope k, then $a_{ki} = a_{kj} = 1$. If they form a maximum boiling azeotrope, then $a_{ik} = a_{jk} = 1$. Otherwise, $a_{ij} = 1$ if $\mathrm{T}_B^i < \mathrm{T}_B^j$, or $a_{ji} = 1$ if $\mathrm{T}_B^i > \mathrm{T}_B^j$.

Step 3: construct all subsystems: let *current_system* involve k components. Then generate k sets of $k-1$ components by removing one component at the time from the set of pure components in *current_system*. Generate the set of fixed points for each subsystem by extracting the respective fixed points from the set of fixed

```
Omega(current_system,host_system)
  If current_system not already explored Then
    If (number of components in current_system) ≥ 4 Then
      For Each sub_system ∈ current_system Do                          (step 3)
        Omega(sub_system,current_system)
      EndFor
    EndIf
    Switch(current_system)
      Case = systems 1, 2, 4, and 5
        Complete unstable boundary limit set of unstable node          (step 4)
      Case = systems 3 and 6
        Complete unstable boundary limit set of unstable node          (step 4)
        Establish connections with stable node                         (step 5)
      Case = systems 7 and 10
        Complete unstable boundary limit sets of unstable nodes        (step 6)
        Construct common unstable boundary limit set (ϖ^uc)            (step 7)
        Evaluate stability of fixed points in ϖ^uc                     (step 8)
        Complete unstable boundary limit sets of fixed points in ϖ^uc  (step 9)
      Case = system 8
        Complete unstable boundary limit sets of unstable nodes        (step 10)
        Construct common unstable boundary limit set (ϖ^uc)            (step 7)
        Evaluate stability of fixed points in ϖ^uc                     (step 8)
        Complete unstable boundary limit sets of fixed points in ϖ^uc  (step 9)
      Case = system 9
        Complete unstable boundary limit sets of unstable nodes        (step 11)
        Construct common unstable boundary limit set (ϖ^uc)            (step 7)
        Evaluate stability of fixed points in ϖ^uc                     (step 8)
        Complete unstable boundary limit sets of fixed points in ϖ^uc  (step 9)
      Case = system 11
        Complete unstable boundary limit sets of unstable nodes        (step 12)
        Construct common unstable boundary limit set (ϖ^uc)            (step 7)
        Evaluate stability of fixed points in ϖ^uc                     (step 8)
        Complete unstable boundary limit sets of fixed points in ϖ^uc  (step 9)
    EndSwitch
  EndIf
  If hostsystem ≠ current_system Then
    Update adjacency matrix of host_system                             (step 13)
  EndIf
```

Figure 4-5: The subroutine **Omega**(current_system).

points in *current_system*. Then determine the stability of each fixed point in every subsystem. Fixed points that are unstable or stable nodes in *current_system* will also be unstable or stable nodes in all subsystems where they are present. Therefore only the stability of saddle points need to be reevaluated when subsystems are analyzed. This can be achieved by performing a new linear stability analysis around each of the saddle points in the subsystems.

Step 4: complete unstable boundary limit set of unstable node: the unstable boundary limit sets of all subsystems are complete. In *current_system* the unstable node is the only fixed point with composition points involving all components in its unstable manifold. The unstable boundary limit set of the unstable node is completed by applying Theorem 4-6. The procedure goes as follows: let i denote the unstable node. Then if $a_{ij} = -1$, set $a_{ij} = 1$.

Step 5a (system 3): establish connections to stable node: the reasoning behind this procedure is presented in Appendix B. Let $\mathbf{x}_q^*$ be the stable node involving all components in *current_system*, and let *current_system* involve k components. Then $\mathbf{x}_q^*$ should be added to the unstable boundary limit sets of all saddle points involving $k-1$ components.

Step 5b (system 6): establish connections to stable node: the reasoning behind this procedure is presented in Appendix B. Let $\mathbf{x}_q^*$ be the stable node involving all components in *current_system*, and let *current_system* involve k components. Then $\mathbf{x}_q^*$ should be added to the unstable boundary limit sets of all $k-1$ component saddle points, except the $k-1$ component saddle points that already have the other stable node in their unstable boundary limit set.

Step 6: complete unstable boundary limit sets of unstable nodes: the unstable boundary limit sets of all subsystems are complete. *Current_system* has two unstable nodes and hence a stable dividing boundary. The unstable boundary limit set of each unstable node must be completed before the common unstable boundary

limit set may be constructed. This is done by applying Theorem 4-11. The pseudo-code for the procedure is shown in Figure 4-6. i denotes an unstable node, $\overline{\omega}^u(i)$ its unstable boundary limit set, and k the number of components in *current_system*.

```
For i ∈ {unstable nodes} Do
   For j ∈ ϖ^u(i) Do
      For l ∈ ϖ^u(j) Do
         If a_il = -1 Then
            a_il = 1
         EndIf
      EndFor
   EndFor
EndFor
```

Figure 4-6: Completion of unstable boundary limit sets for unstable nodes.

Step 7: construct common unstable boundary limit set ($\overline{\omega}^{uc}$): apply Equation (4.3) to the completed unstable boundary limit sets of the two unstable nodes.

Step 8: evaluate stability of fixed points in $\overline{\omega}^{uc}$: a fixed point that is a saddle point in *current_system* may remain a saddle point locally on a stable dividing boundary, or it may have the properties of an unstable or stable node. For example, binary azeotrope AB in Figure 4-2 is a saddle point globally in system A, B, C, and D, but has the properties of an unstable node locally on the stable dividing boundary. This is because all trajectories through composition points located on $\mathrm{SDB}(\mathbf{x}_A^* C, \mathbf{x}_B^*)$ in the neighborhood of AB approach AB as $\xi \to -\infty$. Hence, for each fixed point $\mathbf{x}^*$ on the stable dividing boundary we can associate a set of trajectories located on the boundary that approach the fixed point as $\xi \to -\infty$, and a set of trajectories located on the boundary that approach the fixed point as $\xi \to +\infty$. These sets are denoted by $\overline{W}^u_{sdb}(\mathbf{x}^*)$ and $\overline{W}^s_{sdb}(\mathbf{x}^*)$, respectively. The trajectory through $\mathbf{x}^*$ is $\mathbf{x}^*$ itself, and $\mathbf{x}^*$ therefore belongs to both sets. For convenience the fixed point itself will be allocated to $\overline{W}^u_{sdb}(\mathbf{x}^*)$. $\overline{W}^u_{sdb}(\mathbf{x}^*)$ and $\overline{W}^s_{sdb}(\mathbf{x}^*)$ are evidently subsets of the fixed points unstable

and stable manifolds. In fact, the subscript *sdb* in $\overline{W}^{u}_{sdb}(\mathbf{x}^*)$ indicates the subset of $\overline{W}^{u}(\mathbf{x}^*)$ that is also a subset of the stable dividing boundary. If $\overline{W}^{s}_{sdb}(\mathbf{x}^*) = \emptyset$, then $\mathbf{x}^*$ is unstable locally on the stable dividing boundary. Similarly, if $\overline{W}^{u}_{sdb}(\mathbf{x}^*) = \{\mathbf{x}^*\}$, $\mathbf{x}^*$ is stable locally on the stable dividing boundary. Otherwise, $\mathbf{x}^*$ is a saddle point.

The stability of a fixed point in *current_system* is determined by the number of positive and negative eigenvalues computed from a linear stability analysis in the neighborhood of the fixed point. In a system with k components each fixed point is characterized by $k-1$ eigenvalues. Similarly, the stability of a fixed point on the stable dividing boundary may be determined by the number of positive and negative eigenvalues computed from a linear stability analysis in the neighborhood of the fixed point on the stable dividing boundary. These eigenvalues are a subset of the set of $k-1$ eigenvalues characterizing the stability of the fixed point in *current_system*.

From Theorem 4-11 it follows that if a fixed point $(\mathbf{x}^*)$ is an element of the common unstable boundary limit set its unstable manifold $(\overline{W}^{u}(\mathbf{x}^*))$ will be a subset of the stable dividing boundary provided that *current_system* and all its subsystems have at most two unstable and at most two stable nodes. Hence, $\overline{W}^{u}_{sdb}(\mathbf{x}^*) = \overline{W}^{u}(\mathbf{x}^*)$. Consequently, the number of positive eigenvalues characterizing the stability of the fixed point on the stable dividing boundary must be the same as for *current_system*. Because the stable dividing boundary has dimension $k-2$ the stability of each fixed point on the stable dividing boundary is characterized by $k-2$ eigenvalues. Hence, the local stability of fixed point $\mathbf{x}^*$ on the stable dividing boundary can be found simply by computing the number of positive $(\Lambda^{\oplus}_{sdb}(\mathbf{x}^*))$ and negative eigenvalues $(\Lambda^{\ominus}_{sdb}(\mathbf{x}^*))$ applying Equations (4.9) and (4.10). $\Lambda^{\oplus}(\mathbf{x}^*)$ and $\Lambda^{\ominus}(\mathbf{x}^*)$ represent the number of positive and negative eigenvalues in *current_system*. A similar approach is suggested by Safrit and Westerberg (1996).

$$\Lambda^{\oplus}_{sdb}(\mathbf{x}^*) = \Lambda^{\oplus}(\mathbf{x}^*) \qquad \forall x^* \in \overline{\omega}^{uc}(\mathbf{x}^*_{m_a}, \mathbf{x}^*_{m_b}) \tag{4.9}$$

$$\Lambda^{\ominus}_{sdb}(\mathbf{x}^*) = \Lambda^{\ominus}(\mathbf{x}^*) - 1 \;\; \forall x^* \in \overline{\omega}^{uc}(\mathbf{x}^*_{m_a}, \mathbf{x}^*_{m_b}) \tag{4.10}$$

Step 9: complete unstable boundary limit sets of fixed points in $\overline{\omega}^{uc}$: a stable dividing boundary in a k component system has dimension $k-2$. The topological structure may be characterized according to Table 4.1 by the number of unstable and stable nodes, and whether there is an azeotrope involving all components located on the boundary. Completion of the unstable boundary limit sets is accomplished using the corresponding procedure in Figure 4-5.

Step 10: complete unstable boundary limit set of unstable nodes: the reasoning behind this procedure is presented in Appendix B. The unstable boundary limit sets of all subsystems are complete. Complete the unstable boundary limit set of the unstable node located on the facet the procedure described in Figure 4-6. Let $\mathbf{x}_m^*$ be the unstable node involving all components in *current_system*, and let *current_system* involve k components. Add all the $nc-1$ component saddle points to the unstable boundary limit set of $\mathbf{x}_m^*$, except the $nc-1$ component saddle points that are already elements in the unstable boundary limit set of the unstable node located on the facet. Complete the unstable boundary limit set of $\mathbf{x}_m^*$ by applying the procedure described in Figure 4-6.

Step 11: complete unstable boundary limit set of unstable nodes: the reasoning behind this procedure is presented in Appendix B. The unstable boundary limit sets of all subsystems are complete. Include the stable node in the unstable boundary limit set of both unstable nodes. The unstable boundary limit sets of the unstable nodes are completed by applying the procedure described in Figure 4-6.

Step 12: complete unstable boundary limit set of unstable nodes: include the saddle point in the unstable boundary limit sets of both unstable nodes. The unstable boundary limit sets of the unstable nodes are completed by applying the procedure described in Figure 4-6.

Step 13: update adjacency matrix: whenever a subsystem is completed the adjacency matrix of *host_system* should be updated. If component j is an element

of the unstable boundary limit set of component i in a subsystem, j is also in the unstable boundary limit set of i in *host_system*.

Step 14: complete $\mathbf{A}_{nc}$: in a k component subsystem the unstable boundary limit sets of the fixed points characterized as having composition points involving all k components in their unstable manifold are completed, i.e., unstable nodes, fixed points on a stable dividing boundary, and saddle points connected to stable node located internal to the subsystem. No other fixed points will have elements added to their unstable boundary limit set in that particular subsystem. When all subsystems are explored, the overall system is explored based on the same strategy. Hence, when the unstable boundary limit sets of the overall system are completed no new elements may be added to any unstable boundary limit set. Therefore the remaining elements are set to zero, i.e., if $a_{ij} = -1$, set a_{ij} to zero.

4.2 Enumerate Product Sequences

In Chapter 3 it is demonstrated that at the limiting conditions of very high reflux ratio, large number of trays, and linear pot composition boundaries an nc component mixture located internal to a batch distillation region will produce exactly nc product cuts. The product cuts will have compositions equal to fixed points, and no other product compositions may be produced. In addition, the following relationship between the fixed points in a product sequence must be true: if $\mathbf{p}_k$ represents product cut k, then $\mathbf{p}_{k+1} \in \overline{\omega}^u(\mathbf{p}_l)\ \forall l = 0, \ldots, k$ (Corollary 3-5). To summarize, the properties of a feasible product sequence are:

Property 1 *A sequence consists of nc fixed points.*

Property 2 *Each subsequent product cut has to be an element of the unstable boundary limit sets of all the preceding product cuts.*

These properties lead to the following algorithm for enumerating the feasible product sequences in the composition simplex of an nc component system. The unstable boundary limit sets of the system may be represented as a directed graph with:

- **vertices:** fixed points
- **edges:** an edge exists between two vertices $\mathbf{x}_i^*$ and $\mathbf{x}_j^*$ if $\mathbf{x}_j^*$ is an element of the unstable boundary limit set of $\mathbf{x}_i^*$ ($\mathbf{x}_i^*$ is the head and $\mathbf{x}_j^*$ is the tail of the edge)
- **directionality:** to the highest boiling vertex of each pair

Formally, the problem can be formulated as a graph theoretical problem (Zhang, 1995):

Definition 4-6 PDAG Problem: *given a Directed Acyclic Graph G with each vertex* $\mathbf{x}^*$ *labeled with a unique positive real number* T_B*, which will be called priority, such that the direction of any edge always radiates from the vertex of the lower number. Find a group of nc vertices that includes a predetermined prioritized vertex such that there exists a path which begins with that vertex and end at the highest prioritized vertex in the group and passes through every vertex in the group exactly once. Moreover, the vertices are pairwisely connected.*

A complete algorithm for solving the PDAG problem can be found in Zhang (1995). The resulting chains of points will start with an unstable node, and will be in order of increasing boiling temperature. Let $\{\mathbf{D}\}$ denote this set of chains (sets of *nc* points), and $\{\mathbf{P}\}$ the set of product sequences achievable in a system. Properties 1 and 2 are necessary to define a product sequence. It can therefore be guaranteed that $\{\mathbf{P}\} \subseteq \{\mathbf{D}\}$. However, the two conditions are not sufficient. Hence, it is possible that $\{\mathbf{D}\}$ contains one or more sets of *nc* points which do not represent true product sequences. An additional property is extracted from Theorem 3-4:

Property 3 *The nc fixed points form a geometric* $(nc-1)$*-simplex constrained to lie on the hyperplane* $\sum_{i=1}^{nc} x_i = 1$.

Definition 4-7 *(Hocking and Young, 1961) Two geometric simplices are properly joined if they do not meet at all, or if their intersection is a face of each other.*

Theorem 4-12 *If the simplices constructed from the sets of nc points in* $\{\mathbf{D}\}$ *are properly joined,* $\{\mathbf{P}\} = \{\mathbf{D}\}$.

Proof. The union of the batch distillation regions is equal to the composition simplex. Batch distillation regions may not intersect (except along boundaries), as that would mean that one composition point could give rise to more than one product sequence. A product simplex will be greater than or equal to its respective batch distillation region. Assume that one of the simplices is not a true product simplex. We may then remove this simplex, and the remaining simplices will still contain all the composition points in the composition simplex. However, since the simplices are properly joined this is infeasible. □

Observe that if the product simplices are properly joined, every product simplex coincides with its respective batch distillation region.

In order for the set of nc points to form a geometric $(nc-1)$-simplex the points must be pointwise independent (Hocking and Young, 1961). Figure 4-7 illustrates this criterion. The sequence {m1,n2,q1} satisfies Properties 1 and 2, but not 3.

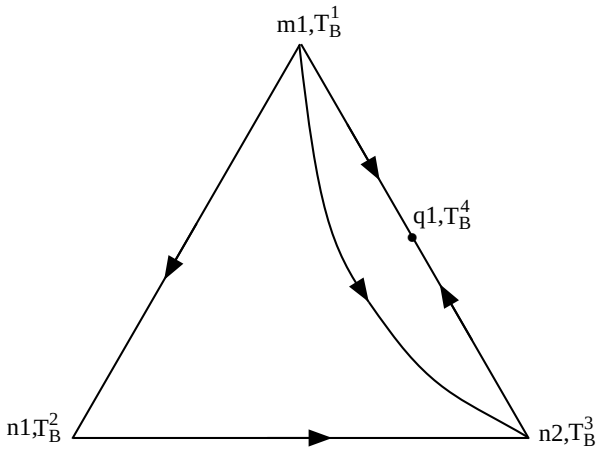

Figure 4-7: The vertices in the sequence {m1,n2,q1} are not pointwise independent.

Consider the possible characteristics of $\{\mathbf{D}\}$:

1. Every set $\mathbf{D} \in \{\mathbf{D}\}$ forms an $(nc-1)$-simplex, and

   (a) the constructed simplices are properly joined.

   (b) the constructed simplices are not properly joined.

2. One or more of the sets $\mathbf{D} \in \{\mathbf{D}\}$ does not form an $(nc-1)$-simplex (the respective nc points are not pointwise independent), and

   (a) the simplices constructed from the remaining sets are properly joined.

   (b) the simplices constructed from the remaining sets are not properly joined.

Assuming that every set $\mathbf{D} \in \{\mathbf{D}\}$ forms an $(nc-1)$-simplex the following procedure may be applied to check if the simplices are properly joined: form $(nc-1)$-simplices from each set $\mathbf{D} \in \{\mathbf{D}\}$. If at least one fixed point can be found that is located internal to or on a facet of a simplex, and this fixed point is not in the set of fixed points defining the simplex, the set of simplices will not be properly joined, since every fixed point is a face (0-simplex) of one or more simplices. Conversely, if no fixed point is located internal to or on a facet of a product simplex, the set of product simplices are properly joined. A geometric $(k-1)$-simplex is defined by Equation (4.11), where $k \leq nc$ (Hocking and Young, 1961):

$$\mathbf{\Delta} = \{\mathbf{h} \in \mathbf{R}^{nc} : \mathbf{h} = \sum_{i=0}^{k-1} f_i \mathbf{d}_i;\ f_i \geq 0\ \ \forall i = 0, \ldots, k-1 \text{ and } \sum_{i=0}^{k-1} f_i = 1\} \qquad (4.11)$$

where $\mathbf{d}_i\ \forall i = 0, \ldots, k-1$ represent the vertices of the k-simplex, and $f_i\ \forall i = 0, \ldots, k-1$ represent barycentric coordinates. An $(nc-1)$-simplex $\mathbf{\Delta}$ in a system with nc components is defined by nc vertices. Hence $k = nc$. The vertices are the fixed points in the set $\mathbf{D}$. Let $\mathbf{h}$ represent a fixed point which is not in $\mathbf{D}$, and E the set of fixed points in the system. For every $\mathbf{h} \in$ E and every $\mathbf{D} \in \{\mathbf{D}\}$ apply Equation (4.11) to $\mathbf{h}$ and $\mathbf{D}$. If no combination of $\mathbf{h}$ and $\mathbf{D}$ satisfies Equation 4.11, $\{\mathbf{D}\}$ represents the set of true product sequences (category 1a).

If no barycentric coordinate is negative, and more than one but less than nc barycentric coordinates are greater than zero this implies that $\mathbf{h}$ is located on a facet of the simplex $\hat{\mathbf{\Delta}}$ (defined by $\hat{\mathbf{D}}$). If nc barycentric coordinates are greater than zero $\mathbf{h}$ is located internal to $\hat{\mathbf{\Delta}}$. In either case the simplices generated from $\{\mathbf{D}\}$ are not properly joined (category 1b).

This procedure may be applied directly if $\{\mathbf{D}\}$ belongs to category 1 above. However, if $\{\mathbf{D}\}$ belongs to category 2 the procedure must be applied with a slight modification: remove the set(s) $\{\mathbf{D}_{npi}\}$ that do not satisfy Property 3. The remaining sets are denoted by $\{\mathbf{D}_{pi}\}$. Let $\mathbf{h}$ represent a fixed point which is neither in $\mathbf{D}_{pi}$ nor in $\{\mathbf{D}_{npi}\}$. For every $\mathbf{h} \in$ E and every $\mathbf{D} \in \{\mathbf{D}_{pi}\}$ apply Equation (4.11) to $\mathbf{h}$ and $\mathbf{D}$. If no combination of $\mathbf{h}$ and $\mathbf{D}$ satisfies Equation 4.11, $\{\mathbf{D}_{pi}\}$ represents the set of true product sequences (category 2a).

Finally, we need to deal with categories 1b and 2b. Consider the ternary system Figure 4-8. Three sequences satisfy Properties 1, 2, and 3: $\mathbf{P}_1 =$ {L,I,I-H}, $\mathbf{P}_2 =$ {L,I-H,L-I-H}, and $\mathbf{P}_3 =$ {L,H,L-I-H}. The 2-simplices formed from these three sequences are not properly joined, since the simplex formed from $\mathbf{P}_2$ and $\mathbf{P}_3$ intersect. In fact, batch distillation region B_3 (bounded by the straight lines connecting L, I, I-H, and L-I-H) is an exception where the simplex bounded by the product compositions does not coincide with the batch distillation region itself. However, $\mathbf{P}_1$, $\mathbf{P}_2$, and $\mathbf{P}_3$ are all true product sequences.

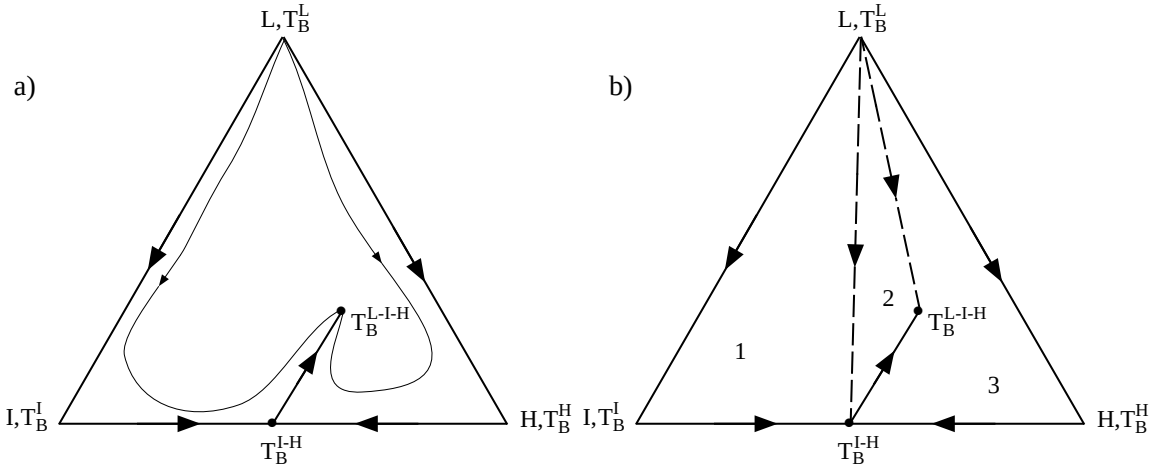

Figure 4-8: Intersecting product simplices. The order of boiling temperatures: $T_B^{L,m} < T_B^{I,n} < T_B^{H,n} < T_B^{L-I,n} < T_B^{L-I-H,q}$.

On the other hand, consider the ternary system in Figure 4-9. In Figure 4-9 there are five batch distillation regions, and hence five feasible product sequences represented by $\mathbf{P}_1 =$ {m1,n1,n3}, $\mathbf{P}_2 =$ {m1,n2,q1}, $\mathbf{P}_3 =$ {m1,n3,q1}, $\mathbf{P}_4 =$ {m2,n2,q1}, and $\mathbf{P}_5 =$ {m2,n3,q1}. In Figure 4-9b the position of the stable node q1 has changed.

However, note that the topological structure of the system, and hence the unstable boundary limit sets have not changed. The sequence of points {m1,n3,q1} satisfies all three properties above. Nevertheless, {m1,n3,q1} does not correspond to a product sequence. Looking closely at this map, it is found that no composition point would give rise to sequence {m1,n3,q1}, but rather one of the other sequences. Consequently, this map only has four batch distillation regions.

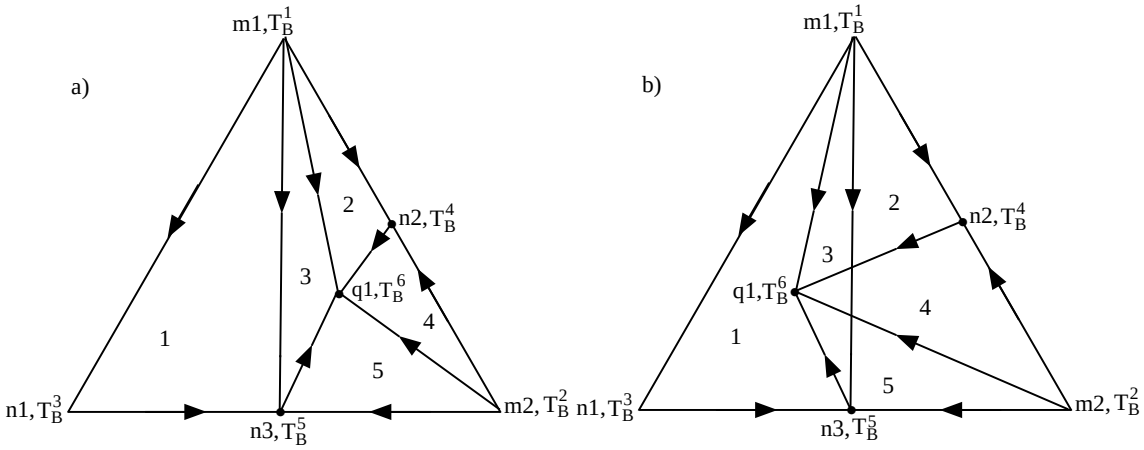

Figure 4-9: a) Five batch distillation regions. b) Four batch distillation regions.

An additional property may therefore be formulated:

Property 4 *For a* $(nc-1)$*-simplex to be a product simplex one or more composition points must give rise to the corresponding sequence of* nc *fixed points when batch distillation is applied. These composition points will form the respective batch distillation region and lie internal to the simplex.*

In fact, observe that Property 4 supplies both necessary and sufficient conditions to characterize a product simplex: following Definition 2-1, the composition points that give rise to the same product sequence form a batch distillation region. The product simplex formed by the nc product cuts coincides or is greater than the respective batch distillation region. Hence, in order for an $(nc-1)$-simplex to be a product simplex, it must contain the respective batch distillation region.

However, Properties 1, 2, and 3 are easier to use, and when the product simplices are properly joined, these three properties are both necessary and sufficient to char-

acterize a product sequence and to enumerate all the true product sequences. When the simplices are not properly joined Properties 1, 2, and 3 only supply necessary conditions to characterize a product sequence. From the many systems we have studied we believe that the following procedure is sufficient to eliminate the simplices that satisfy Properties 1, 2, and 3, but not Property 4, although a proof is currently lacking.

Let $\{\mathbf{\Delta}_{pi}\}$ represent the set of simplices satisfying Properties 1, 2, and 3. Furthermore, let $\{\mathbf{\Delta}_{pi}^{npj}\} \subset \{\mathbf{\Delta}_{pi}\}$ represent the set of simplices for which $\mathbf{h}$ results in positive barycentric coordinates. The simplices containing $\mathbf{h}$ will intersect $\{\mathbf{\Delta}_{pi}^{npj}\}$. Let $\{\mathbf{\Delta}_{pi}^{h}\}$ represent this set of simplices. We are left with determining if one or more of the simplices in $\{\mathbf{\Delta}_{pi}^{h}\}$ does not satisfy Property 4, and hence is not a product simplex, but rather of the type illustrated by Figure 4-9b. Such a simplex is characterized as being a subset of $\{\mathbf{\Delta}_{pi}^{npj}\}$: a simplex in $\{\mathbf{\Delta}_{pi}^{h}\}$ which shares all its vertices except $\mathbf{h}$ with $\{\mathbf{\Delta}_{pi}^{npj}\}$ is a subset of $\{\mathbf{\Delta}_{pi}^{npj}\}$. In addition, there must be at least two other simplices in $\{\mathbf{\Delta}_{pj}^{h}\}$. Remove simplices satisfying these characteristics from $\{\mathbf{\Delta}_{pi}\}$. Enumeration of all product simplices in the system is complete.

4.3 Example: Ternary System

The following example serves to demonstrate the procedure for enumerating the product sequences when the system belongs to category 2b in the previous section. The compositions of the fixed points in the ternary system are listed in Table 4.2, and the unstable boundary limit sets are listed in Table 4.3. For clarity, the composition simplex is shown in Figure 4-10. Observe that the ternary system exhibits a similar topological structure to the one shown in Figure 4-9.

Solving the PDAG problem results in the set $\{\mathbf{D}\}$: $\mathbf{D}_1 = \{$A, C, BC$\}$, $\mathbf{D}_2 = \{$A, AB, ABC$\}$, $\mathbf{D}_3 = \{$A, BC, ABC$\}$, $\mathbf{D}_4 = \{$B, BC, ABC$\}$, and $\mathbf{D}_5 = \{$B, AB, ABC$\}$.

It is found that the respective three points in each of the sets above form a 2-simplex. Therefore, $\{\mathbf{\Delta}_{pi}\} = \{\mathbf{\Delta}_1, \mathbf{\Delta}_2, \mathbf{\Delta}_3, \mathbf{\Delta}_4, \mathbf{\Delta}_5\}$, where $\mathbf{\Delta}_i$ is the 2-simplex formed from the fixed points in $\mathbf{D}_i$. Next, we need to determine whether the 2-

Table 4.2: Fixed points in ternary system.

e	A	B	C
A	1	0	0
B	0	1	0
C	0	0	1
AB	0.5	0.5	0
BC	0	0.6	0.4
ABC	0.3	0.2	0.5

Table 4.3: Unstable boundary limit sets.

e	$\overline{\omega}^u(\mathbf{x}_e^*)$
A	C, AB, BC, ABC
B	AB, BC, ABC
C	BC
AB	ABC
BC	ABC
ABC	$\emptyset$

simplices in $\{\mathbf{\Delta}_{pi}\}$ are properly joined. Let $\{\mathbf{h}_i\}$ represent the set of fixed points that are not in the set $\mathbf{D}_i$. Then $\{\mathbf{h}_1\}$ = {B, AB, ABC}, $\{\mathbf{h}_2\}$ = {B, BC, C}, $\{\mathbf{h}_3\}$ = {B, AB, C}, $\{\mathbf{h}_4\}$ = {A, AB, C}, and $\{\mathbf{h}_5\}$ = {A, BC, C}. Table 4.4 shows the barycentric coordinates computed when Equation 4.11 is applied to $\mathbf{D}_i$ and every $\mathbf{h}_i \in \{\mathbf{h}_i\}$.

Table 4.4 shows that the ternary azeotrope ABC is located inside $\mathbf{\Delta}_1$. Hence, the simplices are not properly joined, and $\{\mathbf{\Delta}_{pi}^{npj}\} = \{\mathbf{\Delta}_1\}$. Furthermore, $\{\mathbf{\Delta}_{pi}^{ABC}\} = \{\mathbf{\Delta}_2, \mathbf{\Delta}_3, \mathbf{\Delta}_4, \mathbf{\Delta}_5\}$. We find that $\mathbf{\Delta}_3$ is a subset of $\mathbf{\Delta}_1$, because $\mathbf{D}_1 \cap \mathbf{D}_3$ = ABC. In addition, there are three more simplices in $\{\mathbf{\Delta}_{pi}^{ABC}\}$. Consequently, simplex $\mathbf{\Delta}_3$ should be removed from $\{\mathbf{\Delta}_{pi}\}$. The true product sequences are $\mathbf{D}_1$, $\mathbf{D}_2$, $\mathbf{D}_4$, and $\mathbf{D}_5$.

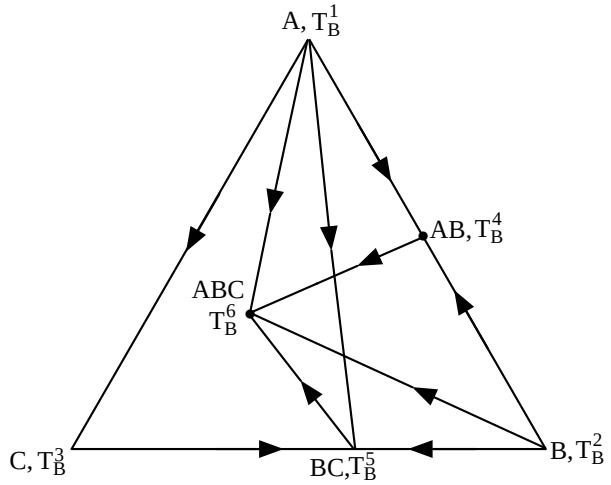

Figure 4-10: Composition simplex with batch distillation regions for the ternary system.

Table 4.4: Barycentric coordinates.

	$\mathbf{D}_1$				$\mathbf{D}_2$				$\mathbf{D}_3$		
$\mathbf{h}_1$	f_A	f_C	f_{BC}	$\mathbf{h}_2$	f_A	f_{AB}	f_{ABC}	$\mathbf{h}_3$	f_A	f_{BC}	f_{ABC}
B	0	-0.67	1.66	B	-1	2	0	B	0.55	2.27	-1.82
AB	0.5	-0.33	0.83	BC	-0.68	0.88	0.8	AB	0.77	1.14	-0.91
ABC	0.3	0.37	0.33	C	-0.2	-0.8	2	C	-0.82	-0.91	2.72

	$\mathbf{D}_4$				$\mathbf{D}_5$			
$\mathbf{h}_4$	f_B	f_{BC}	f_{ABC}	$\mathbf{h}_5$	f_B	f_{AB}	f_{ABC}	
A	1.83	-4.17	3.33	A	-1	2	0	
AB	1.42	-2.08	1.67	BC	0.68	-0.48	0.9	
C	-1.5	2.5	0	C	0.2	-1.2	2	

4.4 Example: Five-Component System

The algorithm for constructing the composition simplex in Figure 4-1 was employed to the system acetone (A), chloroform (C), methanol (M), ethanol (E), and benzene (B) at 1 atmosphere. The fixed points in this system are taken from Fidkowski *et al.* (1993) and are shown in Table 4.5.

The unstable boundary limit set matrix is initialized by applying the procedure in Section 4.1.4. The binary edges are then completed. The resulting matrix is given in Table 4.6. The rows and columns represent the fixed points ordered according to

Table 4.5: Compositions, boiling temperatures, and stability of fixed points for the system acetone, chloroform, methanol, ethanol, and benzene at 1 atmosphere.

e	A	C	M	E	B	T_B[K]	Type
CM	0	0.6481	0.3519	0	0	327.06	un
AM	0.7944	0	0.2056	0	0	328.49	un
A	1	0	0	0	0	329.22	s
ACMB	0.2259	0.16	0.4849	0	0.1282	330.61	s
ACM	0.3234	0.2236	0.4530	0	0	330.73	s
MB	0	0	0.6162	0	0.3838	331.27	s
CE	0	0.8536	0	0.1464	0	333.08	s
C	0	1	0	0	0	334.94	s
ACE	0.3383	0.4642	0	0.1967	0	337.04	s
M	0	0	1	0	0	337.69	s
AC	0.3437	0.6563	0	0	0	338.62	s
EB	0	0	0	0.4514	0.5486	340.98	s
E	0	0	0	1	0	351.44	sn
B	0	0	0	0	1	353.25	sn

boiling temperature.

The five-component system has ten ternary subsystems and five quaternary subsystems. Figure 4-11 shows the ternary and quaternary subsystems that need to be analyzed before the unstable boundary limit sets of the global system can be completed. Observe that a ternary system only needs to be analyzed once even if it appears in several of the quaternary systems.

In order to complete the boundary limit sets of each subsystem, the stability of the fixed points in every subsystem has to be determined. Since unstable and stable nodes in a particular system will remain unstable and stable in all its subsystems, only the fixed points that are saddle points in the five-component system need to be reevaluated in the quaternary subsystems. Likewise, only fixed points that are saddle points in a quaternary system need to be reevaluated in its ternary subsystems. Tables 4.7 and 4.8 list the stability of the fixed points in the ternary and quaternary systems.

Each of the ternary subsystems were analyzed, and the boundary limit sets completed. The elements with value equal to 1 were copied into the unstable boundary limit set matrices for the quaternary systems. Tables 4.9, 4.10, 4.11, and 4.12 give

Table 4.6: The initialized unstable boundary limit matrix for the five-component system with completed binary edges.

	CM	AM	A	ACMB	ACM	MB	CE	C	ACE	M	AC	EB	E	B
CM	0	-1	-1	-1	-1	-1	-1	1	-1	1	-1	-1	-1	-1
AM	0	0	1	-1	-1	-1	-1	-1	-1	1	-1	-1	-1	-1
A	0	0	0	-1	-1	-1	-1	-1	-1	-1	1	-1	1	1
ACMB	0	0	0	0	-1	-1	-1	-1	-1	-1	-1	-1	-1	-1
ACM	0	0	0	0	0	-1	-1	-1	-1	-1	-1	-1	-1	-1
MB	0	0	0	0	0	0	-1	-1	-1	1	-1	-1	-1	1
CE	0	0	0	0	0	0	0	1	-1	-1	-1	-1	1	-1
C	0	0	0	0	0	0	0	0	-1	-1	1	-1	-1	1
ACE	0	0	0	0	0	0	0	0	0	-1	-1	-1	-1	-1
M	0	0	0	0	0	0	0	0	0	0	-1	-1	1	-1
AC	0	0	0	0	0	0	0	0	0	0	0	-1	-1	-1
EB	0	0	0	0	0	0	0	0	0	0	0	0	1	1
E	0	0	0	0	0	0	0	0	0	0	0	0	0	0
B	0	0	0	0	0	0	0	0	0	0	0	0	0	0

the completed unstable boundary limit set matrices for the quaternary subsystems I_2^4, I_3^4, I_4^4, and I_5^4. Table 4.13 gives the incomplete unstable boundary limit set matrix for system I_1^4. The completion of the matrix for I_1^4 will be discussed in more detail below.

There are two unstable nodes in I_1^4, CM and AM. The unstable boundary limit sets of CM and AM were completed by applying the procedure in Figure 4-6. Since CE is an element of $\overline{\omega}^u$(CM) and ACE is an element of $\overline{\omega}^u$(CE), ACE must also be an element of $\overline{\omega}^u$(CM). ACE was therefore added to $\overline{\omega}^u$(CM). Also, since A is an element of $\overline{\omega}^u$(AM) and ACE is an element of $\overline{\omega}^u$(A), ACE must be an element of $\overline{\omega}^u$(AM). ACE was therefore added to $\overline{\omega}^u$(AM). Next, the common unstable boundary limit set was determined (see Equation (4.12)). The subscript in $\overline{\omega}_{41}^{uc}(\mathrm{CM},\mathrm{AM})$ indicates that this is the common unstable boundary limit set for system I_1^4:

$$\begin{aligned} \overline{\omega}_{41}^{uc}(\mathrm{CM},\mathrm{AM}) &= \{\mathrm{ACM,CE,C,ACE,M,AC,E}\} \cap \\ &\quad \{\mathrm{A,ACM,ACE,M,AC,E}\} \\ &= \{\mathrm{ACM,ACE,M,AC,E}\} \end{aligned} \tag{4.12}$$

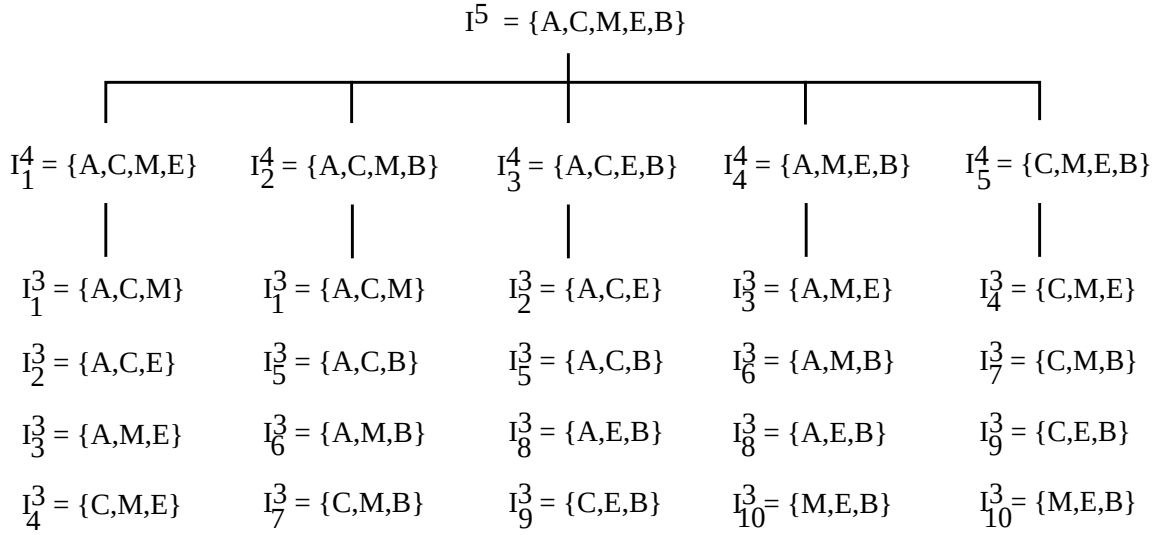

Figure 4-11: The five-component global system with all ternary and quaternary subsystems that need to be analyzed.

The local stability of the fixed points in $\overline{\omega}^{uc}$(CM, AM) on SDB_{41}(CM,AM) was found using Equations (4.9) and (4.10). It was determined that ACM is an unstable node, ACE and M are saddle points, and AC and E are stable nodes. Hence, ACE, M, AC, and E must be elements of $\overline{\omega}^{u}$(ACM). The completed matrix for the quaternary system I_1^4 is shown in Table 4.14.

The elements with values equal to 1 were copied into the unstable boundary limit set matrix for the global system (I^5). The unstable boundary limit sets of the unstable nodes (CM and AM) were completed by applying the procedure in Figure 4-6. However, no new elements needed to be added. Table 4.15 gives the incomplete unstable boundary limit set matrix for I^5 before the stable dividing boundary was analyzed.

The common unstable boundary limit set $\overline{\omega}_5^{uc}$(CM,AM) was determined (see Equation (4.13)).

$$\begin{aligned} \overline{\omega}_5^{uc}(\mathrm{CM},\mathrm{AM}) &= \{\mathrm{ACMB,ACM,MB,CE,C,ACE,M,AC,EB,E,B}\} \cap \\ &\quad \{\mathrm{A,ACMB,ACM,MB,ACE,M,AC,EB,E,B}\} \\ &= \{\mathrm{ACMB,ACM,MB,ACE,M,AC,EB,E,B}\} \end{aligned} \tag{4.13}$$

Table 4.7: Stability of fixed points in ternary subsystems. * indicates that the fixed point is not present in the system.

	CM	AM	A	ACMB	ACM	MB	CE	C	ACE	M	AC	EB	E	B
I_1^3	un	un	s	*	s	*	*	s	*	sn	sn	*	*	*
I_2^3	*	*	un	*	*	*	un	s	s	*	sn	*	sn	*
I_3^3	*	un	s	*	*	*	*	*	*	s	*	*	sn	*
I_4^3	un	*	*	*	*	*	s	sn	*	s	*	*	sn	*
I_5^3	*	*	un	*	*	*	*	un	*	*	s	*	*	sn
I_6^3	*	un	s	*	*	s	*	*	*	sn	*	*	*	sn
I_7^3	un	*	*	*	*	s	*	s	*	sn	*	*	*	sn
I_8^3	*	*	un	*	*	*	*	*	*	*	*	s	sn	sn
I_9^3	*	*	*	*	*	*	un	s	*	*	*	s	sn	sn
I_{10}^3	*	*	*	*	*	un	*	*	*	s	*	s	sn	sn

Table 4.8: Stability of fixed points in quaternary subsystems. * indicates that the fixed point is not present in the system.

	CM	AM	A	ACMB	ACM	MB	CE	C	ACE	M	AC	EB	E	B
I_1^4	un	un	s	*	s	*	s	s	s	s	sn	*	sn	*
I_2^4	un	un	s	s	s	s	*	s	*	sn	s	*	*	sn
I_3^4	*	*	un	*	*	*	un	s	s	*	s	s	sn	sn
I_4^4	*	un	s	*	*	s	*	*	*	s	*	s	sn	sn
I_5^4	un	*	*	*	*	s	s	s	*	s	*	s	sn	sn

The local stability of the fixed points in $\overline{\omega}_5^{uc}(\mathrm{CM}, \mathrm{AM})$ on SDB_5(CM,AM) was found using Equations (4.9) and (4.10). It was determined that ACMB is an unstable node, ACM, MB, ACE, M, AC, and EB are saddle points, and E and B are stable nodes. Hence, ACM, MB, ACE, M, AC, EB, E, and B must be elements of $\overline{\omega}^u$(ACMB). The remaining elements in the unstable boundary limit set matrix were set to zero. The completed matrix for the five-component system I^5 is shown in Table 4.16.

A directed graph based on the matrix in Table 4.16 was generated. Applying the algorithm in Section 4.2 twenty-five product sequences with five product cuts were found. It is determined that the 4-simplices formed from these sequences are properly

Table 4.9: The completed boundary limit set matrix for system I_2^4.

	CM	AM	A	ACMB	ACM	MB	C	M	AC	B
CM	0	0	-1	1	1	1	1	1	1	1
AM	0	0	1	1	1	1	-1	1	1	1
A	0	0	0	-1	-1	-1	-1	-1	1	1
ACMB	0	0	0	0	1	1	-1	1	1	1
ACM	0	0	0	0	0	-1	-1	1	1	-1
MB	0	0	0	0	0	0	-1	1	-1	1
C	0	0	0	0	0	0	0	-1	1	1
M	0	0	0	0	0	0	0	0	0	0
AC	0	0	0	0	0	0	0	0	0	1
B	0	0	0	0	0	0	0	0	0	0

Table 4.10: The completed boundary limit set matrix for system I_3^4.

	A	CE	C	ACE	AC	EB	E	B
A	0	0	-1	1	1	1	1	1
CE	0	0	1	1	1	1	1	1
C	0	0	0	-1	1	-1	-1	1
ACE	0	0	0	0	1	1	1	1
AC	0	0	0	0	0	-1	-1	1
EB	0	0	0	0	0	0	1	1
E	0	0	0	0	0	0	0	0
B	0	0	0	0	0	0	0	0

joined. Hence, they represent the true product sequences. The product sequences are shown in Figure 4-12 and are also listed in Table 4.17. 13 sequences start with CM, and 12 sequences will produce AM as the first cut.

4.5 Summary

An algorithm for characterizing the batch distillation composition simplex is described. Construction of the batch distillation composition simplex is accomplished through completion of the unstable boundary limit sets. The completed unstable boundary limit sets accurately represent the topological structure of the composition simplex, and also makes it possible to extract all product sequences achievable when

Table 4.11: The completed boundary limit set matrix for system I_4^4.

	AM	A	MB	M	EB	E	B
AM	0	1	1	1	1	1	1
A	0	0	-1	-1	1	1	1
MB	0	0	0	1	1	1	1
M	0	0	0	0	-1	1	-1
EB	0	0	0	0	0	1	1
E	0	0	0	0	0	0	0
B	0	0	0	0	0	0	0

Table 4.12: The completed boundary limit set matrix for system I_5^4.

	CM	MB	CE	C	M	EB	E	B
CM	0	1	1	1	1	1	1	1
MB	0	0	-1	-1	1	1	1	1
CE	0	0	0	1	-1	1	1	1
C	0	0	0	0	-1	-1	-1	1
M	0	0	0	0	0	-1	1	-1
EB	0	0	0	0	0	0	1	1
E	0	0	0	0	0	0	0	0
B	0	0	0	0	0	0	0	0

applying batch distillation. The derived algorithm is guaranteed to find the correct unstable boundary limit sets for all fixed points in the system provided that the system itself and all its subsystems have at most two unstable and at most two stable nodes, and that a stable dividing boundary locally exhibits at most two unstable and at most two stable nodes. This restriction ensures that the system is globally determined, i.e., topological requirements of the composition simplex given by the compositions, boiling temperatures, and stability of each fixed point can be met by a unique combination of unstable boundary limit sets. The topological structures included in the algorithm are divided into eleven systems, and are characterized by the number of unstable and stable nodes, and whether the system exhibits an azeotrope involving all components. Other important properties are also demonstrated. In particular:

Table 4.13: The incomplete boundary limit set matrix for system I_1^4.

	CM	AM	A	ACM	CE	C	ACE	M	AC	E
CM	0	0	-1	1	1	1	-1	1	1	1
AM	0	0	1	1	-1	-1	-1	1	1	1
A	0	0	0	-1	-1	-1	1	-1	1	1
ACM	0	0	0	0	-1	-1	-1	1	1	-1
CE	0	0	0	0	0	1	1	-1	1	1
C	0	0	0	0	0	0	-1	-1	1	-1
ACE	0	0	0	0	0	0	-1	-1	1	1
M	0	0	0	0	0	0	0	0	-1	1
AC	0	0	0	0	0	0	0	0	0	0
E	0	0	0	0	0	0	0	0	0	0

Table 4.14: The completed boundary limit set matrix for system I_1^4.

	CM	AM	A	ACM	CE	C	ACE	M	AC	E
CM	0	0	-1	1	1	1	1	1	1	1
AM	0	0	1	1	-1	-1	1	1	1	1
A	0	0	0	-1	-1	-1	1	-1	1	1
ACM	0	0	0	0	-1	-1	1	1	1	1
CE	0	0	0	0	0	1	1	-1	1	1
C	0	0	0	0	0	0	-1	-1	1	-1
ACE	0	0	0	0	0	0	0	-1	1	1
M	0	0	0	0	0	0	0	0	-1	1
AC	0	0	0	0	0	0	0	0	0	0
E	0	0	0	0	0	0	0	0	0	0

- In a system with two unstable nodes the unstable manifolds of the unstable nodes are separated by a *stable dividing boundary*. The boundary is characterized by the *common unstable boundary limit set*, i.e., the fixed points located on the boundary.

- If a system has only one unstable node, the unstable node's unstable boundary limit set will contain all the other fixed points in the system.

- A saddle point involving all components cannot exist in a system with only one unstable or stable node.

Table 4.15: The unstable boundary limit set matrix for the global system before the stable dividing boundary is analyzed.

	CM	AM	A	ACMB	ACM	MB	CE	C	ACE	M	AC	EB	E	B
CM	0	0	0	1	1	1	1	1	1	1	1	1	1	1
AM	0	0	1	1	1	1	0	0	1	1	1	1	1	1
A	0	0	0	0	0	0	0	0	1	0	1	1	1	1
ACMB	0	0	0	0	-1	-1	-1	-1	-1	-1	-1	-1	-1	-1
ACM	0	0	0	0	0	-1	-1	-1	1	1	1	-1	1	-1
MB	0	0	0	0	0	0	-1	-1	-1	1	-1	1	1	1
CE	0	0	0	0	0	0	0	1	1	-1	1	1	1	1
C	0	0	0	0	0	0	0	0	-1	-1	1	-1	-1	1
ACE	0	0	0	0	0	0	0	0	0	-1	1	1	1	1
M	0	0	0	0	0	0	0	0	0	0	-1	-1	1	-1
AC	0	0	0	0	0	0	0	0	0	0	0	-1	-1	1
EB	0	0	0	0	0	0	0	0	0	0	0	0	1	1
E	0	0	0	0	0	0	0	0	0	0	0	0	0	0
B	0	0	0	0	0	0	0	0	0	0	0	0	0	0

- If a system features two unstable nodes, two stable nodes, and a saddle point involving all the components, the saddle point must be in the unstable boundary limit sets of both unstable nodes, and in the stable boundary limit sets of both stable nodes.

- If a system contains three or more unstable nodes, two stable nodes, (or *vice versa*)and a saddle point involving all components the system is globally undetermined.

- If a system and all its subsystems can be characterized as having at most two unstable nodes and at most two stable nodes the unstable boundary limit sets of fixed point $\mathbf{x}_j^*$ is a subset of the unstable boundary limit set of unstable node $\mathbf{x}_{m_a}^*$, provided that $\mathbf{x}_j^*$ is an element of the unstable boundary limit set of $\mathbf{x}_{m_a}^*$.

The algorithm for constructing the composition simplex is applied to the five-component system acetone, chloroform, methanol, ethanol, and benzene. The system exhibits 9 azeotropes. The unstable boundary limit sets for the fixed points are completed. Furthermore, 25 product sequences are enumerated.

Table 4.16: The completed unstable boundary limit matrix for the five-component system.

	CM	AM	A	ACMB	ACM	MB	CE	C	ACE	M	AC	EB	E	B
CM	0	0	0	1	1	1	1	1	1	1	1	1	1	1
AM	0	0	1	1	1	1	0	0	1	1	1	1	1	1
A	0	0	0	0	0	0	0	0	1	0	1	1	1	1
ACMB	0	0	0	0	1	1	0	0	1	1	1	1	1	1
ACM	0	0	0	0	0	0	0	0	1	1	1	0	1	0
MB	0	0	0	0	0	0	0	0	0	1	0	1	1	1
CE	0	0	0	0	0	0	0	1	1	0	1	1	1	1
C	0	0	0	0	0	0	0	0	0	0	1	0	0	1
ACE	0	0	0	0	0	0	0	0	0	0	1	1	1	1
M	0	0	0	0	0	0	0	0	0	0	0	0	1	0
AC	0	0	0	0	0	0	0	0	0	0	0	0	0	1
EB	0	0	0	0	0	0	0	0	0	0	0	0	1	1
E	0	0	0	0	0	0	0	0	0	0	0	0	0	0
B	0	0	0	0	0	0	0	0	0	0	0	0	0	0

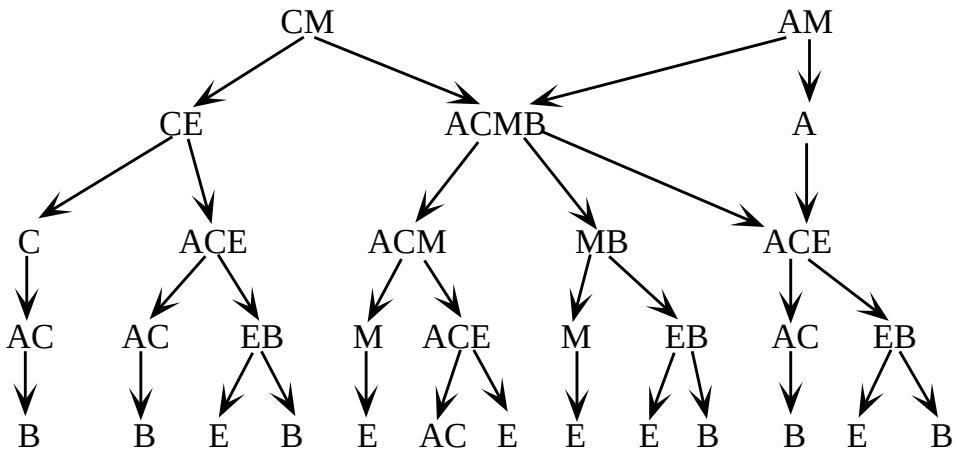

Figure 4-12: 25 product sequences with five product cuts.

Table 4.17: 25 product sequences with five product cuts.

b	Product sequence	b	Product sequence
1	{CM,ACMB,ACM,ACE,AC}	14	{AM, ACMB,ACM,ACE,AC}
2	{CM,ACMB,ACM,ACE,E}	15	{AM,ACMB,ACM,ACE,E}
3	{CM,ACMB,ACM,M,E}	16	{AM,ACMB,ACM,M,E}
4	{CM,ACMB,MB,M,E}	17	{AM,ACMB,MB,M,E}
5	{CM,ACMB,MB,EB,E}	18	{AM,ACMB,MB,EB,E}
6	{CM,ACMB,MB,EB,B}	19	{AM,ACMB,MB,EB,B}
7	{CM,ACMB,ACE,AC,B}	20	{AM,ACMB,ACE,AC,B}
8	{CM,ACMB,ACE,EB,E}	21	{AM,ACMB,ACE,EB,E}
9	{CM,ACMB,ACE,EB,B}	22	{AM,ACMB,ACE,EB,B}
10	{CM,CE,C,AC,B}	23	{AM,A,ACE,AC,B}
11	{CM,CE,ACE,AC,B}	24	{AM,A,ACE,EB,E}
12	{CM,CE,ACE,EB,E}	25	{AM,A,ACE,EB,B}
13	{CM,CE,ACE,EB,B}		

Chapter 5

Solvent Recovery Targeting

In this chapter, we show that the algorithm for characterizing the batch distillation composition simplex for a system with an arbitrary number of components can be exploited in a sequential design strategy where process streams or mixed waste-solvent streams are analyzed for maximum feasible solvent recovery using a targeting approach. We will term this procedure *solvent recovery targeting*. Solvent recovery targeting yields an understanding of the barriers to solvent recovery created by a particular design, e.g., the existence of a particular azeotrope in solvent mixtures. This information can then be used to modify the design, aiming at enhanced solvent recovery and recycling.

We present the application of solvent recovery targeting to two case studies. The first case study is a siloxane monomer process. We will demonstrate that significantly lower emission levels can be achieved by integrating recovery and recycling of solvent as part of the process flowsheet. Furthermore, we will show that dynamic simulation models can be exploited to evaluate proposed process alternatives with respect to effects on the reaction chemistry from recycling intermediates. In particular, models yield detailed insight when designing integrated operating policies to increase yield and selectivity while minimizing formation of undesired byproducts. In the second case study the production of a carbinol is analyzed. Solvent recovery targeting is used to assess several possible process modifications to improve solvent recovery. In particular, evaluation of alternative solvents is emphasized.

5.1 Approach

For a given base case, solvent recovery targeting will, given the composition of the mixture(s) to be separated, predict the correct distillation sequence and calculate the maximum feasible recovery of each product cut in the sequence. It can further provide information about all other feasible distillation sequences involving the same set of pure components. This information is used to evaluate the feasibility of enhancing solvent recovery in the proposed flowsheet. If necessary, the original design is modified, and the targeting approach is next applied to the new process streams to evaluate the modifications. The general structure of solvent recovery targeting is outlined in Figure 5-1. Analyzing the stream for maximum recovery involves two tasks: 1) locating the stream composition in the correct batch distillation region, and 2) calculating the amounts recovered in each product cut. In the subsequent sections the different steps are described.

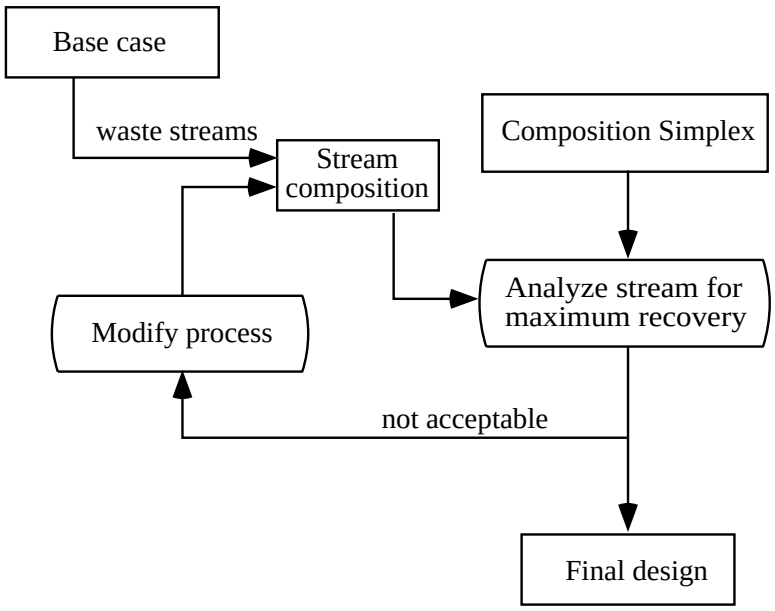

Figure 5-1: Solvent recovery targeting.

5.2 Locate Initial Composition

Let $\mathbf{P} = \{\mathbf{p}_0, \mathbf{p}_1, \ldots, \mathbf{p}_{nc-1}\}$ represent the sequence of product cuts resulting from any composition located in batch distillation region B. From the definition of batch distillation regions (Definition 2-1 in Chapter 2) it follows that if the initial composition of interest ($\mathbf{x}^{p,0}$) is located in batch distillation region B it must also be located in product simplex $\mathbf{\Pi}^{nc}$ formed from the nc fixed points in $\mathbf{P}$. Note that the notation $\mathbf{\Pi}^{nc}$ refers to a product simplex formed from nc fixed points. Furthermore, $\mathbf{\Pi}^{nc}$ is a $(nc-1)$-geometric simplex. Hence, $\mathbf{x}^{p,0}$ must satisfy Equations (5.1) with respect to $\mathbf{\Pi}^{nc}$:

$$\mathbf{\Pi}^{nc} = \{\mathbf{x} \in \mathbf{R}^{nc} : \mathbf{x} = \sum_{k=0}^{nc-1} f_k \mathbf{p}_k;\ f_k \geq 0\ \ \forall k = 0, \ldots, nc-1 \text{ and } \sum_{k=0}^{nc-1} f_k = 1\} \quad (5.1)$$

where $f_k\ \ \forall k = 0, \ldots, nc-1$ are barycentric coordinates. The element p_{ki} represents the molefraction of pure component i in product cut k in the nc vector $\mathbf{p}_k$. Physically, the scalars f_k represent the fractions of $\mathbf{x}^{p,0}$ that will be recovered in each product cut using batch distillation under the limiting conditions. The fact that both $\mathbf{x}^{p,0}$ and the set of points $\{\mathbf{p}_k\ \ \forall k = 0, \ldots, nc-1\}$ lie in the hyperplane $\sum_{i=1}^{nc} x_i = 1$ implies that the criterion $\sum_{k=0}^{nc-1} f_k = 1$ is satisfied. If one or more $f_k = 0$ this implies that $\mathbf{x}^{p,0}$ lies on one of the faces of $\mathbf{\Pi}^{nc}$.

Any composition in the composition space will yield a unique product sequence. However, since the batch distillation regions fill the composition simplex, and a product simplex will either coincide or be larger than its batch distillation region, two or more product simplices can possibly intersect. In that case, two or more product simplices will satisfy Equations (5.1) for the same initial composition. In general, applying Equations (5.1) to initial composition $\mathbf{x}^{p,0}$ may yield three different outcomes depending on the location of $\mathbf{x}^{p,0}$:

1. One of the batch distillation regions satisfies Equations (5.1). Hence, there is only one positive product simplex, and, consequently, the correct product sequence is found.

2. More than one batch distillation region satisfies Equations (5.1), and the predicted product sequences will produce the same unstable node in the first cut.

3. More than one batch distillation region satisfies Equations (5.1), and the predicted product sequences will give rise to different unstable nodes in the first cut.

To illustrate the possible outcomes, consider the ternary system in Figure 5-2a. The system has four batch distillation regions and therefore four product sequences, represented by $\mathbf{P}_1$ = {m1,n1,n3}, $\mathbf{P}_2$ = {m1,n2,q1}, $\mathbf{P}_3$ = {m2,n2,q1}, and $\mathbf{P}_4$ = {m2,n3,q1}. $\mathbf{P}_1$ and $\mathbf{P}_2$ have the unstable node m1 in common, while $\mathbf{P}_3$ and $\mathbf{P}_4$ have m2 in common. Product simplex $\mathbf{\Pi}_1^3$ intersects product simplices $\mathbf{\Pi}_2^3$, $\mathbf{\Pi}_3^3$, and $\mathbf{\Pi}_4^3$. The intersections are represented by the domains 2a, 3a, and 4a, respectively. If $\mathbf{x}^{p,0}$ is located in domains 1, 2b, 3b, or 4b outcome 1 above will result, if $\mathbf{x}^{p,0}$ is located in domain 2a outcome 2 above will result, and if $\mathbf{x}^{p,0}$ is located in domains 3a or 4a outcome 3 will result. If outcome 2 or 3 is encountered further examination is required in order to determine the correct product sequence.

5.2.1 Product Sequences that have an Unstable Node in Common

Consider the ternary system in Figure 5-3. The system has four batch distillation regions (see Figure 5-3b). Hence four product simplices can be generated, defined by $\mathbf{\Pi}_1^3$: $\mathbf{P}_1$ = {m1,n1,n3}, $\mathbf{\Pi}_2^3$: $\mathbf{P}_2$ = {m1,n4,q1}, $\mathbf{\Pi}_3^3$: $\mathbf{P}_3$ = {m1,n3,n4}, and $\mathbf{\Pi}_4^3$: $\mathbf{P}_4$ = {m1,n2,n4} as indicated in Figure 5-3c. They all have the unstable node m1 in common. One of the facets of $\mathbf{\Pi}_3^3$ intersects the stable separatrix connecting the binary azeotrope n4 and the ternary azeotrope at the point t. The composition simplex can therefore be divided into five domains (see Figure 5-3d). When applying Equations (5.1) five possible scenarios can take place depending on the location of the initial composition. The different scenarios are summarized in Table 5.1.

Correct prediction of the true product sequence can be confirmed by placing $\mathbf{x}^{p,0}$ anywhere in the composition space, and then drawing a straight line through $\mathbf{x}^{p,0}$

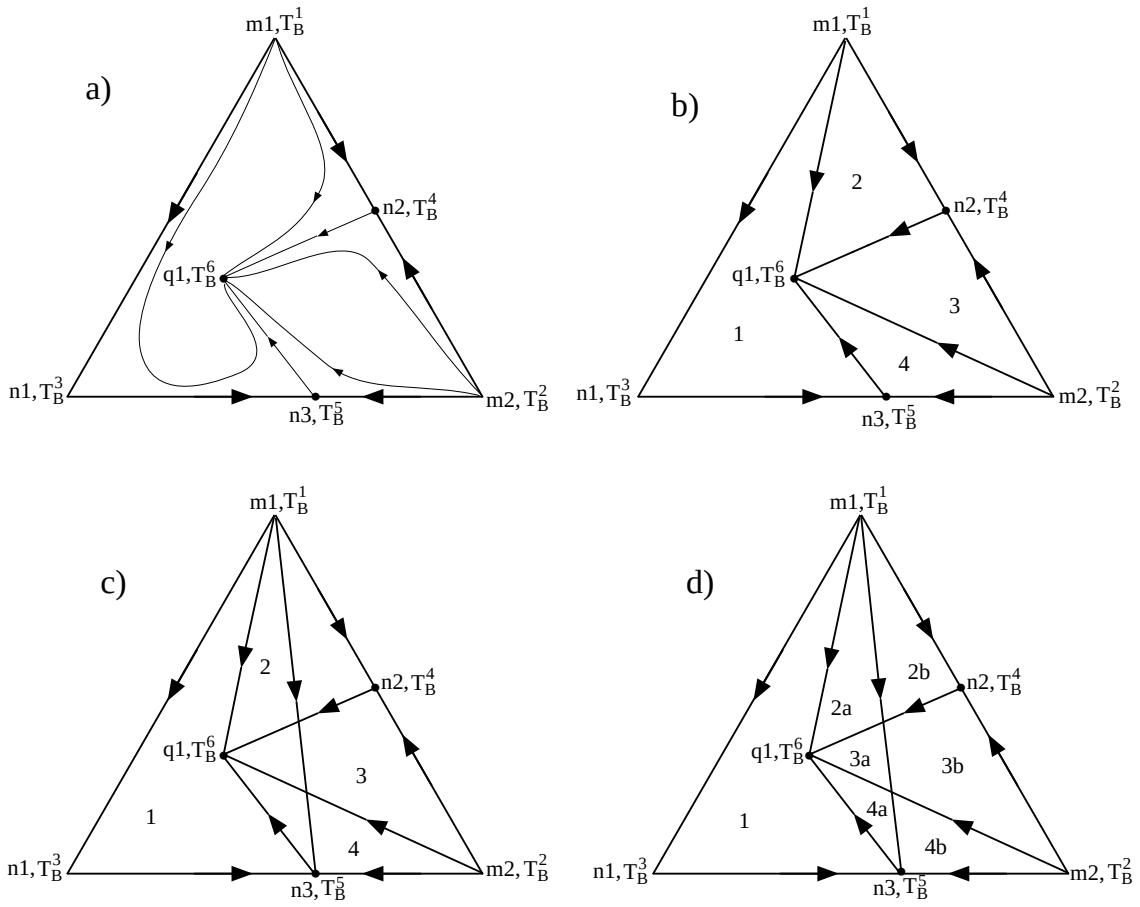

Figure 5-2: Ternary system with intersecting product simplices. a) Simple distillation residue curve map. b) Batch distillation regions. c) Product simplices. d) Intersecting domains.

Case	Location of $\mathbf{x}^{p,0}$	Positive product simplex	True product sequence
1	B_1	$\mathbf{\Pi}_1^3$	$\mathbf{P}_1$
2	B_{2a}	$\mathbf{\Pi}_1^3$, $\mathbf{\Pi}_2^3$	$\mathbf{P}_2$
3	B_{2b}	$\mathbf{\Pi}_2^3$, $\mathbf{\Pi}_3^3$	$\mathbf{P}_2$
4	B_3	$\mathbf{\Pi}_3^3$	$\mathbf{P}_3$
5	B_4	$\mathbf{\Pi}_4^3$	$\mathbf{P}_4$

Table 5.1: Possible scenarios when testing for positive barycentric coordinates.

and m1. The pot composition path will move along this line away from m1 until it encounters a *pot composition boundary* (see Chapter 3). In scenario 3 the pot composition path intersects the pot composition boundary connecting n4 and q1 as

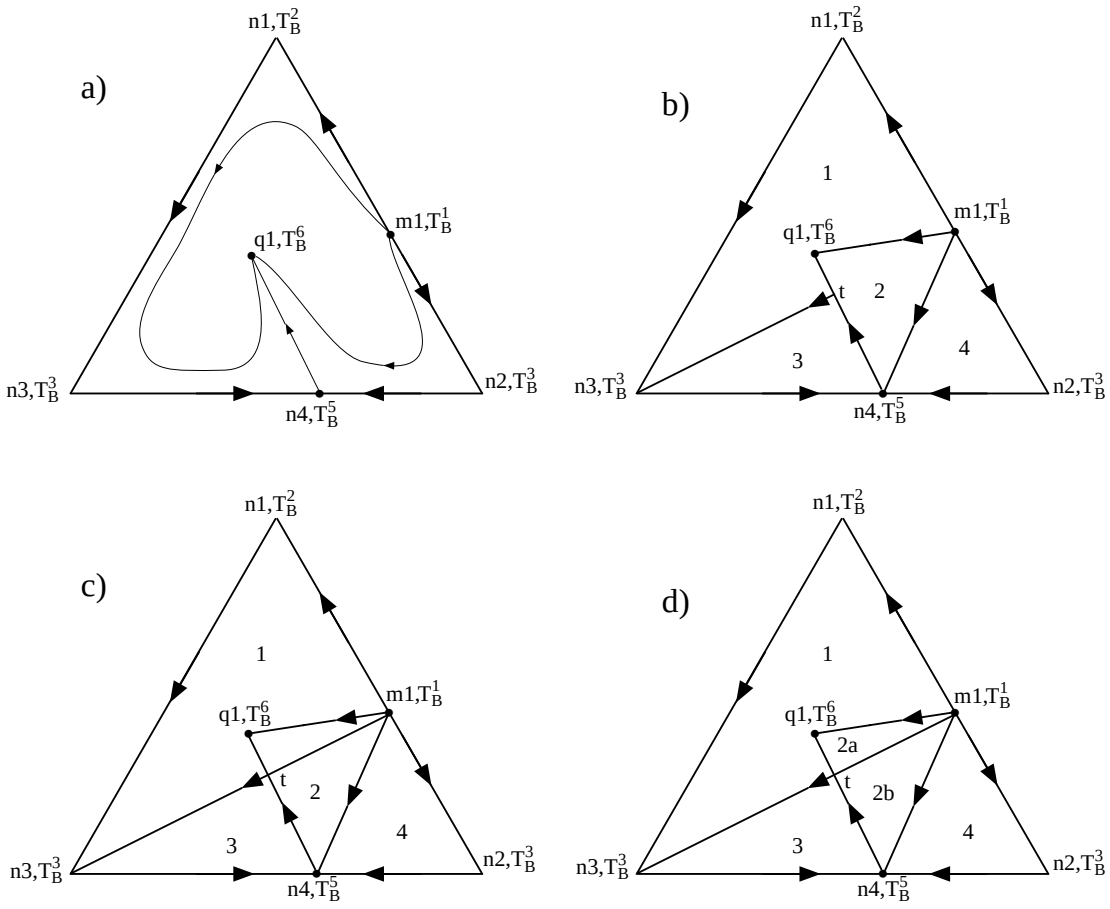

Figure 5-3: Ternary system with intersecting product simplices: a) Simple distillation residue curve map. b) Batch distillation regions. c) Product simplices. d) Intersecting domains.

illustrated by Figure 5-4. The point of intersection is $\mathbf{x}^{1a}$. Further, the line can be extended until it intersects the pot composition boundary connecting n3 and n4 at $\mathbf{x}^{1b}$. The true product sequence is the set of fixed points $\mathbf{P}$ resulting from the batch distillation region that contains the *active pot composition boundary*, defined as the pot composition boundary that is encountered first. *Product simplex boundary* $\hat{\mathbf{\Pi}}^{nc-1}$ of product simplex $\mathbf{\Pi}^{nc}$ is the facet opposite the unstable node $\mathbf{p}_0$, and will be used to approximate the pot composition boundary, in the same manner product simplices are used to approximate batch distillation regions. $\hat{\mathbf{\Pi}}^{nc-1}$ is defined by $nc-1$ vectors formed from the $nc-1$ fixed points that remain when the unstable node is removed from $\mathbf{P}$. Since it is assumed that the pot composition boundary is linear, i.e., either

located on a facet, or a stable dividing boundary and the fixed points located on the pot composition boundary lie on a hyperplane, this approximation is an accurate representation of the actual distance. Obviously, if the number of fixed points located on the pot composition boundary is equal to $nc-1$, the pot composition boundary is linear and equal to the corresponding product simplex boundary. In the case that the number of fixed points on the pot composition boundary is greater than $nc-1$, the approximation may result in an overestimation of the distance. This is because the product simplex either coincide or is greater than its corresponding batch distillation region. However, an overestimation of the distance implies that the pot composition boundary is smaller than its corresponding product simplex boundary, and hence the batch distillation region is smaller than its corresponding product simplex. Therefore, it is not the active batch distillation region.

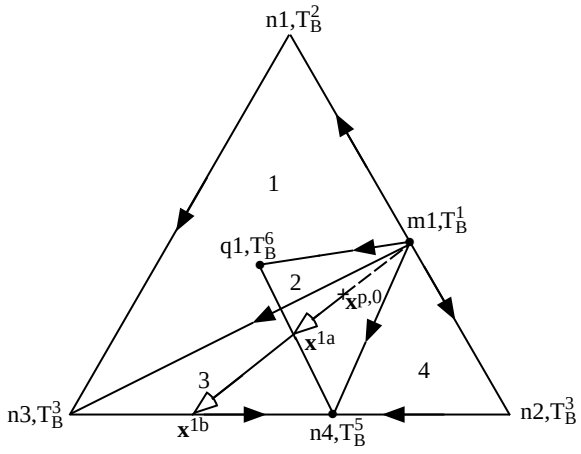

Figure 5-4: The true product sequence is determined by the active pot composition boundary.

Consider Figure 5-5. It shows a product simplex for a quaternary mixture projected into $\mathbf{R}^3$. The relation to the origin ($\mathbf{x} = (0,0,0,0)^T$) is indicated for clarity. The initial composition is defined by:

$$\mathbf{x}^{p,0} = f_0\mathbf{p}_0 + \sum_{k=1}^{nc-1} f_k\mathbf{p}_k = f_0\mathbf{p}_0 + (1-f_0)\mathbf{x}^{p,1} \tag{5.2}$$

where $f_k \ \ \forall k \in \{0,\ldots,nc-1\}$ are the barycentric coordinates from Equations (5.1).

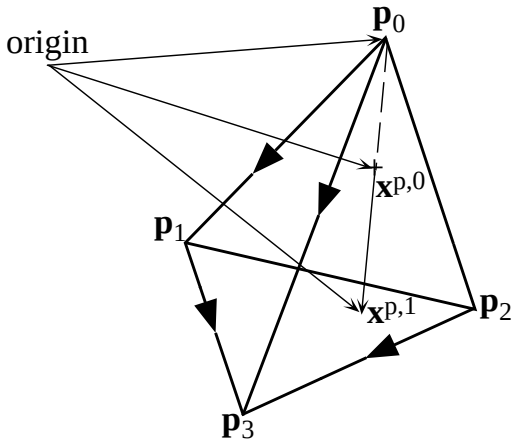

Figure 5-5: Identification of active product simplex boundary.

The intersection with the product simplex boundary (defined by $\mathbf{p}_1, \mathbf{p}_2,$ and $\mathbf{p}_3$) at $\mathbf{x}^{p,1}$ can be expressed in terms of the relative distance α, the number of times we need to take the vector $(\mathbf{x}^{p,0} - \mathbf{p}_0)$ in order to get from $\mathbf{p}_0$ to $\mathbf{x}^{p,1}$.

$$\mathbf{x}^{p,1} = \mathbf{p}_0 + \alpha(\mathbf{x}^{p,0} - \mathbf{p}_0) \tag{5.3}$$

Combining Equations (5.2) and (5.3) results in a simple relationship between α and f_0:

$$\alpha = \frac{1}{1 - f_0} \tag{5.4}$$

Hence, the relative distance to the product simplex boundary can be measured in terms of the barycentric coordinate, f_0, for the first product cut. The larger α is, the further away from the initial composition is $\mathbf{x}^{p,1}$. In order to determine the true product sequence, it is therefore sufficient to compare the barycentric coordinates f_0^s for the positive product simplices. The true product simplex is thus $\mathbf{\Pi}_*^{nc}$ for which

$$f_0^* = \text{MIN}\{f_0^s \;\; \forall s \in \{\text{positive product simplices}\}\} \tag{5.5}$$

If Equation (5.5) does not give a unique minimum, i.e., $f_0^s = f_0^* \; \forall s \in \{$positive product simplices$\}$, then either the product simplex boundaries for the positive prod-

uct simplices are located on the same facet, or on the stable dividing boundary and the stable dividing boundary is linear (i.e., the fixed points in the common unstable boundary limit set are located on a hyperplane). In either case, the product simplex boundaries intersect, in the same manner product simplices may intersect. In order to determine the true product sequence Equation (5.5) has to be repeated by replacing f_0^s with f_1^s.

5.2.2 Product Sequences that do not have an Unstable Node in Common

Clearly, this behavior can only be observed in a system with two unstable nodes, and hence a stable dividing boundary. The correct product sequence is the one for which the unstable node lies on the same side of the stable dividing boundary as the initial composition. Consider Figure 5-6. The stable dividing boundary is composed of the straight lines between n3 and q1 and n2 and q1.

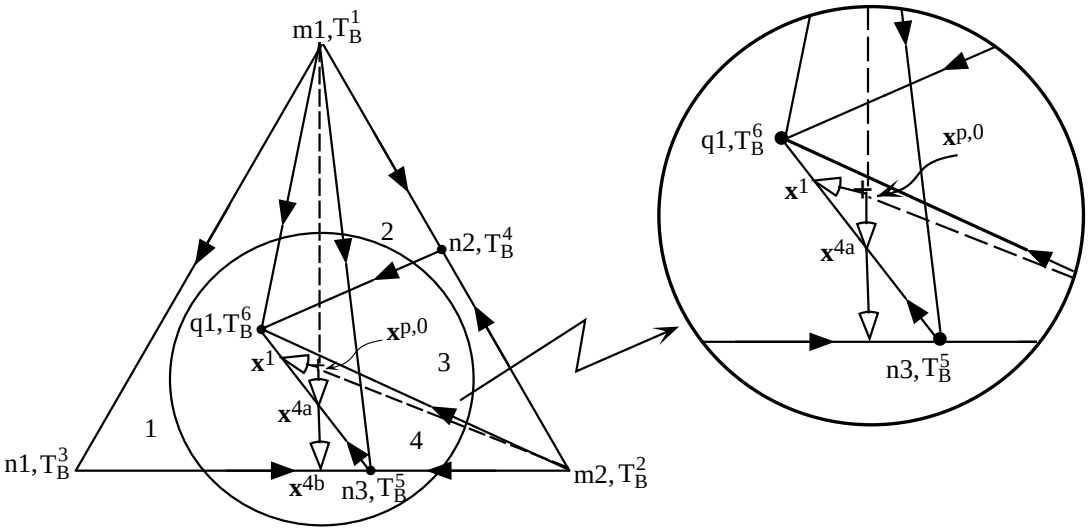

Figure 5-6: Identification of true product sequence.

Both product simplices 1 and 4 will generate positive barycentric coordinates when applying Equations (5.1) to the initial composition $\mathbf{x}^{p,0}$, although $\mathbf{x}^{p,0}$ is truly located in batch distillation region 4. The correct product sequence can be determined by drawing straight lines through $\mathbf{x}^{p,0}$ and each of the unstable nodes, and extending

these lines until they intersect the respective pot composition boundaries of batch distillation regions 1 and 4 ($\mathbf{x}^1$ and $\mathbf{x}^{4b}$). The line from $\mathbf{x}^{p,0}$ to the intersection represents the path the pot composition orbit would travel during distillation of the first product cut (with composition equal to the unstable node). Observe that the line from $\mathbf{x}^{p,0}$ to $\mathbf{x}^{4b}$ also intersects the line connecting n3 and q1, which is part of the stable dividing boundary, at $\mathbf{x}^{4a}$. The path from $\mathbf{x}^{p,0}$ to $\mathbf{x}^{4b}$ is therefore infeasible, and $\mathbf{x}^{p,0}$ cannot give rise to sequence {m1,n1,n3}.

Consider Figure 5-7. It shows product simplex 1 and the stable dividing boundary extracted from Figure 5-6. The stable dividing boundary can be divided into two pot composition boundaries, approximated by product simplex boundaries $\hat{\mathbf{\Pi}}_a^2$: $\hat{\mathbf{P}}_a$ = {n2,q1}, and $\hat{\mathbf{\Pi}}_b^2$: $\hat{\mathbf{P}}_b$ = {n3,q1}. Also note that two 2-simplices (a and b) have been constructed by adding the unstable node m1 to the sets $\hat{\mathbf{P}}_a$ and $\hat{\mathbf{P}}_b$. We can therefore find the relative distance (α_{sdb}) (see Figure 5-8), the number of times we need to take the vector ($\mathbf{x}^{p,0} - \text{m1}$) in order to get from $\mathbf{x}^{p,0}$ to the stable dividing boundary simply by computing the barycentric coordinates for the two simplices with respect to $\mathbf{x}^{p,0}$ and applying Equation (5.4). The relative distance from $\mathbf{x}^{p,0}$ to the pot composition boundary in batch distillation region 1 (α_{ppb}) (approximated by the product simplex boundary formed by $\hat{\mathbf{P}}$ = {n1,n3}) can be computed in a similar manner. If the relative distance from $\mathbf{x}^{p,0}$ to the stable dividing boundary is smaller than the distance to the pot composition boundary in batch distillation region 1, the path from the initial composition to the pot composition boundary will intersect the stable dividing boundary. Since $\mathbf{x}^{p,0}$ is located in simplex a and in product simplex 1, f_0 computed for simplex b will be negative. It is therefore not necessary to compute α_{sdb} for simplex b since a negative f_0 implies that the pot composition would have to travel backwards to intersect $\hat{\mathbf{\Pi}}_b^2$.

The general procedure goes as follows: let $\mathbf{x}_{m_a}^*$ and $\mathbf{x}_{m_b}^*$ represent the two unstable nodes in the system, and let $\mathbf{x}^{p,0}$ represent the initial composition. $\alpha_{\text{sdb}}^{m_i}$ represents the relative distance from the initial composition to the stable dividing boundary, and $\alpha_{\text{pps}}^{m_i}$ represents the relative distance from the initial composition to the product simplex boundary of a positive product simplex. The superscript m_i refers to unsta-

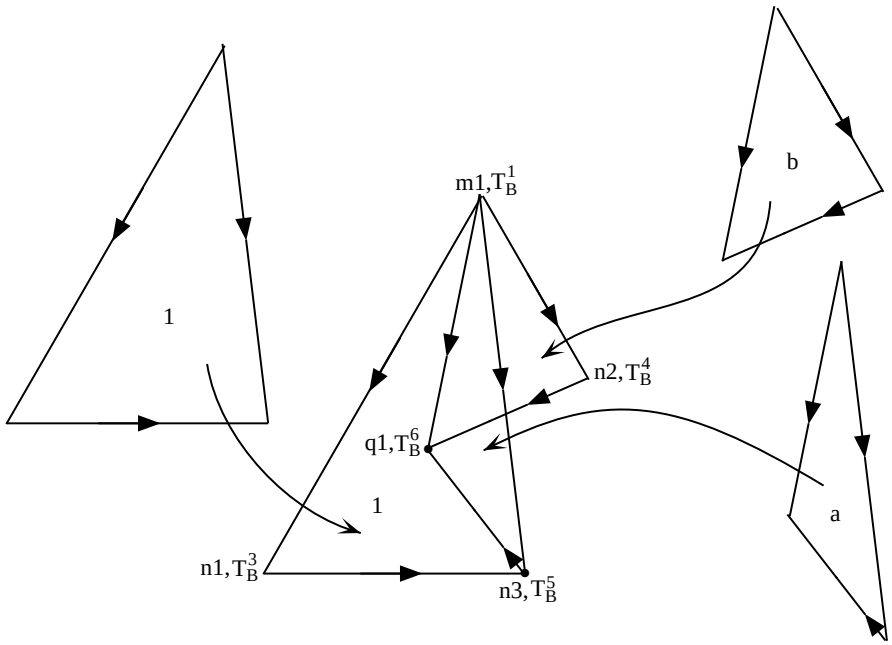

Figure 5-7: Construction of additional simplices.

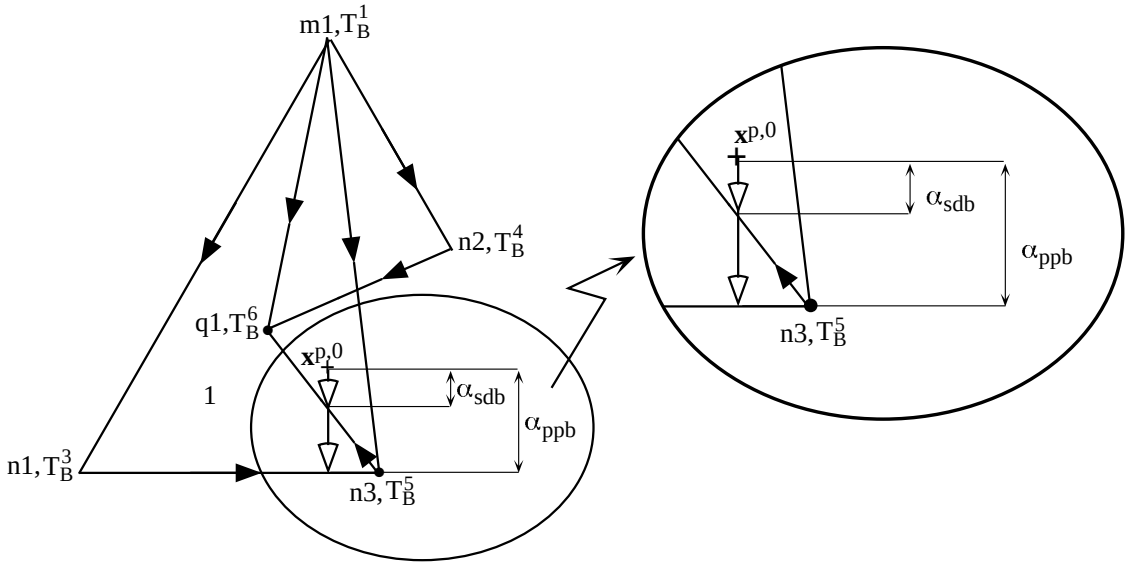

Figure 5-8: Calculation of relative distance from initial composition to intersection.

ble node m_i. The fixed points on the stable dividing boundaries are the points in $\overline{\omega}^{uc}(\mathbf{x}^*_{m_a}, \mathbf{x}^*_{m_b})$, the common unstable boundary limit set.

1. Divide $\overline{\omega}^{uc}(\mathbf{x}^*_{m_a}, \mathbf{x}^*_{m_b})$ into sets of $nc - 1$ points which each define a product simplex boundary. The product simplex boundaries will be used to approximate

the stable dividing boundary.

2. For each unstable node:

   (a) Construct sets of nc points by combining the unstable node with each of the sets of $nc-1$ points. Each set of nc points define an $(nc-1)$-simplex.

   (b) For all the simplices (both the positive product simplex and the new simplices) compute the barycentric coordinates by applying Equations (5.1) to $\mathbf{x}^{p,0}$.

   (c) Finally, compute $\alpha_{\text{sdb}}^{m_i}$ and $\alpha_{\text{ppb}}^{m_i}$ using Equation (5.4). Alternatively, apply Equation (5.5), where s now is the set of simplices (both the original positive product simplex and the new simplices) containing the same unstable node and which have positive barycentric coordinates.

   (d) If $\alpha_{\text{sdb}}^{m_i} < \alpha_{\text{ppb}}^{m_i}$, then $\mathbf{x}^{p,0}$ is not in the batch distillation region giving rise to $\mathbf{x}_{m_i}^{*}$ in the first cut.

The overall strategy for predicting the correct product sequence is summarized in Figure 5-9.

5.3 Calculating Maximum Recovery

Once the correct product sequence has been found the fractions of the initial mixed-solvent stream recovered in each cut must be calculated. Of course, if some of the species are very close boiling, we may not be able to achieve good separation no matter how many trays the column has, and no matter how high reflux ratio the column operates at. However, for the purpose of this work we assume that sharp splits are always obtained. This will give us the theoretical maximum flows - hence targeting.

The amounts recovered in each cut can be computed by solving a simple material

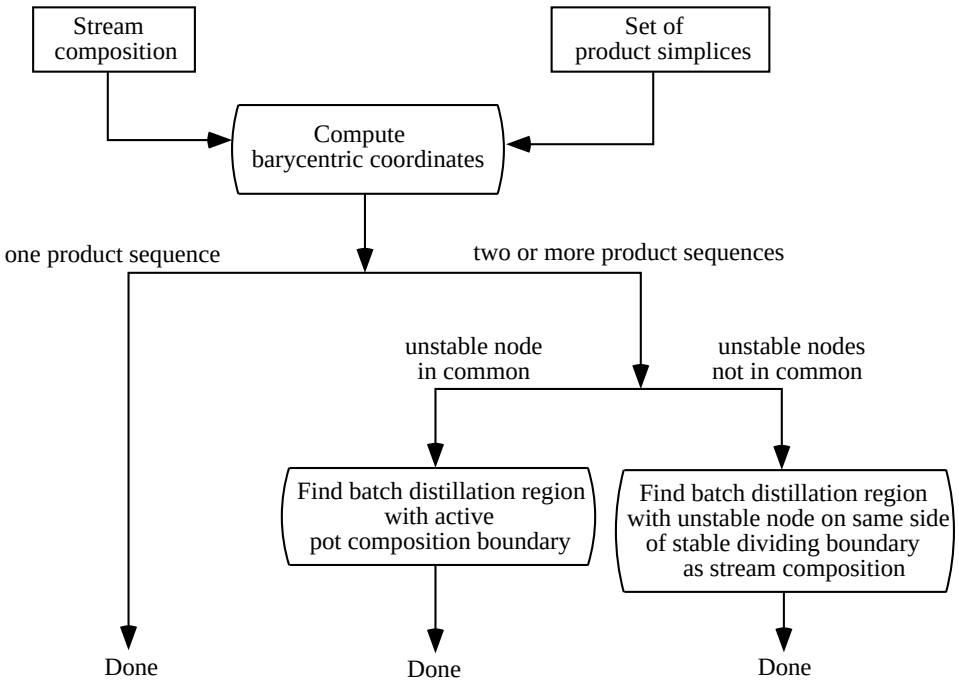

Figure 5-9: Strategy for predicting correct product sequence.

balance for each of the components present:

$$\mathbf{F}^{p,0} = \sum_{k=0}^{nc-1} \mathrm{F}_k \mathbf{p}_k;\ \mathrm{F}_k \geq 0 \ \ \forall k = 0, \ldots, nc-1 \tag{5.6}$$

$\mathrm{F}_i^{p,0}$ is the total number of component i initially in the reboiler, and F_k is the total number of moles recovered in product cut k. The material balance confirms that $\sum_{k=0}^{nc-1} \mathrm{F}_k = \sum_{i=1}^{nc} \mathrm{F}_i^{p,o} = \mathrm{F}^{p,0}$. Hence, we have nc equations and a set of nc unknowns $(\mathrm{F}_0, \mathrm{F}_1, \ldots, \mathrm{F}_{nc-1})$, and the system is therefore fully defined. Division by $\mathrm{F}^{p,0}$ results in equations similar in form to Equations 5.1. The recovered fractions are in fact the barycentric coordinates $f_k \ \ \forall k = 0, \ldots, nc-1$ already computed for locating the feed composition.

5.4 Ternary Example

The presented procedures for locating a stream composition and computing maximum recovery were applied to several ternary mixtures involving the same three compo-

nents. The ternary system is the same as the one in Section 4.3. The compositions of the fixed points in the ternary system can be found in Table 4.2, the composition simplex with the batch distillation regions is shown in Figure 4-10, and the unstable boundary limit sets are listed in Table 4.3. The four product sequences that were found in Section 4.3 are listed in Table 5.2.

Table 5.2: Product sequences in ternary system.

b	Product sequence
1	{A, C, BC}
2	{A, AB, ABC}
3	{B, AB, ABC}
4	{B, BC, ABC}

Three different stream compositions were tested: $\mathbf{x}_1^{p,0} = [0.2, 0.2, 0.6]^T$, $\mathbf{x}_2^{p,0} = [0.5, 0.2, 0.3]^T$, and $\mathbf{x}_3^{p,0} = [0.2, 0.4, 0.4]^T$. The barycentric coordinates were computed for each composition point by applying Equation 5.1 to the four constructed product simplices ($\mathbf{\Pi}_1^3$, $\mathbf{\Pi}_2^3$, $\mathbf{\Pi}_3^3$ and $\mathbf{\Pi}_4^3$). The values are listed in Table 5.3.

Table 5.3: Barycentric coordinates.

	$\mathbf{\Pi}_1^3$			$\mathbf{\Pi}_2^3$			$\mathbf{\Pi}_3^3$			$\mathbf{\Pi}_4^3$		
	f_A	f_C	f_{BC}	f_A	f_{AB}	f_{ABC}	f_B	f_{AB}	f_{ABC}	f_B	f_{BC}	f_{ABC}
$\mathbf{x}_1^{p,0}$	0.2	0.47	0.33	-0.12	-0.08	1.2	0.12	-0.32	1.2	-0.11	0.44	0.67
$\mathbf{x}_2^{p,0}$	0.5	0.17	0.33	0.24	0.16	0.6	-0.24	0.64	0.6	0.22	-0.89	1.67
$\mathbf{x}_3^{p,0}$	0.2	0.13	0.67	-0.28	0.48	0.8	0.28	-0.08	0.8	0.22	0.11	0.67

Composition point $\mathbf{x}_1^{p,0}$ results in positive barycentric coordinates for product simplex $\mathbf{\Pi}_1^3$ only. Hence, the correct product sequence is $\mathbf{P}_1$ = {A,C,BC}. The amounts recovered in each product cut can be extracted directly from Table 5.3. f_A is equal to 0.2, f_{BC} is equal to 0.47, and f_{BC} is equal to 0.33.

Composition point $\mathbf{x}_2^{p,0}$ results in positive barycentric coordinates for both product simplex $\mathbf{\Pi}_1^3$ and $\mathbf{\Pi}_2^3$. The respective product sequences share the same unstable node (A). We therefore need to determine which batch distillation region (B_1 or B_2)

contains the active batch distillation boundary. The relative distance to the boundary may be computed using Equation (5.4). Alternatively, Equation (5.5) may be applied directly to the barycentric coordinates for the first product cut. From Table 5.3 we find that $f_A^1 = 0.5$, while $f_A^2 = 0.24$. Consequently, batch distillation region 2 contains the active batch distillation boundary, and $\mathbf{x}_2^{p,0}$ will give rise to product sequence $\mathbf{P}_2 =$ {A,AB,ABC}. The fractions recovered of each product cut can be extracted directly from Table 5.3. f_A is equal to 0.24, f_{AB} is equal to 0.16, and f_{ABC} is equal to 0.6.

Composition point $\mathbf{x}_3^{p,0}$ results in positive barycentric coordinates for both product simplex $\mathbf{\Pi}_1^3$ and $\mathbf{\Pi}_4^3$. The respective product sequences do not share the same unstable node. Product sequence $\mathbf{P}_1$ has pure component A has its first product cut, while product sequence $\mathbf{P}_4$ has pure component B has its first product cut. We therefore need to determine which batch distillation region (B_1 or B_4) that has the unstable node on the same side of the stable dividing boundary as stream composition $\mathbf{x}_3^{p,0}$. This is done by performing the steps in Section 5.2.2.

The common unstable boundary limit set is determined from Table 4.3 using Equation (4.3) in Chapter 4:

$$\overline{\omega}^{uc}(\text{A,B}) = \{\text{C, AB, BC, ABC}\} \cap \{\text{AB, BC, ABC}\} = \{\text{AB, BC, ABC}\} \qquad (5.7)$$

The stable dividing boundary is approximated by the two product simplex boundaries $\hat{\mathbf{\Pi}}_2^2$ defined by $\hat{\mathbf{P}}_2 = \{\text{AB, ABC}\}$, and $\hat{\mathbf{\Pi}}_4^2$ defined by $\hat{\mathbf{P}}_4 = \{\text{BC, ABC}\}$. Hence, two new 2-simplices are generated by adding A as the first vertex, defined by the vertices $\mathbf{S}_a = \{\text{A, AB, ABC}\}$, and $\mathbf{S}_b = \{\text{A, BC, ABC}\}$. The barycentric coordinates are computed for these new simplices for $\mathbf{x}_3^{p,0}$. The values are shown in Table 5.4.

Table 5.4: Barycentric coordinates for $\mathbf{x}_3^{p,0}$.

	$\mathbf{\Pi}_1^3$			Simplex a			Simplex b		
	f_A	f_C	f_{BC}	f_A	f_C	f_{BC}	f_A	f_C	f_{BC}
$\mathbf{x}_3^{p,0}$	0.2	0.13	0.67	-0.28	0.48	0.8	0.091	0.55	0.36

Simplex a has some negative barycentric coordinates. We therefore only need to

compute the relative distances $\alpha^A_{\text{sdb},b}$ and α^A_{ppb}. This is done by applying Equation (5.4):

$$\alpha^A_{\text{sdb},b} = \frac{1}{1-0.091} = 1.1 \tag{5.8}$$

$$\alpha^A_{\text{ppb}} = \frac{1}{1-0.2} = 1.25 \tag{5.9}$$

$\alpha^A_{\text{sdb},b} < \alpha^A_{\text{ppb}}$. Hence, $\mathbf{x}_3^{p,0}$ is not located in batch distillation region 1. Consequently, it must be located in batch distillation region 4. For completeness, the procedure is repeated for unstable node B.

Two new 2-simplices are generated by adding unstable node B as the first vertex, defined by the vertices $\mathbf{S}_c = \{\text{B, AB, ABC}\}$, and $\mathbf{S}_d = \{\text{B, BC, ABC}\}$. The barycentric coordinates are computed for these new simplices for $\mathbf{x}_3^{p,0}$. The values are shown in Table 5.5.

Table 5.5: Barycentric coordinates for $\mathbf{x}_3^{p,0}$.

	$\mathbf{\Pi}_4^3$			Simplex c			Simplex d		
	f_B	f_{BC}	f_{ABC}	f_B	f_{BC}	f_{ABC}	f_B	f_{BC}	f_{ABC}
$\mathbf{x}_3^{p,0}$	0.22	0.11	0.67	0.28	-0.08	0.8	0.22	0.11	0.67

Simplex c has some negative barycentric coordinates. We therefore only need to compute the relative distances $\alpha^B_{\text{sdb},d}$ and α^B_{ppb}. This is done by applying Equation (5.4):

$$\alpha^B_{\text{sdb},d} = \frac{1}{1-0.22} = 1.28 \tag{5.10}$$

$$\alpha^B_{\text{ppb}} = \frac{1}{1-0.22} = 1.28 \tag{5.11}$$

$\alpha^B_{\text{sdb},d} = \alpha^B_{\text{ppb}}$. Hence, the result above is confirmed. The fractions recovered in each product cut can be extracted directly from Table 5.3. f_B is equal to 0.22, f_{BC} is equal to 0.11, and f_{ABC} is equal to 0.67. For clarity the locations of the composition points in the composition simplex are shown in Figure 5-10.

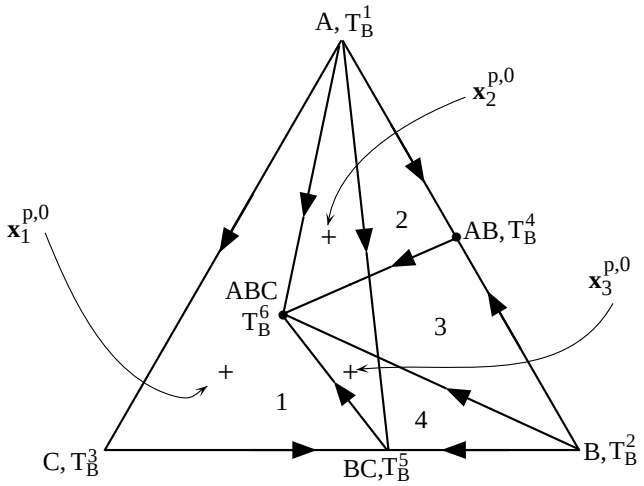

Figure 5-10: Locations of the composition points in the composition simplex.

5.5 Siloxane Monomer Process

Solvent recovery targeting is applied to the production of a siloxane based monomer in a single campaign (Figure 5-11). The process consists of several sequential reaction steps. Solvents and reaction by-products are separated from products through batch distillation. Further details concerning the process can be found in Allgor *et al.* (1996). The different unit operations were simulated using ABACUSS.[¶] The azeotropic behavior was approximated using the Wilson model to calculate the activity coefficients (see, for example, Reid *et al.* (1987)). Binary parameters were extracted from Aspen Plus (Aspen Technology, 1995). Missing binary parameters were estimated using the UNIFAC group contribution method (Fredenslund *et al.*, 1977) as implemented in Aspen Plus (Aspen Technology, 1995). Binary parameters for the pairs involving the non-standard components R2, C, E, A, and D can be found in Appendix D. R1 represents allyl alcohol. The vapor phase was assumed to be ideal. A batch size of 780 kg of product (A + D) was used as a basis for the simulations. The stream compositions for the base case are summarized in Appendix C.

There are two mixed waste-solvent streams generated in the process. Firstly, the

[¶]ABACUSS (Advanced Batch and Continuous Unsteady-State Simulator) Process Modeling Software, a derivative work of gPROMS Software, Copyright 1992 by the Imperial College of Science, Technology and Medicine.

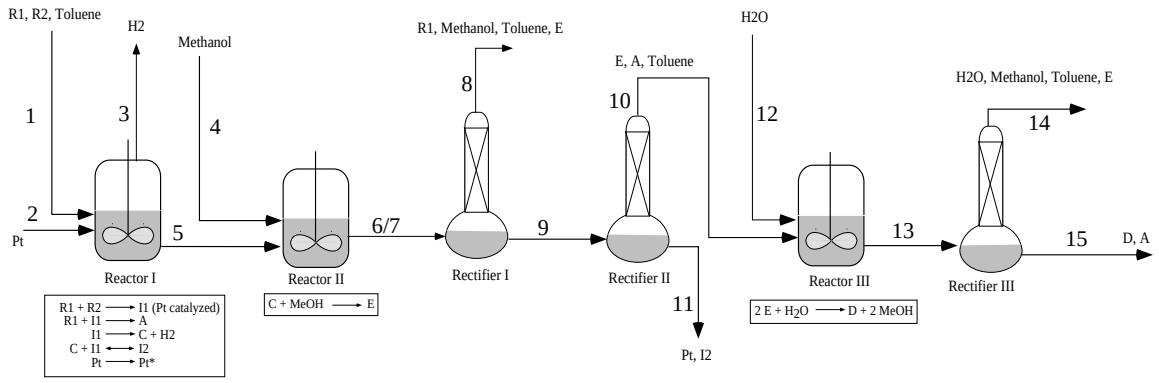

Figure 5-11: Siloxane monomer process: base case

stream leaving overhead from the first rectifier contains large amounts of toluene (T) and methanol (M), about 23% of the reactant R1, and small amounts of the intermediate E. The composition simplex for this system divided into batch distillation regions is presented in Figure 5-12. E is not included as there is very little of this intermediate present in the stream. Also, E does not form an azeotrope with any of the other components. The mixture exhibits a low-boiling binary azeotrope between methanol and toluene (M-T), and a low-boiling binary azeotrope between toluene and R1 (R1-T). There are three batch distillation regions present, each resulting in different product sequences with three cuts: $\mathbf{P}_1$ ={M-T,M,R1}, $\mathbf{P}_2$ ={M-T,R1-T,R1}, and $\mathbf{P}_3$ ={M-T,R1-T,T}. In this case the generated product simplices coincide with their respective batch regions. The initial composition places the stream in region 3. At the limit, 28% or about 2.4 kmol will be recovered as the methanol-toluene azeotrope, 34% or about 2.95 kmol as the R1-toluene azeotrope and 38% or 3.3 kmol as pure toluene. Hence only toluene can possibly be recovered as a pure component. Provided that the fraction of methanol in the R1-toluene cut is very small, this cut could probably be recycled back to reaction step I. To avoid premature reaction of C with methanol, methanol may not enter reaction step I. In addition, recycling of the methanol-toluene azeotrope to reaction step II will result in unacceptable build-up of toluene. Therefore, at least 28% of this stream (the methanol-toluene azeotrope) could not be recovered. In other words, at least 28% of the stream would end up as organic waste.

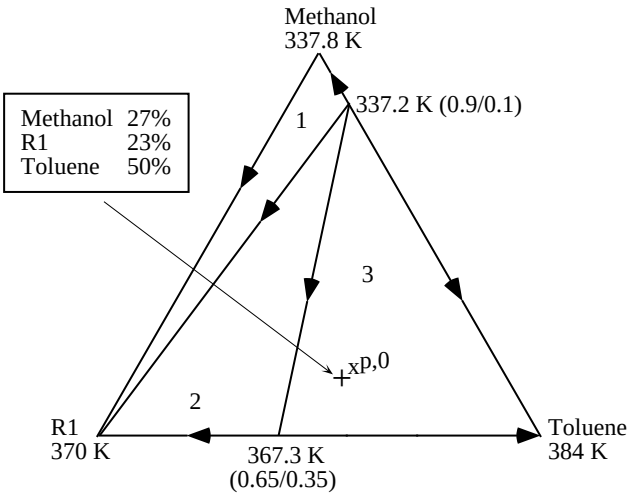

Figure 5-12: Composition simplex for the system methanol, R1, and toluene at 1 atmosphere.

Secondly, the aqueous stream leaving overhead from rectifier III contains about 95% water, and traces of toluene, methanol (formed in reaction step III), and intermediate E. It is assumed that the organic compounds would end up as organic waste. The stream is heterogeneous, forming a water-rich liquid phase and a toluene-rich liquid phase. The components also form three binary azeotropes, one between methanol and toluene, one between water and toluene, and one between water and E. The majority of the toluene and E could be removed in a decanter, while most of the remaining methanol in the aqueous phase could be removed through distillation. The estimated amount of organic waste from this stream is about 170 kg per batch, and the total amount of organic waste from the two mixed waste-solvent streams is 282 kg or about 5 kmol. Can we do better?

5.5.1 Process Alternative

By studying the composition simplices created for all the process streams, several process alternatives were generated. Only the most promising one will be discussed here, but it should be noted that there are other acceptable solutions.

Toluene and intermediate E are relatively narrow boiling, and it is therefore difficult to achieve a sharp split between these two components. Hence, in order to avoid

loss of intermediate E, a large fraction of toluene is left in the reboiler at the end of distillation I, and, consequently, toluene will remain with the product and not be removed until distillation III. This complicates solvent recovery since toluene forms a binary azeotrope with methanol. It was therefore proposed to introduce a batch distillation column between reaction step I and II as indicated in Figure 5-13. Three product cuts were proposed. Intermediate C is recovered for reaction step II, toluene and excess reactants are recycled back to reaction step I, and product A is purified. Methanol and C are recovered in rectifier II, and recycled directly back to reactor II. No toluene is carried through to the last column. The aqueous waste stream is therefore only contaminated with methanol which will greatly simplify the clean-up of the stream. The stream composition is about 45 kmol water and 1.3 kmol methanol. All the toluene is recovered and recycled, and there will be no toluene losses from the process. In fact, since the excess methanol from reaction step II is recycled, only the methanol generated in reaction step III (1.3 kmol) and removed in a water treatment facility will appear as organic waste. The total amount of organic waste is reduced by approximately 70% compared to the base case. Other improvements are also achieved: raw material is saved, and the load on downstream units is reduced.

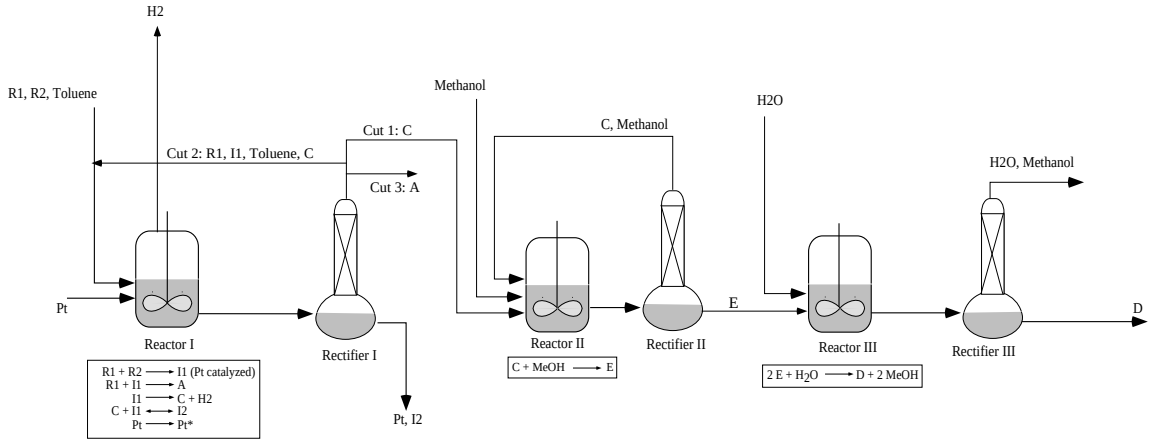

Figure 5-13: Process alternative

An analysis of the new composition simplex for the ternary system C, R1, and toluene indicates that there are two batch distillation regions from which intermediate C can be recovered as a pure species (see Figure 5-14).

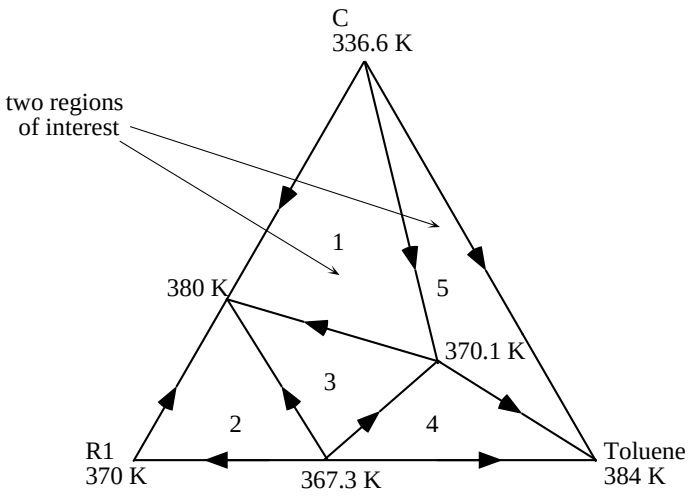

Figure 5-14: Residue curve map for the system toluene, R1, and C at 1 atmosphere.

However, C forms a binary azeotrope with R1 and a ternary azeotrope with R1 and toluene. Hence, while C can be recovered as a pure species, a large fraction of C will also be recycled back to reaction step I. Recycling of C will lead to build-up of C in the reactor to a *cyclic steady-state*[‡‡] concentration. A reversible reaction with C forms the undesired oligmer I2, and recycling of C will encourage formation of I2. Consequently, while solvent recovery targeting has determined that the proposed process modification is indeed feasible, it may not be acceptable as it could possibly lower the selectivity of A over C and increase the formation of undesired byproducts. A more detailed analysis of the effects of recycling C on the chemistry in reaction step I is essential. A feasibility study of the coupled system consisting of Reactor I, Rectifier I, and the recycle stream was therefore performed.

5.5.2 Dynamic Simulation of Coupled Reactor and Distillation Column

The feasibility study has several design objectives: the mixture leaving Reactor I must at cyclic steady-state be in either batch distillation region 1 or 5 to allow recovery of pure C. Also, the formation of undesired oligmer I2 must be minimized. The key

[‡‡]A cyclic dynamic system is said to have reached cyclic steady-state when the variable profiles over a cycle are the same from one cycle to the next.

design variables are the charge and temperature policies for the reactor which will control the amount of solvent and reagent at the end, the concentration of I1, and hence I2.

A dynamic model of the reactor and the column was created to predict the build-up of C in this recycle loop at cyclic steady-state (see Figure 5-15). The coupled reactor-distillation system was modeled using ABACUSS and applying the same models as in the base case calculations. Only the operating policies were modified. In the base case all of R1, R2, toluene, and platinum catalyst was charged at the same time. The mixture was heated to its boiling temperature. The heating jacket was then turned off and the exothermic reaction was allowed to continue until the amount of R1 or R2 was less then 0.1 mol. Once this criteria was met, the reaction was considered complete.

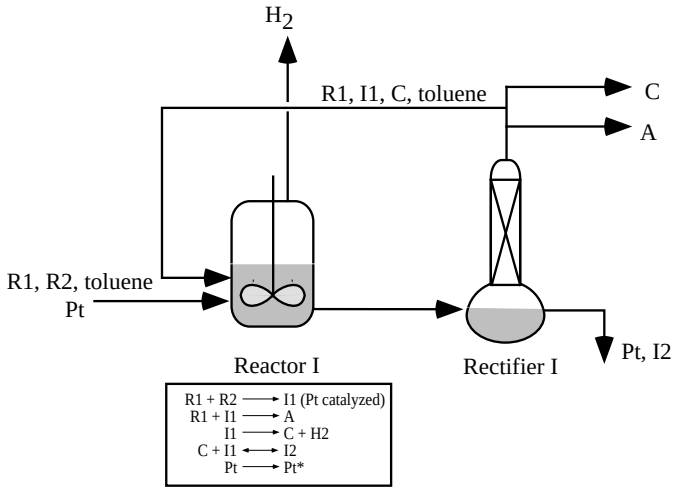

Figure 5-15: Model of coupled reactor and distillation column.

In the modified process all of R1 and toluene was charged initially. The mixture was heated to its boiling temperature and the heating jacket was turned off. The catalyst slurry was then added. Over the next two hours R2 was charged continuously to maintain a high R1/R2 ratio. This feed policy favors formation of A over C. The reaction was allowed to continue until the amount of R1 or R2 was less then 0.1 mol. In the subsequent cycles a stream consisting of R1, toluene, and C and small amounts of I1, R2, and A was recycled from the distillation column. The recycle

stream significantly decreased the amount of fresh R1 and toluene needed.

The composition profile in reaction step I reached cyclic steady-state after four cycles. Only a slight increase in the fraction of C was observed, while the fraction of A consequently was reduced with a similar amount. At cyclic steady-state 1.65 kmol of C and 2.71 kmol of A were produced, compared to 1.82 kmol of C and 2.1 kmol of A in the base case. No noticeable increase in the fraction of I2 was detected. The hold-up in reaction I over three cycles is shown in Figure 5-16.

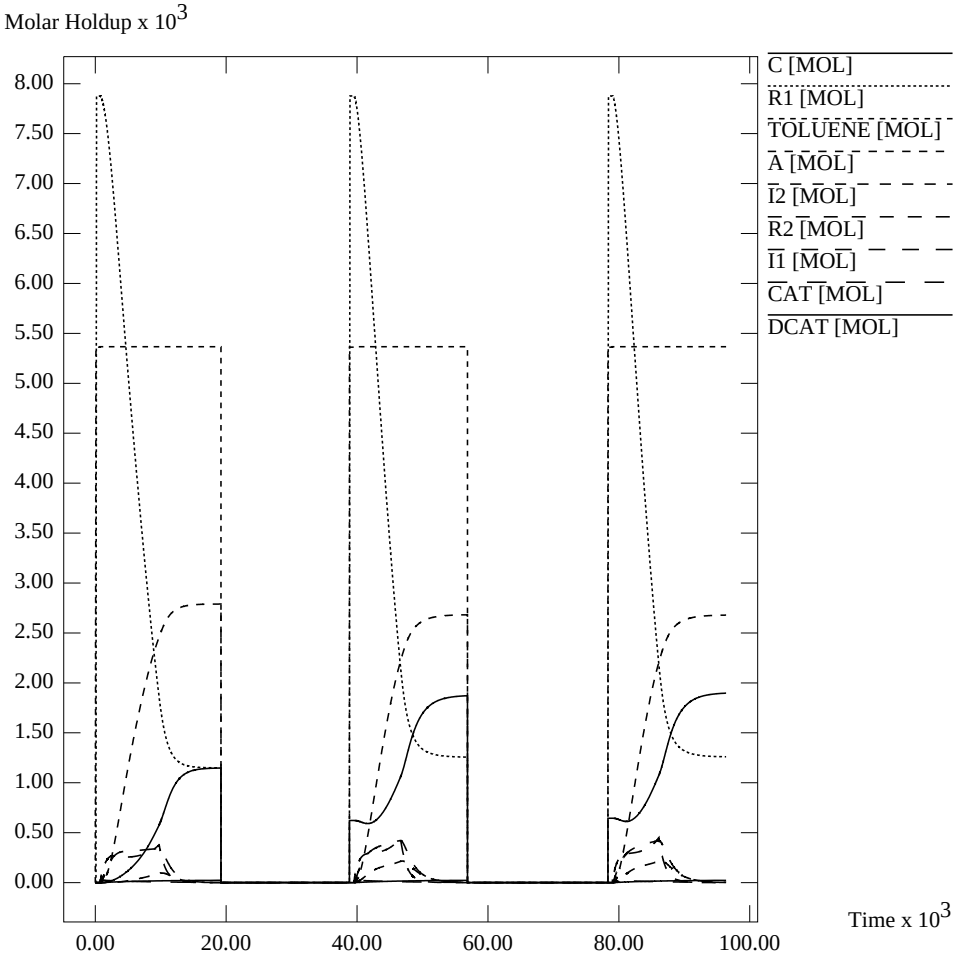

Figure 5-16: Hold-up in reaction step I over three cycles.

The coupled reactor and distillation model was extremely valuable in designing integrated operating policies for the reaction and the distillation task to minimize the formation of I2, and also to ensure that the mixture to be separated remains in the

composition region from which C can be recovered as a pure species.

5.6 Production of a Carbinol

Solvent recovery targeting was applied to the production of a carbinol (5-methyl-5H-dibenzo[a,d]cycloheptene-5-ol) (see Figure 5-17). The synthesis represents one of the 10 steps in a manufacturing process for the production of 5-methyl-10,11-dihydro-5H-dibenzo[a,d]cycloheptene-5,10,imine,maleate.

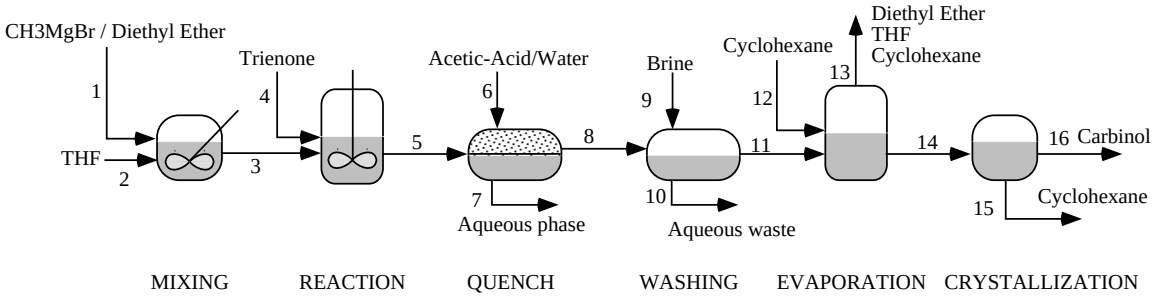

Figure 5-17: Flowsheet for production of a carbinol.

The process consists of a reaction step followed by quenching with an aqueous solution and a two-phase separation, and washing with brine. Then the reaction solvent is replaced by the crystallization medium through evaporation, and the product is crystallized and collected through filtration. In the reaction step trienone is converted to carbinol. A major impurity is tetraene, produced by acid catalyzed elimination of carbinol. Further details about the process can be found in Aumond (1994) and Linninger *et al.* (1994). The azeotropic behavior was approximated using the NRTL (Non-Random-Two-Liquid) model (Renon and Prausnitz, 1968) to calculate the activity coefficients. Binary parameters were extracted from Aspen Plus (Aspen Technology, 1995). A batch size of 500 kg of carbinol was used as basis for the study. The stream compositions for the base case are summarized in Appendix E.

The major organic waste stream results from the replacement of the reaction medium tetrahydrofuran (THF) with crystallization medium cyclohexane. The solvent switch takes place through evaporation, and the resulting waste stream is a

ternary mixture consisting of about 12.1 kmol of diethyl ether (10%), 40.4 kmol of THF (33.3%), and 68.8 kmol of cyclohexane (56.7%). It is desirable to recover the solvents for reuse through batch distillation. The composition simplex for this mixture at 1 atmosphere is shown in Figure 5-18. Cyclohexane and THF exhibit a low-boiling binary azeotrope. Varying the pressure reveals that the azeotrope is not very pressure sensitive. Running the separation at lower pressure therefore does not provide any significant benefits. The pure component diethyl ether is the only unstable node, and the two batch distillation regions will both give rise to diethyl ether as the first product, followed by the binary azeotrope. Depending on the location of the initial composition the final cut will be either pure cyclohexane or pure tetrahydrofuran. The initial composition places the mixed waste-solvent stream in region 1, and therefore diethyl ether (12.1 kmol) and cyclohexane (65.52 kmol) can be recovered as pure components and reused, while THF will be recovered as part of the azeotrope (43.68 kmol). Since cyclohexane is the crystallization medium, recycling the recovered binary azeotrope to the reactor may cause some of the product to crystallize prematurely. The fraction of cyclohexane in the azeotrope is relatively small and may not cause a problem. However, if premature crystallization is not acceptable the binary azeotrope has to be disposed of or possibly be split using an entrainer, an alternative that is not considered here. In that case, the base case will result in at least 43 kmol or about 3190 kg of organic waste per batch. Moving the composition of the mixed waste-solvent stream to region 2 by adding tetrahydrofuran and achieving recovery of pure THF would result in the same problem, as recovery of the azeotrope cannot be avoided. In addition, the binary azeotrope and THF are very close boiling, making it almost infeasible to obtain a sharp split.

The most promising option for process improvement lies in replacing THF with a solvent that allows for easier recovery. It is also advantageous to replace THF because it is miscible with water at atmospheric conditions (Wisniak, 1980), and solvent is often lost to the aqueous phase. Other problems associated with THF include its extreme flammability and the potential for formation of peroxides (Molnar, 1996). Several issues have to be kept in mind when evaluating alternative solvents:

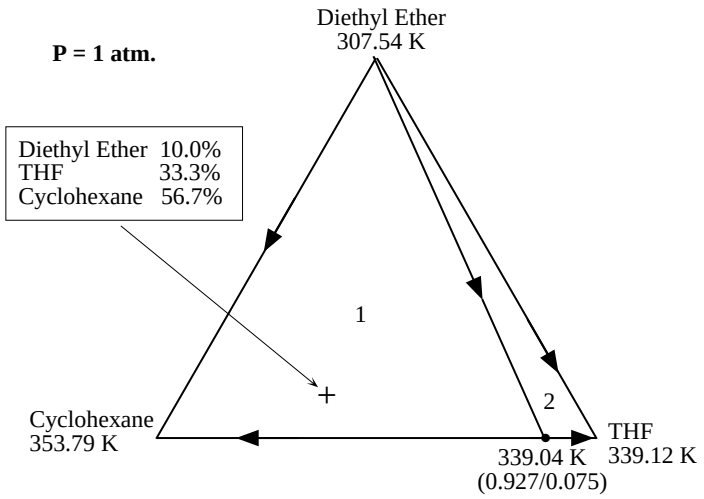

Figure 5-18: Composition simplex for the system diethyl ether, tetrahydrofuran, and cyclohexane.

1. it must be compatible with the process chemistry

2. it should preferably be completely or partially immiscible with water to utilize a two-phase split to remove salts from the organic phase

3. it should preferably be less harmful than the replaced solvent, THF

The reaction is a Grignard addition. Ethers are usually employed as Grignard reaction media, due to the ether group that is attracted by the highly electrophilic magnesium atom in the Grignard compound. An obvious choice in this case is to employ diethyl ether since it is already used as storage medium for the Grignard compound. Diethyl ether is also suggested by Reichardt (1988) as a common solvent for Grignard reactions. Diethyl ether is partially immiscible with water (Wisniak, 1980) and will form the organic rich phase following the two-phase split. Furthermore, the replacement of cyclohexane through evaporation will result in a binary solvent waste stream of diethyl ether and cyclohexane. Returning to the composition simplex in Figure 5-18 reveals that diethyl ether can be easily separated from cyclohexane, resulting in complete recovery of solvents. However, it is expected that the use of diethyl ether will reduce the reaction rate, as the nucleophilic ether group in diethyl ether may not be as efficient as in THF due to the molecule's linear structure.

Laboratory experiments are necessary to resolve this issue.

Another possibility is to replace THF with a novel solvent replacement. For example, Molnar (1996) designs and synthesizes a new class of solvents having similar properties to THF, but which are nonvolatile and can be easily recovered from process streams using simple mechanical separation operations such as ultrafiltration. The polymer solvent system is generated by attaching THF to a polymer backbone and dissolving it in a relatively benign continuous phase. In the example process the polymer based solvent can be recovered from the organic product stream after the washing operation, leaving the product (carbinol) dissolved in the inert solvent. The inert solvent is then replaced by cyclohexane through evaporation as in the base case. Thus, we are again left with a mixed solvent-waste stream consisting of diethyl ether, cyclohexane, and the inert solvent that needs to be analyzed. Molnar (1996) tests different compositions of mixtures of toluene, hexane, and heptane as candidates for the inert continuous phase. Liquid-liquid phase diagrams in Wisniak (1980) show that these three components are all almost completely immiscible in water. Applying solvent recovery targeting discloses that none of the components form azeotropes with diethyl ether or cyclohexane. Consequently, separating the solvent-waste mixture through batch distillation would be relatively easy, and again no unnecessary organic waste is generated. Laboratory experiments should be performed to determine which of the candidate solvents (or mixture of) would result in the optimal reaction conditions. The resulting flowsheet indicating solvent recovery and recycling is shown in Figure 5-19.

5.7 Summary

The algorithm for constructing the batch distillation composition simplex for a system with an arbitrary number of components has been exploited in a sequential design approach where process streams or mixed waste-solvent streams are analyzed for maximum feasible solvent recovery using a targeting approach. The procedure is termed *solvent recovery targeting*. For a given base case, solvent recovery targeting

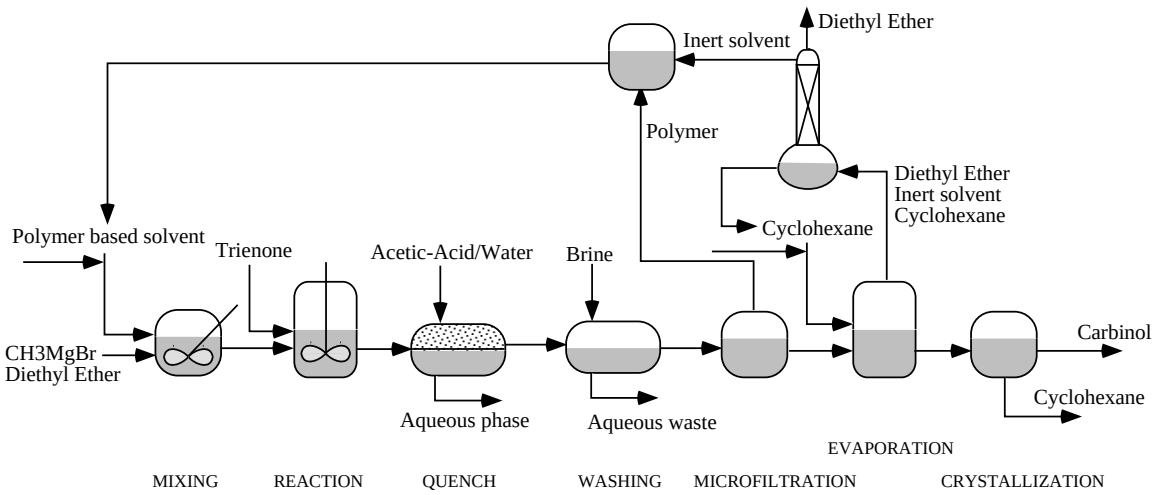

Figure 5-19: Improved process flowsheet.

will, given the composition of the mixture(s) to be separated, predict the correct distillation sequence and calculate maximum feasible recovery of each product cut in the sequence. It can further provide information about all other feasible distillation sequences involving the same set of pure components. The information is used to evaluate the feasibility of enhancing solvent recovery in the proposed flowsheet, and to guide the process of improving the flowsheet.

Solvent recovery targeting has been applied to two case studies. The first case study involves a siloxane monomer process. By using the targeting algorithm to explore the feasible separation alternatives, it was found that a reduction of about 70% in the organic waste compared to the base case could be achieved by integrating solvent recovery and recycling into the flowsheet. Also, it is demonstrated how a dynamic simulation model can be exploited to evaluate the proposed process alternative with respect to effects on the chemistry when an intermediate is recycled. The model yields insight into designing integrated operating policies to increase yield and selectivity and minimize formation of an undesired byproduct.

Similarly, in the second case study involving the manufacture of a carbinol solvent recovery targeting was used to evaluate several possible process modifications to improve solvent recovery. In particular, replacing the original solvent, THF, with a novel polymer based solvent proved very promising.

Chapter 6

Process-wide Design of Solvent Mixtures

This chapter presents a systematic approach to the generation of batch process designs that have solvent recovery and recycling integrated into the flowsheet. The design approach is based on the proposition that highly non-ideal phase behavior, in particular azeotropy, creates barriers to solvent recovery and recycling, and solvent mixtures that cannot be recycled inevitably becomes toxic waste. The systematic alteration of the mixtures formed in a batch process in order to facilitate solvent recovery and recycling is therefore investigated. The primary objective is to design the compositions of stream candidates that will (or can be) subject to recovery such that the quantity of solvents crossing the plant boundary is minimized, subject to a variety of constraints such as reaction stoichiometry, solvation of reactions, selectivity achievable, etc.

The approach is realized as a mathematical programming problem. The advantage of a mathematical programming formulation is that it facilitates the analysis and integration of very complex networks where the trade-offs are not obvious. For this approach to be valuable, the model employed must be abstract but reflect accurately the complex physical behavior that drives the decision process (e.g., azeotropy), the resulting mathematical program must be compact and solvable efficiently for problem sizes of industrial relevance, and the results must be generated in a form that can

be interpreted easily by the engineer to improve the process design. The formulation presented satisfies all these criteria.

6.1 Problem Statement

The problem that is addressed can be stated as follows:

> *Given a set of reaction tasks with known stoichiometry and a set of acceptable solvent and entrainer candidates, synthesize a batch reaction and separation network that satisfies production demand while integrating solvent recovery and recycling in order to minimize waste generated.*

The amount of waste generated is measured as the amount of material other than final products that leave the process and cross the system boundary. Consequently, solvent recovery and integrated recycling of the recovered material should be maximized. However, unless the magnitudes of the recycled streams are restricted, they may take on arbitrary values. This issue is illustrated by the example in Figure 6-1. The lost solvent (waste) is replaced through the make-up stream. The more solvent is recovered and recycled, the less make-up is needed, until the maximum possible amount of solvent is recovered and recycled and the level of waste has reached its minimum. Beyond that the recycle stream may take on any value provided that the total amount of solvent added to the reactor in each batch is sufficient to solvate the reaction.

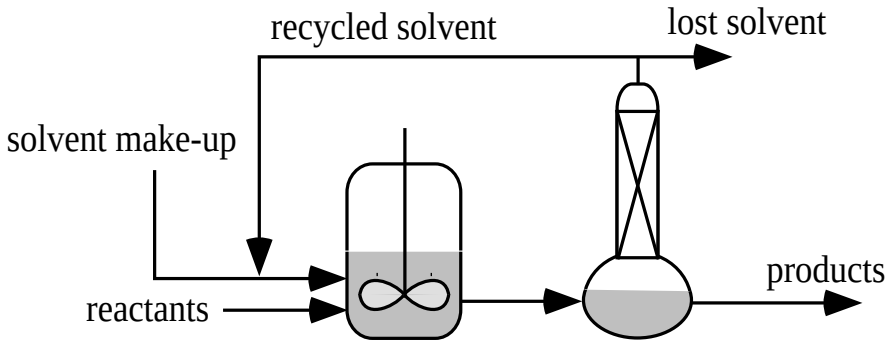

Figure 6-1: Recycling of solvent.

The optimization problem may therefore be formulated as an embedded optimization problem, where an inner optimization problem constraints the outer one (Clark and Westerberg, 1983):

$$\begin{aligned} & \min \sum_{i \in I} \mathrm{F}_i^{rec} \\ \text{s.t.} \quad & \min \sum_{i \in I} \mathrm{C}_i \mathrm{W}_i \end{aligned} \tag{6.1}$$

I represents the set of pure components, F_i^{rec} is the amount of pure component i that is recycled, W_i is the amount of component i that will end up as hazardous waste, and C_i is a weighting factor, for example, representing the relative harm of component i, or waste treatment cost. Hence, in the outer problem we attempt to minimize the magnitude of the streams recycled subject to the constraints that any feasible solution must be a minimum waste solution as measured by the weighting factors.

In general, the embedded optimization problem is very difficult to solve. A special case of the embedded optimization problem is the multi-criteria decision making problem where several objective functions are optimized simultaneously. The solution to this problem is a family of points called a *pareto optimal surface* or the set of *noninferior* solutions. Each such solution has the property that it is not possible to improve any of the objectives without simultaneously degrading the value of another.

As will be demonstrated in Chapter 7, the structure of our design problem is such that a sequential approach can be used to solve (6.1). First, the minimum level of waste emitted to the environment is determined as measured by the weighting factors. Second, the recycle flowrates are minimized subject to minimum waste emitted. In fact, this feature also allows us to readily generate the pareto optimal surface by specifying an acceptable level of waste, and then minimizing the recycle flows. As a first approximation, the magnitude of the streams entering the separation tasks is assumed to be proportional to the cost of separating and recycling solvent, and only material leaving a separation task can cross the system boundary. The objective function can therefore be reformulated as:

$$\begin{aligned} & \min \sum_{d \in D} \sum_{i \in I} \mathrm{FD}_{di}^{in} \\ \text{s.t.} \quad & \min \sum_{d \in D} \sum_{e \in \hat{E}} \mathrm{C}_e \mathrm{FD}_{de}^{w} \end{aligned} \tag{6.2}$$

where D is the set of separation tasks, FD_{di}^{in} is the flow of component i into separation task d, $\hat{\mathrm{E}}$ represent the set of product cuts (separated compositions) that will end up as waste if they cross the system boundary, and FD_{de}^{w} is the amount of composition e from separation task d crossing the system boundary.

The design approach is based on the derivation of a superstructure (Hwa, 1965; Umeda *et al.*, 1972) that embeds a large set of possible process configurations and separation sequences. Streams may be mixed, split, and extra solvent or entrainer added. Figure 6-2 outlines the general modeling framework. It is composed of three components: the *environment* which serves as a source or sink for all material streams crossing the *system boundary* (e.g., raw material, solvents, entrainers, products, waste), a reactor block containing all *reaction tasks* in the process, and a separation block containing all *separation tasks* in the process. Material leaving a reaction task may be separated in a separation task or sent directly to the next reaction task. Recovered material in a separation task may be sent upstream or downstream to a reaction task or another separation task, or emitted to the environment.

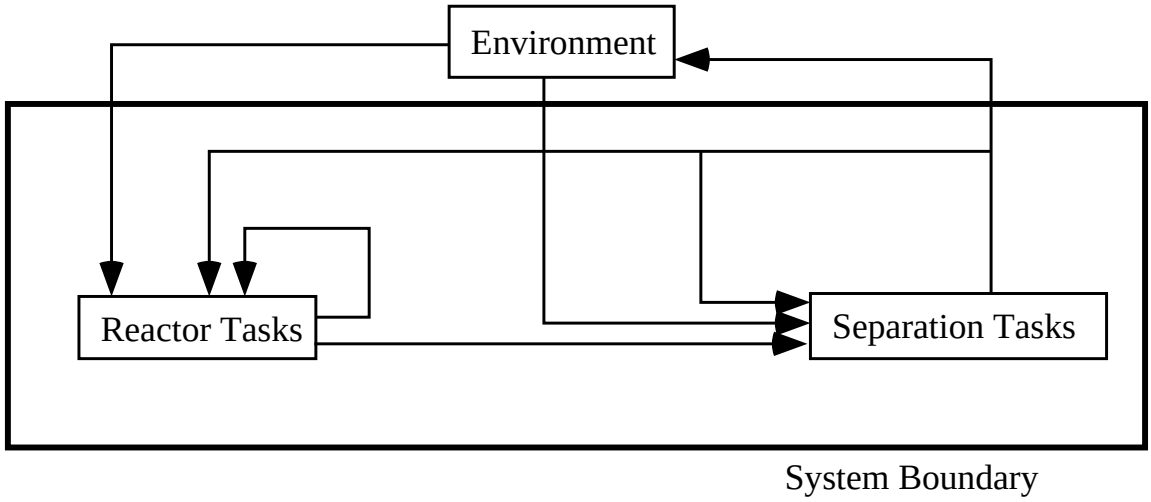

Figure 6-2: General modeling framework.

The basic assumptions that will be made for this synthesis problem, in addition to the ones mentioned above, are:

- The process flowrates are computed as time averaged flows in a batch process based on overall mole balances.
- Batch distillation is the separation method of choice.
- All streams to be separated are homogeneous.
- Perfect splits can be achieved.

The first assumption avoids the issue of time-dependency. The last three assumptions permit the separation tasks to be modeled using the results derived in Chapters 3-5. As a consequence, the product cuts (distillate compositions) can have compositions only equal to fixed points (pure components and azeotropes), and the feasible separation sequences can be predicted *a priori*. As will be demonstrated in Section 6.2 this will allow us to formulate the feasible separation tasks as linear constraints in terms of a mixed set of real and binary variables. Providing all other constraints can also be formulated such that they are linear, the overall synthesis problem can be formulated as a *mixed integer-linear programming* (MILP) problem.

The strategy for synthesizing the overall reaction-separation network consists of the following three steps as indicated in Figure 6-3:

1. Three modeling concepts are required to represent the reaction-separation superstructure: that of the reaction tasks, that of the feasible separation alternatives, and that of the material flows between tasks.
2. The overall superstructure is formulated as an MILP-problem which has as its objective Equation (6.2), and which is constrained by overall material balances and design constraints such as reaction stoichiometry, solvation of reactions, selectivity achievable, etc.

3. The solution to the MILP-problem will provide stream compositions to achieve optimal separation sequences, stream flowrates, reaction conversions, selected solvents and entrainers, and recycle stream structure.

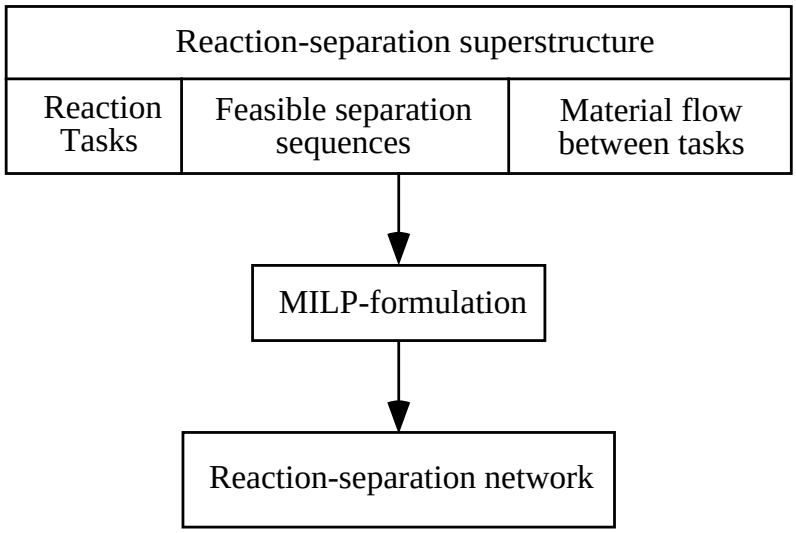

Figure 6-3: Strategy for the synthesis of the overall reaction-separation network.

6.2 Feasible Separation Sequences

A batch distillation region B is the set of compositions that leads to the same sequence of product cuts $\mathbf{P} = \{\mathbf{p}_0, \mathbf{p}_1, \ldots\}$ upon distillation under the limiting conditions of high reflux ratio and large number of equilibrium stages (see Definition 2-1 in Chapter 2). Theorems 3-3 and 3-4 in Chapter 3 prove that under the assumptions of very high reflux ratio, large number of equilibrium trays, and linear pot composition boundaries an nc component mixture will produce exactly nc product cuts (pure components and/or azeotropes) (i.e., $\mathbf{P} = \{\mathbf{p}_0, \mathbf{p}_1, \ldots \mathbf{p}_{nc-1}\}$), and that these nc vertices bound an $(nc-1)$-simplex. Such a simplex is termed the *product simplex* $\mathbf{\Pi}(\mathbf{P})$ of the corresponding batch distillation region B($\mathbf{P}$).

A product simplex $\mathbf{\Pi}^{nc}$ for an nc component mixture can be characterized by the

set of vectors $\{\mathbf{p}_k \in \mathbf{R}^{nc} \ \ \forall k = 0, \ldots, nc-1\}$ such that:

$$\mathbf{\Pi}^{nc} = \{\mathbf{x} \in Q : \mathbf{x} = \sum_{k=0}^{nc-1} f_k \mathbf{p}_k;\ f_k \geq 0 \ \ \forall k = 0, \ldots, nc-1 \text{ and } \sum_{k=0}^{nc-1} f_k = 1\} \quad (6.3)$$

where $f_k \ \ \forall k = 0, \ldots, nc-1$ are the barycentric coordinates, and Q is the whole composition simplex. The element p_{ki} represents the molefraction of pure component i in product cut k in the nc vector $\mathbf{p}_k$. Hence, if a point $\hat{\mathbf{x}}$ in the composition simplex satisfies the condition for positive barycentric coordinates with respect to $\mathbf{\Pi}^{nc}$ then $\hat{\mathbf{x}} \in \mathbf{\Pi}^{nc}$.

From the definition of batch distillation regions it follows that if the initial composition of interest $\mathbf{x}^{p,0}$ is located in batch distillation region $\mathrm{B}(\mathbf{P})$, the corresponding product sequence $\mathbf{P}$ will result. Any point in $\mathrm{B}(\mathbf{P})$ must be a point in the corresponding product simplex defined by $\mathbf{\Pi}(\mathbf{P})$. $\mathbf{x}^{p,0}$ therefore must satisfy Equations (6.3) with respect to $\mathbf{\Pi}(\mathbf{P})$. This can be confirmed by solving the system of linear equations above for $\mathbf{f}$ given $\mathbf{x}^{p,0}$, $\mathbf{p}_0, \mathbf{p}_1, \ldots, \mathbf{p}_{nc-1}$ and examining the values of $f_k \ \ \forall k = 0, \ldots, nc-1$. Physically, the scalars f_k represent the fractions of $\mathbf{x}^{p,0}$ that will be recovered in each product cut through batch distillation. The fact that both $\mathbf{x}^{p,0}$ and the set of points $\{\mathbf{p}_k \ \ \forall k = 0, \ldots, nc-1\}$ lie in the hyperplane $\sum_{i=1}^{nc} x_i = 1$ implies that the criteria $\sum_{k=0}^{nc-1} f_k = 1$ is also satisfied. If one or more $f_k = 0$ this implies that $\mathbf{x}^{p,0}$ lies on one of the faces of $\mathbf{\Pi}(\mathbf{P})$.

No loss of generality is induced by expressing Equations (6.3) on a mole basis. When multiplying both sides by the total number of moles initially in the reboiler ($\mathrm{F}^{p,0}$) Equations (6.3) take the form:

$$\mathbf{F}^{p,0} = \sum_{k=0}^{nc-1} \mathrm{F}_k \mathbf{p}_k;\ \mathrm{F}_k \geq 0 \ \ \forall k = 0, \ldots, nc-1 \quad (6.4)$$

$\mathrm{F}_i^{p,0}$ is the total number of component i initially in the reboiler, and F_k is the total number of moles recovered in product cut k. The material balance confirms that $\sum_{k=0}^{nc-1} \mathrm{F}_k = \sum_{i=1}^{nc} \mathrm{F}_i^{p,0} = \mathrm{F}^{p,0}$.

Any composition in the composition space will yield a unique product sequence.

Unfortunately, since the batch distillation regions fill the composition simplex, and a product simplex will either coincide or be larger than its batch region, two or more product simplices can possibly intersect. In that case two or more product simplices will satisfy Equations (6.4) for the compositions in the intersection. This dilemma is discussed in Chapter 5. Criteria that can be used to distinguish intersecting product simplices, and, hence, two batch distillation regions claiming the same initial composition are provided. However, the mathematical formulation presented here assumes that all product simplices coincide with their respective batch distillation regions (category 1a in Section 4.2). This is a reasonable assumption since systems that give rise to intersecting product simplices are relatively rare. Given the initial composition $\mathbf{x}^{p,0}$, Equations (6.4) therefore provide us with a simple test for predicting the correct separation sequence. For a composition simplex with NB batch distillation regions NB linear equation systems as defined by Equations (6.4) can be generated. By computing the barycentric coordinates for each region the correct product sequence can be determined. $\mathbf{x}^{p,0}$ is located in the batch distillation region that has all $\mathrm{F}_k \geq 0 \quad \forall k = 0, \ldots, nc-1$, and hence will give rise to the corresponding product sequence when batch distillation is employed.

6.3 Separation Superstructure

As argued above, when distilled an nc component mixture will give rise to at most nc product (distillate) cuts. The product cuts can only have compositions equal to fixed points, and the set of product cuts achieved is dependent on which batch distillation region the feed composition is located. A distillation task can therefore be represented as shown in Figure 6-4. The nodes 1, 2, ..., ep represent fixed points in a system, and hence are the known feasible product compositions achievable when employing batch distillation. The flows to each of the nodes will be greater or equal to zero. Note that the pure component compositions in the system are a subset of the fixed points. The fixed point nodes play a crucial role in the mathematical formulation, and may be thought of as unlimited intermediate storage tanks.

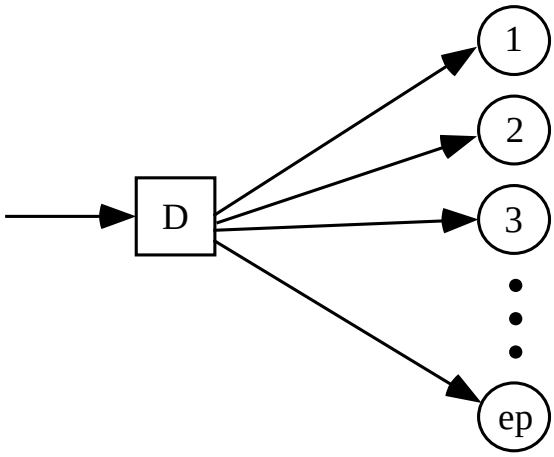

Figure 6-4: Representation of distillation task in reaction-separation superstructure.

To demonstrate how the superstructure for feasible separations can be derived, suppose that there is a mixture with three components, A, B, and C, and that the composition simplex contains four fixed points (three pure components and one azeotrope (AB)) and two batch distillation regions. The ternary residue curve map is shown in Figure 6-5a. Batch distillation region 1 gives rise to sequence $\mathbf{P}_1 = \{\mathbf{p}_{11}, \mathbf{p}_{12}, \mathbf{p}_{13}\}$ ={A,AB,C}, and batch distillation region 2 gives rise to $\mathbf{P}_2 = \{\mathbf{p}_{21}, \mathbf{p}_{22}, \mathbf{p}_{23}\}$ ={B,AB,C}. The postulated superstructure for the distillation of this mixture is then shown in Figure 6-5b.

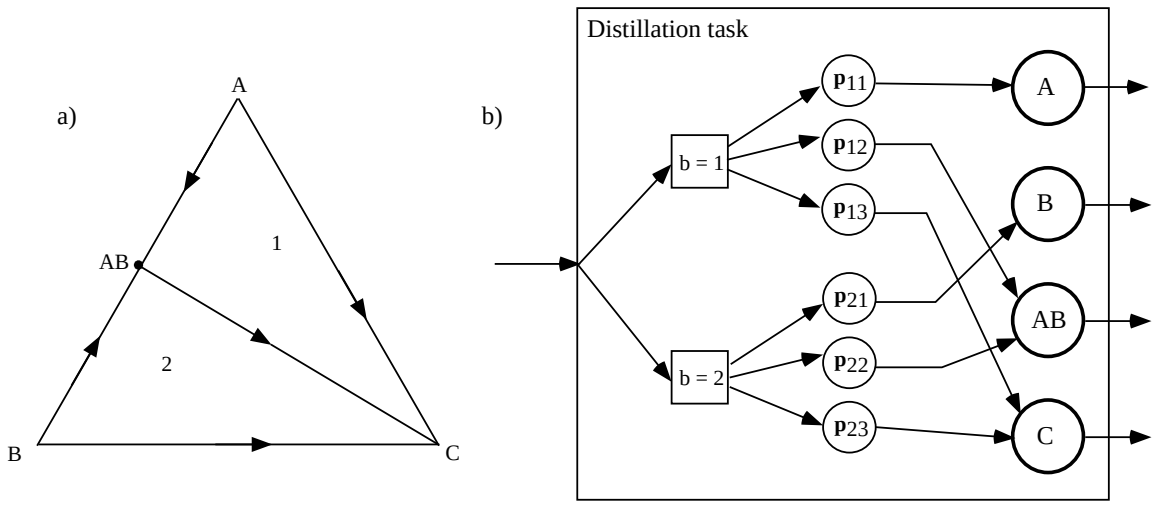

Figure 6-5: Superstructure of distillation task for a ternary mixture with one azeotrope and two batch distillation regions.

Each recovered stream can either be recycled upstream to a reaction or distillation task, sent downstream to a reaction or distillation task, or emitted to the environment. The streams crossing the system boundary can be divided into four categories:

- pure products
- reaction by-products
- certain azeotropic compositions
- purge streams

The three latter stream categories will typically end up as hazardous waste. An undesired reaction by-product that cannot be used anywhere else in the process must leave the process to avoid build-up. The same applies to azeotropic compositions involving components where, for example, one (or more) is forbidden in a certain reaction task while the other(s) is needed only in that particular task. Furthermore, in order to avoid build-up of trace contaminants, recycled streams must be purged. The splitting of material entering each fixed point node is therefore represented as illustrated in Figure 6-6. This representation allows complete control of the source and destination of each recovered material stream.

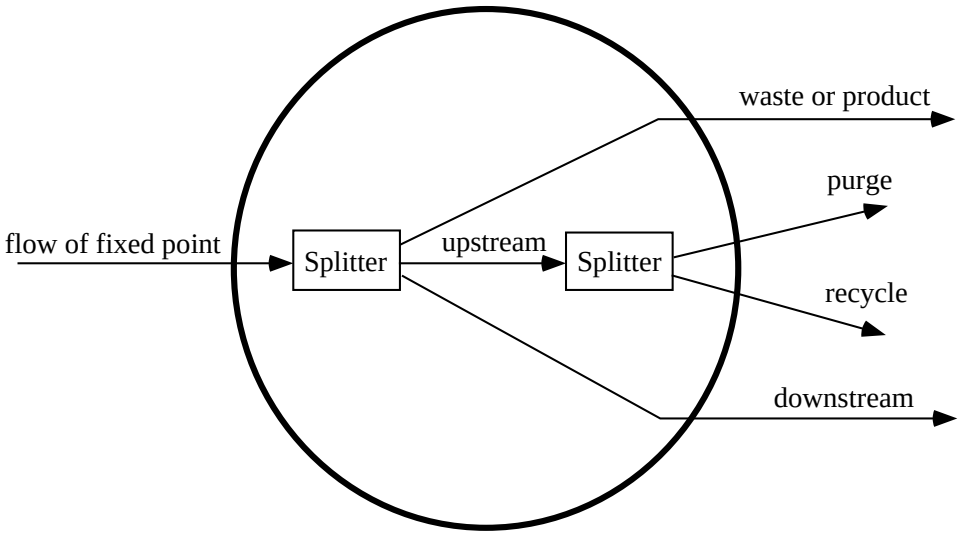

Figure 6-6: Representation of splitting of streams in fixed point node.

6.4 Super Simplex

The notion of the composition simplex divided into a series of batch distillation regions leads to the conception of a *super simplex* corresponding to the overall composition simplex of mixtures of all the components that may appear in the process. This set of components will include raw material and products, in addition to several candidate solvents and entrainers. The super simplex will represent the search space for feasible separation. Optimization in this super simplex may drive the mixtures formed in the process to lower dimensional faces, thus choosing between candidate solvents, or, alternatively, identify potential entrainers. The derivation of the super simplex is based on the assumptions of high reflux ratio, large number of trays, linear pot composition boundaries, and homogeneous mixtures, and can be derived using the algorithm in Chapter 4 for a given set of components.

6.5 Reaction-Separation Superstructure

The overall reaction-separation superstructure is shown in Figure 6-7. Each reaction task is assumed to be followed by a distillation task. However, the formulation allows the optimization to omit the distillation task and let a reaction task feed directly to the next reaction task. Each separation task is represented by a node for each fixed point (see Figure 6-4). A fixed point node may only take input from the corresponding separation task, and output to the environment, to all separation tasks, and to all reaction tasks.

6.6 Mathematical Formulation

To derive the mathematical formulation, the following index sets will be used to characterize the topology of the superstructure. The fixed points will be represented by the index set E = $\{e\}$. The set of pure components, which is a subset of E, will be represented by I = $\{i\}$. J = $\{j\}$ represents the set of reaction tasks. The set of reactions taking place in a particular reaction task is denoted by $R_j = \{\pi\}$. The

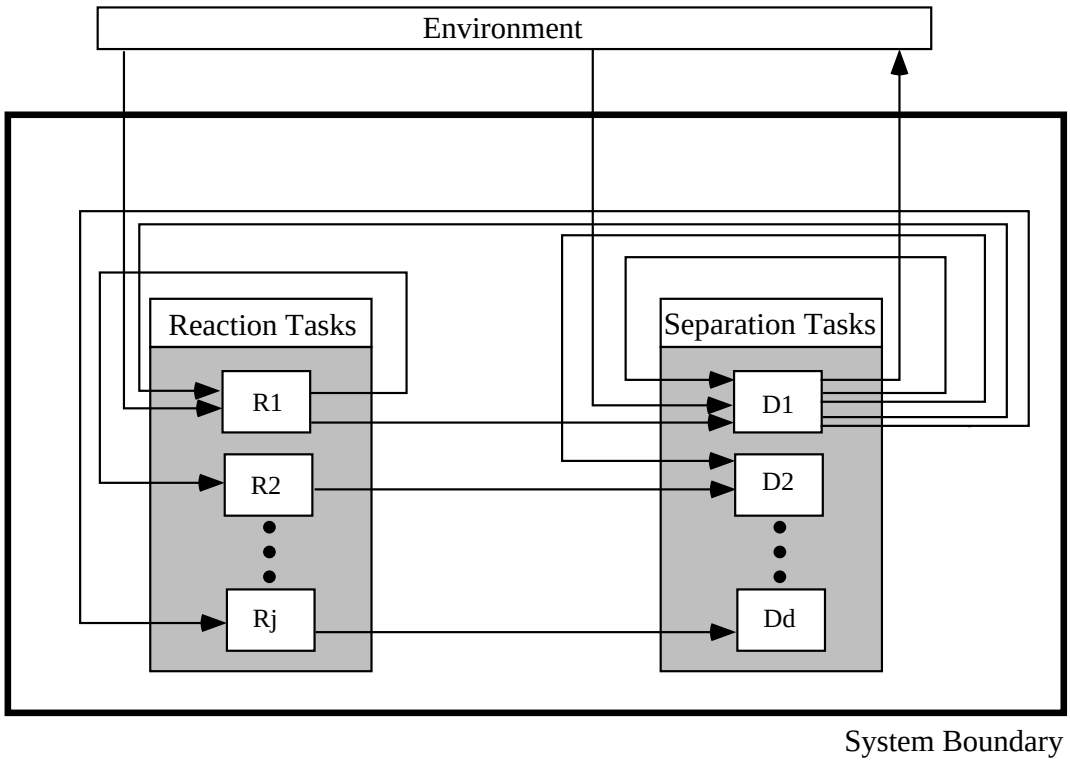

Figure 6-7: Reaction-separation superstructure.

distillation tasks are represented by D = $\{d\}$. In the mathematical formulation each batch distillation region in the super simplex will be represented by its corresponding product simplex. NB = $\{b\}$ denotes the batch distillation regions. $K_b = \{k\}$ denotes the individual product cuts, and K_{be} denotes the set of product cuts in batch distillation region b with composition equal to fixed point e.

Each reaction task is modeled as a simple extent reactor. The individual reactions are specified in terms of stoichiometry. The flows into and out of reaction task j of component i are given by FR_{ji}^{in} and FR_{ji}^{out}. Although FR_{j}^{out} is a single stream, it is represented by separate flowrates for each individual pure component. This is done in order to avoid using molefractions, which would result in nonlinearities in the model. The flow of component i from reaction task j to reaction task $\hat{j}$ is given by $FR_{j\hat{j}i}^{out}$, and the flow of component i from reaction task j to distillation task d is given by FR_{jdi}^{out}. The flow of material with composition equal to fixed point e from distillation task d to reaction task j is given by FDR_{dje}, and the flow of material equal to fixed

point e from the environment to reaction task j is given by FE_{je}^{out}. The overall mole balances are defined by:

$$\mathrm{FR}_{ji}^{in} + \sum_{\pi \in \mathrm{R}_j} \xi_{j\pi}\nu_{j\pi i} = \mathrm{FR}_{ji}^{out} \quad \forall j \in \mathrm{J},\ i \in \mathrm{I} \tag{6.5}$$

$$\mathrm{FR}_{ji}^{in} = \sum_{e \in E} \mathrm{SS}_{ie}\Big(\sum_{d \in D} \mathrm{FDR}_{dje} + \mathrm{FE}_{je}^{out}\Big) + \sum_{\hat{j} \in J} \mathrm{FR}_{\hat{j}ji}^{out} \quad \forall j \in \mathrm{J},\ i \in \mathrm{I} \tag{6.6}$$

$$\mathrm{FR}_{ji}^{out} = \sum_{\hat{j} \in J} \mathrm{FR}_{j\hat{j}i}^{out} + \sum_{\hat{j} \in J} \mathrm{FR}_{jdi}^{out} \quad \forall j \in \mathrm{J},\ i \in \mathrm{I} \tag{6.7}$$

where $\nu_{j\pi i}$ is the stoichiometric coefficient for component i in reaction π in reaction task j. The molar extent of reaction $\xi_{j\pi}$ is the same for all species taking part in reaction π. Note that for species that do not take part in reaction π, $\nu_{j\pi i} = 0$. Hence, $\mathrm{FR}_{ji}^{in} = \mathrm{FR}_{ji}^{out}$. The element SS_{ie} is the molefraction of component i in fixed point e, which is data provided to the formulation. Also note that $\mathrm{FR}_{j\hat{j}i}^{out}$ must be set to zero for all reaction tasks $\hat{j}$ that are not directly downstream to reaction task j, and $\mathrm{FR}_{jdi}^{out} = 0$ for all distillation tasks d that are not directly downstream to reaction task j. Likewise, $\mathrm{FR}_{\hat{j}ji}^{out} = 0$ for all reaction tasks $\hat{j}$ that are not directly preceding reaction task j. The flows in and out of reaction task j are shown in Figure 6-8.

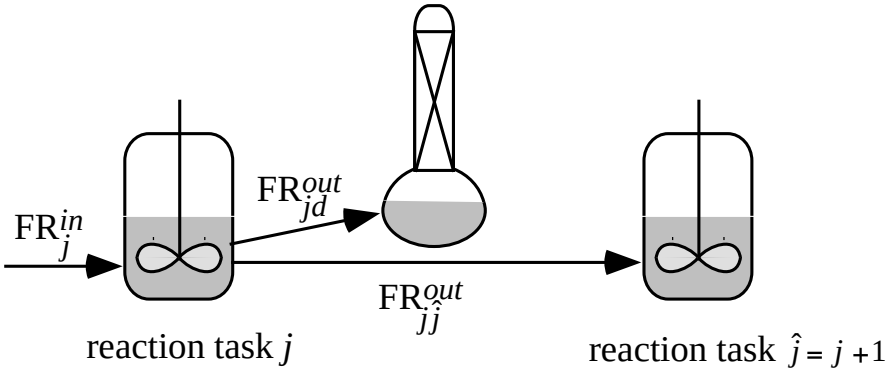

Figure 6-8: Input and output flows for reaction task j.

Following the discussion in Section 6.4, the material balance characterizing the distillation of an nc component mixture can be expressed in terms of p_{bki}, the mole fraction of pure component i in product cut k from batch distillation region b. Flow

into batch distillation column d of component i is represented by FD_{di}^{in}. The flow of distillation cut k in batch distillation region b from column d is denoted by FD_{dbk}^{out}, and the total amount of material recovered in column d exhibiting the composition of fixed point e is denoted by FDT_{de}^{out}. FE_{de}^{out} is the flow of material with composition equal to fixed point e from the environment to distillation task d, and $\mathrm{FDD}_{\hat{d}de}$ is the flow of material from distillation task $\hat{d}$ to distillation task d with composition equal to fixed point e. The resulting equations are:

$$\mathrm{FD}_{di}^{in} = \sum_{b \in \mathrm{NB}} \sum_{k \in K_b} p_{bki} \mathrm{FD}_{dbk}^{out} \quad \forall d \in \mathrm{D}, \;\; i \in \mathrm{I} \tag{6.8}$$

$$\mathrm{FD}_{di}^{in} = \sum_{j \in J} \mathrm{FR}_{jdi}^{out} + \sum_{e \in E} \mathrm{SS}_{ie} (\mathrm{FE}_{de}^{out} + \sum_{\hat{d} \in D} \mathrm{FDD}_{\hat{d}de}) \quad \forall d \in \mathrm{D}, \; i \in \mathrm{I} \tag{6.9}$$

$$\mathrm{FDT}_{de} = \sum_{b \in \mathrm{NB}} \sum_{k \in K_{be}} \mathrm{FD}_{dbk}^{out} \quad \forall d \in \mathrm{D}, \; e \in \mathrm{E} \tag{6.10}$$

Note that $\mathbf{p}_{bk}$ are data for the mathematical programming formulation that can be generated automatically by the algorithm presented in Chapter 4. As the feed mixture $\mathrm{FD}_{di}^{in} \;\; \forall i \in \mathrm{I}$ cannot be located in more than one batch distillation region simultaneously, $\mathrm{FD}_{dbk}^{out} = 0 \;\; \forall b \in \mathrm{NB} \neq b^*$ where b^* denotes the active region for column d. Binary variables $\mathrm{Y}_{db} \in \{0, 1\}$ are introduced to denote active and inactive regions. $\mathrm{Y}_{db} = 1$ if the initial reboiler composition in column d is located in region b, otherwise $\mathrm{Y}_{db} = 0$. The following constraints are therefore introduced:

$$\sum_{k \in K_b} \mathrm{FD}_{dbk}^{out} \leq \mathrm{MY}_{db} \quad \forall d \in \mathrm{D}, \; b \in \mathrm{NB} \tag{6.11}$$

$$\sum_{b \in \mathrm{NB}} \mathrm{Y}_{db} = 1 \;\; \forall d \in \mathrm{D} \tag{6.12}$$

Inequality (6.11) will ensure that when $\mathrm{Y}_{d\hat{b}} = 0$, $\mathrm{FD}_{d\hat{b}k}^{out} = 0 \;\; \forall k \in \mathrm{K}_{\hat{b}}$ where $\hat{b}$ is an inactive region. M is a large scalar. The value of M is selected carefully such that if $\mathrm{Y}_{db} = 1$, the values of FD_{dbk}^{out} are not constrained. Equality (6.12) will ensure that only one batch distillation region is active in each column.

To illustrate this formulation, assume that the ternary mixture in Figure 6-5 is located internal to batch distillation region 1. Constraints (6.8), (6.9), (6.10), (6.11),

and (6.12) will then yield the flows indicated in Figure 6-9b where the zero flows are not included.

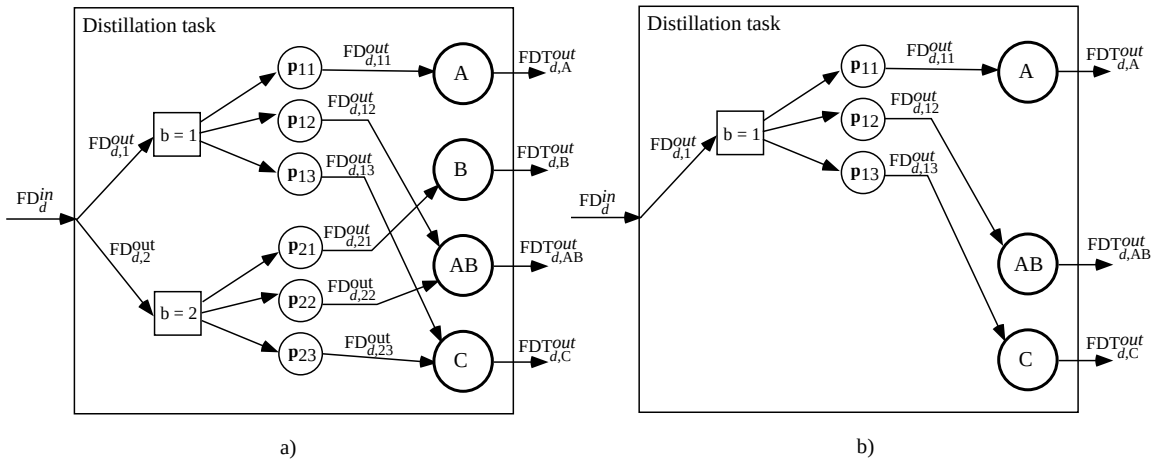

Figure 6-9: Distillation of ternary mixture located in batch distillation region 1.

Further, as Figure 6-8 shows the optimization can choose to omit a distillation task and send material directly from one reaction task to the next. Binary variables are therefore introduced to denote an active or inactive distillation task. $\mathrm{L}_d = 1$ if material is fed to distillation task d, otherwise $\mathrm{L}_d = 0$. The additional constraints are:

$$\sum_{i \in I} \mathrm{FD}_{di}^{in} \quad \leq \quad \mathrm{ML}_d \quad \forall d \in \mathrm{D} \tag{6.13}$$

Inequality (6.13) will ensure that when $\mathrm{L}_d = 0$, FD_{di}^{in}, and, consequently, FR_{jdi}^{out} are zero.

The constraints that ensure overall mole balance around each fixed point node are given by Equations (6.14). FE_{de}^{in} denotes flow of fixed point e from distillation task d to the environment, and PURGE_{de} is the amount of purge with composition equal to fixed point e from column d.

$$\mathrm{FDT}_{de} \quad = \quad \sum_{j \in J} \mathrm{FDR}_{dje} + \sum_{\hat{d} \in D} \mathrm{FDD}_{d\hat{d}e} + \mathrm{FE}_{de}^{in} + \mathrm{PURGE}_{de} \; \forall d \in \mathrm{D}, e \in \mathrm{E} \tag{6.14}$$

The purge streams are computed using Equation (6.15). The choice of purge

fraction will depend on the purity requirements in the particular problem of interest.

$$\mathrm{PURGE}_{de}(1-\alpha_{de}) = \left(\sum_{j \in J^{du}} \mathrm{FDR}_{dje} + \sum_{\hat{d} \in D^{du}} \mathrm{FDD}_{d\hat{d}e} \right) \quad \forall d \in \mathrm{D},\ e \in \mathrm{E} \qquad (6.15)$$

where J^{du} represents the set of reaction tasks upstream of distillation task d, and D^{du} represents the set of distillation tasks upstream of distillation task d. Note that D^{du} includes the distillation task d itself. α_{de} is the purge fraction of streams with composition equal to fixed point e from column d, and is data provided to the formulation. Typically, the same purge fraction is used throughout the formulation.

Finally, it must be required that all flowrates are non-negative.

6.7 Stripper or Rectifier Configuration

A batch stripper is configured in a similar manner to a batch rectifier. However, the material is fed to the column from a holding tank where the mixture is held at its boiling temperature by a condenser. The product is taken out at the bottom of the column, and the recycled material is evaporated in a reboiler. Hence, the heaviest species is separated off first. A more detailed discussion concerning the stripper configuration is provided in Appendix A.

When constructing the residue curve map for the mixture of interest, the arrows indicating the direction of residue path should be reversed, as we will now be moving from heavier to lighter species in the holding tank. Therefore, all residue curves will reverse direction. As a result, the nodes that are unstable when a rectifier is assumed will become stable, and *vice versa* for the stable nodes. From this point the analysis is analogous to the analysis for a rectifier configuration, based on the same limiting assumptions of high reflux ratio, large number of trays, and linear pot composition boundaries. Batch distillation regions corresponding to a stripper configuration can therefore be constructed in a similar manner, providing new separation alternatives. A choice between the two column configurations can be simply expressed as choosing between the total set of batch distillation regions, i.e., $\mathrm{NB} = \mathrm{NB}^r \cup \mathrm{NB}^s$, and

constraints (6.8), (6.9), (6.10), (6.11), and (6.12) remain unchanged. NB^r and NB^s represent batch distillation regions for the rectifier and the stripper configuration, respectively. Observe that it does not matter if members of these sets intersect in the composition simplex. The optimization is simply choosing from two super simplices: one which represents the separation alternatives when a rectifier configuration is used, and one which represents the separation alternatives when a stripper configuration is used. The mathematical model could be modified in a similar manner to allow other column configurations such as a middle vessel configuration, provided that a means of enumerating the product sequences and batch distillation regions is developed.

6.8 Other Constraints

In addition to constraints incorporating conservation of mass and feasible separations, constraints specific to the chemistry and operation of a particular process are required. Additional index sets are introduced to characterize these constraints: $\mathrm{S} = \{s\}$ is the set of candidate solvents, and $\mathrm{R} = \{r\}$ is the set of reagents. Categories of constraints include:

- A lower bound on solvent to reagent ratio. Such constraints can be expressed as:

$$\mathrm{FR}_{js}^{in} \geq \mathrm{Ratio}_{jsr}\mathrm{FR}_{jr}^{in} \tag{6.16}$$

- Upper and lower bounds on extents of reaction, e.g., minimum acceptable and maximum feasible yield (Equation (6.17)), or linear combinations of extents yielding the range of selectivity achievable (Equations (6.18) and (6.19)):

$$\mathrm{LowerBound}_{j\pi} \leq \xi_{j\pi} \leq \mathrm{UpperBound}_{j\pi} \tag{6.17}$$

$$\xi_{j1} \geq \mathrm{RatioLow}_{j1,2}\xi_{j2} \tag{6.18}$$

$$\xi_{j1} \leq \mathrm{RatioHigh}_{j1,2}\xi_{j2} \tag{6.19}$$

- If the presence of a component causes undesired side reactions in a particular reaction task, the flow of this component either as pure species or as part of an azeotrope to this reaction task should be forbidden, or the use of an upper bound may be appropriate:

$$\mathrm{FR}_{ji}^{in} \leq \mathrm{UpperBound}_{ji} \tag{6.20}$$

Ratio_{jsr}, $\mathrm{LowerBound}_{j\pi}$, $\mathrm{UpperBound}_{j\pi}$, $\mathrm{RatioLow}_{j1,2}$, $\mathrm{RatioHigh}_{j1,2}$, and $\mathrm{UpperBound}_{ji}$ are scalars. Such data may be obtained through collaboration with the chemist, through experiments or computer simulations.

6.9 Summary

A mixed-integer linear programming (MILP) formulation for the design of batch processes with integrated solvent recovery and recycling has been presented. A *super simplex* is introduced, which corresponds to the overall composition simplex for mixtures of several candidate solvents, and in general will contain multiple azeotropic compositions. It is demonstrated that, under reasonable assumptions, the feasible sequences of pure component and azeotropic cuts that can be separated from mixtures in the super simplex can be formulated as linear constraints in terms of a mixed set of real and binary variables. This result is especially significant since it facilitates a compact and efficient mathematical abstraction of the complex azeotropic behavior that drives the decision process. For example, the choice of a particular solvent corresponds to driving the mixture to a lower dimensional face of the super simplex.

The super simplex is embedded in a novel reaction-separation superstructure to yield a modeling framework for the process-wide design of the mixtures formed in a batch process (primarily design of the mixtures leaving the reaction tasks). The modeling framework is flexible, new constraints can be easily added to produce more realistic alternatives, and leads to a compact MILP that can be solved efficiently to guaranteed optimality. A very promising feature is the scalability of the formulation,

since the number of binary variables can be expressed roughly as the product of the number of batch distillation regions with the number of distillation tasks embedded in the super structure. The number of binary variables is a measure of the complexity of the problem, and if this number grows slowly with process size it will greatly improve the solvability of the problem. For example, the realistic industrial example solved in the next chapter leads to an MILP probably two orders of magnitude smaller than those that can be solved by current general purpose codes on a routine basis. This enables us to be very ambitious with the problem formulations that can be contemplated.

By its nature, the formulation is approximate and does not embed all constraints on the design. Hence the engineer must interact with the formulation in an evolutionary manner: the problem is first formulated as an MILP and an optimal flowsheet is found. The methodology can then be employed to generate various designs by adding or removing design constraints, thereby furnishing the engineer with a set of different process designs that can be evaluated based on other criteria not embedded into the program like reaction rates (which is a function of selected solvent), production times, safety, etc. The evolutionary character of the design approach is demonstrated in the second case study in Chapter 7.

Chapter 7

Optimization of a Siloxane Monomer Process

The synthesis formulation for process-wide design of mixtures has been applied to a process for the production of a siloxane based monomer in a single campaign. The process is the same as the one analyzed in Chapter 5 where an ad hoc method was used to improve solvent recovery. In this chapter it is demonstrated that the process can be further improved through use of an automated optimization procedure.

The first case study is a subsystem of the process and is used to illustrate the concept of a super simplex to represent separation alternatives in combination with mathematical programming. The second case study involves the entire process. The mathematical programming formulation is used to generate several different process alternatives by adding design constraints to the formulation. The process alternatives generated show that an intuitive and automated formulation can produce minimum emission designs very rapidly. Furthermore, it is verified that the formulation can be extended to explore the space of noninferior solutions corresponding to the trade-offs between quantity of waste emitted and the cost of recovering and recycling solvent.

7.1 Base Case

Figure 7-1 shows the base case design from the pilot plant. Appendix C contains the stream data. The process consists of several sequential reaction steps. Solvents and

reaction by-products are removed through batch distillation. Further details can be found in Chapter 5.

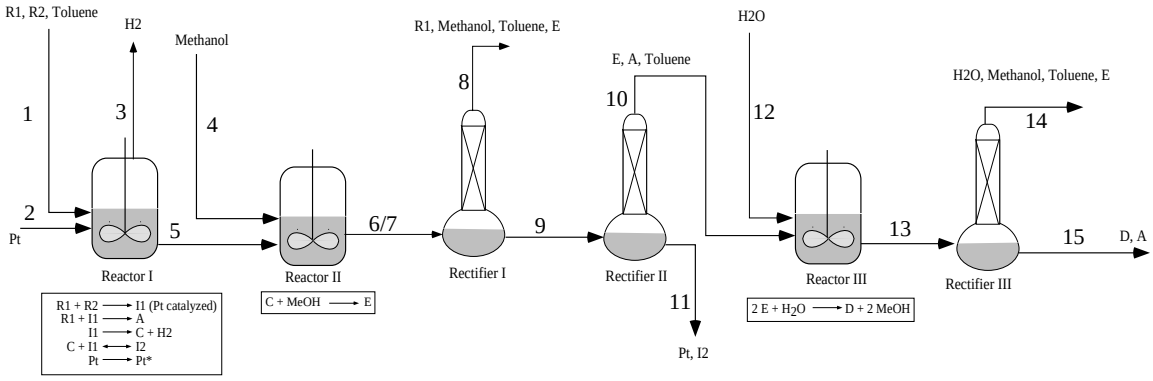

Figure 7-1: Siloxane monomer process: base case

7.2 Case Study 1

A subsystem of the above process was chosen for the first case study. The problem formulation includes, in sequence, reaction step I and a batch distillation column for recovery of the pure products. However, although simple, the system is sufficiently complicated to test the targeting methodology for derivation of the super simplex, and to test the concept of a super simplex in combination with mathematical programming to determine the optimal composition of the final mixture in the reactor. These ideas are demonstrated here.

The first reaction step has a relatively complicated reaction mechanism. The reactants are R1 and R2, while toluene serves as a solvent. The main products are C and A. A is one of the final products, while C is an intermediate which is processed further in reaction steps II and III. To make the points of the problem clearer a few simplifications and assumptions have been made:

1. Only include the two overall reactions in reaction step I:

$$\begin{aligned} 2\mathrm{R1} + \mathrm{R2} &\rightarrow \mathrm{A} \\ \mathrm{R1} + \mathrm{R2} &\rightarrow \mathrm{C} + \mathrm{H_2} \end{aligned}$$

2. Run reaction step I to 100% conversion of R2, the most expensive reactant.

Any of the components can be accepted in a recycle stream, and the overall material balance shows that only A and C need to leave the system. The total number of moles of A and C produced is equal to the number of moles of R2 converted. For this particular setup, an appropriate objective would therefore be to minimize the flow of the recycled streams, while allowing only A and C to cross the system boundary.

7.2.1 Separation Sequences

There are five pure components in this system. However, as reaction step I is run to extinction of R2, only four components will enter the batch distillation columns, hence form the super simplex. These are C, R1, A, and toluene (T). The azeotropic behavior was approximated using the Wilson model to calculate the activity coefficients (see, for example, Reid *et al.* (1987)). Binary parameters were extracted from Aspen Plus (Aspen Technology, 1995). Missing binary parameters were estimated using the UNIFAC group contribution method (Fredenslund *et al.*, 1977) as implemented in Aspen Plus (Aspen Technology, 1995). Binary parameters for the pairs involving the non-standard components C, and A can be found in Appendix D. R1 represents allyl alcohol. The vapor phase was assumed to be ideal. The components involved form two binary azeotropes, one between R1 and toluene, and one between C and R1. Components C, R1, and toluene also form a ternary azeotrope. Table 7.1 lists the fixed points in the system at 1 atmosphere with compositions, boiling temperatures, and whether a point is an unstable node (un), stable node (sn), or a saddle point (s).

The super simplex was generated using the algorithm described in Chapter 4 and the feasible distillation sequences were extracted. There are five batch distillation regions in the super simplex (see Figure 7-2), each producing 4 product cuts (see Table 7.2).

Table 7.1: Compositions, boiling temperatures, and stability of fixed points at 1 atmosphere. *) Since R2 will not enter the column it is not included in the super simplex.

e	C	R2	R1	T	A	T_B[K]	type
C	1	0	0	0	0	336.6	un
R2	0	1	0	0	0	346.0	*
R1-T	0	0	0.65	0.35	0	367.5	un
R1	0	0	1	0	0	370.0	s
C-R1-T	0.18	0	0.3	0.52	0	373.6	s
C-R1	0.31	0	0.69	0	0	378.8	s
T	0	0	0	1	0	383.8	s
A	0	0	0	0	1	532	sn

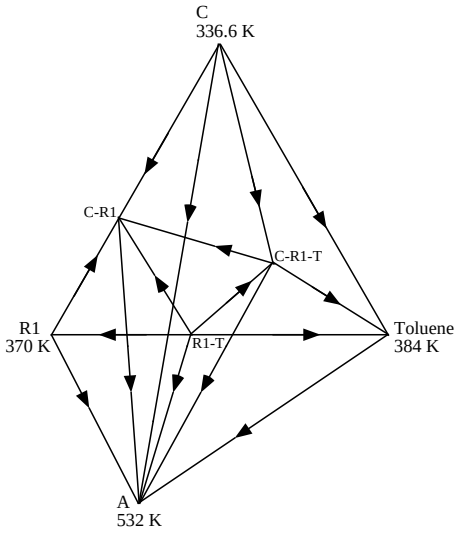

Figure 7-2: Super simplex for C, R1, toluene, and A.

Table 7.2: Feasible distillation sequences for case study I.

b	Product sequence
1	{C, C-R1-T, C-R1, A}
2	{C, C-R1-T, T, A}
3	{R1-T, R1, C-R1, A}
4	{R1-T,C-R1-T, C-R1, A}
5	{R1-T, C-R1-T, T, A}

7.2.2 Formulation of Optimization Problem

The reactor should be operated such that there is stoichiometric excess of R1 in order to drive the reaction to completion, as specified by the following constraint:

$$\mathrm{FR}_{1,R1}^{out} \geq 0.15\mathrm{FR}_{1,R2}^{in} \tag{7.1}$$

We assume 100% conversion of R2:

$$\mathrm{FR}_{1,R2}^{out} = 0 \tag{7.2}$$

This constraint can also be expressed in terms of the fractional conversion X_{ji}, the fraction of component i that is consumed in reaction task j, defined as:

$$X_{ji} = \frac{\mathrm{FR}_{ji}^{in} - \mathrm{FR}_{ji}^{out}}{\mathrm{FR}_{ji}^{in}} \tag{7.3}$$

However, in order to avoid introducing nonlinearities the relationship should be written as:

$$X_{ji}\mathrm{FR}_{ji}^{in} = \mathrm{FR}_{ji}^{in} - \mathrm{FR}_{ji}^{out} \tag{7.4}$$

Constraint (7.2) is therefore enforced by specifying $X_{1,R2} = 1$. A lower limit on the ratio of solvent to reactant fed to the reactor is specified in order to guarantee adequate solvation:

$$\mathrm{FR}_{1,R2}^{in} \leq 0.734\mathrm{FR}_{1,T}^{in} \tag{7.5}$$

In order to analyze selectivity to A versus C in the two parallel reactions the dynamic behavior of the reactor was modeled using ABACUSS. The operating policies were varied and the following upper and lower bounds on the relative extent of reaction for the two parallel reactions, $\xi_{1,1}$ and $\xi_{1,2}$, respectively, were established:

$$\xi_{1,1} \geq 1.78\xi_{1,2} \tag{7.6}$$

$$\xi_{1,1} \leq 4.92\xi_{1,2} \tag{7.7}$$

It should be noted that these bounds are not strictly rigorous, since a global solution to the relevant dynamic optimization problem was not obtained. However, they serve as suitable bounds for illustration purposes.

The feed of R2 ($FE^{out}_{1,R2}$) to the reactor was set to 3.93836 kmol (529.0 kg) as a basis. Also, the recycled streams were not purged. The problem was formulated in GAMS (Brooke *et al.*, 1992) as an MILP with 35 equations and 5 binary variables, and solved on an HP 9000/735 workstation by OSL (IBM Corporation, 1991) in 0.1s.

7.2.3 Results

The degrees of freedom for the optimization can be viewed as the feed of solvent toluene, the feed of reagent R1, and a linear combination of the extents of reactions. From Table 7.2 note that both pure products (C and A) can only be recovered from a mixture in batch distillation region 1 or 2. Product A alone can be recovered as a pure species from any of the regions. In fact, the mathematical program places the solution in region 2. The value of the objective function was found to be 6.311 kmol of recycled material. 3.938 kmol of C and A is produced (0.665 kmol of C and 3.273 kmol of A). The flows of the other streams are indicated in Figure 7-3. Inequality (7.7) is active, indicating that as some C is inevitably recycled as azeotropes, selectivity to A is maximized.

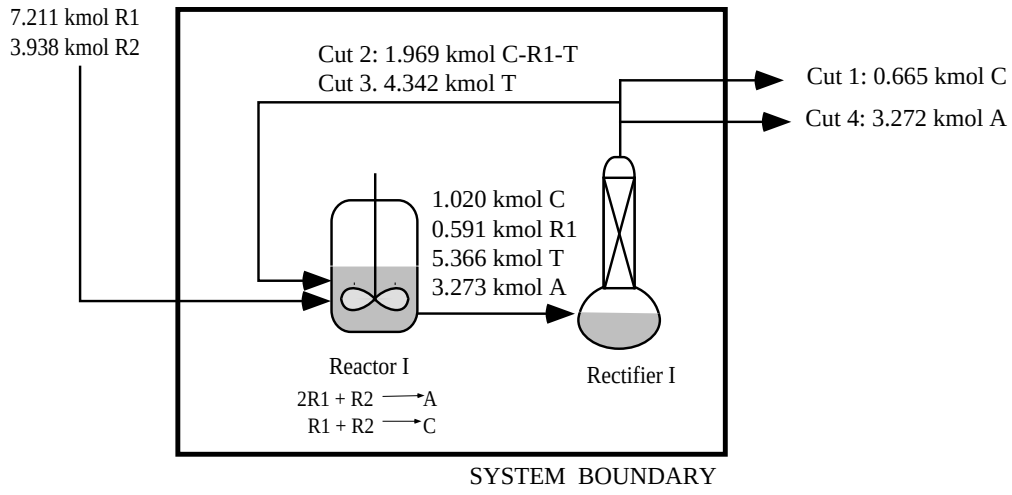

Figure 7-3: Optimized flowsheet of case study 1.

7.3 Case Study 2

The second case study involves all three reaction tasks in the siloxane monomer process. Reaction step I was modeled as in the first case study. In reaction step II intermediate C reacts with methanol (M) to form another intermediate E. Methanol also serves as a solvent. In reaction step III E is converted to the second final product D in a hydrolysis reaction, and methanol is a byproduct. In Chapter 5 an analysis applying solvent recovery targeting to the waste streams emitted from the base case reveals that the design will generate approximately 5 kmol of organic waste per batch.

7.3.1 Separation Sequences

As in the first case study, R2 is not included in the super simplex, as this component will never enter a distillation column. Water and toluene are immiscible, and therefore would lead to the formation of two liquid phases in certain regions of the super simplex. Since the use of the super simplex is based on the assumption of homogeneous mixtures, constraints preventing toluene and water from mixing are required. Consequently, the optimized solution will move on the lower dimensional faces of the super simplex omitting stream compositions containing both toluene and water, and only product sequences on these faces are permitted. Two super simplices are therefore constructed, one representing the composition simplex formed by the pure components C, M, R1, W, E, A, and D, and the other representing the composition simplex formed by the pure components C, M, R1, T, E, A, and D. It should be noted that the requirement to avoid heterogeneous mixtures places an unnecessary restriction on our design. Heterogeneous mixtures appear frequently in the class of processes we are studying, and an extension of the formulation to also permit such mixtures is imperative in order to include all possible design alternatives. The azeotropic behavior was approximated using the Wilson model to calculate the activity coefficients (see, for example, Reid *et al.* (1987)). Binary parameters were extracted from Aspen Plus (Aspen Technology, 1995). Missing binary parameters were estimated using the UNIFAC group contribution method (Fredenslund *et al.*,

1977) as implemented in Aspen Plus (Aspen Technology, 1995). Binary parameters for the pairs involving the non-standard components C, R2, E, A and D can be found in Appendix D. R1 represents allyl alcohol. The vapor phase was assumed to be ideal. Table 7.3 lists the fixed points in these two subsystems at 1 atmosphere with compositions, boiling temperatures, and whether a point is an unstable node (un), stable node (sn), or a saddle point (s).

Table 7.3: Compositions, boiling temperatures, and stability of fixed points at 1 atmosphere.

e	C	M	R2	R1	W	T	E	A	D	$T_B[K]$	type
C-M	0.675	0.325	0	0	0	0	0	0	0	323.4	un
C	1	0	0	0	0	0	0	0	0	336.6	s
M-T	0	0.89	0	0	0	0.11	0	0	0	337.3	s
M	0	1	0	0	0	0	0	0	0	337.8	s
R2	0	0	1	0	0	0	0	0	0	346.0	*
R1-W	0	0	0	0.4	0.6	0	0	0	0	365.4	s
R1-T	0	0	0	0.65	0	0.35	0	0	0	367.5	s
R1	0	0	0	1	0	0	0	0	0	370.0	s
W-E	0	0	0	0	0.914	0	0.086	0	0	370.8	s
W	0	0	0	0	1	0	0	0	0	373.2	s
C-R1-T	0.18	0	0	0.3	0	0.52	0	0	0	373.6	s
C-R1	0.31	0	0	0.69	0	0	0	0	0	378.8	s
T	0	0	0	0	0	1	0	0	0	383.8	s
E	0	0	0	0	0	0	1	0	0	416.5	s
A	0	0	0	0	0	0	0	1	0	532	s
D	0	0	0	0	0	0	0	0	1	752	sn

The feasible distillation sequences were extracted from the two super simplices. There are six batch distillation regions in the simplex containing water (1 to 6 in Table 7.4), and eight regions in the simplex containing toluene (7 to 14 in Table 7.4). Each of these regions involves seven components. Hence, each region produces seven product cuts.

7.3.2 Formulation of Optimization Problem

In addition to the constraints introduced in the first case study governing reaction step I, constraints governing reaction steps II and III were added. The conversion of

Table 7.4: Feasible product sequences for case study 2.

b	Product sequence
1	{C-M, C, R1-W, R1, E, A ,D}
2	{C-M, C, R1-W, W-E, W, A ,D}
3	{C-M, C, R1-W, W-E, E, A ,D}
4	{C-M, M, R1-W, R1, E, A ,D}
5	{C-M, M, R1-W, W-E, W, A ,D}
6	{C-M, M, R1-W, W-E, E, A ,D}
7	{C-M, M-T, M, R1, E, A ,D}
8	{C-M, M-T, R1-T, R1, E, A ,D}
9	{C-M, M-T, R1-T, T, E, A ,D}
10	{C-M, C, C-R1-T, T, E, A, D}
11	{C-M, C, C-R1-T, C-R1, E, A, D}
12	{C-M, R1-T, C-R1-T, C-R1, E, A, D}
13	{C-M, R1-T,C-R1-T, T, E, A, D}
14	{C-M, R1-T, R1, C-R1, E, A, D}

C to E was set to 98%:

$$\mathrm{FR}_{2,C}^{out} = 0.02\mathrm{FR}_{2,C}^{in} \tag{7.8}$$

Reaction step II takes place in excess methanol:

$$\mathrm{FR}_{2,M}^{in} \geq 3.15\mathrm{FR}_{2,C}^{in} \tag{7.9}$$

Conversion of E was set to 85%:

$$\mathrm{FR}_{3,E}^{out} = 0.15\mathrm{FR}_{3,E}^{in} \tag{7.10}$$

The hydrolysis reaction in step III takes place in large excess of water (W):

$$\mathrm{FR}_{3,W}^{in} \geq 25\mathrm{FR}_{3,E}^{in} \tag{7.11}$$

In order to avoid build-up of trace contaminants, a purge fraction of 0.02 was specified. Furthermore, it was required that no water entered reaction step I and II, no methanol entered step I, and no R1 entered reaction step III. The feed of R2

(FR_{R2}^{in}) to reaction step 1 was set to 3.938 kmol as a basis. The problem was solved in a sequential manner. First, the objective function was formulated as minimizing the amount of waste emitted to the environment computed as the total flow crossing from the system to the environment of all fixed points except the final products (A and D). However, this problem has a nonunique solution. The recycle flowrates can take on arbitrary values unless additional constraints are introduced. Therefore, the optimal design was found by formulating a second optimization problem where the recycle flowrates were minimized subject to minimum waste as found in the first optimization problem. The problem was formulated in GAMS (Brooke *et al.*, 1992) as an MILP with 345 equations and 44 binary variables, and solved on an HP 9000/735 workstation by OSL (IBM Corporation, 1991) in 2.41s.

7.3.3 Results

The optimized flowsheet is shown in Figure 7-4. There is no separation between reaction step I and II. The feed to rectifier I is placed in the subsystem C, M, R1, T, E, and A in region 9 and the feed to rectifier II is located in the subsystem M, W, E, A, and D in region 5. Pure E and A recovered in rectifier I are fed to reaction step III. The binary azeotrope C-M and the binary azeotrope M-T are recovered and recycled to reaction step II, while the binary azeotrope R1-T and pure toluene are recovered and recycled to reaction step I. Pure water and the W-E azeotrope are recovered in rectifier II and recycled to reaction step III. Methanol generated in reaction step III is recovered and recycled to reaction step II. 3272 mol of product A and 331 mol of product D are recovered in rectifier II. The amount of waste emitted is 189 mol resulting only from the purge streams. This is a reduction of about 95% compared to the base case. Hence, embedding the super simplex in the reaction-separation synthesis formulation has resulted in a design without azeotropic mixtures that cannot be recycled, and therefore would become hazardous waste. Furthermore, since the consumption of methanol in reaction step I balances the generation of methanol in reaction step III, and methanol can be recovered in pure form in rectifier II, there is no net production of undesired byproducts.

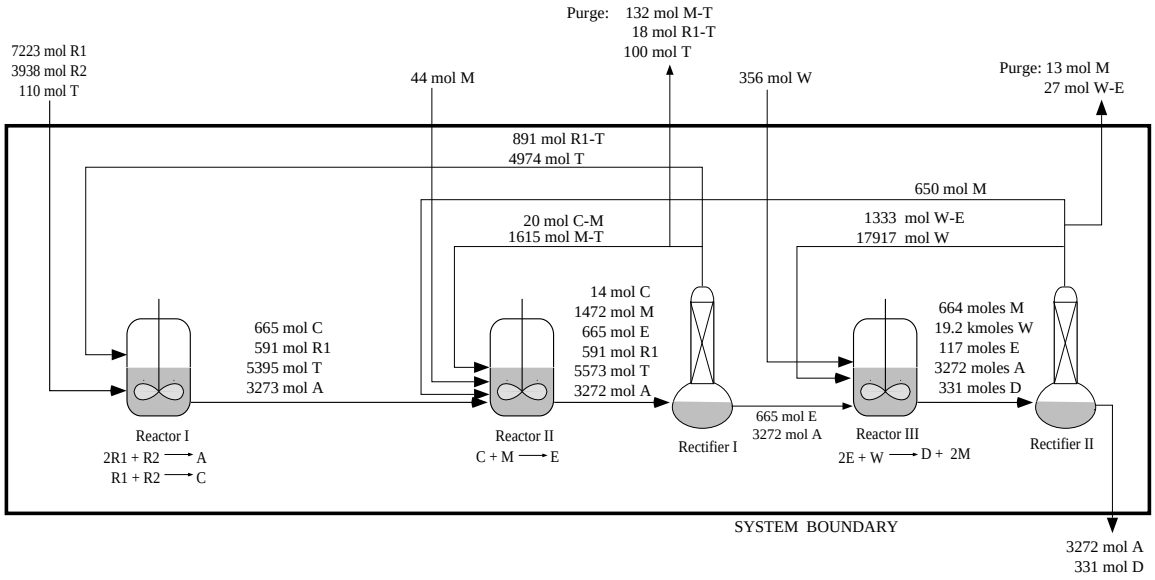

Figure 7-4: Case study 2: optimized flowsheet.

The trade-off of recovery cost versus waste generated may also be studied. The special properties of this problem allows us to readily generate the *pareto optimal surface* (Clark and Westerberg, 1983) of this bicriteria optimization problem. This is because the MILP can be solved to guaranteed global optimality. As a first approximation, the magnitude of the recycled streams is assumed to be proportional to the cost of separating and recycling solvent. The pareto optimal surface is then generated by minimizing the recycle flowrates while varying the level of maximum allowable discharge. Figure 7-5 shows how an increase in the allowable discharge level will decrease the amount recycled. It also shows that increased discharge results in lower yield of A and D, as some intermediate C and E are lost through the discharge. If the level of discharge permitted is set to 2.3 kmol or higher the optimal solution chooses to omit the production of D and instead emits the intermediate C as part of the azeotropes C-R1 and C-R1-T.

The mathematical programming formulation was used to generate other process alternatives by adding additional design constraints to the formulation. The alternative flowsheets will yield slightly higher emissions and are discussed below.

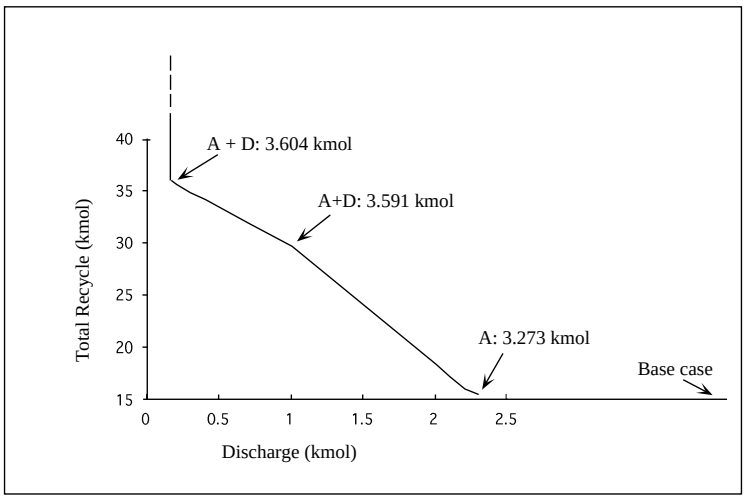

Figure 7-5: Discharge versus recycle flowrates and production rate.

7.3.4 Alternative 1

Toluene and intermediate E are relatively narrow boiling and it is therefore difficult to achieve sharp split between these two components. Detailed dynamic simulations of rectifier I in Figure 7-4 reveal that in order to avoid loss of intermediate E a large fraction of toluene is left in the reboiler at the end of the distillation. Hence, toluene will proceed to reaction step III and rectifier II. Toluene cannot be recovered in pure form from the mixture entering rectifier II due to a heterogeneous azeotrope between water and toluene. Consequently, allowing toluene to enter reaction step II will inevitably result in some toluene as organic waste. By adding a constraint forbidding toluene to enter reaction step II, an alternative design was generated as shown in Figure 7-6. The ternary azeotrope C-R1-T and pure toluene is recycled to reaction step I, and only pure C is sent to reaction step II. Unreacted C is recovered as part of the binary azeotrope C-M in rectifier II and recycled to reaction step II together with recovered methanol, while E is sent to reaction step III. In rectifier III pure methanol is recovered and recycled to reaction step II, while the azeotrope W-E and water are recovered and recycled to reaction step III. The total amount of waste generated is 192 mol, an increase of only 2 % compared to the optimized flowsheet in Figure 7-4.

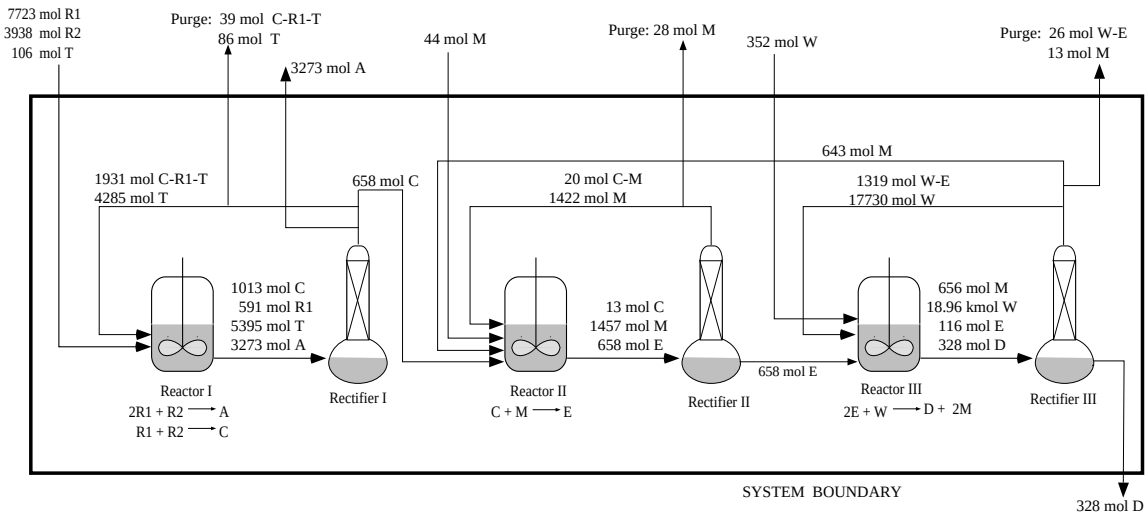

Figure 7-6: Alternative 1: no toluene should enter rectifier II.

7.3.5 Alternative 2

Recovered methanol from reaction step III may possibly contain some water. However, no water should enter reaction step II as this may result in premature reaction of E to produce D. Hence, if methanol from reaction step III is to be recycled to reaction step II drying of the stream is necessary. This may not be desirable, and an alternative design has been generated forbidding such recycle. The resulting flowsheet is shown in Figure 7-7. Observe that the flowsheet is identical to the flowsheet in Figure 7-6 except that recovered methanol is not recycled from rectifier III but disposed of as waste. The design emits 821 mol of waste, mainly due to the generation of methanol in reaction step III.

Table 7.5 summarizes the emission levels, yield, and total amounts recycled for each process design.

7.4 Summary

Two realistic case studies are presented to illustrate the design approach introduced in Chapter 6. The mathematical programming formulation is used to generate several different process alternatives by adding design constraints to the formulation. The

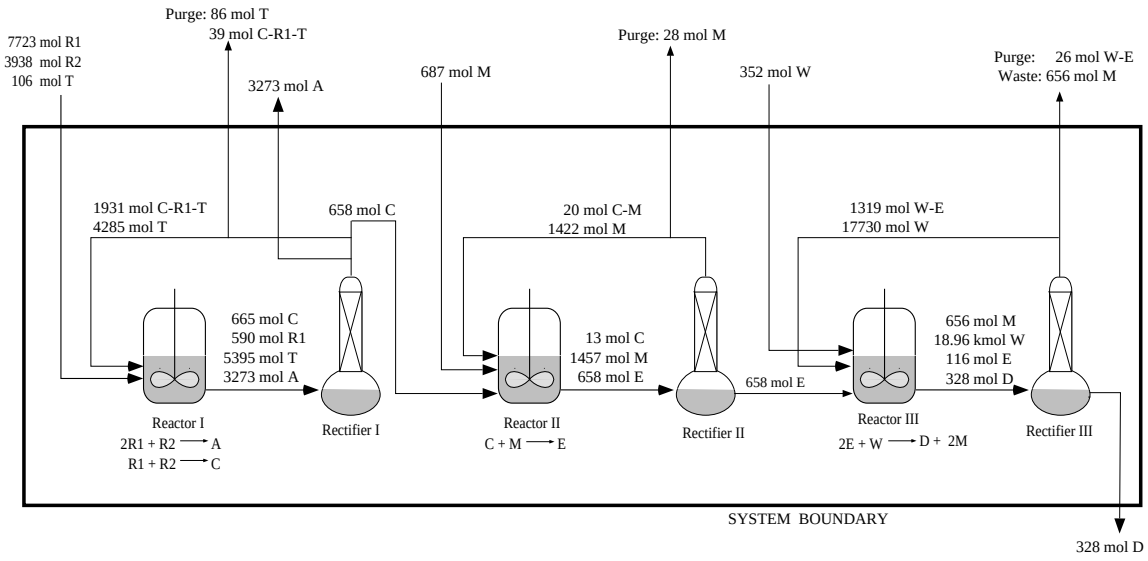

Figure 7-7: Alternative 2: no methanol recycled from rectifier III to reaction step II.

Table 7.5: Summary of emission levels, yield, and total amounts recycled [kmol per batch].

	Emissions	Yield (A + D)	Recycle
Base case	5	2.7	0
Opt. flowsheet	0.189	3.604	27.41
Alternative 1	0.192	3.601	27.35
Alternative 2	0.821	3.601	26.71

process alternatives generated show that an intuitive and automated formulation can produce minimum emission designs very rapidly. It is believed that this decision support tool will be particularly useful in the early stages of process development enabling the engineer to automatically generate and explore minimum emission designs interactively by adding constraints in an evolutionary manner.

Furthermore, it is verified that the formulation can be extended to explore the space of noninferior solutions corresponding to the trade-offs between quantity of waste emitted and the cost of recovering and recycling solvent. The mathematical properties of the formulation guarantee this space to be generated efficiently and correctly. In fact, it is believed that the primary value of the work will be the ability

to generate noninferior solutions in a systematic and automated manner, omitting the need for an ad hoc and manual generation of (possibly inferior) design alternatives as currently practiced in industry.

Chapter 8

Plant-wide Design of Solvent Mixtures

In this chapter the mathematical programming formulation presented in Chapter 6 is extended to provide a general framework for the design of multi-product batch manufacturing facilities in which solvent use is integrated across parallel processes. The goal is to integrate the reaction steps and separation network of the processes such that the generation of waste streams that cross the plant boundary is minimized.

Solvent integration across parallel processes may be advantageous if, for example, the processes have different purity requirements. High purity requirements will typically require a larger purge fraction. It may therefore be beneficial to recycle the recovered solvent to a process with lower purity requirements and lower purge fraction. Thereby the amount of purge will be lower. Improvements from integrating across processes may also be achieved if an azeotrope formed in one process cannot be recycled within the process, but can be accepted in another process. For example, if an azeotrope formed between components where one or more is needed as solvent in a particular reaction task, while the other component(s) are restricted from entering the same reaction task because this may lower the yield, result in undesired side-reactions, etc. It may instead be acceptable to recycle the azeotrope to another process if one or more of the components involved are required in the process and the other component(s) will not result in undesired side-effects. Breaking the azeotrope

may also be accomplished by recycling the azeotrope to another process where a component is present that acts naturally as an entrainer. The recovered solvent can then be recycled back to the original process. Similarly, a solvent that is used in one process may be used as an entrainer in another process and therefore sent to the other process. Depending on the sizes of the entrainer stream and the azeotropic stream it may be more advantageous to allow the solvent stream rather than the azeotropic stream to cross the process boundaries. Several of these benefits are demonstrated in the case studies in Chapter 9.

The methodology is best suited to processes with parallel campaigns that coincide or are relatively close in time. Recovery and recycling of solvent in batch manufacturing will always require some intermediate storage. Because of the generally hazardous (in particular, flammable) nature of the solvents it is desirable to limit quantities and also the time span required for storage.

Trace contaminants are often a concern in the pharmaceutical industry. In such situations solvent integration across processes should be used with caution, and probably restricted to recycling between stages for the production of a single product.

8.1 Problem Statement

The problem that is addressed can be stated as follows:

> *Given a set of parallel processes each described by a set of reaction tasks with known stoichiometry and a set of acceptable solvent and entrainer candidates, synthesize a batch reaction and separation network for each process that satisfies production demand while integrating solvent recovery and recycling in order to minimize the waste generated.*

The same assumptions as those of the process-wide design formulation presented in Chapter 6 apply:

- The magnitude of the streams entering the separation tasks is assumed to be proportional to the cost of separating and recycling solvent.

- A separation task is assumed to follow each reaction task. However, the optimization may choose to omit the distillation task, and instead let the reaction task feed directly to the next reaction task
- Only material leaving a separation task can cross the system boundary.
- The process flowrates are computed as time averaged flows in a batch process based on overall mole balances.
- Batch distillation is the separation method of choice.
- All streams to be separated are homogeneous.
- Perfect splits can be achieved.

The objective function is a modified version of (6.2) presented in Chapter 6:

$$\begin{aligned} & \min \sum_{s \in S} \sum_{d \in D_s} \sum_{i \in I} \mathrm{FD}_{sdi}^{in} \\ \text{s.t.} \quad & \min \sum_{s \in S} \sum_{d \in D_s} \sum_{e \in \hat{E}} \mathrm{C}_e \mathrm{FD}_{sde}^{w} \end{aligned} \tag{8.1}$$

where S represents the set of parallel processes, D_s is the set of separation tasks in process s, FD_{sdi}^{in} is the flow of component i into separation task d in process s, I is the set of pure components, $\hat{\mathrm{E}}$ represents the set of product cuts (separated compositions) that will end up as waste if they cross the system boundary, and FD_{sde}^{w} is the amount of composition e from separation task d in process s crossing the system boundary.

8.2 Reaction-Separation Superstructure

The overall reaction-separation superstructure is illustrated in Figure 8-1 using two parallel processes. Each separation task is represented by a node for each fixed point. A fixed point node may take input only from the corresponding separation task, and output material to the environment, to all separation tasks in all processes, and to all reaction tasks in all processes as shown in Figures 6-4 and 6-6. The *super*

simplex introduced in Chapter 6 is embedded into the modeling framework and will correspond to the overall composition simplex of mixtures of all the components that may appear in all the processes included in the reaction-separation superstructure. This set of components will include raw material and products, in addition to several candidate solvents and entrainers.

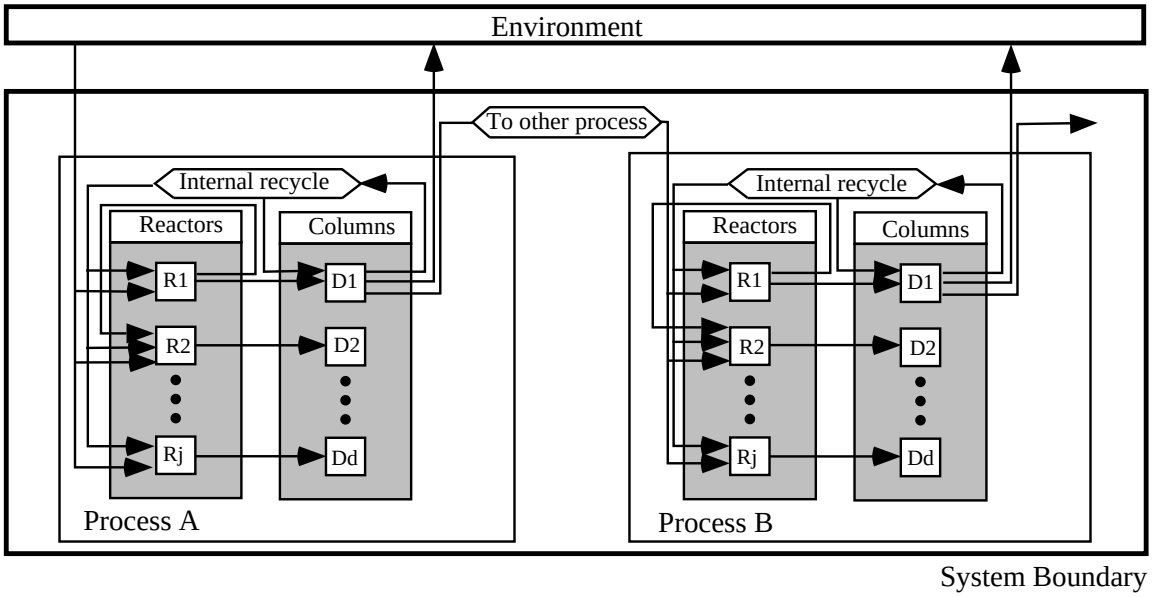

Figure 8-1: Reaction-separation superstructure for plant-wide design of solvent mixtures involving two processes.

8.3 Mathematical Formulation

To derive the mathematical formulation, the following index sets will be used to characterize the topology of the superstructure. The fixed points will be represented by the index set E = $\{e\}$. The set of pure components, which is a subset of E, will be represented by I = $\{i\}$. S = $\{s\}$ represents the number of parallel processes, and J_s = $\{j\}$ represents the number of reaction tasks in process s. The number of reactions taking place in a particular reaction task is denoted by R_j = $\{\pi\}$. Each of the reaction tasks will be followed by a distillation task. The distillation tasks in process s are represented by D_s = $\{d\}$. In the mathematical formulation each batch distillation region in the super simplex will be represented by its corresponding

product simplex. NB = $\{b\}$ denotes the batch distillation regions. $K_b = \{k\}$ denotes the individual product cuts, and K_{be} denotes the product cuts in batch distillation region b with composition equal to fixed point e.

The flows into and out of reaction task j in process s of component i are given by FR^{in}_{sji} and FR^{out}_{sji}. Although FR^{out}_{sj} is a single stream, it is represented by separate flowrates for each individual pure component. This is done in order to avoid using molefractions, which would result in nonlinearities in the model. The flow of component i from reaction task j to reaction task $\hat{j}$ in process s is given by $FR^{out}_{sj\hat{j}i}$, and the flow of component i from reaction task j to distillation task d in process s is given by FR^{out}_{sjdi}. The flow of material with composition equal to fixed point e from distillation task d in process $\hat{s}$ to reaction task j in process s is given by $FDR_{sd\hat{s}je}$, and the flow of material equal to fixed point e from the environment to reaction task j in process s is given by FE^{out}_{sje}. Flow into batch distillation column d in process s of component i is represented by FD^{in}_{sdi}. The flow of distillation cut k in batch distillation region b from column d in process s is denoted by FD^{out}_{sdbk}, and the total amount of material recovered in column d in process s exhibiting the composition of fixed point e is denoted by FDT^{out}_{sde}. $FR^{out}_{sj_di}$ is the flow of component i out of reaction task j_d in process s preceding distillation task d in process s. FE^{out}_{sde} is the flow of material with composition equal to fixed point e from the environment to distillation task d in process s, and $FDD_{\hat{s}\hat{d}sde}$ is the flow of material from distillation task $\hat{d}$ in process $\hat{s}$ to distillation task d in process s with composition equal to fixed point e. $Y_{sdb} \in \{0, 1\}$ is a binary variable denoting an active or inactive region. $Y_{sdb} = 1$ if the initial reboiler composition in column d in process s is located in region b. Otherwise, $Y_{sdb} = 0$. L_{sd} is a binary variable denoting an active or inactive distillation task. $L_{sd} = 1$ if material is fed to distillation task d, otherwise $L_{sd} = 1$ if material is fed to distillation task d in process s. Otherwise, $L_{sd} = 0$. M is a large scalar. The value of M is selected carefully such that if $Y_{db} = 1$ or $L_{sd} = 1$, the values of the flowrates are not constrained. FE^{in}_{sde} denotes flow of fixed point e from distillation task d in process s to the environment, and $PURGE_{sde}$ is the amount of purge with composition equal to fixed point e from column d in process s. The resulting mixed-integer linear

programming (MILP) problem is:

$$\mathrm{FR}^{in}_{sji} + \sum_{\pi \in \mathrm{R}_j} \xi_{sj\pi}\nu_{sj\pi i} = \mathrm{FR}^{out}_{sji} \;\; \forall s \in \mathrm{S},\; j \in \mathrm{J}_s,\; i \in \mathrm{I} \tag{8.2}$$

$$\mathrm{FR}^{in}_{sji} = \sum_{e \in E} \mathrm{SS}_e \mathrm{FR}^{in}_{sje} + \sum_{\hat{j} \in J} \mathrm{FR}^{out}_{s\hat{j}ji} \; \forall s \in \mathrm{S}, j \in \mathrm{J}_s, i \in \mathrm{I} \tag{8.3}$$

$$\mathrm{FR}^{in}_{sje} = \sum_{\hat{s} \in S} \sum_{d \in D_s} \mathrm{FDR}_{\hat{s}dsje} + \mathrm{FE}^{out}_{sje} \; \forall s \in \mathrm{S}, \forall j \in \mathrm{J}_s,\; e \in \mathrm{E} \tag{8.4}$$

$$\mathrm{FR}^{out}_{sji} = \sum_{\hat{j} \in J} \mathrm{FR}^{out}_{sj\hat{j}i} + \sum_{\hat{j} \in J} \mathrm{FR}^{out}_{sjdi} \;\; \forall s \in \mathrm{S},\; j \in \mathrm{J},\; i \in \mathrm{I} \tag{8.5}$$

$$\mathrm{FD}^{in}_{sdi} = \sum_{b \in \mathrm{NB}} \sum_{k \in K_b} p_{bki} \mathrm{FD}^{out}_{sdbk} \;\; \forall s \in \mathrm{S},\; d \in \mathrm{D}_s,\; i \in \mathrm{I} \tag{8.6}$$

$$\mathrm{FD}^{in}_{sdi} = \sum_{j \in J} \mathrm{FR}^{out}_{sjdi} + \sum_{e \in E} \mathrm{SS}_{ie} (\mathrm{FE}^{out}_{sde} + \sum_{\hat{s} \in S} \sum_{\hat{d} \in D} \mathrm{FDD}_{\hat{s}\hat{d}sde}) \;\; \forall s \in \mathrm{S},\; d \in \mathrm{D}_s,\; i \in \mathrm{I} \tag{8.7}$$

$$\mathrm{FDT}_{sde} = \sum_{b \in \mathrm{NB}} \sum_{k \in K_{be}} \mathrm{FD}^{out}_{sdbk} \;\; \forall s \in \mathrm{S},\; d \in \mathrm{D}_s,\; e \in \mathrm{E} \tag{8.8}$$

$$\sum_{k \in K_b} \mathrm{FD}^{out}_{sdbk} \leq \mathrm{M} Y_{sdb} \quad \forall s \in \mathrm{S},\; d \in \mathrm{D}_s,\; b \in \mathrm{NB} \tag{8.9}$$

$$\sum_{b \in \mathrm{NB}} \mathrm{Y}_{sdb} = 1 \;\; \forall s \in \mathrm{S},\; d \in \mathrm{D}_s \tag{8.10}$$

$$\sum_{i \in I} \mathrm{FD}^{in}_{sdi} \leq \mathrm{ML}_{sd} \quad \forall s \in \mathrm{S},\; d \in \mathrm{D} \tag{8.11}$$

$$\mathrm{FDT}_{sde} = \sum_{j \in J_s} \mathrm{FDR}_{sdje} + \sum_{\hat{d} \in D_s} \mathrm{FDD}_{sd\hat{d}e} + \mathrm{FE}^{in}_{sde} + \mathrm{PURGE}_{sde} \;\; \forall s \in \mathrm{S},\; d \in \mathrm{D}_s,\; e \in \mathrm{E} \tag{8.12}$$

where $\nu_{sj\pi i}$ is the stoichiometric coefficient for component i in reaction π in reaction task j in process s. The extent of reaction $\xi_{sj\pi}$ is the same for all species taking part in reaction π. The element SS_{ie} is the molefraction of component i in fixed point e. p_{bki} is the mole fraction of pure component i in product cut k from batch distillation region b. Also note that $\mathrm{FR}^{out}_{s\hat{j}ji}$ must be set to zero for all reaction tasks $\hat{j}$ that are not directly downstream to reaction task j (both tasks j and $\hat{j}$ are in process s), and $\mathrm{FR}^{out}_{sjdi} = 0$ for all distillation tasks d that are not directly downstream to reaction task j in process s. Likewise, $\mathrm{FR}^{out}_{s\hat{j}ji} = 0$ for all reaction tasks $\hat{j}$ that are not directly preceding reaction task j.

The purge streams are computed using Equations (8.13) and (8.14). It is assumed that all streams that are integrated across processes are purged.

$$\text{PURGE}_{sd\hat{s}e}(1-\alpha_{sd\hat{s}e}) = \left(\begin{array}{c} \sum_{j \in J_{\hat{s}}^{sdu}} \text{FDR}_{sd\hat{s}je} + \\ \sum_{\hat{d} \in D_{\hat{s}}^{sdu}} \text{FDD}_{sd\hat{s}\hat{d}e} \end{array} \right) \quad \forall s \in \text{S},\ d \in \text{D},\ e \in \text{E} \quad (8.13)$$

$$\text{PURGE}_{sde} = \sum_{\hat{s} \in S} \text{PURGE}_{sd\hat{s}e} \quad \forall s \in \text{S},\ d \in \text{D}_s\ e \in \text{E} \quad (8.14)$$

where $\text{J}_{\hat{s}}^{sdu}$ represents the set of reaction tasks in process $\hat{s}$ that are upstream of distillation task d in process s, and $\text{D}_{\hat{s}}^{sdu}$ represents the set of distillation tasks in process $\hat{s}$ that are upstream of distillation task d in process s. Note that $\text{J}_{\hat{s}}^{sdu}$ includes all reaction tasks in processes other than s in addition to the ones that are upstream in process s. $\text{D}_{\hat{s}}^{sdu}$ includes all distillation tasks in processes other than s in addition to the ones that are upstream in process s and the distillation task d itself. $\alpha_{sd\hat{s}e}$ is the purge fraction of streams with composition equal to fixed point e from column d in process s to process $\hat{s}$. $\text{PURGE}_{sd\hat{s}e}$ denotes the purge of streams with composition e from column d in process s to process $\hat{s}$, and PURGE_{sde} denotes the overall amount of purge with composition e from column d in process s.

The choice of purge fraction will depend on the purity requirements in the particular problem of interest. A process with high purity requirements will require larger purge fractions on recycled streams than a process with lower purity requirements. For processes with similar purity requirements the same purge fraction can be used on all recycled streams. However, in order to make the optimization favor internal recycle to recycle across process boundaries a slightly lower purge fraction should be chosen on internal recycle streams compared to streams that are recycled across processes.

8.4 Summary

A mixed-integer linear programming formulation for the design of multi-product manufacturing facilities in which solvent use is integrated across parallel processes is pre-

sented. The formulation is an extension to the formulation for design of single batch processes presented in Chapter 6. A novel reaction-separation superstructure that yields a modeling framework for the plant-wide design of the mixtures formed in a batch process is introduced. The *super simplex* presented in Chapter 6 is embedded into the modeling framework and will correspond to the overall composition simplex of mixtures of all the components that may appear in all the processes included in the reaction-separation superstructure.

Solvent integration across parallel processes may be advantageous if the processes have different purity requirements, and thereby different requirements on purging. It may be acceptable to run a reaction step in an azeotropic composition recovered in a parallel process rather than in the pure solvent as specified by the chemist. A naturally present entrainer may be exploited by recycling an azeotropic composition to a parallel process. The recovered solvent can then be recycled back to the original process. Several of these benefits are demonstrated in two case studies in Chapter 9.

Chapter 9

Case Studies on Plant-wide Design of Solvent Mixtures

This chapter presents results from two case studies where the formulation for plant-wide design of solvent mixtures was applied. The first case study involves the manufacture of benzonitrile intermediates and shows that integrating solvent usage across parallel processes is beneficial when the processes have different purity requirements. The second case study demonstrates the advantages of plant-wide integration of solvent usage when a recovered azeotrope cannot be recycled internal to the process. The case study also demonstrates how a solvent can act as a naturally present entrainer to break an azeotrope recovered in a parallel process.

9.1 Case Study 1

The first case study involves the production of two substituted benzonitrile compounds (Ar1 and Ar2). These compounds are used as intermediates to dyes and other specialty chemicals. Figure 9-1 shows the base case. Ar1 is processed through three synthetic steps (process 1), a Sandmeyer reaction, Nitration, and Béchamp reduction, respectively, from R1 via intermediates I11 and I12. Ar2 is processed through two synthetic tasks (process 2), a Sandmeyer reaction and Béchamp reduction, respectively, from R2 via intermediate I21. More details about the synthetic steps can

be found in Knight and McRae (1993) and Knight (1994). Five different solvents are used in the two processes (Clarke and Read, 1932; Groggins, 1958; Streitwieser *et al.*, 1992). In the base case toluene is used in reaction steps 1.1 and 2.1. However, either benzene or toluene may be used for the Sandmeyer reaction. For reaction steps 1.3 and 2.2 a 50/50 mixture of methanol and ethanol on a mole basis is used, but both methanol and ethanol are acceptable alone. Water is consumed in some steps and formed in others. In the base case aqueous waste is separated from the organic phase in a decanter after both reaction tasks 1.1 and 2.1. It is assumed that the intermediate remains in the organic phase (primarily toluene). Acetic acid may not enter any other reaction tasks than 1.2, and the intermediate I12 is therefore recovered through crystallization after reaction step 1.2. Likewise, Ar1 and Ar2 are crystallized out and recovered after reaction tasks 1.3 and 2.2, respectively. The stream compositions for the base case can be found in Appendix F.

9.1.1 Separation Sequences

It is assumed that the key reagents react to complete conversion, and that the intermediates can be recovered through either crystallization or a liquid-liquid phase split after each synthetic step. Hence, only the solvents that are used will enter the batch distillation columns. Six solvents therefore form the super simplex: water (W), methanol (M), ethanol (E), benzene (B), toluene (T), and acetic acid (A). The azeotropic behavior was approximated using the UNIQUAC (Universal Quasi-Chemical Theory) (Abrams and Prausnitz, 1975) model to calculate the activity coefficients. The binary interaction parameters were extracted from Aspen Plus (Aspen Technology, 1995). Missing parameters were estimated using the UNIFAC group contribution method (Fredenslund *et al.*, 1977) implemented in Aspen Plus (Aspen Technology, 1995). The vapor phase was assumed to be ideal. The components form eight binary azeotropes and two ternary azeotropes. The fixed points are listed in Table 9.1.

When applying the algorithm described in Chapter 4 twenty-seven separation sequences were found. However, benzene and toluene form heterogeneous mixtures

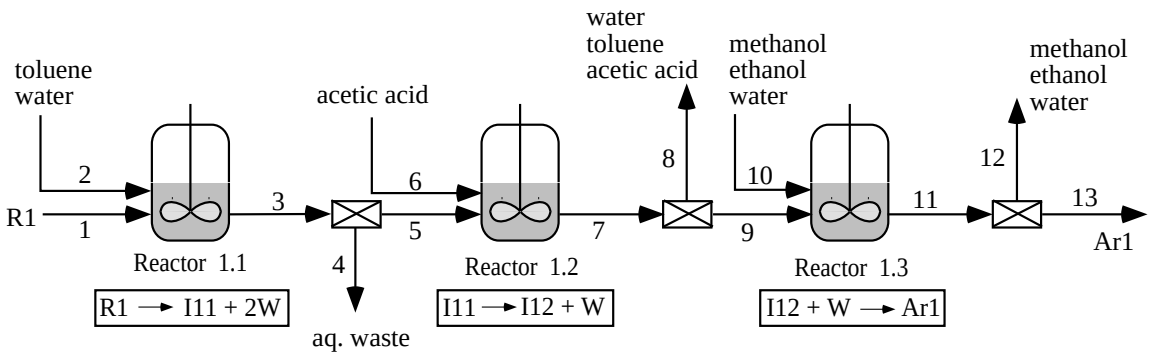

PROCESS 1

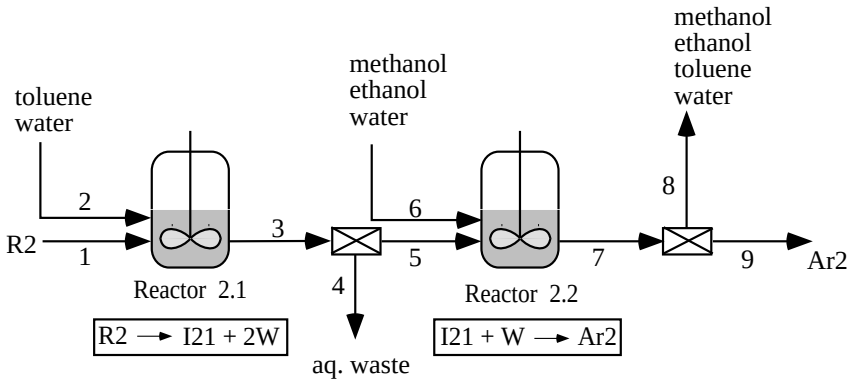

PROCESS 2

Figure 9-1: Base case with solvent requirements.

with water. The composition simplex involving all six components therefore will have domains which are heterogeneous. The algorithm for constructing the super simplex assumes that the mixtures to be separated are homogeneous. Hence, some of the distillation sequences that were found may not be feasible. In order to ensure feasible separation, we constrain the problem so that water may never mix with benzene and toluene in any of the columns. Note that this amounts to introducing two super simplices, which is what was also done in the case study in Chapter 7. The optimization will be constrained to operate only on the face involving all components except water, or on the face involving water but not toluene and benzene. Each sequence will produce six product cuts as shown in Table 9.2. The binary azeotrope

Table 9.1: Compositions, boiling temperatures, and stability of fixed points at 1 atmosphere. un indicates unstable node, s indicates saddle point, and sn indicates stable node. * indicates that the azeotrope is heterogeneous.

e	M	E	B	W	T	A	T_B[K]	type
MB	0.69	0	0.31	0	0	0	331.1	un
MT	0.9	0	0	0	0.1	0	336.8	s
M	1	0	0	0	0	0	337.6	s
EBW	0	0.26	0.56	0.18	0	0	340.1	s*
EB	0	0.45	0.55	0	0	0	340.9	s
BW	0	0	0.7	0.3	0	0	342.4	s*
EWT	0	0.46	0	0.28	0.26	0	349.8	s*
ET	0	0.81	0	0	0.19	0	350	s
EW	0	0.9	0	0.1	0	0	351.3	s
E	0	1	0	0	0	0	351.5	s
B	0	0	1	0	0	0	353.3	s
WT	0	0	0	0.56	0.44	0	357.6	s*
W	0	0	0	1	0	0	371.3	s
TA	0	0	0	0	0.62	0.38	380.9	s
T	0	0	0	0	1	0	384	sn
A	0	0	0	0	0	1	391.2	sn

between methanol and benzene (MB) is the only unstable node and therefore all product sequences will start with the methanol-benzene azeotrope as the first product cut.

9.1.2 Analysis of Base Case

For the base case it is assumed that there is no internal recovery and recycling of solvents. Instead the mixed waste-solvent streams (streams 8 and 12 in process 1, and stream 8 in process 2) are collected and sent to a central waste-treatment facility. The mixture to be treated contains both toluene and water and is therefore heterogeneous. The mixture is first separated into an organic phase and an aqueous phase (see Table 9.3), and the organic layer is sent to a batch distillation column. The liquid-liquid phase split was simulated using Aspen Plus (Aspen Technology, 1995) with UNIQUAC (Abrams and Prausnitz, 1975) to approximate the nonideal liquid behavior.

Table 9.2: Separation sequences in the composition simplex.

b	Product sequences	b	Product sequences
1	{MB, MT, M, EW, W, A}	15	{MB, EWB, BW, B, TA, T}
2	{MB, MT, M, EW, E, A}	16	{MB, EWB, BW, B, TA, A}
3	{MB, MT, EWT, ET, E, A}	17	{MB, EWB, BW, WT, TA, T}
4	{MB, MT, EWT, ET, TA, T}	18	{MB, EWB, BW, WT, TA, A}
5	{MB, MT, EWT, ET, TA, A}	19	{MB, EWB, EWT, ET, E, A}
6	{MB, MT, EWT, WT, TA, T}	20	{MB, EWB, EWT, ET, TA, T}
7	{MB, MT, EWT, WT, TA, A}	21	{MB, EWB, EWT, ET, TA, A}
8	{MB, MT, EWT, EW, E, A}	22	{MB, EWB, EWT, EW, E, A}
9	{MB, MT, EWT, EW, H, A}	23	{MB, EWB, EWT, EW, W, A}
10	{MB, EWB, EB, B, TA, T}	24	{MB, EWB, EWT, WT, TA, T}
11	{MB, EWB, EB, B, TA, A}	25	{MB, EWB, EWT, WT, TA, A}
12	{MB, EWB, EB, ET, E, A}	26	{MB, EWB, WB, WT, W, A}
13	{MB, EWB, EB, ET, TA, T}	27	{MB, MT, EWT, WT, W, A}
14	{MB, EWB, EB, ET, TA, A}		

Table 9.3: Composition of mixed waste-solvent stream in base case to central treatment facility [kmol per batch].

Component	Waste stream	Organic layer	Aqueous layer
Toluene	22.61	21.07	1.54
Acetic Acid	17.69	3.51	14.19
Methanol	11.87	2.05	9.82
Ethanol	11.87	5.23	6.65
Water	34.08	1.24	32.84
Total	98.13	33.1	65.03

It was assumed that the organics in the aqueous layer would end up as waste (about 32.1 kmol). Solvent recovery targeting was applied to the stream composition of the organic layer (the small amount of water was ignored). The stream was placed on the boundary of batch distillation region 4 giving rise to the sequence {MT, ET, TA, T}. It was found that about 36% of organic waste would be generated from this stream assuming no use of entrainers. For example, the distillation would produce the binary azeotrope methanol-toluene. Since toluene can only be fed to reaction tasks 1.1 and 2.1, and it is not desirable to introduce methanol in these reaction tasks,

the azeotrope must be disposed of. Also, the binary azeotrope toluene-acetic acid is generated and cannot be recycled. Hence, a total of 44 kmol of organic waste per batch would be generated from the base case.

9.1.3 Formulation of Optimization Problem

The mathematical synthesis formulation presented in Chapter 8 was applied to the two processes. In addition to the constraints discussed above, a set of design requirements was specified. Lower bounds on solvent requirements specified in terms of moles were introduced:

- The amount of water in reaction task 1.1 has to be greater or equal to 50 times the amount of R1.
- The total amount of benzene and toluene in reaction task 1.1 has to be greater or equal to three times the amount of R1.
- The amount of acetic acid in reaction task 1.2 has to be greater or equal to 4.5 times the amount of I11.
- The amount of water in reaction task 1.3 has to be greater or equal to 5 times the amount of I12.
- The total amount of methanol and ethanol in reaction task 1.3 has to be greater or equal to 3.15 times the amount of I12.
- The amount of water in reaction task 2.1 has to be greater or equal to 50 times the amount of R2.
- The total amount of benzene and toluene in reaction task 2.1 has to be greater or equal to 3 times the amount of R2.
- The amount of water in reaction task 2.2 has to be greater or equal to 5 times the amount of I21.

- The total amount of methanol and ethanol in reaction task 2.2 has to be greater or equal to 3.15 times the amount of I21.

No water can be added to reaction task 1.2 as this would lower the yield, and acetic acid may not enter any other reaction task than 1.2. The purity requirements are higher for product Ar1 than for product Ar2. A purge fraction of 0.019 was used for recycled streams internal to process 1, and 0.02 was used for recycled streams from process 2 to process 1. A purge fraction of 0.009 was specified for recycled streams internal to process 2, and 0.01 was used for recycled streams from process 1 to process 2. The incremental higher purge fractions for streams integrated across processes were chosen to favor internal recycling if possible. A weighting factor of 1 was used for all waste. The feed of R1 was set to 3.932 kmol producing about 600 kg of Ar1, and the feed of R2 was set to 3.605 kmol producing about 550 kg of Ar2. The problem was formulated in GAMS (Brooke *et al.*, 1992) as an MILP with 1005 equations and 129 binary variables, and solved on an HP 9000/735 workstation by OSL (IBM Corporation, 1991) in 4.39s.

9.1.4 Results

The optimized flowsheet with the integrated solvent streams is shown in Figure 9-2. Toluene is recovered through filtration after the aqueous phase split and is recycled internally to the first reaction task in both processes. In addition, toluene is recycled from process 1 to process 2 to make up for lost toluene through purging. Make-up for toluene and methanol is only introduced in process 1. It is advantageous to use as much fresh material as possible for the process with the higher purity requirement, in this case process 1, and it reduces the overall loss due to different purge fractions. Similarly, methanol is recovered through batch distillation after the last reaction task and recycled internally in both processes. In addition methanol is recycled from process 1 to process 2 to make up for lost methanol through purging. Acetic acid is recovered and recycled internally in process 1, while water is recovered in process 1 and recycled to process 2. The amount of organic waste generated is

1261 mol resulting only from the purge streams as indicated in the figure. About 391.9 kmol of aqueous waste is also emitted. No azeotropic mixtures are produced. Hence, optimization in the super simplex has driven the mixtures formed in the process to lower dimensional faces, thus avoiding systems with azeotropic compositions. Also observe that methanol was chosen as the solvent for reaction tasks 1.3 and 2.2. Ethanol forms a binary azeotrope with water, and the use of ethanol would therefore generate additional waste. Toluene was chosen as solvent for reaction tasks 1.1 and 2.1. However, use of benzene instead would not change the value of the objective function. Introducing different weighting factors to reflect differences in toxicity or treatment cost would help to discriminate components in such cases.

For comparison, forbidding the processes to integrate, but allowing recycling internal to each process would result in process designs that would generate about 1400.4 mol of organic waste (see Figures 9-3 and 9-4). Hence, integrating solvent use across parallel processes has lead to a 10% reduction in the amount of organic waste generated compared to recycling only internal to each process. Compared to the use of a central recovery facility as in the base case an overall reduction in organic waste of about 95% has been achieved. Stream tables for the flowsheets in Figures 9-2, 9-3, and 9-4 can be found in Appendix F.

9.2 Case Study 2

This case study involves two parallel processes, each with two reaction steps. The chemistry and solvent requirements are indicated in Figure 9-5. Four different solvents are used in the two processes. Methanol (M) is used in reaction task 1.1, and toluene (T) is used in reaction task 1.2. Methanol is one of the products in reaction task 1.2. Reaction task 2.1 requires iso-propanol (IP), while reaction task 2.2 requires a mixture of ethyl-acetate (EA) and methanol.

9.2.1 Separation Sequences

The compounds involved in the reactions (except methanol) do not form azeotropes with any of the solvents. Furthermore, they are heavy boiling and can be taken out

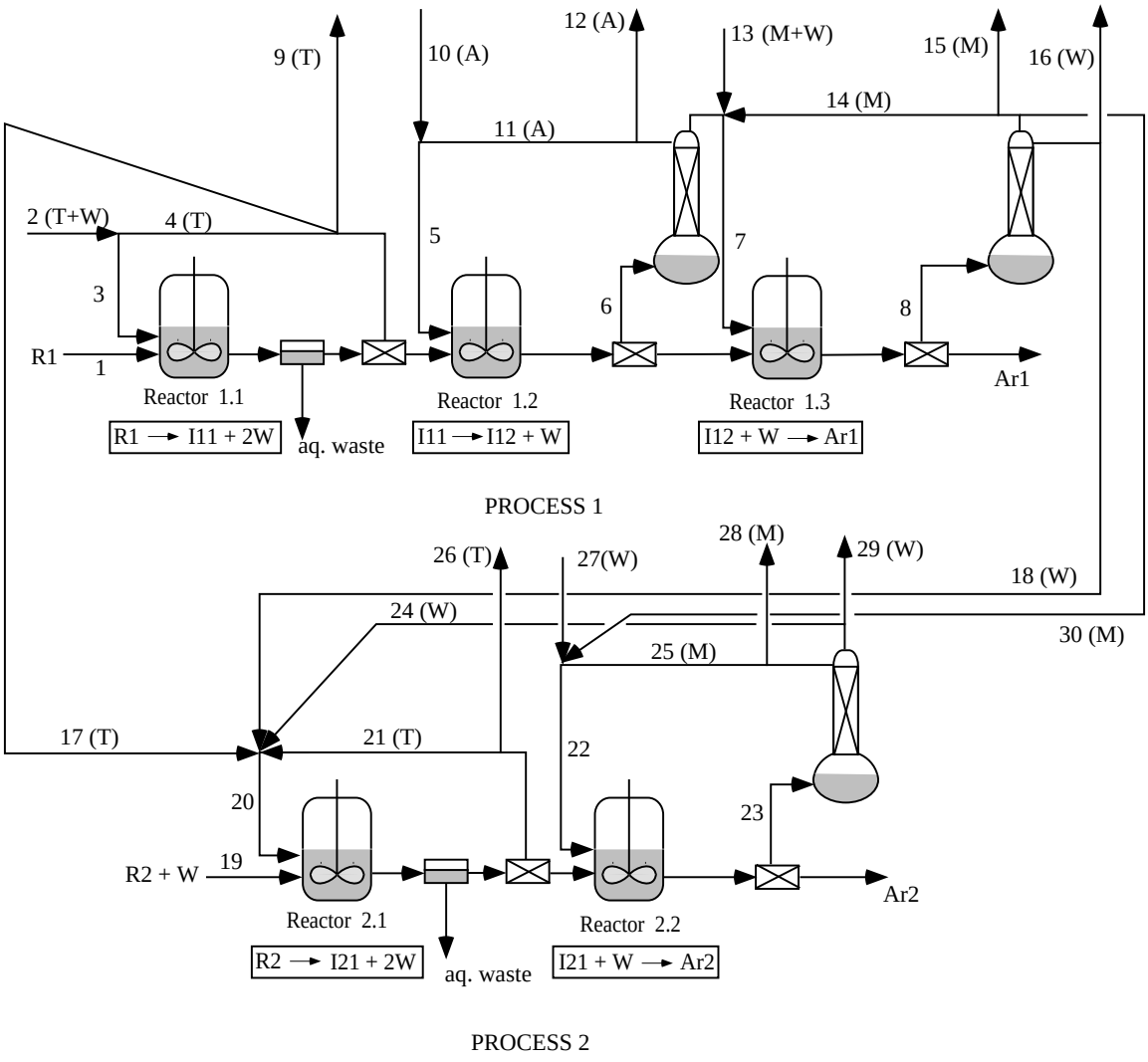

Figure 9-2: Case study 1: integrated flowsheet.

as bottom products in the distillation tasks. Hence, only the solvents are included in the super simplex. The azeotropic behavior was approximated using the UNIQUAC (Universal Quasi-Chemical Theory) (Abrams and Prausnitz, 1975) model to calculate the activity coefficients. The binary interaction parameters were extracted from Aspen Plus (Aspen Technology, 1995). Missing binary interaction parameters were estimated using the UNIFAC group contribution method (Fredenslund *et al.*, 1977) implemented in Aspen Plus (Aspen Technology, 1995). The vapor phase was assumed to be ideal. The components form three binary azeotropes (see Table 9.4).

When applying the algorithm described in Chapter 4 four separation sequences

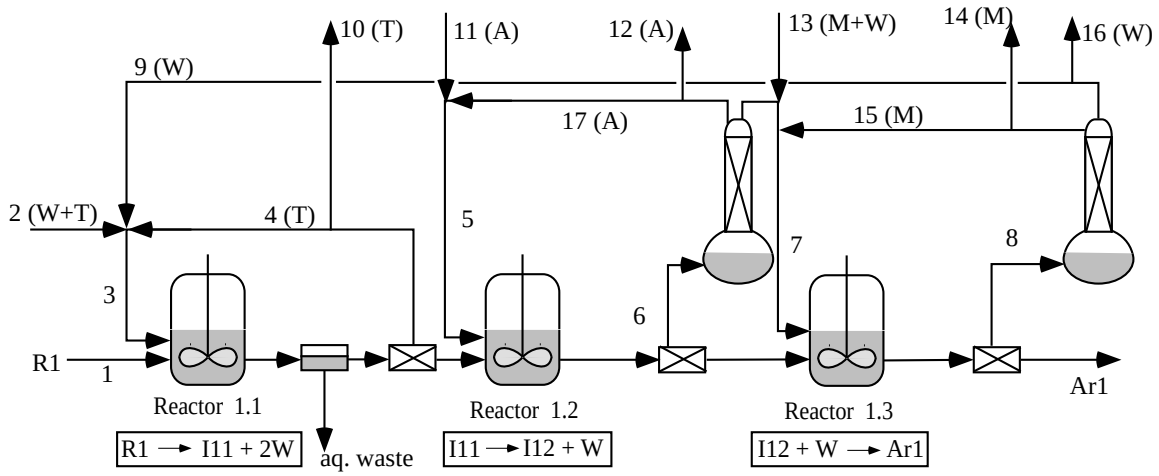

PROCESS 1

Figure 9-3: Case study 1: process 1 with no integration.

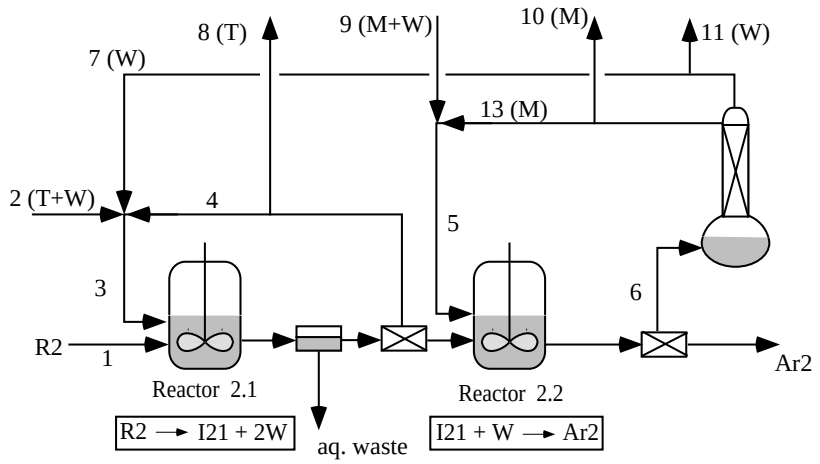

PROCESS 2

Figure 9-4: Case study 1: process 2 with no integration.

were found. Each sequence will produce four product cuts as shown in Table 9.5. The binary azeotrope between methanol and ethyl-acetate (MEA) is the only unstable node and therefore all product sequences will start with this azeotrope as the first product cut.

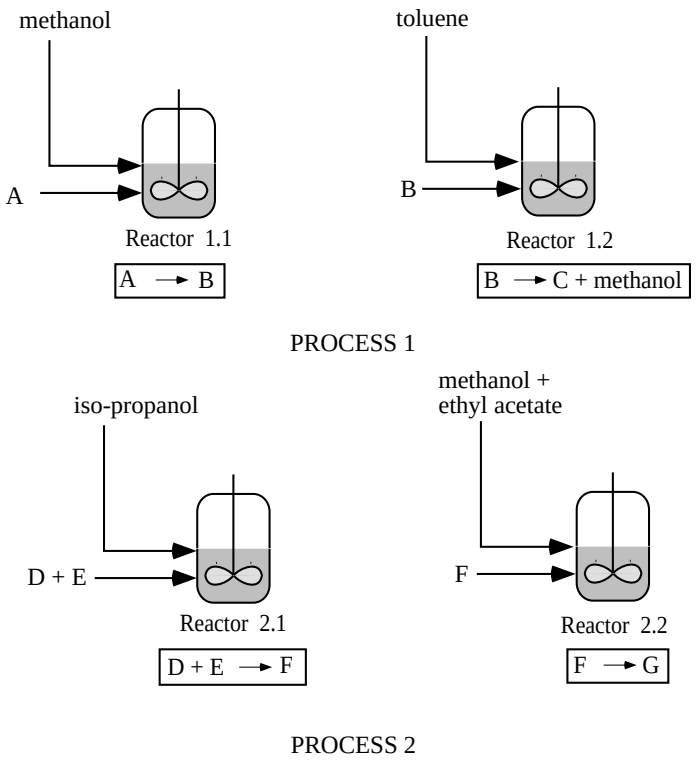

Figure 9-5: Case study 2: solvent requirements.

Table 9.4: Compositions, boiling temperatures, and stability of fixed points at 1 atmosphere. un indicates unstable node, s indicates saddle point, and sn indicates stable node.

e	M	EA	IP	T	T_B[K]	type
MEA	0.7	0.3	0	0	335.3	un
MT	0.9	0	0	0.1	336.8	s
M	1	0	0	0	337.6	s
EAIP	0	0.71	0.29	0	348.6	s
EA	0	1	0	0	350.3	s
IP	0	0	1	0	356.2	s
T	0	0	0	1	384	sn

9.2.2 Formulation of Optimization Problem

The mathematical synthesis formulation presented in Chapter 8 was applied to the two processes. In addition to the constraints discussed above, a set of design requirements was specified. Lower bounds on solvent requirements specified in terms of mol were introduced:

Table 9.5: Separation sequences in the composition simplex.

b	Product sequences
1	{MEA, MT, M, IP}
2	{MEA, MT, IPA, T}
3	{MEA, EAIP, EA, T}
4	{MEA, EAIP, IP, T}

- The ratio of methanol to reagent A for reaction task 1.1 should be greater or equal to 3.
- The ratio of toluene to intermediate B for reaction task 1.2 should be greater or equal to 3.5.
- The ratio of iso-propanol to reagent D in reaction task 2.1 should be greater or equal to 5.
- The ratio of methanol to intermediate F in reaction task 2.2 should be greater or equal to 2.
- The ratio of ethyl-acetate to intermediate F in reaction task 2.2 should be greater or equal to 1.5.

Toluene should not enter reaction task 1.1 as this would result in undesired side-reactions. Methanol should not be fed to reaction task 1.2. Methanol is generated in this reaction task and methanol in the feed will prevent complete conversion. A purge fraction of 0.019 was specified for streams being recycled internal to each process, and a purge fraction of 0.02 was used on streams recycled across process boundaries. The incremental higher purge fractions for streams integrated across processes were chosen to favor internal recycling if possible. The weighting factors were initially set to 1 for all waste streams. A basis of 4000 mol of A was used in process 1, and a basis of 3200 mol of D was used in process 2. The problem was formulated in GAMS (Brooke *et al.*, 1992) with 213 equations and 16 binary variables and solved on an HP 9000/735 workstation by OSL (IBM Corporation, 1991) in 0.51s.

9.2.3 Results

Two scenarios were proposed:

1. No integration between processes.

2. Integration between processes.

Permitting no integration between processes will result in approximately 7200 mol of waste emitted, while scenario 2 will result in 5180 mol of emissions. Hence, we have achieved an improvement of 28% compared to only allowing recycling within the individual processes. Figures 9-6 an 9-7 show the flowsheets resulting from not allowing integration between the processes. The stream data can be found in Appendix G.

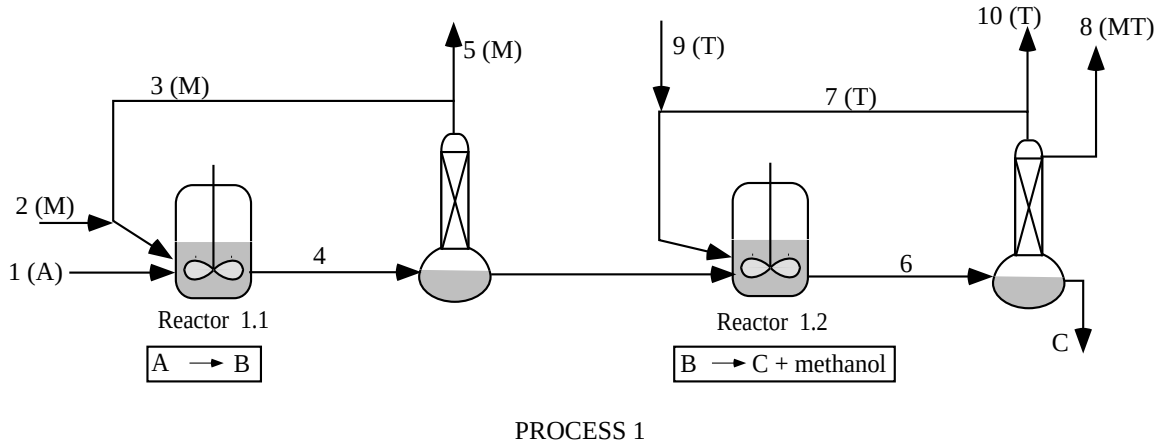

Figure 9-6: Case study 2: process 1 with no integration.

Figure 9-8 shows the optimized flowsheet for scenario 2. Methanol and toluene form a unavoidable binary azeotrope since methanol is generated in reaction task 1.2 while toluene is used as a solvent in the same task. Since toluene cannot be recycled back to reaction task 1.1 where methanol is used as a solvent, the methanol-toluene azeotrope must either be disposed of or recycled to process 2. In the integrated flowsheet a combination takes place: some of the azeotrope is recycled to distillation task 2.2, where the azeotrope is effectively broken by the presence of ethyl acetate, and toluene is recovered in pure form and recycled back to reaction task 1.2. The binary azeotrope methanol-ethyl acetate is also recovered, but can be recycled to reaction

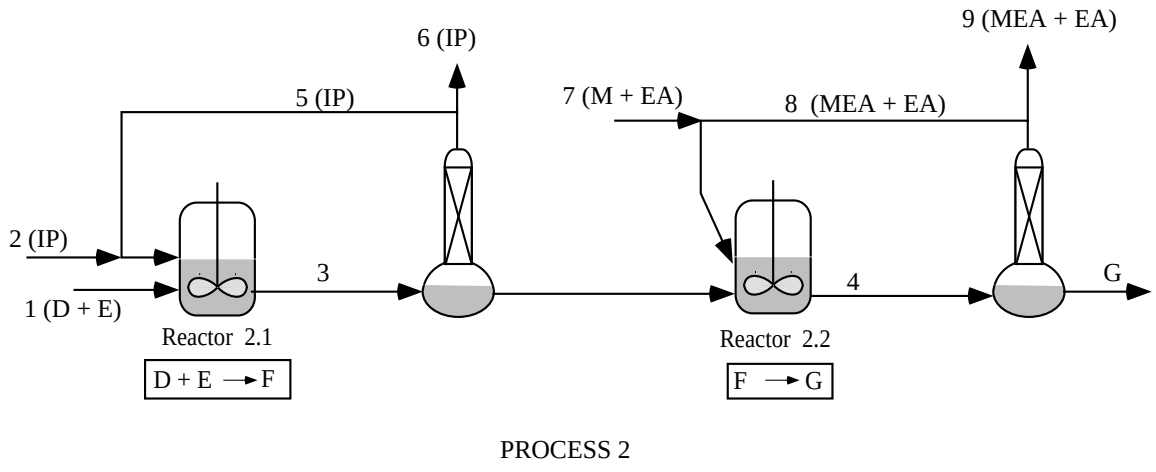

Figure 9-7: Case study 2: process 2 with no integration.

task 2.2 where both components are required as solvents. The binary azeotrope is also recycled to reaction task 1.1 where methanol is used as solvent. Hence, the synthesis in reaction task 1.2 takes place in the methanol-ethyl acetate azeotrope. Since there is a net generation of methanol, some methanol has to be disposed of. This is accomplished through the emission of the remaining of the methanol-toluene azeotrope, and the methanol-ethyl acetate purges. Furthermore, note that no methanol make-up is required. The losses of methanol and ethyl acetate in process 1 are replaced through stream 9 from process 2. Stream tables for the integrated flowsheets can be found in Appendix G.

The breaking of the methanol-toluene azeotrope is illustrated in Figure 9-9. The mixture that enters distillation task 2.2 is composed of methanol, ethyl acetate, and toluene. The methanol-toluene azeotrope is recycled from process 1, while a mixture of the methanol-ethyl acetate azeotrope and ethyl acetate make-up (labeled $\mathbf{x}^a$ in Figure 9-9) is fed from reaction task 2.2. The make-up of ethyl acetate is exactly balanced to place the mixture on the straight line between the methanol-ethyl acetate azeotrope and pure toluene (labeled $\mathbf{x}^b$ in Figure 9-9), resulting in recovery of pure toluene. Also note that the vertex for pure ethyl acetate, and the composition points $\mathbf{x}^a$ and $\mathbf{x}^b$ must lie on a straight line to satisfy the overall material balance.

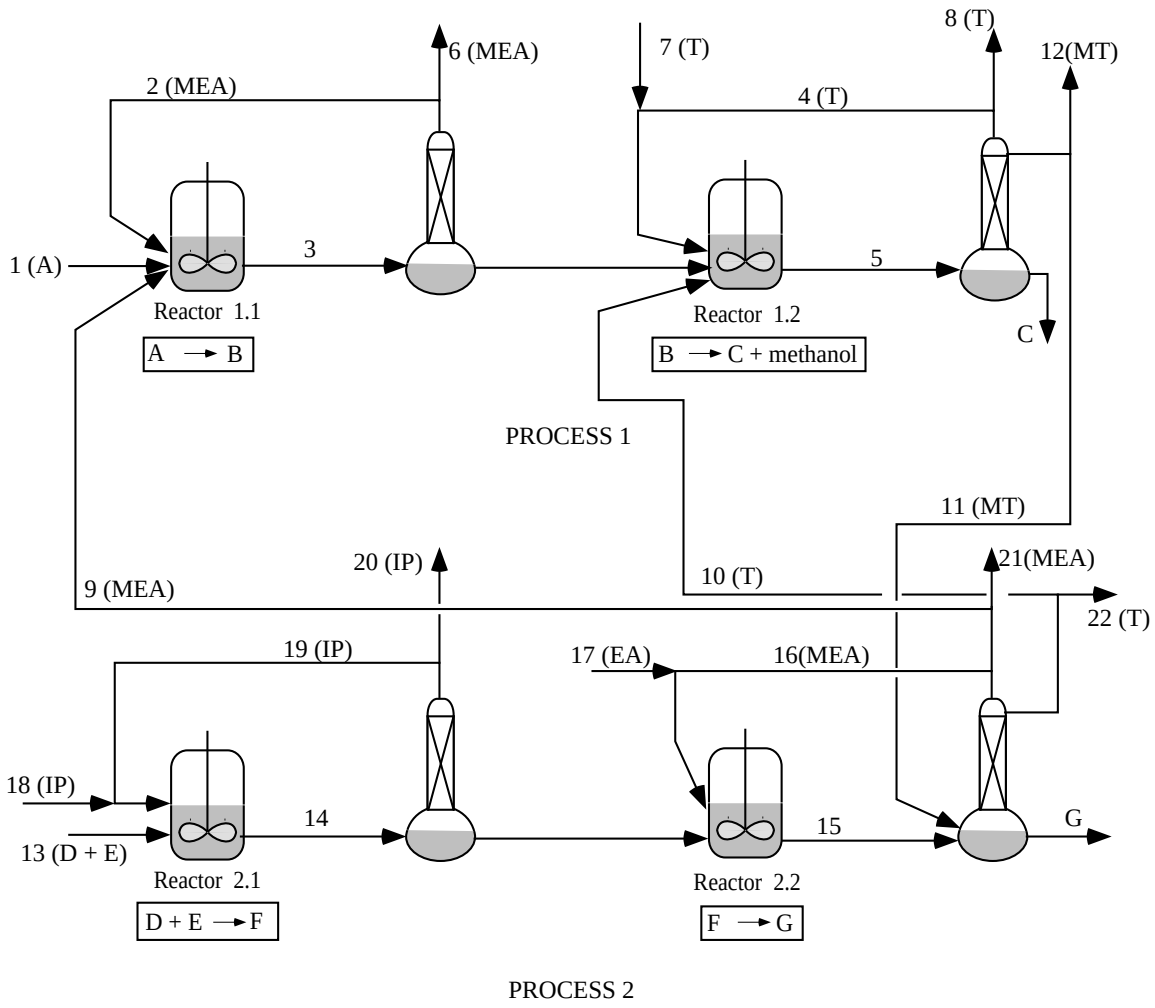

Figure 9-8: Optimized flowsheet for integration of recovered solvent across process boundaries.

9.2.4 Alternative Flowsheets

In the above formulation the weighting factors for all the different waste compositions were set to 1. However, different weighting factors can be introduced to discriminate between different compositions or components. In order to reflect the difference in toxicity of toluene compared to the other components it was decided to increase the weighting factors of discharge of pure toluene as well as of the methanol-toluene azeotrope. Table 9.6 shows the weighting factors that were used. The values in case 1 is the same as for the flowsheet in Figure 9-8. The weighting factors in case 2 was found by assuming that toluene is 2.5 times as toxic as the other components.

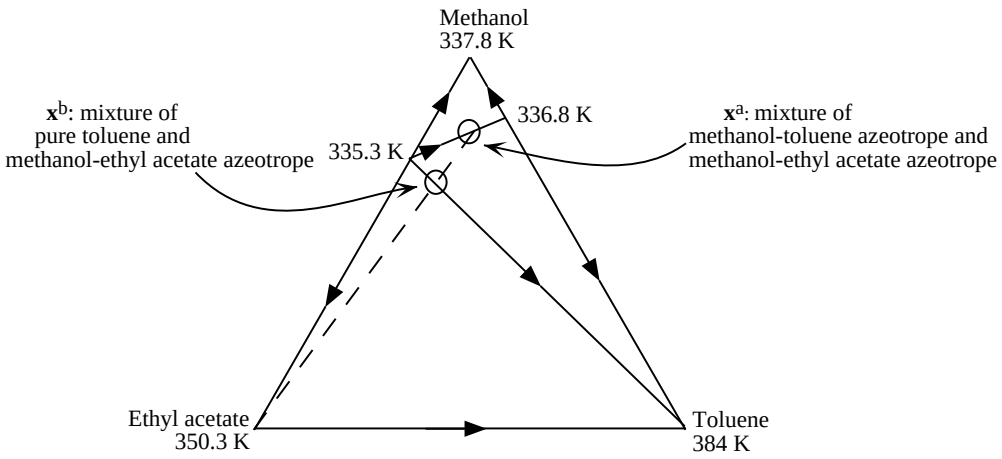

Figure 9-9: Ethyl acetate acts as an entrainer to break the methanol-toluene azeotrope.

The weighting factor for the methanol-toluene azeotrope was found by multiplying the fraction of methanol by 1 and adding 2.5 times the fraction of toluene. In case 3 it was assumed that toluene is 3.5 times as toxic as the other components. The weighting factor for the methanol-toluene azeotrope was found by multiplying the fraction of methanol by 1 and adding 3.5 times the fraction of toluene.

Table 9.6: Weighting factors.

	MEA	MT	M	EAIP	EA	IP	T
Case 1	1	1	1	1	1	1	1
Case 2	1	1.17	1	1	1	1	2.5
Case 3	1	1.28	1	1	1	1	3.5

It is expected that an increase in the weighting factor of toluene will discourage discharge of toluene and instead favor increased recovery and recycling. Figure 9-10 reflects the results of these calculations. Note that the amount of methanol that is discharged remains constant and equal to 4000 mol, which is the amount of methanol generated in reaction task 1.2. Also, the amount of iso-propanol emitted remains constant. The recovery and recycling of iso-propanol is isolated from the rest of the flowsheet and is not effected by the change in weighting factors.

Figure 9-10 reveals that there is only a slight decrease in the discharge of toluene

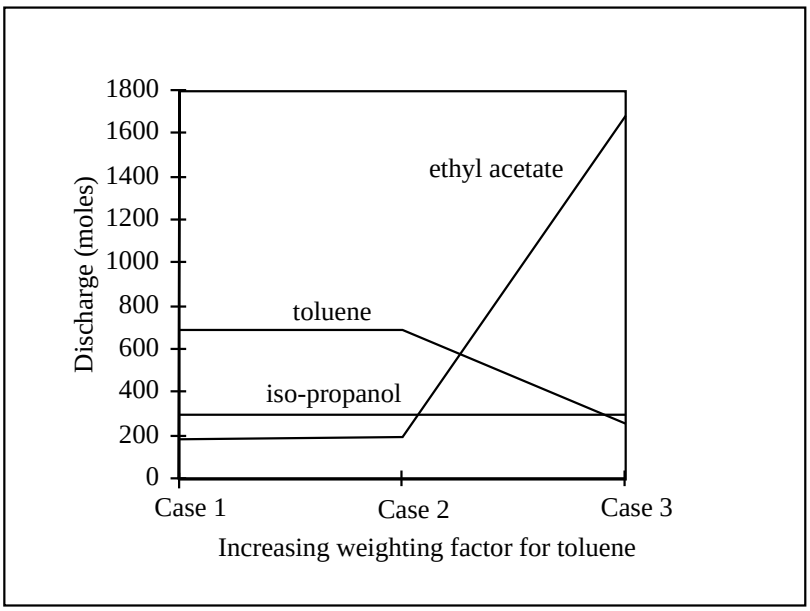

Figure 9-10: Distribution of discharge when weighting factor of toluene is varied.

in case 2. Likewise, there is only a slight increase in the discharge of ethyl acetate. In contrast, a dramatic change is observed when the weighting factor of toluene is increased from 2.5 to 3.5. The integrated flowsheet for case 3 is shown in Figure 9-11 with the stream data in Appendix G. The excess methanol that is generated in process 1 and which in the flowsheet in Figure 9-8 is emitted through the methanol-toluene azeotrope, is now emitted through the methanol-ethyl acetate azeotrope from distillation task 1 in process 1. The generated methanol necessarily has to leave the system. Methanol can only be recovered as a pure component from batch distillation region 1 (see Table 9.5). However, the design constraints placed on the processes do not allow a mixture to be placed in that region. For example, with the amount of toluene required in reaction step 1.2 the composition out will always be located in batch distillation regions 2, 3, or 4. Methanol therefore has to escape the system through an azeotrope (either methanol-toluene or methanol-ethyl acetate) resulting in additional losses due to the fraction of the other component involved in the azeotrope. The methanol-toluene azeotrope is initially favored because the fraction of toluene (about 10%) is relatively small compared to methanol. However, as the weighting factor is increased it becomes less favorable to emit the methanol-toluene azeotrope,

until the fraction of toluene times the weighting factor equals the fraction of ethyl acetate in the methanol-ethyl acetate azeotrope. In this case when the weighting factor is about 3. If the weighting factor is increased further the optimization chooses to emit the methanol-ethyl acetate azeotrope.

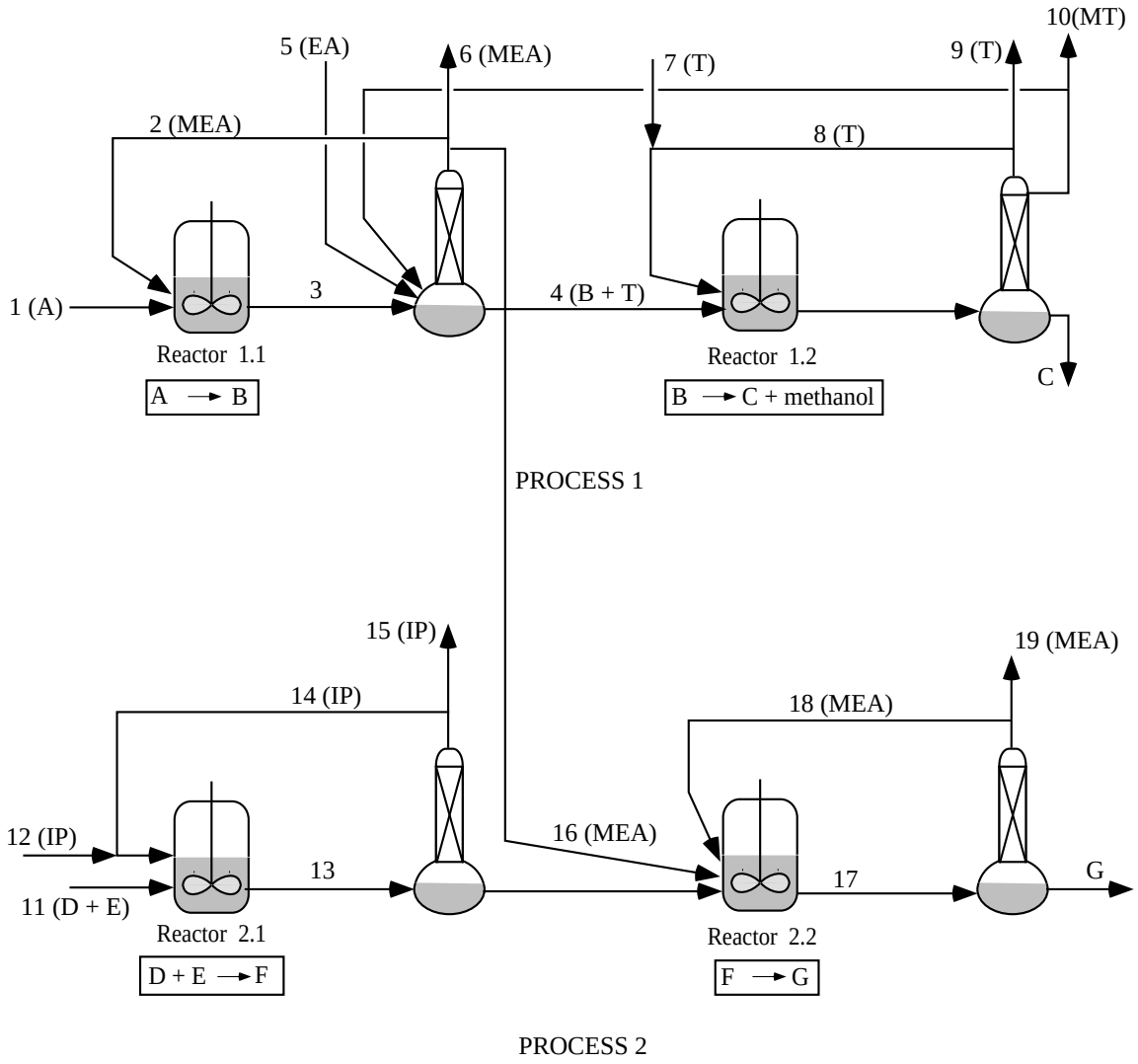

Figure 9-11: Alternative flowsheet.

9.3 Summary

The results from two case studies where the mathematical synthesis formulation for plant-wide design of solvent mixtures was applied are presented. In both case studies

improvements in the range of 10-30% compared to not allowing integrated recycling of recovered solvent between parallel processes were achieved.

In the first case study the main improvement was due to differences in purity requirements in the two parallel processes, which was reflected in different purge fractions. As a result it became advantageous to recycle material from the process with the higher purity requirements and hence higher purge fraction to the process with lower purity requirements and hence lower purge fraction, and introducing as much fresh material through make-up streams to the process with high purity requirements.

The second case study achieved the greatest improvements of about 30% compared to not integrating the two processes. Methanol was a by-product in process 1, but could not be recovered in pure form. Hence, the excess methanol could only escape the system through an azeotrope. With no integration this caused additional losses due to the fraction of the other component involved in the azeotrope. However, when integration was permitted some of the azeotrope could be recycled to the parallel process, where a solvent acted as a natural entrainer to break the azeotrope. In the second case study it was also demonstrated how the use of different weighting factors could be used to discriminate between components to, for example, reflect differences in toxicity or treatment cost, and that this can have a major impact on the process structures chosen by the optimization.

Chapter 10

Conclusions and Recommendations

10.1 Conclusions

One of the many environmental challenges faced by the synthetic pharmaceutical and specialty chemical industries is the widespread use of organic solvents. Cleaning solvents are relatively easy to change or eliminate. However, solvents in process reactions are much more difficult to substitute. With a solvent-based chemistry, the solvent necessarily has to be separated from the product stream. Although intermediate storage may be required before the solvent can be recycled to subsequent batches, this should be preferred to disposal of the solvent as toxic waste. This issue provides the motivation for this work, which focuses on the development of analysis and design tools to address the pollution prevention challenges posed by the use of organic solvents in the pharmaceutical and specialty chemical industries. In particular, the effective recovery and recycling of solvents is a primary concern.

So far, research activities have been successful only to a limited extent in addressing the problems of waste generation in chemical processes. It is our opinion that much of this deficiency has arisen from a failure to recognize that the environmental problems faced by the chemical industries require new approaches, as opposed to adapting current design technologies. The real opportunities lie in how the environmental debate should change the way design is performed, rather than *vice versa*. This thesis serves as a modest example of how this approach can yield concrete technical

solutions leading to significant environmental benefits.

Chemical species in waste-solvent streams generated by the pharmaceutical and specialty chemical industries typically form multicomponent azeotropic mixtures. This highly nonideal behavior often complicates separation and hence recovery of the solvents. Our approach is based on understanding and mitigating such obstacles. A prototype technology is proposed which combines rigorous dynamic simulation models and/or plant data to predict the compositions and magnitude of waste-solvent streams with residue curve maps to target for the maximum feasible recovery when using batch distillation.

As such, a complete theoretical understanding of residue curve maps applied to batch distillation of homogeneous multicomponent mixtures is required. It is demonstrated that earlier work on ternary residue curve maps for batch distillation is not complete. The theory is further generalized to homogeneous systems with an arbitrary number of components. The concepts of unstable and stable manifolds, and unstable and stable boundary limit sets are introduced to characterize simple distillation. Moreover, based on the limiting assumptions of very high reflux ratio, large number of trays, linear pot composition boundaries, and a rectifier configuration, properties of the batch distillation composition simplex are introduced. It is demonstrated that the pot composition orbit will be constrained by pot composition barriers present in the composition simplex, and that a pot composition barrier can be divided into one or more pot composition boundaries. An initial composition located interior to a batch distillation region will give rise to exactly nc product cuts, and these nc cuts form an nc product simplex. It is also found that a batch distillation region and its corresponding product simplex do not necessarily coincide.

An algorithm for elucidating the structure of the batch distillation composition simplex for a multicomponent system is described. Identification of the batch distillation regions is accomplished through completion of the unstable boundary limit sets. The completed boundary limit sets accurately represent the topological structure of the composition simplex, and also makes it possible to extract all product sequences achievable when applying batch distillation. The algorithm only requires information

of the compositions, boiling temperatures, and stability of the fixed points, and is guaranteed to find the correct unstable boundary limit sets for all fixed points in the system provided that the system itself and all its subsystems have at most two unstable and at most two stable nodes. The topological structures included in the algorithm are categorized by the number of unstable and stable nodes, and whether the system exhibits an azeotrope involving all components.

The algorithm for identifying the batch distillation regions has been exploited in a sequential design procedure where process streams or mixed waste-solvent streams are analyzed for maximum feasible solvent recovery. The procedure is termed *solvent recovery targeting*. For a given base case, solvent recovery targeting will, given the composition of the mixture(s) to be separated, predict the correct distillation sequence and calculate maximum feasible recovery of each product cut in the sequence. It can further provide information about all other feasible distillation sequences involving the same set of pure components. The information is used to evaluate the feasibility of enhancing solvent recovery in the proposed flowsheet, and to guide in improving the flowsheet.

A mixed-integer linear programming (MILP) formulation for the automated design of batch processes with integrated solvent recovery and recycling is also presented. A super simplex is introduced, which corresponds to the overall composition simplex for mixtures of several candidate solvents and entrainers, and in general will contain multiple azeotropic compositions. It is demonstrated that, under reasonable assumptions, the feasible sequences of pure component and azeotropic cuts that can be separated from mixtures in the super simplex can be formulated as linear constraints in terms of a mixed set of real and binary variables. This result is especially significant since it facilitates a compact and efficient mathematical abstraction of the complex azeotropic behavior that drives the decision process.

The super simplex is embedded in a novel reaction-separation superstructure to yield a modeling framework for the process-wide design of the mixtures formed in a batch process (primarily design of the mixtures leaving the reaction tasks). The modeling framework is flexible, new constraints can be easily added to produce more

realistic alternatives, and leads to a compact MILP that can be solved efficiently to guaranteed optimality. The methodology can be employed to generate various designs by adding or removing design constraints in an evolutionary manner, thereby furnishing the engineer with a set of different process designs that can be evaluated based on other criteria not embedded in the mathematical program, such as reaction rates (which are functions of selected solvent), production times, safety, etc.

The mathematical programming formulation for the design of a single batch process is extended to the design of multi-product manufacturing facilities in which solvent use is integrated across parallel processes.

In conclusion, the tangible product of this research work is a set of synthesis tools that can be employed to guide process modifications leading to significantly lower emission levels through integrated recovery and recycling of solvent as part of the process flowsheet. The application of the synthesis tools is successfully demonstrated in several case studies.

10.2 Recommendations for Future Research

The theoretical results on residue curve maps applied to batch distillation derived in Chapters 2 and 3 form the basis for the synthesis tools developed in this research. As such, the assumptions imposed on the theoretical derivations will also restrict the applicability of the synthesis tools. The significance of the limiting assumptions of very high reflux ratio, large number of theoretical stages, and linear pot composition boundaries are touched upon in Section 3.4. It is concluded that only slight deviation from the predicted behavior may be observed if any of these assumptions are relaxed. However, the assumption that the liquid phase remains homogeneous throughout the distillation has much more fundamental implications. The assumption is not restrictive when analyzing a single homogeneous stream as in solvent recovery targeting. However, it dramatically limits the problems that can be investigated with the mathematical programming formulation for process-wide (as well as plant-wide) design of mixtures. The super simplex embeds a range of solvents and entrainers, and it is

almost certain that some of these components will form partially miscible pairs. For example, water is often used in some part of a flowsheet, and will typically form a partially miscible pair with one or more of the other components in the flowsheet. In the first case study in Chapter 9 water is almost completely immiscible with both benzene and toluene. A constraint forbidding water to mix with either benzene or toluene is therefore included in the mathematical program, which in practice means that the optimal solution is restricted to lie on one of the facets of the super simplex. Hence, the constraint will greatly limit the alternative designs that can be considered. In the worst case, we may fail to find the most environmentally favorable design. Extending the theory of multicomponent azeotropic batch distillation to mixtures containing partially miscible pairs is therefore critical in order to allow solvent recovery targeting as well as the mathematical programming formulation to be applied to a broader class of manufacturing processes.

The algorithm for identifying batch distillation regions only applies to systems were the system itself and all its subsystems exhibit at most two unstable and at most two stable nodes (or globally determined systems). This assumption is not very restrictive since systems that do not satisfy this requirement are rarely encountered. In fact, we are not aware of a physical mixture that is globally undetermined. Although elaborate, integration of the equations governing simple distillation may be performed to determine the correct boundary limit sets in such cases. Recent progress in the area of dynamic analysis may lead to a more promising solution. For example, the concept of *trapping regions* to bound families of trajectories connecting two fixed points might possibly lend itself to resolving this issue (see, for example, Guckenheimer and Holmes (1983) or Strogatz (1994)).

Two further issues that will greatly enhance the applicability of the synthesis tools are related to the type of unit operations and separation technologies that might be considered. Firstly, the algorithm for identifying the batch distillation regions assumes the use of a single batch distillation column with a rectifier configuration, although one can easily envision that other more sophisticated configurations may be employed. Benefits of the stripper configuration, the middle-vessel configuration, and

the multi-vessel configuration have been demonstrated (Bernot *et al.*, 1991; Davidyan *et al.*, 1994; Safrit *et al.*, 1995; Skogestad *et al.*, 1995). The presented methodology should be extended to include a set of specific rules associated with each alternative technology. These rules could then be applied automatically for each relevant technology to generate more separation alternatives for the engineer. As demonstrated in Appendix A, the algorithm can be extended in a relatively straight forward manner to a stripper configuration. Advances on this issue will benefit both the usefulness of solvent recovery targeting as well as the mathematical programming formulation. Secondly, inclusion of appropriate abstract models to describe other common unit operations involving solvent usage such as crystallization, extraction, decanting, etc., in the mathematical programming formulation should be investigated. The latter two separation technologies rely on a liquid-liquid phase split for the feasibility of the operation. Progress on this issue will therefore strongly depend on advancements in extending the theory of multicomponent azeotropic batch distillation to heterogeneous mixtures.

A related issue concerns the column pressure. Knapp (1991) demonstrates that the qualitative features of the composition simplex depend on the pressure. In fact, in some systems azeotropes may appear or disappear as the pressure is varied. The column pressure could therefore be introduced as an additional design variable.

Another area of importance deals with the form of the objective function in the mathematical programming formulation. As a measure of the cost of recycling the solvent, the magnitude of the feed stream to a column is used. In order to appropriately reflect the actual cost, the manufacturing cost associated with the additional energy required as well as equipment usage should be included, while taking into account reduced solvent consumption, waste treatment, and raw material consumption (e.g., loss of products in non-product streams).

Furthermore, the formulation of the super simplex assumes that all product simplices coincide with their respective batch distillation regions. An extension to permit systems where this is not the case should be considered.

The two last issues concern the plant-wide design of solvent mixtures. In the

current formulation a slightly lower purge fraction must be chosen on internal recycle streams compared to streams that are recycled across processes in order to make the optimization favor internal recycle to recycle across process boundaries. However, while writing up this thesis we realized that the proper way to solve this design problem is as a *triple embedded* optimization: first, the minimum level of waste is determined as measured by the weighting factors. Second, the minimum level of integration across parallel processes is determined subject to minimum waste emitted. Third, internal recycle is minimized subject to minimum waste emitted and minimum integration across parallel processess.

Finally, the scheduling aspect of integrating solvent usage across parallel or nearly parallel process should be investigated. Of particular importance are the problems related to intermediate storage.

Appendix A

The Theory Applied to a Batch Stripper

A batch stripper is configured in a similar manner to a batch rectifier. However, the material is fed to the column from a holding tank where the mixture is held at its boiling temperature by a condenser. The product is taken out at the bottom of the column, and the recycled material is evaporated in a reboiler. Hence, the heaviest species is separated off first. This is illustrated by Figure A-1. When constructing the residue curve map for the mixture of interest, the arrows indicating direction of residue path should be reversed, as we now will be moving from heavier to lighter species in the holding tank. Therefore, all residue curves will reverse direction. As a result, the fixed points that are unstable when a rectifier is assumed will become stable, and vice versa for the stable nodes. From there the analysis is analogous to the analysis when a rectifier configuration is used, based on the same limiting assumptions of high reflux ratio, large number of trays, and linear pot composition boundaries.

Example: The residue curve map when using a batch stripper has been derived for the ternary system in Figure 2-12a. The resulting batch distillation regions are shown in Figure A-2. Observe that the batch distillation regions and their corresponding product simplices coincide. An initial composition located in batch distillation region 1 will produce $\mathbf{P}_1 = \{$L-I-H,I-H,I$\}$, any composition in region 2 will produce $\mathbf{P}_2 = \{$L-I-H,I-H,H$\}$, region 3 will result in the product sequence $\mathbf{P}_3 = \{$L-I-H, I,L$\}$,

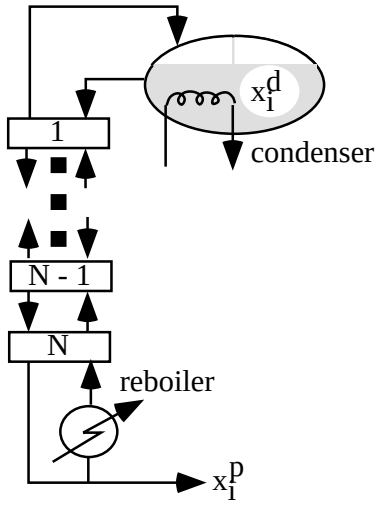

Figure A-1: Setup for stripper configuration.

and region 4 will result in $\mathbf{P}_1 = \{\text{L-I-H,H,L}\}$. Because ternary azeotrope L-I-H is the unstable node in all batch distillation regions, it will always appear as the first product when a stripper configuration is used. In contrast, only initial compositions located in batch distillation region 2 in Figure 2-12b have the ternary azeotrope as a product cut. Since it is always desirable to achieve products involving less components, this simple analysis implies that for distilling such a mixture the rectifier configuration should be chosen.

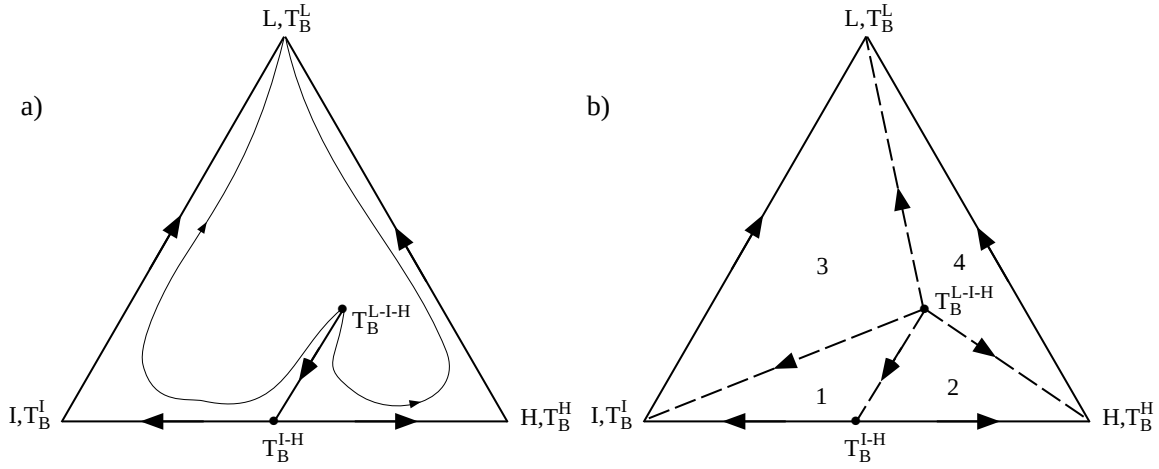

Figure A-2: Residue curve map with batch distillation regions and product simplices for a stripper configuration.

For mixtures with highly curved separatrices Bernot *et al.* (1991) demonstrated that using the stripper configuration may reduce the number of cuts necessary to achieve the desired products. It should be noted, however, that the stripper configuration is less likely to be adopted as any solids (e.g. catalysts, crystals) in the process stream will complicate such an operation.

Appendix B

Saddle Points connected to Stable Node involving all Components

Foucher (1991) shows that in a ternary system a ternary node (unstable or stable) must be connected to a binary saddle point through a separatrix (unstable or stable). Here we will demonstrate that this criterion extends to systems of nc components.

Doherty and Perkins (1979) conclude that the only types of fixed points which can occur are: unstable and stable nodes, saddle points, and armchair-like points. The three first types are elementary fixed points, while the latter type is a non-elementary fixed point. Non-elementary fixed points have one or more eigenvalues equal to zero, and may correspond to bifurcation points with respect to a parameter such as pressure, i.e., the global structure is changing from one type to another (see, for example, Knapp (1991)). It will be assumed that all the fixed points are elementary. In that case the eigenvalues of the linearized system in the neighborhood of a fixed point must be real and nonzero. Note that fixed points on a facet must satisfy the same conditions. The fact that we only consider the orbits for which $x_i \geq 0 \ \forall i = 1, \ldots, nc$, does not alter this requirement. For example, in Figure B-1 a and d represent non-elementary ternary fixed points, B-1 b and e represent non-elementary binary fixed points, and c represents a non-elementary pure component. It will be demonstrated that unless the criterion above is satisfied, the system will exhibit non-elementary fixed points.

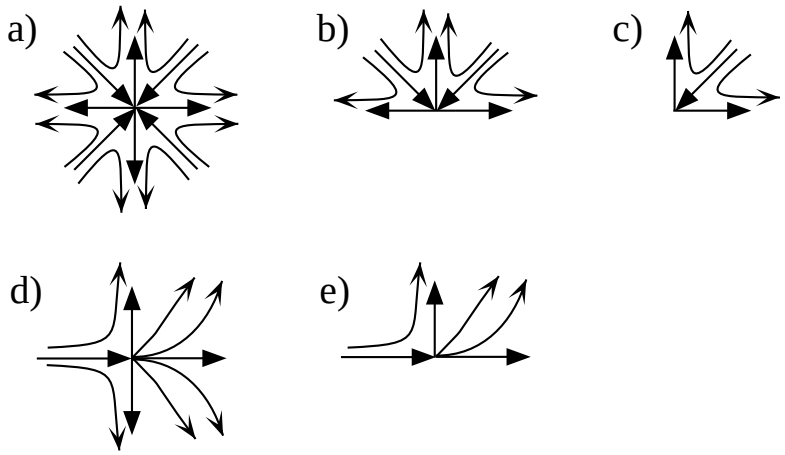

Figure B-1: Examples of non-elementary fixed points in a ternary system.

The case of the *nc* component node being unstable will be dealt with. The same arguments apply to the case of the *nc* component node being stable. All orbits through composition points in the neighborhood of the unstable node will approach the unstable node as $\xi \to -\infty$. In a ternary system the same orbits may only approach pure component nodes or binary saddle points as $\xi \to +\infty$. In fact, at least one orbit must approach a binary saddle point as $\xi \to +\infty$ (Foucher *et al.*, 1991). Figure B-2 demonstrates that any other topology will result in non-elementary fixed points. The system in Figure B-2a exhibits one unstable node, one stable node, one binary saddle point, and two pure component saddle points. The binary saddle point (b1) must have at least one orbit approaching as $\xi \to +\infty$, and b1 is therefore connected to the unstable node (t1). Note that this is necessary to make the binary azeotrope a saddle point. However, as Figure B-2b shows, t1 may not connect to any other saddle point as this will result in a non-elementary fixed point. In this case the connection between t1 makes the pure component saddle point (p1) into a saddle-node, i.e., it exhibits the properties of a saddle point in one sector of the neighborhood, and the properties of a stable node in another sector of the neighborhood.

The ternary system in Figures B-2c-d exhibits two unstable nodes, one stable node, two binary saddle points, and one pure component saddle point. Figure B-2c shows the correct topological structure. It is obvious from the discussion above that the ternary component unstable node (t1) may not connect to the pure component

saddle point (p1). However, as Figure B-2d shows it may neither connect to the binary saddle point b2. The connection between b2 and the stable node is necessary to make b2 a saddle point. The connection between b2 and t1 therefore makes b2 into a non-elementary fixed point. Observe that b2 is in the common unstable boundary limit set, and hence, located on the stable dividing boundary.

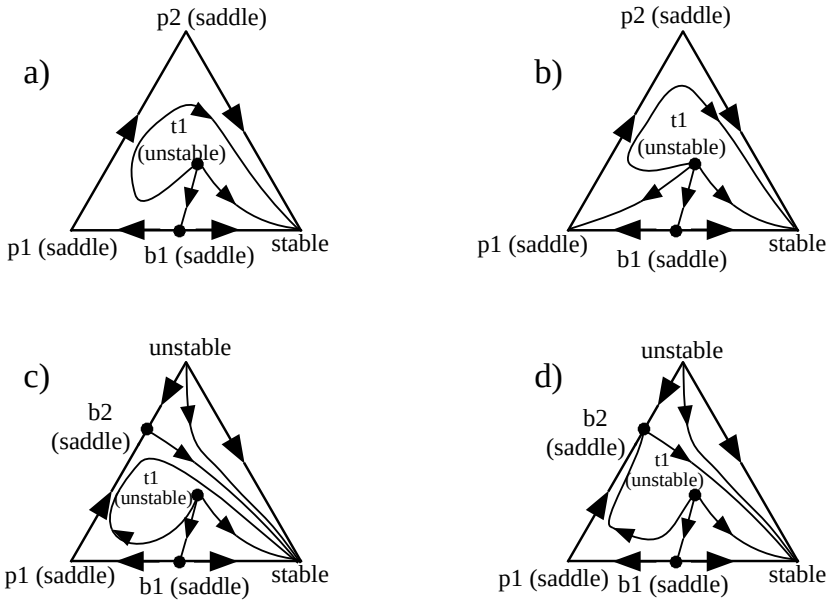

Figure B-2: Unstable node may be connected to binary saddle points only.

Similarly, although it is more elaborate, it can be shown graphically that in a quaternary system a quaternary unstable node must be connected to stable nodes and ternary saddle points only, and that it must be connected to at least one ternary saddle point. Any other topological configuration would result in non-elementary fixed points.

The linearized system in the neighborhood of each fixed point in a ternary system is defined by two eigendirections (2 eigenvalues). For a pure component the two eigendirections coincide with the binary edges. A binary saddle point has one eigendirection along the binary edge. The second eigendirection must therefore point into the composition simplex. Hence, in a system which exhibits a ternary unstable node, a binary saddle point must either be located on a stable dividing boundary, or be connected to a ternary unstable node, but not both, as this will make the

point non-elementary. Similarly, in a quaternary system the linearized system in the neighborhood of each fixed point is defined by three eigendirections (3 eigenvalues). For pure component saddle points and binary saddle points all three eigendirections will be parallel to the facets of the composition simplex, while a ternary saddle point has two eigendirections parallel to the ternary facet in which it is located. The third eigendirection must therefore point into the composition simplex. Hence, in a system which exhibits a quaternary unstable node, a ternary saddle point must either be located on a stable dividing boundary, or be connected to an quaternary unstable node, but not both, as this will make the point non-elementary. Although it is not possible to confirm graphically the same behavior for systems with more than four components, similar arguments apply.

In conclusion, we have established that in an nc component system with an unstable node involving nc components a saddle point involving $nc-1$ components must either be connected to the nc component unstable node through an unstable separatrix or be located on a stable dividing boundary, but not both. Also, saddle points involving less than $nc-1$ components may not be connected to the unstable node. Similarly, by reversing time, it follows that in an nc component system with a stable node involving nc components a saddle point involving $nc-1$ components must either be connected to the nc component stable node through an stable separatrix or be located on an unstable dividing boundary, but not both. Also, saddle points involving less than $nc-1$ components may not be connected to the stable node.

An orbit connecting two fixed points implies that the fixed point with the higher boiling temperature is in the unstable boundary limit set of the lower boiling fixed point. However, it is important to note that the converse is not necessarily true. In Figure B-2a there is an orbit between b1 and t1. Hence, b1 is in the unstable boundary limit set of t1. On the other hand, note that p1 is also in the unstable boundary limit set of t1, but there is no orbit connecting the two fixed points.

From the above discussion, a set of rules has been derived to analyze an nc component system with an nc component node. In particular, it is described how we determine which $nc-1$ saddle points are connected to this node, keeping in mind

that the ultimate goal is to complete the unstable boundary limit sets of the system (refer to Table 4.1 for the system numbers):

System 2 (one unstable and one stable node, where the unstable node involves nc components): from Theorem 4-6 we learn that all the other fixed points are in the unstable boundary limit set of the unstable node. The $nc-1$ component saddle points connected to the unstable node through unstable separatrices are obviously included. Hence, we are done.

System 3 (one unstable and one stable node, where the stable node involves nc components): from above we conclude that all fixed points are in the unstable boundary limit set of the unstable node. However, since the nc component node is stable, one or more $nc-1$ saddle points must be connected to the stable node through stable separatrices. Since there is only one stable node in the system, the system does not exhibit an unstable dividing boundary. Hence, all $nc-1$ saddle points must be connected to the stable node. It follows that the stable node must be in the unstable boundary limit sets of these saddle points.

System 5 (one unstable node and two stable nodes, where the unstable node involves nc components): using similar arguments as for system 2, we conclude that the same procedure can be applied.

System 6 (one unstable node and two stable nodes, where one stable node involves nc components): one or more $nc-1$ saddle points must be connected to the nc component stable node through stable separatrices. Since there are two stable nodes in the system, the system must exhibit an unstable dividing boundary. Hence, an $nc-1$ component saddle point that already has a stable node (i.e., the stable node located on one of the facets) in its unstable boundary limit set may not be connected to the nc component stable node as this will place the saddle point in the common stable boundary limit set and hence on the unstable dividing boundary. In conclusion, only the $nc-1$ component saddle points that do not already have a stable node in

their unstable boundary limit are connected to the nc component stable node. The nc component stable node must therefore be in the unstable boundary limit set of these saddle points.

System 8 (two unstable nodes (termed $\mathbf{x}_{m_a}$ and $\mathbf{x}_{m_b}$) and one stable node, where one unstable node ($\mathbf{x}_{m_b}$) involves nc components): one or more $nc-1$ saddle points must be connected to $\mathbf{x}_{m_b}$ through unstable separatrices. Since there are two unstable nodes in the system, the system must exhibit a stable dividing boundary. Hence, an $nc-1$ component saddle point that is already in the unstable boundary limit set of $\mathbf{x}_{m_a}$ may not be connected to $\mathbf{x}_{m_b}$, as this will place the saddle point in the common unstable boundary limit set and on the stable dividing boundary. In conclusion, only the $nc-1$ component saddle points that are not already elements of the unstable boundary limit set of the unstable node located on one of the facets are connected to the nc component unstable node. These saddle points are therefore in the unstable boundary limit set of the nc component unstable node.

System 9 (two unstable nodes and one stable node, where the stable node involves nc components): the stable node must obviously be an element of the unstable boundary limit sets of both unstable nodes. The stable node must therefore be located on the stable dividing boundary. Consequently, the $nc-1$ saddle points connected to the stable node must also be located on the boundary. If not, the stable separatrices connecting the saddle points to the stable node will result in additional boundaries in the composition simplex, which is not feasible. The unstable boundary limit sets of these saddle points may be completed when the stable dividing boundary is analyzed. The procedure for completing the unstable boundary limit sets for the fixed point on the stable dividing boundary is described in Section 4.1.4.

Appendix C

Stream Data for Siloxane Monomer Process

The following assumptions and simplifications were made for the base case:

- Final conversion specification for reactor I: amount of R1 or R2 should be less or equal to 0.1 mol.
- Conversion of C to E in reactor II is assumed to be 0.98.
- Conversion of E to D in reactor III is assumed to be 0.85.
- The distillation columns were simulated by lumping components C, R2, I1, and R1 into R1, and using the properties of R1. I2 and Pt were lumped into I2, and using the properties I2.
- The purity specifications on product (A + D) from distillation III was set to 99% on mass basis.

Table C.1: Stream data for Siloxane Monomer base case [kmol per batch]. Stream 6 is the stream out of reactor II, and stream 7 is the lumped stream into column I.

Component	1 + 2	3	4	5	6	7	8
R1 - Allyl Alcohol	7.87707	0	0	1.86563	1.86563	1.9218	1.9218
R2	3.93836	0	0	0.01696	0.01696	0	0
I1	0	0	0	0.028	0.028	0	0
A	0	0	0	2.09004	2.09004	2.09004	0
I2	0	0	0	0.00403	0.00403	0.02903	0
C	0	0	0	1.8205	0.03641	0	0
Toluene	5.36443	0	0	5.36443	5.36443	5.36443	4.2879
Pt	0.025	0	0	0.025	0.025	0	0
H2	0	1.82453	0	0	0	0	0
Methanol	0	0	3.93234	0	2.14825	2.14825	2.14825
E	0	0	0	0	1.78409	1.78409	0.27101
Water	0	0	0	0	0	0	0
D	0	0	0	0	0	0	0
Total	17.20485	1.82453	3.93234	13.33764	13.33764	13.33764	8.62901

Component	9	10	11+12	13	14	15	
R1 - Allyl Alcohol	0.00004	0	0.00004	0.00004	0	0	
R2	0	0	0	0	0	0	
I1	0	0	0	0	0	0	
A	2.9004	0.03735	2.0526	2.0526	0	2.0526	
I2	0.02907	0.02907	0	0	0	0	
C	0	0	0	0	0	0	
Toluene	1.0765	0	1.0765	1.0765	1.0765	0.00074	
Pt	0	0	0	0	0	0	
H2	0	0	0	0	0	0	
Methanol	0	0	0	1.28614	1.28614	0	
E	1.5131	0	1.5131	0.22697	0.18573	0.04143	
Water	0	0	45.393	44.74993	44.75	0	
D	0	0	0	0.64307	0	0.64295	
Total	4.70866	0.06642	50.03524	50.03524	47.29837	2.73772	

Appendix D

Binary Parameters for Wilson Activity Coefficient Model

The binary parameters in the Wilson activity coefficient model for the non-standard components C, E, A, and D that were used to compute the fixed points in the process are listed in Tables D.1 and D.2. R1 represents allyl-alcohol. * indicates that the data can be extracted from Aspen Plus (1995). The form of the model is:

$$\gamma_i = \exp\left(1 - \mathrm{B}_i - \sum_{j=1}^{nc}\left(\exp\left(a_{ji} + \frac{b_{ji}}{\mathrm{T}} - \mathrm{B}_j\right) x_j\right)\right) \tag{D.1}$$

$$\exp \mathrm{B}_i = \sum_{j=1}^{nc}\left(\exp\left(a_{ij} + \frac{b_{ij}}{\mathrm{T}}\right) x_j\right) \tag{D.2}$$

γ_i denotes the activity coefficient of component i, a_{ij} and b_{ij} represent binary interaction parameters between component pairs i and j, and T denotes the temperature (in Kelvin) of the system.

Table D.1: Binary parameters for Wilson activity coefficient model.

a_{ij}	C	Methanol	R1	Water	Toluene	E	A	D
C	0	3.787622	1.490857	0	-.5262635	-4.044775	-2.082101	0
Methanol	13.55363	0	*	*	*	1.116	1.558	1.845
R1	-3.092109	*	0	*	*	1.255	1.079	1.313
Water	0	*	*	0	*	-0.5128	-0.1479	-0.022
Toluene	0.9162579	*	*	*	0	0.8763	1.226	1.581
E	-2.175137	-1.344	0.9424	-6.273	-0.1774	0	0	0
A	2.99377	-0.052	0.2916	-4.377	1.625	-182.6	0	0
D	0	2.669	2.877	-5.526	4.567	-179.4	0	0

Table D.2: Binary parameters for Wilson activity coefficient model.

b_{ij}	C	Methanol	R1	Water	Toluene	E	A	D
C	0	-1603.069	-196.9849	0	-172.3204	-4.044775	865.0983	0
Methanol	-5112.675	0	*	*	*	-122.4	-80.24	-160.4
R1	1607.231	*	0	*	*	-441.7	38.64	-21.11
Water	0	*	*	0	*	61.36	168.5	72.18
Toluene	-118.064	*	*	*	0	-91.69	-265.5	-265.8
E	-2.175137	-1.655	131.6	-1411	-503.7	0	0	0
A	-1256.716	-1306	-1134	-2937	-2087	0	0	0
D	0	-3136	-2815	-5702	-3915	0	0	0

Appendix E

Stream Data for Carbinol Case Study

When computing the stream compositions the following assumptions and simplifications were made:

- 87% conversion of trienone to carbinol.
- A 7% loss of carbinol to tetraene.
- All water, acetic acid, and salts are removed in the phase split. No organic material is lost here.
- The brine is removed completely in the washing, and no organic material is lost here.

Table E.1: Stream data for Carbinol case study [kmol per batch].

Component	1	2	3	4	5	6	7	8
Trienone	0	0	0	0.182	0.02	0	0	0.02
CH3MgBr	3.8	0	3.8	0	3.6	0	3.6	0
Et2O	12.1	0	12.1	0	12.1	0	0	12.1
THF	0	42.4	42.4	0	42.4	0	0	42.4
AceticAcid	0	0	0	0	0	2.5	2.5	0
H_2O	0	0	0	0	0	1	1	0
Brine	0	0	0	0	0	0	0	0
Cyclohexane	0	0	0	0	0	0	0	0
Carbinol	0	0	0	0	0.147	0	0	0.147
Tetraene	0	0	0	0	0.01	0	0	0.01
Total	15.9	42.4	58.3	0.182	58.3	3.5	7.1	54.7

Component	9	10	11	12	13	14	15	16
Trienone	0	0	0.02	0	0	0.02	0	0.02
CH3MBr	0	0	0	0	0	0	0	0
Et2O	0	0	12.1	0	12.1	0	0	0
THF	0	0	42.4	0	40.4	1.98	1.98	0
AceticAcid	0	0	0	0	0	0	0	0
H_2O	0	0	0	0	0	0	0	0
Brine	0.5	0.5	0	0	0	0	0	0
Cyclohexane	0	0	0	130	68.8	61.4	61.4	0
Carbinol	0	0	0.147	0	0	0.147	0	0.147
Tetraene	0	0	0.01	0	0	0.01	0	0.01
Total	0.5	0.5	57.1	130	121.3	63.4	63.3	0.188

Appendix F

Stream Data for Benzonitrile Production

Table F.1: Case study 1: process 1 base case [kmol per batch].

Component	1	2	3	4	5	6	7
Toluene	0	11.8	11.8	0	11.8	0	11.8
Methanol	0	0	0	0	0	0	0
Acetic Acid	0	0	0	0	0	17.69	17.69
Ethanol	0	0	0	0	0	0	0
Water	0	196.6	204.5	204.5	0	0	3.932
R1	3.932	0	0	0	0	0	0
I11	0	0	3.932	0	3.932	0	0
I12	0	0	0	0	0	0	3.932
AR1	0	0	0	0	0	0	0
Total	3.932	208.4	220.2	204.5	15.73	17.69	33.42

Component	8	9	10	11	12	13	
Toluene	11.8	0	0	0	0	0	
Methanol	0	0	6.193	6.193	6.193	0	
Acetic Acid	17.69	0	0	0	0	0	
Ethanol	0	0	6.193	6.193	6.193	0	
Water	3.932	0	19.66	15.73	15.73	0	
R1	0	0	0	0	0	0	
I11	0	0	0	0	0	0	
I12	0	3.932	0	0	0	0	
AR1	0	0	0	3.932	0	3.932	
Total	29.49	3.932	32.05	35.98	28.12	3.932	

Table F.2: Case study 1: process 2 base case [kmol per batch].

Component	1	2	3	4	5	6	7	8	9
Toluene	0	10.815	10.815	0	10.815	0	10.815	10.815	0
Methanol	0	0	0	0	0	5.678	5.678	5.678	0
Ethanol	0	0	0	0	0	5.678	5.678	5.678	0
Water	0	180.25	187.46	187.46	0	18.02	14.42	14.42	0
R1	3.605	0	0	0	0	0	0	0	0
I21	0	0	3.605	0	3.605	0	0	0	0
Ar2	0	0	0	0	0	0	3.605	0	3.605
Total	3.605	191.1	194.7	187.5	14.42	29.38	40.2	36.6	3.605

Table F.3: Case study 1: integration across process boundaries [kmol per batch].

Compound	1	2	3	4	5	6	7	8	9	10
Methanol	0	0	0	0	0	0	12.385	12.385	0	0
Ethanol	0	0	0	0	0	0	0	0	0	0
Water	0	196.6	196.6	0	0	3.932	19.966	15.728	0	0
Toluene	0	0.316	11.796	11.48	0	0	0	0	0.219	0
Acetic Acid	0		0	0	17.694	17.694	0	0	0	0.33
R1	3.932		0	0	0	0	0	0	0	0
R2	0		0	0	0	0	0	0	0	0
Total	3.932	196.9	208.4	11.48	17.694	21.626	32.351	28.113	0.219	0.33

Compound	11	12	13	14	15	16	17	18	19	20
Methanol	0	0	0.33	12.054	0.23	0	0	0	0	0
Ethanol	0	0	0	0	0	0	0	0	0	0
Water	0	0	15.728	0	0	0.156	0	15.572	150.386	29.9
Toluene	0	0	0	0	0	0	0.096	0	0	10.815
Acetic Acid	17.364	0.33	0	0	0	0	0	0	0	0
R1	0	0	0	0	0	0	0	0	0	0
R2	0	0	0	0	0	0	0	0	3.605	0
Total	17.364	0.33	16.058	12.054	0.23	0.156	0.096	15.572	153.991	40.7

Compound	21	22	23	24	25	26	27	28	29	30
Methanol	0	11.356	11.356	0	11.254	0	0	0.101	0	0.101
Ethanol	0	0	0	0	0	0	0	0	0	0
Water	0	18.025	14.42	14.291	0	0	18.025	0	0.129	0
Toluene	10.719	0	0	0	0	0.096	0	0	0	0
Acetic Acid	0	0	0	0	0	0	0	0	0	0
R1	0	0	0	0	0	0	0	0	0	0
R2	0	0	0	0	0	0	0	0	0	0
Total	10.791	29.381	25.8	14.291	11.254	0.096	18.025	0.101	0.129	1.01

Table F.4: Case study 1: process 1 with no integration across process boundaries [kmol per batch].

Component	1	2	3	4	5	6	7	8	9
Methanol	0	0	0	0	0	0	12.385	12.385	0
Ethanol	0	0	0	0	0	0	0	0	0
Water	0	181.2	196.6	0	0	3.932	19.66	15.728	15.429
Toluene	0	0.22	11.796	11.576	0	0	0	0	0
Acetic Acid	0	0	0	0	17.694	17.694	0	0	0
R1	3.932	0	0	0	0	0	0	0	0
I11	0	0	0	0	0	0	0	0	0
I12	0	0	0	0	0	0	0	0	0
Ar1	0	0	0	0	0	0	0	0	0
Total	3.932	181.42	208.396	11.576	17.694	21.626	32.045	28.113	15.429

Component	10	11	12	13	14	15	16	17	
Methanol	0	0	0	0.231	0.231	12.154	0	0	
Ethanol	0	0	0	0	0	0	0	0	
Water	0	0	0	15.429	0	0	0.299	0	
Toluene	0.22	0	0	0	0	0	0	0	
Acetic Acid	0	0.329	0.329	0	0	0	0	17.4	
R1	0	0	0	0	0	0	0	0	
I11	0	0	0	0	0	0	0	0	
I12	0	0	0	0	0	0	0	0	
Ar1	0	0	0	0	0	0	0	0	
Total	0.22	0.329	0.329	15.66	0.231	12.154	0.299	17.4	

Table F.5: Case study 1: process 2 with no integration across process boundaries [kmol per batch].

Compound	1	2	3	4	5	6
Methanol	0	0	0	0	11.356	11.356
Ethanol	0	0	0	0	0	0
Water	0	167.21	180.25	0	18.025	14.42
Toluene	0	0.096	10.815	10.719	0	0
R2	3.605	0	0	0	0	0
I21	0	0	0	0	0	0
Ar2	0	0	0	0	0	0
Total	3.605	167.306	191.065	10.719	29.381	25.776

Compound	7	8	9	10	11	
Methanol	0	0	0.1	0.1	0	
Ethanol	0	0	0	0	0	
Water	14.29	0	14.42	0	0.13	
Toluene	0	0.096	0	0	0	
R2	0	0	0	0	0	
I21	0	0	0	0	0	
Ar2	0	0	0	0	0	
Total	14.29	0.096	14.42	0.1	0.13	

Appendix G

Stream Data for Case Study 5

Table G.1: Case study 2: process 1 no integration across process boundaries [mol per batch].

Compound	1	2	3	4	5	6	7	8	9	10
Methanol	0	224	11776	12000	224	4000	0	4045	0	0
Ethyl Acetate	0	0	0	0	0	0	0	0	0	0
Toluene	0	0	0	0	0	14000	13254	449	252	746
Iso-Propanol	0	0	0	0	0	0	0	0	0	0
A	4000	0	0	0	0	0	0	0	0	0
B	0	0	0	4000	0	0	0	0	0	0
C	0	0	0	0	0	4000	0	0	0	0
D	0	0	0	0	0	0	0	0	0	0
E	0	0	0	0	0	0	0	0	0	0
F	0	0	0	0	0	0	0	0	0	0
G	0	0	0	0	0	0	0	0	0	0
Total	4000	12000	16000	224	22000	13254	4494	252	746	

Table G.2: Case study 2: process 2 with no integration across process boundaries [mol per batch].

Compound	1	2	3	4	5	6	7	8	9
Methanol	0	0	0	6400	0	0	119	6281	119
Ethyl Acetate	0	0	0	4800	0	0	1812	2988	1812
Toluene	0	0	0	0	0	0	0	0	0
Iso-Propanol	0	298	16000	0	15702	298	0	0	0
A	0	0	0	0	0	0	0	0	0
B	0	0	0	0	0	0	0	0	0
C	0	0	0	0	0	0	0	0	0
D	3200	0	0	0	0	0	0	0	0
E	3200	0	0	0	0	0	0	0	0
F	0	0	3200	0	0	0	0	0	0
G	0	0	0	3200	0	0	0	0	0
Total	6400	298	19200	14400	15702	298	1931	9269	1931

Table G.3: Case study 2: integration across process boundaries [mol per batch].

Compound	1	2	3	4	5	6	7	8
Methanol	0	11772	12000	0	4000	228	0	0
Ethyl Acetate	0	3046	5143	0	0	98	0	0
Toluene	0	0	0	13303	14000	0	649	252
Iso-Propanol	0	0	0	0	0	0	0	0
A	4000	0	0	0	0	0	0	0
B	0	0	4000	0	0	0	0	0
C	0	0	0	0	4000	0	0	0
D	0	0	0	0	0	0	0	0
E	0	0	0	0	0	0	0	0
F	0	0	0	0	0	0	0	0
G	0	0	0	0	0	0	0	0
Total	4000	16818	21143	13303	22000	326	649	252

Compound	9	10	11	12	13	14	15	16
Methanol	227	0	445.4	3590	0	0	10760	10759
Ethyl Acetate	98	0	0	0	0	0	4800	4612
Toluene	0	49	49.5	398.6	0	0	0	0
Iso-Propanol	0	0	0	0	0	16000	0	0
A	0	0	0	0	0	0	0	0
B	0	0	0	0	0	0	0	0
C	0	0	0	0	0	0	0	0
D	0	0	0	0	3200	0	0	0
E	0	0	0	0	3200	0	0	0
F	0	0	0	0	0	3200	0	0
G	0	0	0	0	0	0	3200	0
Total	5897	49	494.9	3988.6	3200	19200	18760	15371

Compound	17	18	19	20	21	22		
Methanol	0	0	0	0	213	0		
Ethyl Acetate	189	0	0	0	91	0		
Toluene	0	0	0	0	0	1		
Iso-Propanol	0	298	15702	298	0	0		
A	0	0	0	0	0	0		
B	0	0	0	0	0	0		
C	0	0	0	0	0	0		
D	0	0	0	0	0	0		
E	0	0	0	0	0	0		
F	0	0	0	0	0	0		
G	0	0	0	0	0	0		
Total	189	298	15702	298	304	1		

Table G.4: Case study 2: alternative flowsheet [mol per batch].

Compound	1	2	3	4	5	6	7	8	9	10
Methanol	0	6329	12000	0	0	3711	0	0	0	76
Ethyl Acetate	0	2712	5143	0	1682	1590	0	0	0	0
Toluene	0	0	0	485	0	0	261	13254	252	8
Iso-Propanol	0	0	0	0	0	0	0	0	0	0
A	4000	0	0	0	0	0	0	0	0	0
B	0	0	4000	4000	0	0	0	0	0	0
C	0	0	0	0	0	0	0	0	0	0
D	0	0	0	0	0	0	0	0	0	0
E	0	0	0	0	0	0	0	0	0	0
F	0	0	0	0	0	0	0	0	0	0
G	0	0	0	0	0	0	0	0	0	0
Total	4000	9041	21143	4485	1682	5301	261	13254	252	84

	11	12	13	14	15	16	17	18	19	
Methanol	0	0	0	0	0	5885	11200	5315	214	
Ethyl Acetate	0	0	0	0	0	2522	4800	2278	92	
Toluene	0	0	0	0	0	0	0	0	0	
Iso-Propanol	0	298	16000	15702	298	0	0	0	0	
A	0	0	0	0	0	0	0	0	0	
B	0	0	0	0	0	0	0	0	0	
e C	0	0	0	0	0	0	0	0	0	
D	3200	0	0	0	0	0	0	0	0	
E	3200	0	0	0	0	0	0	0	0	
F	0	0	3200	0	0	0	0	0	0	
G	0	0	0	0	0	0	3200	0	0	
Total	6400	298	19200	15702	298	8407	19200	7593	306	

Bibliography

W. Abrams and J. Prausnitz. Statistical thermodynamics of liquid mixtures: a new expression for the excess gibbs free energy of partly or completely miscible systems. *AIChE Journal*, 21:116, 1975.

B. S. Ahmad and P. I. Barton. Solvent recovery targeting for pollution prevention in pharmaceutical and specialty chemical manufacturing. *AIChE Symposium Series*, 90(303):59–73, 1994.

B. S. Ahmad and P. I. Barton. Synthesis of batch processes with integrated solvent recovery and recycling. *Presented at AIChE Annual Meeting: Paper No. 187d*, November 1995.

B. S. Ahmad and P. I. Barton. Design of multiproduct batch manufacturing facilities with integrated solvent recovery. *Presented at 5th World Congress in Chemical Engineering, San Diego*, July 1996.

B. S. Ahmad and P. I. Barton. Homogeneous multicomponent azeotropic batch distillation. *AIChE Journal*, 42(12):3419–3433, 1996.

R. J. Allgor, M. D. Barrera, P. I. Barton, and L. B. Evans. Optimal batch process development. *Computers chem. Engng*, 20(6/7):885–896, 1996.

Aspen Technology. *BATCHFRAC User Manual release 6.2-2.* Aspen Technology Inc., Cambridge, MA 02139, USA, 1991.

Aspen Technology. *ASPEN PLUS User Manual Release 9.* Aspen Technology Inc., Cambridge, MA 02139, USA, 1995.

J. P. Aumond. Plant-wide solvent identification for pharmaceutical and fine chemical processes. Technical report, Doctoral Thesis Proposal, Massachusetts Institute of Technology, 1994.

R. W. Baker, E. L. Cussler, W. Eykamp, W. K. Koros, R. L. Ryley, and H. Strathmann. Membrane separation systems: Research needs assessment. Technical report, U.S. Department of Energy, DE-AC01-88ER30133, April 1990.

M. D. Barrera and L. B. Evans. Optimal design and operation of batch processes. *Chem. Eng. Comm.*, 82:45–66, 1989.

R. C. Berglund and C. T. Lawson. Preventing pollution in the CPI. *Chemical Engineering*, September 1991.

C. Bernot, M. F. Doherty, and M. F. Malone. Patterns of composition change in multicomponent batch distillation. *Chem. Eng. Science.*, 45(5):1207–1221, 1990.

C. Bernot, M. F. Doherty, and M. F. Malone. Feasibility and separation sequences in multicomponent batch distillation. *Chem. Eng. Science.*, 46(5/6):1311–1326, 1991.

A. Brooke, D. Kendrick, and A. Meeraus. *GAMS A User's Guide Release 2.25*. The Scientific Press, San Francisco, CA, 1992.

E. C. Carlson. Don't gamble with physical properties for simulations. *Chemical Engineering Progress*, pages 35–46, October 1996.

N. Chadha and C. S. Parmele. Minimize emissions of air toxics via process changes. *Chemical Engineering Progress*, pages 37–42, January 1993.

P. A. Clark and A. W. Westerberg. Optimization for design problems having more than one objective. *Computers chem. Engng*, 7(4):259–278, 1983.

H. T. Clarke and R. R. Read. 0-tolunitrile and p-tolunitrile. *Organic Synthesis Collective*, 1:514–516, 1932.

T. H. Cormen, C. E. Leiserson, and R. L. Rivest. *Introduction to Algorithms*. McGraw - Hill Company, New York, 1993.

E. W. Crabtree and M. M. El-Halwagi. Synthesis of acceptable reactions. *AIChE Symposium Series*, 90(303):117–127, 1994.

A. G. Davidyan, V. N. Kiva, G. A. Meski, and M. Morari. Batch distillation in a column with a middle vessel. *Chemical Engineering Science*, 49(18):3033–3051, 1994.

K. De Wahl and D. Peterson. Waste reduction in solvent cleaning: Process change vs. recycling. *Pollution Prevention Review*, Winter 1991.

U. M. Diwekar and S. E. Zitney. Chemical process simulation technology for solving environmental problems. *Presented at AIChE National Meeting, Seattle: Paper No. 69b*, Summer, 1993.

U. M. Diwekar. A process analysis approach to pollution prevention. *AIChE Symposium Series*, 90(303):168–179, 1994.

M. F. Doherty and G. A. Caldarola. Design and synthesis of homogeneous azeotropic distillation - 3: The sequence of columns for azeotropic and extractive distillations. *Ind. Eng. Chem. Fundam.*, 24:474–485, 1985.

M. F. Doherty and J. D. Perkins. Properties of liquid-vapour composition surfaces at azeotropic points. *Chem. Eng. Science*, 32:1112–1114, 1977.

M. F. Doherty and J. D. Perkins. On the dynamics of distillation processes - I: The simple distillation of multicomponent non-reacting, homogeneous liquid mixtures. *Chem. Eng. Science*, 33:281–301, 1978.

M. F. Doherty and J. D. Perkins. On the dynamics of distillation processes - II: The simple distillation of model solutions. *Chem. Eng. Science*, 33:569–578, 1978.

M. F. Doherty and J. D. Perkins. On the dynamics of distillation processes - III: The topology structure of ternary residue curve maps. *Chem. Eng. Science*, 34:1401–1414, 1979.

J. M. Douglas. *Conceptual Design of Chemical Processes*. McGraw - Hill Publishers, New York, 1988.

J. M. Douglas. Process synthesis for waste minimization. *Ind. Eng. Chem. Res.*, 31:238–243, 1992.

R. H. Ewell and L. M. Welch. Rectification in ternary systems containing binary azeotropes. *Industrial and Engineering Chemistry*, 37(112):1224–1231, 1945.

Z. T. Fidkowski, M. F. Malone, and M. F. Doherty. Computing azeotropes in multicomponent mixtures. *Computers chem. Engng*, 17(12):1141–1155, 1993.

E. R. Foucher, M. F. Doherty, and M. F. Malone. Automatic screening of entrainers for homogeneous azeotropic distillation. *Ind. Eng. Chem. Res.*, 30:760, 1991.

Aa. Fredenslund, J. Gmehling, and P. Rasmussen. *Vapor-Liquid Equilibria using UNIFAC*. Elsevier, Amsterdam, 1977.

H. Freeman, T. Harten, J. Springen, P. Randall, M.A. Currant, and K. Stone. Industrial pollution prevention: A critical review. *Journal for Air and Waste Managment Association*, 42(5):618–656, 1992.

S. K. Friedlander. The implications of environmental isssues for engineering R & D and education. *Chemical Engineering Progress*, pages 22–28, November 1989.

J. Ghemling, U. Onken, and W. Arlt. *Vapor-Liquid Equilibrium Data Collection*. DECHEMA, 6000 Frankfurt/Main, F.R.Germany, 1980.

P. H. Groggins. *Unit Processes in Organic Synthesis, 5th ed.* McGraw-Hill, Inc., New York, 1958.

I. E. Grossman, R. Drabbant, and R. K. Jain. Incorporating toxicology in the synthesis of industrial complexes. *Chem. Eng. Comm.*, 17:151–170, 1982.

J. Guckenheimer and P. Holmes. *Nonlinear Oscillations, Dynamical Systems, and Bifurcations of Vector Fields*. Springer-Verlag, 1983.

J. Hale and H. Koçak. *Dynamics and Bifurcations*. Springer-Verlag, 1991.

S. Q. Hassan and D. L. Timberlake. Steam stripping and batch distillation for the removal and/or recovery of volatile organic compunds from industrial waste. *Air Waste Manage. Assoc.*, 42:936–943, 1992.

T. Hatipoglu and D. W. T. Rippin. The effects of optimal temperature and feed addition rate profiles on batch reactions and sequences of batch operations - the development of a catalogue of attainable regions. In *Institution of Chemical Engineering Symposium Series No. 87*, pages 447–454. Pergamon Press, 1984.

R. A. Heckman. Alternatives for hazardous industrial solvents and cleaning agents. *Pollution Prevention Review*, Summer 1991.

J. G. Hocking and G. S. Young. *Topology*. Addison-Wesley Publishing Company, Inc., 1961.

C. S. Hwa. Mathematical formulation and optimization of heat exchanger networks using separable programming. *AIChE-I Chem. E. Symp. Ser.*, 4:101–106, 1965.

IBM Corporation. *Optimization Subroutine Library Guide and Referance*. IBM Corporation, SC23–0519–8 1991.

R. A. Jacobs. Waste minimization-part 2: Design your process for waste minimization. *Chemical Engineering Progress*, pages 55–59, June 1991.

E. M. Kirschner. Environment, health concerns force shift in use of organic solvents. *Chemical & Engineering News*, pages 13–20, June 20, 1994.

J. P. Knapp. *Exploiting Pressure Effects in the Distillation of Homogeneous Azeotropic Distillation*. PhD thesis, University of Massachusets, Amherst, June 1991.

J. R. Knight and M. F. Doherty. Systematic approaches to the synthesis of separation schemes for azeotropic mixtures. In *Proceedings of third International Conferance on Foundations of Computer-Aided Process Designs*, pages 417–434, Snowmass, Colorado, July 9-14, 1989.

J. P. Knight and G. J. McRae. An approach to process integration based on the choice of system chemistry. *Presented at AIChE Annual Meeting: Paper No. 153d*, November 1993.

J. P. Knight. *Computer-Aided Design Tools to Link Chemistry and Design in Process Development*. PhD thesis, Massachusetts Institute of Technology, 1994.

A. Lakshmanan and L. T. BIegler. Reactor network targeting for waste minimization. *AIChE Symposium Series*, 90(303):128–138, 1994.

S. G. Levy, D. B. Van Dongen, and M. F. Doherty. Design and synthesis of homogeneous azeotropic distillation - 2: Minimum reflux calculations for nonideal and azeotropic columns. *Ind. Eng. Chem. Fundam.*, 24:463–474, 1985.

A. A. Linninger, S. A. Ali, E. Stephanopoulos, C. Han, and G. Stephanopoulos. Synthesis and assessment of batch processes for pollution prevention. *AIChE Symposium Series*, 90(303):46–58, 1994.

Y. I. Malenko. Physicochemical analysis of fractional distillation diagrams. I. Theoretical basis of method. *Russ. J. Phys. Chem.*, 44(6):824–826, 1970.

Y. I. Malenko. Physicochemical analysis of fractional distillation diagrams. II. Quaternary systems. *Russ. J. Phys. Chem.*, 44(7):916–919, 1970.

Y. I. Malenko. Physicochemical analysis of fractional distillation diagrams. III. Multicomponent (n-component) systems. *Russ. J. Phys. Chem.*, 44(7):920–922, 1970.

C. D. Maranas, C. M. McDonald, S. T. Harding, and C. A. Floudas. Locating all azeotropes in homogeneous azeotropic mixtures. *Computers chem. Engng*, 20(Suppl.A):S413–S418, 1996.

H. Matsuyama and H. Nishimura. Topological and thermodynamic classification of ternary vapor-liquid equilibria. *J. Chem. Eng. Japan*, 10:181, 1977.

L. K. Molnar. *Polymer-Based Solvent for Minimizing Pollution during the Synthesis of Fine Chemicals*. PhD thesis, Massachusetts Institute of Technology, 1996.

Y. Naka, T. Komatsu, I. Hashimoto, and T. Takamatsu. Changes in distillation composition during ternary azeotropic batch distillation. *Int. Chem. Engng.*, 16:272–279, 1976.

F. B. Petlyuk, V. Ya. Kievskii, and L. A. Serafimov. Thermodynamic and topologic analysis of the phase diagrams of polyazeotropic mixtures. I. Definition of distillation regions using a computer. *Russ. J. Phys. Chem.*, 49(12):1834–1835, 1975.

F. B. Petlyuk, V. Ya. Kievskii, and L. A. Serafimov. Thermodynamic and topologic analysis of the phase diagrams of polyazeotropic mixtures. II. Algorithm for constructing of structural graphs for azeotropic ternary mixtures. *J. of Am. Chem. Soc.*, 49(12):1836–1837, 1975.

F. B. Petlyuk, V. Ya. Kievskii, and L. A. Serafimov. Thermodynamic and topologic analysis of the phase diagrams of polyazeotropic mixtures. V. The use of the phase equilibrium model in combined thermodynamic and topological analysis. *J. of Am. Chem. Soc.*, 51(3):338–340, 1977.

E. N. Pistikopoulos, S. K. Stefanis, and A. G. Livingston. A method for minimum environmental impact analysis. *AIChE Symposium Series*, 90(303):139–150, 1994.

J. M. Prausnitz, R. N. Lichtenhaler, and E. G. Azevedo. *Molecular Thermodynamics of Fluid-Phase Equilibria, 2nd ed.* Prentice-Hall, Engelwood Cliffs, N.J., 1986.

C. Reichardt. *Solvents and Solvent Effects in Organic Chemistry, 2nd ed.* VCH Verlagsgesellschaft mbH, Germany, 1988.

R. C. Reid, J. M. Prausnitz, and B. E. Poling. *The Properties of Gases and Liquids, 4th ed.* McGraw-Hill, Inc, New York, 1987.

W. Reinders and C. H. De Minjer. Vapour-liquid equilibrium in ternary systems. *Recl. Trans. Chim.*, 59:207–230, 1940.

G. V. Reklaitis. Progress and issues on computer aided batch process design. In *Proceedings Third International Conferance on Foundations of Computer-Aided Process Design*, pages 241–276, Snowmass, Colorado, 1989.

H. Renon and J. M. Prausnitz. Local compositions in thermodynamic excess functions for liquid mixtures. *AIChE Journal*, 14(1):135–144, 1968.

D. W. T. Rippin. Design and operation of multiproduct and multipurpose batch chemical plants. *Computers Chem. Engng.*, 7(4):463–481, 1983.

D. W. T. Rippin. Review paper: Simulation of single- and multiproduct batch chemical plants for optimal design and operation. *Computers Chem. Engng.*, 7(3):137–156, 1983.

D. W. T. Rippin. Batch process systems: A retrospective and prospective review. *Computers Chem. Engng.*, 17:S1–S13, 1993.

A. P. Rossiter. Process integration and pollution prevention. *AIChE Symposium Series*, 90(303):12–22, 1994.

W. Rudin. *Principles of Mathematical Analysis.* McGraw-Hill, Inc., New York, 1976.

B. T. Safrit and A. W. Westerberg. Algorithm for generating the distillation regions for azeotropic multicomponent mixtures. *Presented at AIChE Spring Meeting, New Orleans: Paper No. 84b*, February 1996.

B. T. Safrit, A. W. Westerberg, U. Diwekar, and O. M. Wahnschafft. Extending continuous conventional and extractive distillation feasibility insights to batch distillation. *Ind. Eng. Chem. Res.*, 34:3257–3264, 1995.

H. E. Salomone and O. A. Iribarren. Posynomial modeling of batch plants: A procedure to include process decision vaiables. *Computers Chem. Engng.*, 16(3):173–184, 1992.

L. A. Serafimov, F. B. Petlyuk, and I. B. Aleksandrov. The number of trajectory clusters representing continuous rectification of azeotropic multicomponent mixtures. *Theor. Found. Chem. Eng.*, 8:847–850, 1974.

R. A. Sheldon. Consider the environmental quotient. *CHEMTECH*, pages 38–47, March 1994.

Shell. *Shell Briefing Service Report on Petrochemicals.* Shell Briefing Service, 1990.

S. Skogestad, B. Wittgens, E. Sørensen, and R. Litto. Multivessel batch distillation. *Presented at AIChE Annual Meeting: Paper No. 184i*, November 1995.

J. Stichlmair and J. R. Herguijuela. Separation regions and processes of zeotropic and azeotropic ternary distillation. *AIChE Journal*, 38:1523–1535, 1992.

J. Stichlmair, H. Offers, and R. W. Potthoff. Minimum reflux and minimum reboil in ternary distillation. *Ind. Eng. Chem. Res.*, 32:2438–2445, 1993.

S. C. Stinson. Custom chemicals. *C & EN*, pages 34–59, February 8, 1993.

A. Streitwieser, C. H. Heathcock, and E. M. Kosower. *Introduction to Organic Chemistry.* MacMillian Publishing Company, USA, 1992.

S. H. Strogatz. *Nonlinear Dynamics and Chaos.* Addison-Wesley Publishing Company, 1994.

W. Swietoslawski. *Azeotropy and Polyazeotropy.* Pergamon Press, Oxford, 1963.

C. H. Twu and J. E. Coon. Accurately estimate binary interaction parameters. *Chemical Engineering Progress*, pages 46–53, December 1995.

T. Umeda, A. Hirai, and A. Ichikawa. Synthesis of optimal processing systems by an integrated approach. *Chem. Engng. Sci.*, 27:795–804, 1972.

U.S. Congress. Resource Conservation and Recovery Act, 1984.

U.S. Congress. Clean Air Act Amendments, P.C. 101-549, 1990.

U.S. Congress. Pollution Prevention Act, 1990.

U.S. Environmental Protection Agency. Pharmaceutical industry: hazardous waste generation, treatment, and disposal; NTIS referance: PB-258 800, 1976.

D. B. Van Dongen and M. F. Doherty. On the dynamics of distillation processes - V: The topology of the boiling temperature surface and its relation to azeotropic distillation. *Chem. Eng. Science*, 39:883–892, 1984.

D. B. Van Dongen and M. F. Doherty. Design and synthesis of homogeneous azeotropic distillation - 1: Problem formulation for a single column. *Ind. Eng. Chem. Fundam.*, 24:454–463, 1985.

D. B. Van Dongen and M. F. Doherty. On the dynamic of distillation processes-VI: Batch distillation. *Chem. Eng. Science*, 40:2087–2093, 1985.

O. M. Wahnschafft, J. W. Koehler, E. Blass, and A. W. Westerberg. The product composition regions of single-feed azeotropic distillation columns. *Ind. Eng. Chem. Res.*, 31:2345–2362, 1992.

O. M. Wahnschafft, J. P. LeRudulier, and A. W. Westerberg. A problem decomposition approach for the synthesis of complex separation processes with recycle. *Ind. Eng. Chem. Res.*, 32:1121, 1993.

S. Watson, X. Joulia, S. Macchietto, J. M. Le Lann, G. Vayrette, and J. J. Letourneau. Azeotropic distillation: New problems and some solutions. *Computers chem. Engng*, 19:s589–s596, 1995.

J. A. Wilson. Dynamic model based optimization in the design of a batch process involving simultaneous reaction and distillation. In *Institution of Chemical Engineering Symposium Series No.100*, pages 163–181. Pergamon Press, 1987.

J. Wisniak. *Liquid-liquid Equilibrium and Extraction: A Literature Source Book, V.1.* Elsevier Scientific Pub. Co., 1980.

Y. Zhang. Development and implmentation of algorithms for pollution prevention in pharmaceutical and specialty chemical manufacturing. Technical report, Massachusetts Institute of Technology, December 1995.